National Library of Canada
Bibliothèque nationale du Canada

Canadian Theses Service
Service des thèses canadiennes

Ottawa, Canada
K1A 0N4

NOTICE

The quality of this microform is heavily dependent upon the quality of the original thesis submitted for microfilming. Every effort has been made to ensure the highest quality of reproduction possible.

If pages are missing, contact the university which granted the degree.

Some pages may have indistinct print especially if the original pages were typed with a poor typewriter ribbon or if the university sent us an inferior photocopy.

Reproduction in full or in part of this microform is governed by the Canadian Copyright Act, R.S.C. 1970, c. C-30, and subsequent amendments.

AVIS

La qualité de cette microforme dépend grandement de la qualité de la thèse soumise au microfilmage. Nous avons tout fait pour assurer une qualité supérieure de reproduction.

S'il manque des pages, veuillez communiquer avec l'université qui a conféré le grade.

La qualité d'impression de certaines pages peut laisser à désirer, surtout si les pages originales ont été dactylographiées à l'aide d'un ruban usé ou si l'université nous a fait parvenir une photocopie de qualité inférieure.

La reproduction, même partielle, de cette microforme est soumise à la Loi canadienne sur le droit d'auteur, SRC 1970, c. C-30, et ses amendements subséquents.

NL-339 (r. 88/04) c

Canada

THE UNIVERSITY OF ALBERTA

IN SITU STRESS DETERMINATION IN OIL SANDS BY HYDRAULIC FRACTURING

by

SAMUEL ALBERT PROSKIN

(C)

A THESIS

SUBMITTED TO THE FACULTY OF GRADUATE STUDIES AND RESEARCH

IN PARTIAL FULFILMENT OF THE REQUIREMENTS FOR THE DEGREE

OF MASTER OF SCIENCE

IN

GEOTECHNIQUE

DEPARTMENT OF CIVIL ENGINEERING

EDMONTON, ALBERTA

SPRING 1989

National Library of Canada
Bibliothèque nationale du Canada

Canadian Theses Service
Service des thèses canadiennes

Ottawa, Canada
K1A 0N4

The author has granted an irrevocable non-exclusive licence allowing the National Library of Canada to reproduce loan, distribute or sell copies of his/her thesis by any means and in any form or format, making this thesis available to interested persons.

L'auteur a accordé une licence irrévocable et non exclusive permettant à la Bibliothèque nationale du Canada de reproduire, prêter, distribuer ou vendre des copies de sa thèse de quelque manière et sous quelque forme que ce soit pour mettre des exemplaires de cette thèse à la disposition des personnes intéressées.

The author retains ownership of the copyright in his/her thesis. Neither the thesis nor substantial extracts from it may be printed or otherwise reproduced without his/her permission.

L'auteur conserve la propriété du droit d'auteur qui protège sa thèse. Ni la thèse ni des extraits substantiels de celle-ci ne doivent être imprimés ou autrement reproduits sans son autorisation.

ISBN 0-315-53007-3

Canada

THE UNIVERSITY OF ALBERTA

RELEASE FORM

NAME OF AUTHOR: Samuel Albert Proskin

TITLE OF THESIS: In Situ Stress Determination in Oil Sands by Hydraulic Fracturing

DEGREE: Master of Science

YEAR THIS DEGREE GRANTED: 1989

Permission is hereby granted to THE UNIVERSITY OF ALBERTA LIBRARY to reproduce single copies of this thesis and to lend or sell such copies for private, scholarly or scientific research purposes only.

The author reserves other publication rights, and neither the thesis nor extensive extracts from it may be printed or otherwise reproduced without the author's written permission.

signed: Samuel A. Proskin

Permanent address:
4316 - 105 Avenue
Edmonton, Alberta
T6A 0Z9

Date: 26 April 1989

THE UNIVERSITY OF ALBERTA

FACULTY OF GRADUATE STUDIES AND RESEARCH

The undersigned certify that they have read, and recommend to the Faculty of Graduate Studies and Research for acceptance, a thesis entitled *In Situ Stress Determination in Oil Sands by Hydraulic Fracturing* submitted by Samuel Albert Proskin in partial fulfilment of the requirements for the degree of Master of Science in Geotechnique.

J. D. Scott
Supervisor

D. Cam Schmitt

N. R. Morgenstern

P K Robertson

Date: April 6, 1989

To my wife, Moira,

and our unsuspecting expected child.

ABSTRACT

A critique of the hydraulic fracture stress measurement method as applied to Alberta oil sands was conducted. This entailed extensive reviews of hydraulic fracture theory, of the relevant geomechanical behaviour of oil sands, and of previous oil sands hydraulic fracture research and practice. From these reviews, it was concluded that it is difficult to analyze the fracture initation pressure because of (i) the inability to analyze cased borehole microfracs and (ii) the complicated effects of oil sands behaviour.

However, it seems possible to determine the minimum principal stress from the shut-in pressure data. Because shut-in data may be distorted by the effect of oil sands behaviour, a shut-in pressure analysis method, based on well test analyses used by reservoir and groundwater engineers, was proposed. This approach uses graphical techniques derived from analytical models of fluid flow into wells intercepted by fractures. The method is limited by its improper treatment of fracture closure and by its inability to consider other complicating factors, such as geologic discontinuities and climbing fractures.

The data from four oil sands microfrac tests, obtained from AOSTRA, were analyzed in order to determine the in situ stresses. Only one test had conditions which allowed an analysis of the breakdown pressure. Some tests exhibited unusually high breakdown pressures. The shut-in pressure analyses usually agreed with the inflection point analyses. The minimum principal stresses for the Athabasca deposit tests were consistent with other stress data for this deposit. However, the Cold Lake deposit tests gave a minimum principal stress of approximately 5000 kPa, which is significantly lower than previous Cold Lake stress data.

ACKNOWLEDGEMENTS

Throughout my prolonged studies at the University of Alberta, many people have provided help along the way. I would like to briefly acknowledge those who provided financial assistance, scholarly inspiration, and emotional and spiritual support.

The first among these was my supervisor, Dr. J.D. Scott, who introduced me to the subject of my study and with whom I have spent many hours in fruitful discussion. His patience, expertise, and willingness to listen have provided an atmosphere conducive to scholarship.

Under Dr. Scott's tutelage, much appreciated financial assistance was provided by the National Science and Engineering Research Council through NSERC operating grant A0872.

I would like to thank the Alberta Oil Sands Technology and Research Authority for supplying the oil sands microfrac data, and Dr. D.A. Best and the staff at the Calgary office for helping me with the data. I would especially like to acknowledge the assistance of Harbir Chhina who, while with AOSTRA, offered his reservoir engineering and hydraulic fracturing expertise in many informative discussions.

My geotechnical colleagues at the University were a major part of the graduate research experience. Besides augmenting scholastic and research activities, they also provided a welcome social milieu through Saturday morning soccer, intramural hockey and Jim Cassie's house parties. In particular I would like to thank Jim Cassie, John McKay, Wim Van Gassen, Dwayne Tannant and Chris Neville.

My occasional research trips to the AOSTRA office in Calgary were made easier thanks to Brian Prokop and Dan and Janet Babaluk who provided temporary accomodation to the "poor graduate student".

Since I left my home in Winnipeg to pursue my studies, my parents have continued to encourage me to finish my thesis. They funded a large portion of my education for which I will always be grateful.

Finally, not only did I finally get a degree while at the University of Alberta, but also a wife -- and soon a baby. Both of these developments helped provide incentive to complete the thesis. I do not think I could have endured these final months without the encouragement, understanding, and patience of the woman I love.

This document proves that prayers *are* answered.

TABLE OF CONTENTS

Chapter		Page
1. INTRODUCTION		1
	1.1 Background	1
	1.2 Objectives and Scope	2
	1.3 Organization of the Thesis	3
2. HYDRAULIC FRACTURE THEORY		5
	2.1 Introduction	5
	2.2 Hydraulic Fracturing in Rock	6
	2.2.1 Classic Theory	7
	2.2.2 Haimson and Fairhurst's Theory	10
	2.2.3 Poroelastic Theory	12
	2.2.4 Field Test Verification	21
	2.3 Further Developments	24
	2.3.1 Complications in Hydraulic Fracture Behaviour	25
	2.3.1.1 Wellbore Condition	25
	2.3.1.2 Stress Orientation	27
	2.3.1.3 Geologic Structure	29
	2.3.1.4 Material Behaviour	32
	2.3.1.5 Packers	33
	2.3.2 Alternate Failure Mechanisms	34
	2.3.2.1 Fracture Mechanics	34
	2.3.2.2 Shear Failure	39
	2.3.2.3 Plastic Material	42
	2.4 Hydraulic Fracturing in Soil	43
	2.4.1 Hydraulic Fracture Theory for Soil	43
	2.4.2 Field Test Verification	47
	2.5 Summary	48
3. HYDRAULIC FRACTURING IN OIL SANDS		68
	3.1 Introduction	68
	3.2 Geomechanical Behaviour of Oil Sands	69

3.2.1 General Description 70
3.2.2 Implications for Hydraulic Fracture Theory 72
3.2.2.1 Classic Assumptions 73
3.2.2.2 Oil Sands Tensile Strength 74
3.2.2.3 Fluid Diffusion 75
3.2.2.4 Stress Path 77
3.2.2.5 Wellbore Condition 79
3.3 Hydraulic Fracture Studies in Oil Sands 84
3.3.1 Theoretical Studies 84
3.3.1.1 Numerical Modelling 85
3.3.1.2 Conceptual Modelling 87
3.3.2 Laboratory Observations 89
3.3.3 Field Studies 90
3.4 Summary 94
4. MINIMUM PRINCIPAL STRESS INTERPRETATION IN OIL SANDS MICROFRAC TESTS 121
4.1 Introduction 121
4.2 Determination of the Minimum Principal Stress 122
4.2.1 Relationship Between ISIP and the Minimum Principal Stress 122
4.2.2 Oil Sands Behaviour and Shut-In Pressure Response 125
4.2.3 Shut-in Pressure Response Models 127
4.2.2.1 False Shut-In Pressure Response Model 128
4.2.2.2 Multiple Shut-In Pressure Response Model 129
4.2.2.3 Indistinct Shut-In Pressure Response Model 130
4.3 Shut-In Pressure Interpretation Methodology 130
4.3.1 Laboratory Analyses 131
4.3.2 Theoretical Analyses 133
4.3.3 Empirical Analyses 137
4.3.4 Summary 140
4.4 An Interpretation Method for Oil Sands Tests 141
4.4.1 Application of Well Test Analysis Methodology 142

4.4.1.1 Vertically Fractured Wells....143
4.4.1.2 Horizontally Fractured Wells....144
4.4.1.3 Minimum Principal Stress Interpretation....145
4.4.2 Limitations of Well Test Analysis Methodology....147
4.5 Conclusions....148
5. OIL SANDS MICROFRAC CASE STUDIES....173
5.1 Introduction....173
5.1.1 Background....173
5.1.2 Injection Rate Data....175
5.2 Alberta Oil Sands Stress Data....176
5.3 AOSTRA-AMOCO Gregoire Lake Pilot Project Tests....179
5.3.1 Test and Site Description....179
5.3.1.1 General Description....179
5.3.1.2 Limestone Tests....180
5.3.1.3 Shale Tests....181
5.3.1.4 Oil Sands Test....182
5.3.2 Interpretation of Microfrac Data....183
5.3.2.1 Limestone Tests....184
5.3.2.2 Shale Test....185
5.3.2.3 Oil Sands Test....186
5.4 AOSTRA-CANTERRA TENNECO Kearl Lake Pilot Project Tests....188
5.4.1 Test and Site Description....188
5.4.1.1 General Description....188
5.4.1.2 BP 1 Test....190
5.4.1.3 BP 4 Test....191
5.4.2 Interpretation of BP1 and BP4 Microfrac Data....192
5.5 AOSTRA-BP B Unit Pilot Project Tests....194
5.5.1 Test and Site Description....194
5.5.1.1 General Description....194
5.5.1.2 OB-B01 Tests....196
5.5.1.3 OB-B02 Tests....197

5.5.2 Interpretation of the OB-B01 and OB-B02 Microfrac Data 199
5.6 AOSTRA-COLD LAKE-BOW VALLEY Pilot Project Test 201
5.6.1 Test and Site Description 201
5.6.1.1 General Description 201
5.6.1.2 ABC CH#3 Test 202
5.6.2 Interpretation of the Microfrac Data 204
5.7 Review of the Microfrac Results 206
5.7.1 In Situ Stress Results 206
5.7.2 Hydraulic Fracture Initiation 206
5.7.3 Minimum Principal Stress Interpretation 207
6. CONCLUSIONS AND RECOMMENDATIONS 245
6.1 Conclusions 245
6.2 Practical Implications for Conducting Field Tests 248
6.3 Recommendations for Future Research 250
REFERENCES 252

List of Tables

Table		Page
2.1	Factors which may affect hydraulic fracture initiation	51
2.2	Basic concepts of hydraulic fracture propagation	52
3.1	Reported permeability values for Alberta oil sands	97
3.2	Effect of confined drained and unconfined drained stress path tests on the stress strain properties of Athabasca and Cold Lake oil sands	98
3.3	Effect of stress path on the isotropic compressibility (K) and the confined compressibility (D) of Athabasca and Cold Lake oil sands	99
3.4	Oil sands factors affecting hydraulic fracture initiation theories	100
3.5	Oil sands factors affecting hydraulic fracture propagation	102
4.1	Summary of interpretation methods for determining σ_3	150
4.2	Summary of the experimental, theoretical and empirical evidence for σ_3 interpretation methods	152
5.1	Microfrac case data summary	208
5.2	Microfrac case reservoir data	209
5.3	Steady-state fluid flow parameters	209
5.4	Hydraulic fracture stress measurement data for Alberta oil sands deposits	210
5.5	Pressure difference and stress ratio data for the Amoco tests.	212
5.6	Summary of minimum principal stress determinations: Amoco shale, oil sands, and limestone tests	213
5.7	Minimum principal stress analysis for the Canterra BP1 test	214
5.8	Minimum principal stress analysis for the Canterra BP4 test.	214
5.9	Pressure and stress ratio data for the Canterra tests	215
5.10	Pressure and stress ratio data for the BP tests	216

5.11 Minimum principal stress analysis for the BP tests.....217

5.12 Pressure difference and stress ratio data for the ABC test.....218

5.13 Minimum principal stress analysis for the ABC test.....218

List of Figures

Figure		Page
2.1	Schematic representations of (a) openhole hydraulic fracturing tool and (b) an inflatable impression packer	53
2.2	Schematic drawing of a hydraulic fracture stress measurement pressure-time record which defines the nomenclature used in the thesis	54
2.3	Relationship between the principal stresses and fracture orientation for the classic vertical fracture analysis	55
2.4	Plane strain model of a circular hole in a externally loaded plate (Kirsch's model)	55
2.5	The influence of rigid packers in a hydraulic fracture test: (a) model of the pressurized zone and packers and (b) the tangential and vertical stresses induced during borehole pressurization (fluid injection)	56
2.6	Comparison of experimental fracture initiation pressure data and theoretical calculations (classic and Haimson and Fairhurst equations)	57
2.7	Comparison of the fracture initiation pressure data for (a) non-penetrating fluid (heavy grease) and (b) penetrating fluid (vacuum pump oil)	57
2.8	Comparison of hydraulic fracture stress measurement data and overcoring stress measurement data for two sites	58
2.9	Schematic drawing of a downhole hydraulic fracturing tool assembly used in perforated cased boreholes	59
2.10	Comparison between experimental and linear elastic fracture mechanics model predictions of fracture initiation pressure for varying pressurization rates	60
2.11	Laboratory results of deviatoric stress vs effective confining stress at fracture initiation indicating either tensile or shear failure	61
2.12	Theoretical radial pore pressure distribution for laboratory samples all experiencing shear failure at varying injection rates: (a) small samples and (b) large sample	62
2.13	Hydraulic fracture initiation curves for experiments with varying deviatoric stress values resulting in two different failure modes	63

2.14 Laboratory fracture initiation curves with the associated acoustic emission records suggesting four possible failure modes....64

2.15 Four possible failure modes as a function of injection rate, temperature and differential (deviatoric) stress....66

2.16 Possible vertical fracture orientations associated with shear failure....67

3.1 Oil sands deposits of Alberta....103

3.2 Typical shear strength envelope for Athabasca oil sands....104

3.3 Drained and undrained triaxial extension tests results....105

3.4 Relation between pore pressure parameter B and oil sands compressibility....106

3.5 Stress paths used in geomechanics tests....107

3.6 Comparison of undrained and drained shear strength data for oil sands....108

3.7 Stress paths to failure in triaxial stress space for triaxial tests on Syncrude oil sands....109

3.8 Possible stress path for oil sands at depth which undergoes a drained response to borehole drilling and pressurization....110

3.9 Localized shear failure around a wellbore leading to a wellbore breakout....111

3.10 Potential shear failure surfaces around a borehole based on a Mohr-Coulomb failure criteria....111

3.11 Possible borehole rupture modes....112

3.12 Total stresses developed around a borehole along a radial direction normal to the minimum principal stress calculated using poroelastic theory (deviatoric loading mode only)....113

3.13 Effective stresses developed around a borehole along a radial direction normal to the minimum principal stress for poroelastic theory (deviatoric loading mode only)....113

3.14 Evaluation of shear failure around a borehole based on poroelastic theory (hydrostatic and deviatoric stress loading modes)....114

3.15 Elastic stress evaluation of possible shear failure around a borehole for (a) two Athabasca oil sand stress states and (b) a Cold Lake oil sands stress state 115

3.15 Continued 116

3.16 Unstable rupture modes for underground openings 117

3.17 Stress-strain curves for Athabasca Clearwater Formation oil sands 118

3.18 Sectioned oil sands sample indicating fluid penetration which occurred during an hydraulic fracture experiment (a) photograph of the sample and (b) schematic drawing of the sample 119

3.18 Continued 120

4.1 False shut-in pressure response curve 153

4.2 Multiple shut-in pressure response curve 154

4.3 Indistinct shut-in pressure response curve 155

4.4 Application of the inflection point method to shut-in pressure data for the determination of the minimum principal stress 156

4.5 Correlation between applied load and the inflection point method interpretation of the minimum principal stress 157

4.6 Horner analysis of the minimum principal stress from shut-in pressure data 158

4.7 Application of the exponential decay model of Lee and Haimson (1988) to laboratory shut-in pressure data 159

4.8 Schematic of the minimum principal stress contours for the application of the shut-in pressure curve inversion technique proposed by Charlez *et al.* (1988) 160

4.9 Comparison of the field data and the model prediction of the shut-in pressure response 161

4.10 Effect of horizontal stress ratio on the predicted shut-in pressure response 162

4.11 Effect of fluid loss coefficient on the predicted shut-in pressure response 163

4.12 Two of the shut-in pressure response interpretation techniques employed by Aggson and Kim (1987) 164

4.12 Continued 165

4.13 Injection rate vs time models for simulating (a) pressure build-up and (b) pressure fall-off tests 166

4.14 Model of a well intercepted by a single vertical fracture 167

4.15 Characteristic pressure curves of an infinite conductivity vertical fracture for various fracture lengths 168

4.16 Four possible flow regimes exhibited by a vertically fractured well 169

4.17 Model of a well intercepted by a single horizontal fracture 170

4.18 Characterstic pressure curves of a uniform flux horizontal fracture centered at the borehole for various dimensionless formation thicknesses 171

4.19 Three possible flow periods exhibited by a horizontally fractured well 172

5.1 Location of the microfrac test sites 219

5.2 Hydraulic fracture in situ stress data for the Cold Lake deposit 220

5.3 Hydraulic fracture in situ stress data for the Athabasca deposit 221

5.4 Lithologic log of the Amoco H1 well (shale and limestone tests) 222

5.5 Lithologic log of the Amoco H3 well (oil sands test) 223

5.6 Pressure-time graph for the Amoco H1 well limestone microfrac test consisting of four injection/shut-in cycles 224

5.7 Pressure-time graph for the Amoco H1 well shale microfrac test consisting of four injection/shut-in cycles 224

5.8 Variation in the minimum principal stress for the Amoco H1 shale microfrac test 225

5.9 Pressure-time graph for the Amoco H3 well oil sands microfrac test consisting of three injection/shut-in cycles 225

5.10 Shut-in pressure interpretation graphs for the Amoco H3 well oil sands microfrac-cycle 1 226

5.10 Continued 227

5.11 Lithologic logs of the Canterra BP1 and BP4 wells....228

5.12 Pressure-time graph for the BP1 well microfrac test consisting of three injection/shut-in cycles....229

5.13 Pressure-time graph for the BP4 well microfrac test consisting of three injection/shut-in cycles....229

5.14 Shut-in pressure interpretation graphs for the BP4 well microfrac-cycle 2....230

5.14 Continued....231

5.15 Representative lithologic log of the BP OB-B01 and OB-B02 wells....232

5.16 Shut-in pressure interpretation graphs for the OB-B01 well microfrac-cycle 1....233

5.16 Continued....234

5.17 Variation in the minimum principal stress for the OB-B01 well microfrac test....235

5.18 Log-log interpretation graph for OB-B02 well-cycle 1....236

5.19 Variation in the minimum principal stress for the OB-B02 well microfrac test....237

5.20 Lithologic log of the ABC CH#3 well....238

5.21 Pressure-time graph for the ABC CH#3 well microfrac test consisting of three injection/shut-in cycles....239

5.22 Shut-in pressure interpretation graphs for the ABC CH#3 well microfrac-cycle 1....240

5.22 Continued....241

5.22 Continued....242

5.23 Variation in the minimum principal stress for the ABC CH#3 well microfrac test....242

5.24 Thesis microfrac stress data plotted along with previous in situ stress data for the Cold Lake deposit....243

5.25 Thesis microfrac stress data plotted along with previous in situ stress data for the Athabasca deposit....244

Nomenclature

The nomenclature attempts to follow the ISRM (1987) guidelines for hydraulic fracture tests and the recommendations of the Canadian Geotechnical Society. Conventional petroleum/engineering nomenclature has also been adopted for some aspects of hydraulic fracturing and reservoir description. A lower case p denotes that pressure is referenced to the reservoir pressure. A prime (') denotes effective stress.

a	borehole radius
AOSTRA	Alberta Oil Sands Technology and Research Authority
b	radius of finite acting reservoir
B	Skempton's undrained pore pressure parameter
c	generalized consolidation coefficient
c'	effective cohesion intercept
c_v	coefficient of consolidation
c_w	leakoff coefficient (Charlez *et al.* 1988)
C_i	isotropic compressibility
C_c	constrained compressibility
D	constrained bulk modulus
E	modulus of linear deformation (Young's modulus)
E_i	initial tangent modulus of linear deformation
F*, G*	dimensionless stress intensity factors
G	modulus of shear deformation
h	height of the confined pay zone
h_f	horizontal fracture width
hydrostatic stress	state of stress in which all principal stresses are equal
ISIP	instantaneous shut-in pressure
J_1	first invariant of the stress tensor
k	absolute permeability
k*	coefficient of permeability (hydraulic conductivity)
K	isotropic bulk modulus
K_f	pore fluid bulk modulus

K_s	grain (solid) bulk modulus
K_u	undrained bulk modulus
K_{IC}	critical stress intensity factor for tensile (Mode I) failure
K_o	coefficient of earth pressure at rest
K	Haimson and Fairhurst's poroelastic parameter
L	one-half of the fracture length
LEFM	linear elastic fracture mechanics
m_v	coefficient of volume change
n	porosity
P	pressure
P_b	reservoir/formation hydraulic fracture breakdown pressure
P_c	hydraulic fracture closure pressure (stress)
P_e	fracture re-opening pressure (Aamodt and Kuriyagawa 1983)
P_f	hydraulic fracture initiation pressure
P_L	pressure losses in the fracture
P_o	initial reservoir pore fluid pressure
P_{open}	pressure required to keep the fracture open
P_p	fracture propagation/extension pressure
P_{pk}	packer inflation pressure
P_r	fracture reopening pressure or secondary breakdown pressure
P_s	instantaneous shut-in pressure (ISIP)
P_{si}	pressure at shut-in ($\Delta t=0$)
P_{ss}	steady-state fluid flow pressure
P_w	wellbore pressure
P_l	pressure at which fracture closure occurs and radial flow dominates the wellbore pressure response (Cheung and Haimson 1988)
P_u	pressure derived from the extrapolation of the Muscat exponential best fit line to zero shut-in time (Cheung and Haimson 1988)

poroelasticity	an elastic theory which was developed for porous materials containing pore fluid
q	volumetric fluid injection rate
q_{ss}	steady-state fluid flow rate
r	radial distance from the centre of the borehole
S	function representative of the difference between experimental shut-in pressure data and the model predictions of Charlez *et al.* 1988
S_w	water saturation
t	time
t_{inj}	duration of fluid injection
t^*	normalized time (Detournay and Cheng 1988)
t_c	characteristic time for the development of poroelastic effects
T	temperature
UTF	AOSTRA's Underground Test Facility
V_{inj}	volume of fluid injected in one hydraulic fracture injection cycle
Δt	time elapsed since shut-in
Δu	excess pore pressure
α	Biot's coefficient (or poroelastic parameter)
α_1, α_2, $\alpha 3$, $\alpha 4$	borehole stress concentration factors (Cleary 1979)
α^*,β^*	stress factors (Bjerrum *et al.* 1972)
γ	soil/rock unit weight
γ_w	unit weight of water
ε	linear strain
η	Detournay *et al.*'s (1988) poroelastic parameter
θ	angle measured from the radius parallel to σ_{hmax} in the plane containing the horizontal principal stresses
μ	pore fluid dynamic viscosity
ν	Poisson's ratio
ν_u	undrained Poisson's ratio

σ_{ii}	tensor notation for the three principal stresses
$\sigma_1, \sigma_2, \sigma_3$	total principal stresses (major, intermediate and minor, respectively)
σ_b	back stresses or the increase in total stresses due to poroelastic effects
σ_{hmin}	minor horizontal principal stress
σ_{hmax}	major horizontal principal stress
σ_v	vertical principal stress
σ_t	rock/soil tensile strength
$\sigma_{\theta\theta}, \sigma_{rr}, \sigma_{zz}$	tangential, radial and axial stresses
ϕ'	effective angle of internal friction

Interpretation Graphs

P vs t	pressure vs time
P vs Δt	pressure vs shut-in time
log (P_{si} - P) vs log Δt	log-log graph
P vs $\frac{t_{inj} + \Delta t}{\Delta t}$	Horner graph
P vs $\sqrt{(t_{inj} + \Delta t)} - \sqrt{\Delta t}$	Tandem square root graph (TSR)
$\delta P/\delta t$ vs Pavg	incremental pressure decay rate (slope of the P vs Δt curve) vs the average pressure over that increment (also known as the pressure decay rate graph-PDR)

Microfrac Tests

ABC	AOSTRA-COLD LAKE-BOW VALLEY Pilot Project
AMOCO	AOSTRA-AMOCO Gregoire Lake Pilot Project
BP	AOSTRA-BP B Unit Pilot Project
CANTERRA	AOSTRA-CANTERRA TENNECO Kearl Lake Pilot Project

1. INTRODUCTION

1.1 Background

Knowledge of the in situ stress state in oil sands is necessary for the design of in situ bitumen recovery schemes, surface mining projects and shaft and tunnel access projects. At present, hydraulic fracture tests, also known as microfracs or minifracs by the petroleum industry, have been the primary method used to determine the in situ stresses in oil sand deposits of Alberta.

Hydraulic fracturing procedures have been employed in rock and soil strata for many years in order to determine the in situ stress state and stress measurement theory has been developed for both materials. The method has been sufficiently field tested and validated against other techniques and has become a widely accepted procedure for stress measurement in rock, but less so for stress measurement in soils.

Extensive research has been conducted in order to study the effect of complicating factors on the hydraulic fracture intiation. The initial classic theory proposed by Hubbert and Willis (1957) for impermeable rock has since been modified for permeable rock by Haimson and Fairhurst (1967) and then for coupled deformation-diffusion conditions by Rice and Cleary (1976) and by Detournay and Cheng (1988). Additional research has shown deviations from theory occur due to such factors as non-linear stress-strain behaviour and geologic discontinuities. Also, in many cases in the petroleum industry, hydraulic fracture tests are performed in perforated cased boreholes rather than in the usual openhole. Alternative hydraulic fracture initiation theories which have been proposed based on different failure criteria, such as fracture mechanics theory and shear failure, have added to the complexity of this technique.

Often hydraulic fracture data is affected by these extraneous factors making it difficult to interpret the in situ stresses from the pressure-time data. Several methods have been proposed for interpreting complicated pressure-time records resulting from the effect of natural conditions and test

procedures. Unfortunately, no consensus exists for the analysis of hydraulic fracture stress measurement pressure-time data.

Before applying the hydraulic fracture stress measurement method to oil sands, it is important to examine the potential influence of oil sands material properties and behaviour on these results. Research performed at the University of Alberta has shown that oil sands are a unique geotechnical material (Dusseault 1977a; Barnes 1980; Agar 1984; Kosar 1989). Although it is an unconsolidated, uncemented rock, it has been subjected to high overburden stresses since burial that have resulted in a material possessing an interlocked fabric and rock-like properties in situ. Dusseault (1980b) proposed a geomechanics conceptual model of hydraulic fracturing in oil sands in an attempt to explain how these unique properties affect the application of hydraulic fracture theory to oil sands.

1.2 Objectives and Scope

The primary objective of this thesis was to examine the validity of hydraulic fracture stress measurement theory for oil sands. Hydraulic fracture stress measurement theory can be divided into (i) hydraulic fracture initiation theory and (ii) hydraulic fracture propagation theory. Therefore, the primary objective can be stated in the form of two questions. Which one of the hydraulic fracture initiation theories is best suited to the interpretation of tests in oil sands? Do the fundamentals of hydraulic fracture propagation theory apply to oil sand hydraulic fracture tests? The delineation of the limits of hydraulic fracture theory in consideration of oil sand's unique geomechanical behaviour is necessary to meet this objective.

If hydraulic fracture stress measurement theory is an acceptable approach to measuring in situ stress in oil sands, then a further question arises. What is the relationship between the pressures observed during hydraulic fracture tests and the in situ stresses in oil sands?

Because of the extensive nature of hydraulic fracture theory and practice, the scope of this thesis had to be confined to fulfilling the objectives

defined above. Various hydraulic fracture stress measurement theories proposed in the literature for both consolidated and unconsolidated materials were reviewed in order to determine the limitations of hydraulic fracture initiation and propagation This was followed by a study of the relevant aspects of oil sands geomechanics and a review of previous theoretical, experimental and field studies of hydraulic fracturing in oil sands.

Once the applicability of hydraulic fracture stress measurement theory for oil sands was determined, a specific analysis was conducted of the relationship between shut-in pressure data and in situ stress.

The in situ stress determination analysis was then applied to actual hydraulic fracture stress measurement tests (often identified as microfrac and minifrac tests in the petroleum industry) from Athabasca and Cold Lake sites. These field test data were obtained from the Alberta Oil Sands Technology and Research Authority (AOSTRA).

Based on the restrictions inferred from the objectives, the following items remain outside the scope of the thesis: (i) numerical and laboratory work assessing the validity of the various theories; (ii) the effect of large scale ($> 10\ m^3$) fluid injections; (iii) the consideration of fracture fluids other than KCl water; and (iv) a detailed review of other stress measurement techniques.

1.3 Organization of the Thesis

Chapter 2 reviews the literature on hydraulic fracture stress measurement theories. The various factors which affect hydraulic fracture initiation theory are identified. The fundamental principles of hydraulic fracture propagation are summarized. At the conclusion of this chapter there is a summary of the essential factors which must be considered in an evaluation of hydraulic fracture stress measurement theory for oil sands.

Chapter 3 contains a study of the implications of oil sands geomechanical behaviour on hydraulic fracture theory. This study is combined with a review of previous oil sands hydraulic fracturing research in

order to evaluate the viability of the hydraulic fracture stress measurement method for oil sands.

Chapter 4 is predicated on the conclusions of chapter 3. If the hydraulic fracture stress measurement method is valid for oil sand, the relationship between in situ stress and pressure-time data recorded during the test must be found. Consequently, an interpretation method is proposed for determining the minimum principal stress from oil sands hydraulic fracture stress measurement tests.

Chapter 5 analyzes four Alberta oil sand hydraulic fracture tests (microfracs) obtained from AOSTRA. The interpretation method of chapter 4 is applied in the analysis of two tests in the Athabasca oil sands deposit and two tests in the Cold Lake oil sands deposit. The in situ stress results are compared with previous data for Alberta oil sand deposits. Problems observed with the analysis of these tests are also summarized.

Chapter 6 summarizes the findings of the previous chapters. The implications of the results on the use of the hydraulic fracture stress measurement procedure for oil sands are discussed.

2. HYDRAULIC FRACTURE THEORY

2.1 Introduction

Hydraulic fracturing was first proposed by Clark (1949) as the phenomena responsible for the unusual behaviour exhibited by oil wells subjected to fluid injection. Since then the petroleum industry has been a major sponsor of research in the application of hydraulic fracturing for petroleum extraction. Initial studies of the mechanics of hydraulic fracturing revealed its potential use for evaluating in situ stresses in a wide range of engineering and scientific studies. This has resulted in a plethora of theoretical, laboratory and field studies of the hydraulic fracturing technique in the disciplines of petroleum reservoir engineering, rock mechanics, soil mechanics, and geophysics.

A survey of hydraulic fracture literature was conducted in order to trace the development of the hydraulic fracturing stress measurement technique. This chapter summarizes this survey by explaining the fundamentals of classic hydraulic fracture theory first for impermeable rock and then for permeable rock. Laboratory investigations have confirmed the classic hydraulic fracture theory, but these investigations have also identified the limitations of the theory because of its restrictive assumptions. Subsequent research has attempted to modify and generalize the theory in order to make it more compatible with laboratory and field observations. Numerous field studies in which hydraulic fracture stress measurements were compared with other stress results have shown the hydraulic fracturing stress measurement technique to be a valid and valuable method as confirmed by its current popularity in various disciplines.

Further theoretical, experimental and field research has emphasized the restrictions of the general hydraulic fracture theory with regard to some of the theory's most important principles. In some cases hydraulic fracture stress measurement theory is viable as long as restrictions are observed regarding the condition of the rock/soil near the wellbore, the assumed stress

orientation, the influence of geologic structure, the possibility of material anisotropy and the influence of packers. Other research, however, has suggested that hydraulic fracture theory is invalidated by other processes occurring during fluid pressurization of the borehole. This research has centered on the application of fracture mechanics theory, the possibility of shear failure rather than tensile failure being the dominant failure mechanism and the role of plasticity in hydraulic fracture.

Hydraulic fracturing theory for soil (using the engineering definition of soil which includes regolith) has undergone a separate development in geotechnical engineering. Differences in the test method from those used in rock and in material behaviour have resulted in a later, parallel development in the theory and practice of hydraulic fracture stress measurement for soil. Soil hydraulic fracturing is, therefore, treated in a separate section.

2.2 Hydraulic Fracturing in Rock

Hydraulic fracture theory for rock has been studied extensively since Hubbert and Willis (1957) first discussed the mechanics of hydraulic fracturing. The theory has been progressively modified to first consider the effects of penetrating fluid and then to consider other factors which have been observed in laboratory and field experiments. Hydraulic fracture stress measurement procedure and theory have matured to the point where they are now used as the basis of evaluating new stress measurement techniques.

A typical hydraulic fracture stress measurement test in rock consists of injecting fluid (preferably similar to the pore fluid) at a constant rate in a section of borehole isolated by packers (Figure 2.1). Evenutally the fluid pressure rises to a level sufficient to cause fracture initiation, P_f (Figure 2.2). Additional injection is allowed to extend the planar fracture, at the propagation pressure, P_p, to a radial distance where the rock stresses are not affected by the borehole. After an adequate duration, the well is then shut-in (injection stops but the pressure is not released) and the transient pressure response during shut-in is monitored. Normally there is a characteristic

pressure at shut-in known as the instantaneous shut-in pressure, P_s(ISIP). The borehole pressure in the packed-off interval is monitored either downhole or at the surface and can be analyzed according to hydraulic fracture theory in order to calculate the in situ stresses. If test conditions permit it, the fracture orientation is measured downhole, thereby allowing calculation of the in situ stress orientations

2.2.1 Classic Theory

The analysis of hydraulic fracture theory first began with the work of Hubbert and Willis (1957). Refinements were added by a series of researchers (Scheidegger 1962; Dunlap 1963; Kehle 1964; and Fairhurst 1964) until Haimson and Fairhurst (1967) superceded this work with a theory which considered the implications of fluid flow from the borehole into the rock. However, the classic hydraulic fracture theory of the early 1960's remains a common method of analyzing hydraulic fracture test data and and many of its principles are basic to more recent hydraulic fracture theories.

The classic impermeable rock theory is comprised of the following assumptions:

1. Three unequal principal stresses (where $\sigma_v > \sigma_{hmax} > \sigma_{hmin}$), with one of them oriented vertically (parallel to the borehole axis) and the other two in a horizontal plane (Figure 2.3);
2. A smooth, circular, vertical borehole;
3. An isotropic, homogeneous linearly elastic rock; and
4. No fluid diffusion occurs and the pore pressure in the rock remains fixed at the initial pore pressure.

The physical model of a packed-off section of a borehole subjected to internal pressurization was replicated by combining the following two models:

1. A circular hole in an infinite plate subjected to a biaxial stress state under plane strain conditions as shown in Figure 2.4 (Kirsch's solution);
2. Internal pressurization of a thick walled cylinder.

Since the stress solutions to these two models are known, they can be superposed to derive the stress distribution around the borehole.

The stress distribution around the borehole suggests that the tangential stress $\sigma_{\theta\theta}$ will become tensile at two points (0^o and 180^o from the σ_{hmax} direction) around the borehole wall. When $\sigma_{\theta\theta}$ reaches the tensile strength of the rock (σ_t), vertical fracture initiation occurs at these two points. Since fluid pressurization does not induce tensile radial stresses (σ_{rr}) and no axial stresses (σ_{zz}) are induced by pressurization in a smooth borehole, no horizontal fractures are created.

Vertical fracture initiation occurs at the wellbore pressure P_f (in excess of the original pore pressure):

$$P_f - P_o = p_f = 3\sigma_{hmin} - \sigma_{hmax} + \sigma_t - 2P_o \quad \text{(total stresses)} \qquad [2.1]$$

$$P_f - P_o = p_f = 3\sigma'_{hmin} - \sigma'_{hmax} + \sigma_t \quad \text{(effective stresses)} \qquad [2.2]$$

where σ_{hmin} = minimum horizontal principal stress; σ_{hmax} = maximum horizontal principal stress; σ'_{hmin} = minimum horizontal principal effective stress; σ'_{hmax} = maximum horizontal principal effective stress; σ_t = rock tensile strength; and P_f, p_f and P_o are defined in Figure 2.2.

The vertical fracture extends in a plane perpendicular to σ_{hmin} in accordance with the principal of least work as injection is continued at the propagation pressure, P_p. When fluid injection stops upon shut-in, the fracture ceases propagating. An immediate pressure drop caused by the sudden cessation in viscous pressure losses at the fracture entrance leads to a stable equilibrium pressure. This equilibrium pressure reflects a combination of the stress acting normal to the fracture, pressure losses in the fracture and the extra pressure required to keep the fracture open. Assuming the latter two factors to be negligible, the minimum horizontal principal stress can be obtained from the relationship in terms of effective stress:

$$p_s \cong \sigma'_{hmin} \qquad [2.3]$$

and in terms of total stress:

$$P_s \cong \sigma_{hmin} \qquad [2.4]$$

Hubbert and Willis (1957) made some portentous comments in their initial study of hydraulic fracturing. Ordinarily, vertical fracturing would occur in a plane normal to minimum horizontal principal stress, but under special circumstances, horizontal fractures could be created. Horizontal fracturing may be recognized by a borehole pressure which exceeds the overburden weight (vertical stress). Such fractures are feasible only when sufficient axial stresses are induced during injection which may due to borehole irregularities or high packer pressures (Kehle 1964). Furthermore, their simplified analysis showed that fluid diffusion would result in a decreased fracture initiation pressure.

Dunlap (1963) recognized the potential of deriving in situ stresses from hydraulic fracture pressures. He developed equations for both horizontal and vertical fracture initiation and proposed that the propagation pressure was equivalent to the stress normal to the fracture plane. Dunlap argued that the initial in situ stress state controlled fracture behaviour.

Kehle (1964) reaffirmed Hubbert and Willis's analysis by using a different model to analyze the stress distribution created by borehole pressurization and packers. This was performed by using a band of uniform pressure to represent the borehole pressurization and two bands of uniform shear stress to represent the two rigid packers (Figure 2.5). His results showed that sufficient axial stresses were induced at the packers causing horizontal fracturing if $\sigma_{zz} = \sigma_t$. The concept of fracture reorientation was introduced for the case when the minimum principal stress assumed a different orientation away from the borehole. By virtue of the principal of least work, the fracture would then re-orientate once it had propagated beyond the borehole influence. He also argued that the shut-in pressure was approximately equal to the minimum principal stress, rather that the propagation pressure as suggested by Dunlap (1963).

Finally, Fairhurst (1964) concluded that hydraulic fracturing could be employed solely for the purpose of determining in situ stresses. By incorporating the analysis of prior researchers, Fairhurst presented formulae for calculating in situ stresses for tests in impermeable rock. He discussed some complications, such as inelastic deformations and anisotropic formations, which he recommended needed further study.

2.2.2 Haimson and Fairhurst's Theory

The next development in hydraulic fracture theory was re-analyzing the theory for the case of fluid diffusion from the borehole into the surrounding rock. Haimson and Fairhurst (1967) and Haimson (1968) proposed a theory which included the stresses induced by fluid diffusion. They argued that fluid injection would create a pressure difference between the borehole fluid pressure (P_w) and the formation fluid pressure (P_o) thereby causing an outward radial flow. However, this theory considers only the long-term steady-state fluid diffusion (fluid leakoff) problem and, therefore, does not consider any transient effects at the start of fluid diffusion. Consequently, the formation permeability is not required to calculate the induced stresses.

Their theory incorporated this phenomena by superposing the stresses created by radial fluid flow in the rock onto the stresses created by (i) the presence of a borehole in a non-hydrostatic stress field and (ii) by the internal pressurization of a borehole. Haimson (1968) observed that the stresses created by radial fluid flow were analagous to the stresses induced by heat conduction in solids. By adapting the solution for thermoelastic stress in a thick cylinder to the case of borehole fluid diffusion in the surrounding rock, Haimson and Fairhurst (1967) derived the following equations for vertical fracture initiation in terms of total stress:

$$P_f = \frac{\sigma_t + 3\sigma_{hmin} - \sigma_{hmax} - \alpha \frac{1-2\nu}{1-\nu} P_o}{K} \qquad [2.5]$$

and in terms of effective stress:

$$P_f - P_o = p_f = \frac{\sigma_t + 3\sigma'_{hmin} - \sigma'_{hmax}}{K} \qquad [2.6]$$

where p_f, σ_t, σ_{hmax}, σ_{hmin}, σ'_{hmax}, and σ'_{hmin} are as defined previously; and

$$K = 2 - \alpha\left(\frac{1 - 2\nu}{1 - \nu}\right) \qquad [2.7]$$

where $1 \leq K \leq 2$; and $\alpha = 1 - K/K_s$ with K_s = grain (solid) modulus, K = rock bulk modulus, and ν = Poisson's ratio of the rock.

In the formulation of this equation, Haimson and Fairhurst (1967) stated that for the case of nonporous rock, the stress component due to radial flow would be omitted. Haimson (1978) gave the limits of K as (i) $K = 1$ for impermeable rock, and (ii) $K = 2$ for either $\alpha = 0$ ($K = K_s$) or $\nu = 0.5$. He also advised that K and σ_t could be evaluated from a graph of p_f versus $(3\sigma_3 - \sigma_1)$ derived from laboratory experiments with applied loads.

The validity of equations (2.5 and 2.6) has since been tested experimentally. Haimson (1968) and Haimson and Fairhurst (1969), in hydraulic fracture tests conducted on permeable hydrostone samples (an absolute permeability of 11 md and a porosity of 26%), found relatively good agreement (± 10%) between the experimental and theoretical p_f (Figure 2.6). In both vertical and horizontal fracture cases, the Haimson and Fairhurst's equation for fluid diffusion conditions is a lower bound for p_f. Haimson also observed a dependence of p_f on pressurization rate (rate of borehole pressure change). In tests on "impermeable" Tennessee marble and hydrostone samples, p_f increased as pressurization rate increased. Haimson (1968) suggested two possible explanations: (i) rate dependency of σ_t; and (ii) small increases in pore pressure near the wellbore at high injection rates. According to Alexander (1983), Edl (1973) found Haimson and Fairhurst's equation to be applicable for rocks of both low and high porosity and rocks made relatively impervious at high confining stresses. Haimson and Edl

(1972), however, stated that experimental variations precluded a distinction between the classic and Haimson and Fairhurst equations.

Further developments have revealed the limitations of the Haimson and Fairhurst analysis. In an analysis of pressurization rate controlled experiments on unstressed sandstone samples, Zoback *et al.* (1977) concluded that Haimson's equation represents an upper limit of the effect of fluid diffusion. Examination of the equation reveals that it is time independent and makes no direct reference to the rock fluid flow properties. The pressurization rate dependency of p_f suggests that the time dependency of fluid diffusion cannot be dismissed. Consequently, other researchers have invoked poroelastic theory in the analysis of hydraulic fracturing (e.g. Rice and Cleary 1976 and Detournay and Cheng 1988). Furthermore, Nur and Byerlee (1971) suggested that Terzaghi's effective stress law, which was used in Haimson's analysis, may not be appropriate for inelastic processes, such as hydraulic fracturing. Additional research has been conducted in order to identify the limitations of Haimson's theory and to prepare more general treatments of hydraulic fracture theory.

2.2.3 Poroelastic Theory

Since the arrival of Haimson and Fairhurst's (1967) hydraulic fracture analysis, several researchers have identified the limitations of their fluid diffusion analysis. Poroelastic theory is an elastic theory developed for porous materials containing pore fluids. Primarily, it attempts to couple fluid diffusion with stress-deformation for the entire time scale of the associated responses in porous materials, that is, during excess pore pressure dissipation and during steady-state pressure conditions. A large portion of subsequent research has concentrated on the difficult task of fully incorporating the theory of poroelasticity in hydraulic fracture theory. Laboratory and theoretical studies have revealed the complexity of the coupled deformation-diffusion effects of poroelasticity evident in hydraulic fracturing.

Several investigations have revealed the pressurization rate dependency of p_f (Zoback *et al.* 1977; Bredehoeft *et al* 1976; Medlin and Masse 1979). In two series of hydraulic fracture laboratory tests, one with pressurization rate held constant and the other with flow rate held constant, Zoback *et al* (1977) found p_f to increase with pressurization rate, while it was independent of flow rate. Zoback et al. (1977) proposed that in the pressurization rate experiments, fracture initiation occurred at a pressure lower than the breakdown pressure p_f. The breakdown pressure is misleading because it is caused by unstable fracture propagation when the fluid pump is incapable of sustaining the borehole pressure. The direct relationship between p_f and pressurization rate is due to the increasing pressure losses in the fracture associated with the higher rates. For low porosity rock, which would be expected in deeper boreholes or in hard rock, the rate dependence of p_f is much less. Since the fracture intersects less pore space, the resulting fracture width is limited which causes higher fracture pressure losses regardless of the pressurization rate.

Medlin and Masse (1979) confirmed the findings of Zoback *et al.* (1977) through their laboratory hydraulic fracture initiation tests on limestone core. They also independently derived their own equations for predicting hydraulic fracture initiation for no-fluid diffusion and fluid diffusion conditions. More importantly, their hydraulic fracture experiments in spherical and cylindrical cavities for no-fluid diffusion conditions agreed with the classic equation. Although they independently arrived at Haimson and Fairhurst's equation, experiments under fluid diffusion conditions indicated a discrepancy with the Haimson and Fairhurst equation. This theory predicts both a reduction in intercept and slope in a p_f versus σ_{33} (confining stress) curve as shown in Figure 2.7, but the experimental results showed no slope reduction for low confining stresses. At high confining stresses the data for both the no-fluid diffusion and fluid diffusion conditions converge. At stresses beyond the elastic range, lower p_f values are associated with inelastic failure modes (Medlin and Masse 1979).

Rice and Cleary (1976) developed general solutions for deformation-fluid diffusion in fluid saturated porous elastic media based on Biot's treatment of poroelastic theory. Among the solutions was one for fracture initiation in a pressurized cylindrical cavity. This was the first time that the time dependency inherent in poroelasticity was considered in hydraulic fracture theory. Their analysis of the time dependency of fracture initiation clarified the role of pressurization rate on fluid diffusion and fracture initiation. Assuming zero confining stresses and tensile fracture failure criterion, Rice and Cleary (1976) proposed equations for fracture initation according to three degrees of fluid diffusion:

(1) negligible fluid diffusion (for $b^2 >> a^2$);

$$P_f \equiv \sigma_t \qquad [2.8]$$

(2) fluid diffusion to distance equivalent to the borehole radius, a (for $b^2 >> a^2$);

$$P_f \equiv \frac{\sigma_t}{2 - (1 - \eta)} \qquad [2.9]$$

(3) overall fluid diffusion to the outer boundary;

$$Pf \equiv \frac{\sigma_t}{\frac{\eta}{\log\{b/a\}} + 2(1 - \eta)} \qquad [2.10]$$

where $\eta = \left(1 - \frac{K}{K_s}\right)\left(\frac{1 - 2\nu}{2 - 2\nu}\right)$ and a = borehole radius and b = outer boundary radius of the poroelastic media. When non-hydrostatic in situ stresses replace the assumption of zero confining stresses, equation (2.8) becomes equivalent to the classic equation (2.2) while equation (2.9) can be shown to be equivalent to Haimson and Fairhurst's equation (2.5). They concluded that fracture initiation in boreholes is dependent on the duration of fluid pressurization prior to fracture initiation. Rice and Cleary's theoretical clarification of the rate dependency of fracture initiation explains the experimental results of

Zoback *et al.* (1977), but fails to explain the inadequacy of equations (2.5) and (2.9) for matching Medlin and Masse's (1979) experimental results.

Lockner and Byerlee (1977) suggested a deviation from hydraulic fracture theory that had not been considered at that time: the possibility of shear failure. They inferred from their laboratory results that shear failure, rather than tensile failure, may occur at low injection rates resulting in lower breakdown pressures. They suggested that the pore pressure distribution induced by fluid injection controlled the failure mode. This was attributed to injection rate affecting the permeability, deviatoric stress ($\sigma_{hmax} - \sigma_{hmin}$) and the effective stress around the borehole, which all, in turn, influence the pore pressure distribution. At lower rates, the pore pressure increased around the borehole, reducing the effective stress until shear failure occurred. At higher rates, the samples failed in tension at higher pressures. The possibility of shear failure is critical because it would invalidate the classic and Haimson analysis of fracture initiation by contradicting the assumption of tensile failure. The possibility of shear failure is discussed in more detail in section 2.3.2.

The effect of fluid diffusion on hydraulic fracture initiation was summarized by Alexander (1983). He concluded that the Haimson and Fairhurst equation, being valid for a wider range of tests, gave no greater error than the classic equation for no-fluid diffusion conditions. The relationship between pressurization rate and breakdown pressure was reviewed in terms of the development of (1) the poroelastic compression and (2) pore pressure reduction of the effective tensile strength. Although these two effects develop at different rates, they are both dependent on the pressurization rate. In an argument similar to that of Rice and Cleary (1976), Alexander stated that Haimson and Fairhurst's equation is valid when the pressurization rate is low enough to allow the adequate development of (i) the poroelastic compression to the required radius and (ii) the pressurization of wellbore micro-cracks to the borehole pressure (effectively reducing the formation tensile strength σ_t). Higher pressurization rates would allow the poroelastic compression to develop, but preclude the necessary pressurization

of the micro cracks resulting in breakdown pressures exceeding predictions of both the classic and Haimson and Fairhurst equations. Only at extremely high rates would both effects be prevented from occurring, thereby providing the appropriate conditions for the classic equation.

Calculations by Rice and Cleary (1976) indicated that for most rock-fluid combinations, the coefficient of consolidation [$c_v = \frac{k^*}{\gamma_w m_v}$] where k^* is the hydraulic conductivity, γ_w is the unit weight of water and m_v is the coefficient of volume change] value would not be low enough for the classic equation to be acceptable for field pressurization rates. Although poroelastic theory suggests that the effect of fluid diffusion is not negligible, laboratory tests suggest that, for most tests, there would be no significant error in stress calculations when using the classic equation. In comparison with the uncertainity associated with determining the in situ rock properties necessary for poroelastic calculations, the error associated with the classic equation is not critical. It should be recalled that Haimson emphasized that hydraulic fracture method only provides an estimate of the in situ stresses.

Building on his previous work in poroelasticity, Cleary (1979) discussed the poroelastic aspects of the period between the drilling of the borehole and fluid injection. He argued that, in an isotropic material, once the borehole has been drilled and contains drilling fluid, two pore pressure redistributions are evident if allowed sufficient time to develop. The most rapid pore pressure redistribution is caused by the flow of fluid from the most highly compressed region around the borehole, due to the stress concentration abound the borehole, to areas of lower pore pressure. Once this pore pressure redistribution is complete, the near wellbore material exhibits a drained elastic behaviour characteristic of the original isotropic idealization. The second pore pressure redistribution is analagous to Haimson and Fairhurst's (1967) treatment of fluid diffusion. The difference between the drilling fluid pressure and the in situ pore fluid pressure causes fluid flow towards the borehole so that the near wellbore pressure equalizes with the borehole pressure. If this second pore pressure redistribution overlaps with borehole pressurization, the near wellbore stresses will be increased from the originial

stress concentration because of the decrease in pore pressure. Cleary (1979) suggests that these two pore pressure responses will result in a time dependent stress distribution around the borehole with implications for hydraulic fracture initiation.

Detournay *et al.* (1987), Detournay *et al.* (1988), and Detournay and Cheng (1988) further clarified the poroelastic effects of borehole pressurization in an hydraulic fracture initiation analysis based on Rice and Cleary's (1976) analysis. Detournay and Cheng (1988) summarized the poroelastic effects as (i) the induced pore pressure associated with externally applied loads (as measured by pore pressure parameter B), (ii) the dissipation of this excess pore pressure according to a diffusion law, (iii) the bulk volumetric deformation caused by the change in effective stress and (iv) the pore pressure gradient which acts as a body or seepage force.

Their model divides the mechanism of borehole pressurization in a non-hydrostatic stress field in poroelastic material into three loading components: (i) a far-field isotropic stress; (ii) an initial pore pressure; and (iii) a far-field deviatoric stress. While the first loading component can be reduced to an elastic solution independent of time, the other two components are time dependent. However, these solutions depend on whether the mechanical properties of the porous media allow the development of the poroelastic effects. Detournay and Cheng's analysis places Haimson and Fairhurst's analysis in the context of poroelastic theory and provides insight into when poroelastic effects become an important consideration.

Detournay and Cheng (1988) stated that poroelastic theory should be considered when a substantial difference exists between the drained and undrained mechanical properties, that is, in terms of the drained and undrained bulk modulus, K and K_u, where $K_u >> K^2$. Detournay *et al.* (1988) stated that:

$$K_u = \frac{K}{1 - \alpha B} \qquad [2.11]$$

where $\alpha = 1 - K/K_s$, K_s being the solid bulk modulus, and the Skempton pore pressure coefficient $B = \frac{1}{1 + n\,(K/K_f)}$ where K_f is the pore fluid bulk modulus and n is the porosity. For complete poroelastic effects to occur, that is, the second and third loading components to be non-zero, both α and B must be greater than zero. In the first case, $\alpha \rightarrow 0$ as the drained bulk modulus approaches the grain bulk modulus, thereby implying that the rock porosity also approaches zero. In the second case, if $K_f \rightarrow 0$, as it becomes an infinitely compressible fluid, then $B = 0$ and no excess pore fluid pressure is generated.

For the latter case, where no excess pore pressure is induced, the interaction between pore fluid pressure and stress becomes uncoupled as the pore pressure interacts with the solid as a body force through Biot's coefficient α. This case is identical to Haimson and Fairhurst's treatment of fluid diffusion during hydraulic fracturing. Haimson and Fairhurst's analysis can be interpreted as steady-state fluid diffusion analysis. When it is apparent that $B > 0$ and there is an initial transient pore pressure response, Detournay and Cheng's poroelastic theory should be used because of its complete treatment of the coupling between induced pore pressure (diffusion) and stress (deformation).

The influence of the transient pore pressure response and the role of the formation permeability is indicated by the effect of the deviatoric stress component's solution on short and long term stress solutions around the borehole. The long-time deviatoric stress solution around the borehole is for steady-state fluid flow conditions and is equivalent to Haimson and Fairhurst's (1967) analysis. However, for typical rock properties, they found that the short-time transient poroelastic effects occurred at a normalized time, $t^* = ct/a^2 < 10^{-2}$, where c is a generalized consolidation coefficient,

$$c = \frac{2\,k/\mu\; B^2\, G(1 - \nu)(1 + \nu_u)^2}{9(1 - \nu_u)(\nu_u - \nu)} \qquad [2.12]$$

t is time, a is the borehole radius, k is the absolute permeability, μ is the pore fluid dynamic viscosity, G is the modulus of shear deformation, and ν_u is the

undrained Poissons ratio. These transient poroelastic effects result in a tangential stress at the borehole wall of:

$$\sigma_{\theta\theta} = -4[(1 - \nu_u)(1 - \nu)][1/2(\sigma_{hmax} - \sigma_{hmin})] \cos 2\theta. \qquad [2.13]$$

Meanwhile the elastic tangential stress is $\sigma_{\theta\theta} = -[1 + 3a^4/r^4][1/2(\sigma_{hmax} - \sigma_{hmin})] \cos 2\theta$, which is valid for $r > a$. After the transient poroelastic effects have dissipated at approximately at $t^*=1$, the tangential stress concentration at the borehole wall increases to the long-time elastic value.

Comparison of these two tangential stress solutions shows the importance of considering initial transient pore pressure effects. For the borehole case, the maximum tangential stress does not necessarily occur at the borehole wall, but possibly away from it inside the porous material. Detournay and Cheng (1988) extended these findings to propose that immediately after borehole pressurization, the short time tangential stress solution may result in shear failure inside the rock prior to tensile fracturing. This hypothesis has implications for wellbore stability (prior to the fluid injection period of hydraulic fracturing) and the failure mode associated with hydraulic fracturing, both of which are discussed in section 2.3.

The complete short-time solutions of the stresses near a borehole for both the mode 1 and 2 loading components are given in an appendix in Detournay and Cheng (1988). The solutions are the result of an analytical inversion of the expansion of the Laplace transform solution of the field equations. The generalized consolidation coefficient c and, thus, the permeability are components of the complete short-time solutions. Therefore, the permeability is important not only in calculating the transient undrained (short-time) stresses around a borehole, but also in evaluating whether a particular problem should consider the short-time transient poroelastic effects.

Fracture mechanics theory was invoked by Cleary (1979) to explain the smooth transitions in time dependency of fracture initiation pressure among the three time frames observed in the poroelastic theory of hydraulic fracture

(which Haimson and Fairhurst's (1967) theory failed to do). Cleary was convinced that the poroelastic nature of hydraulic fracture initiation could be adequately explained only by the propagation of pre-existing micro-cracks or flaws in the material around the borehole. Three fracture mechanics models were proposed by Cleary (1979) in order to explain the time dependency of fracture initiation in hydraulic fracturing: (a) healed crack for high pressurization rates, (b) transmissive open flaw, modeled by fluid flow in a crack, representing lower injection rates, and (c) micro-crack linking mechanisms (where no pre-existing macro cracks can be found). It appears that the classic and Haimson and Fairhurst theories of hydraulic fracture initiation, which are based on the continuum approach to geologic materials, have been replaced by fracture mechanics theory because the latter better predicts poroelastic effects in hydraulic fracturing. Fracture mechanics theory is discussed in more detail in section 2.3.2.1.

In response to the limitations of the classic and the Haimson and Fairhurst theories of hydraulic fracture initiation, researchers and practitioners have proposed measures that avoid using some of the more troublesome restrictions of these theories. Bredehoeft *et al.* (1976) recommended using the secondary breakdown pressure, P_r (also known as the refracturing pressure) instead of the initial breakdown pressure (i.e., the first cycle fracture initiation pressure) because it avoids the problem of using laboratory measured values of rock tensile strength. Cornet and Valette (1984) proposed an alternate hydraulic fracture stress measurement technique which does not use the fracture initiation pressure and is more general in its assumptions of the hydraulic fracture behaviour. Their technique is based on the pressurization of boreholes which either initiates new fractures or propagates pre-existing fractures with the instantaneous shut-in pressure representing the normal stress acting on the fracture plane. Depending on the assumptions made in the tests, a number of tests are necessary to measure the complete stress tensor. This method, however, greatly increases the cost of the operation.

Despite the limitations of hydraulic fracture stress measurement theories, this method has been used extensively around the world in a variety of applications. A large quantity of field test evidence supports the validity of the hydraulic fracture stress measurement method and it has now become a common stress measurement method.

2.2.4 Field Test Verification

By the early 1970's the validity of the hydraulic fracture stress measurement theory had been established in laboratory tests (Haimson 1968; Haimson and Fairhurst 1970; Edl 1973; Komar and Frohne 1973) and in a limited number of field tests (Von Schonfeldt 1970; Roegiers 1974; Haimson 1975). The next step in the evaluation of the hydraulic fracture stress measurement theory was full scale field testing in regions of known in situ stress, however, there are some problems with this approach. Knowledge of the in situ stress for a particular region is obtained either directly through measurements based on proven methods or indirectly through appropriate analytical (or numerical) models. Confidence in the stress measurements is usually assessed by a comparison among various stress measurement techniques used in the region. Most of the evidence supporting hydraulic fracture stress measurement theory is based on this approach. The larger the in situ stress measurement data base, the greater the confidence in the data.

In general, stress measurement methods used in geotechnical engineering, such as overcoring methods and borehole deformation gauges, are restricted to areas accessible through shafts or tunnels. While most in situ stress data is for shallow depths (e.g., < 500 m), one of the advantages of the hydraulic fracture method is its capability of measurements at great depths (e.g. > 5000 m). Since there is a large number of shallow-depth in situ stress measurements, the best evaluation of hydraulic fracture stress measurements involve comparisons for shallow-depth stress measurements (e.g., comparison of overcoring and hydraulic fracture stress measurements by Haimson 1981). The evaluation of deep hydraulic fracture stress measurements must resort to

comparison with indirect stress measurement techniques. These techniques include borehole breakouts, earthquake focal mechanism solutions and surface and subsurface fracture studies. Evidence supporting hydraulic fracturing stress measurement theory is drawn from field studies in reservoir engineering, underground excavation design, crustal stress and seismic investigations.

The best verification approach is a comparison of established stress measurement techniques and the hydraulic fracture technique in regions where both have been extensively used. Haimson (1978) summarized hydraulic fracture tests conducted at a variety of projects, including earthquake studies, underground power stations, hard rock tunnels and plate tectonics research. The results at the Nevada Test Site showed fair agreement between the hydraulic fracture measurements and the borehole deformation and seismic investigation measurements. The underground powerhouse investigation revealed a close agreement between the calculated vertical (overburden) stress and the stress inferred from horizontal hydraulic fracture tests. In a survey of six case histories where overcoring results were compared with hydraulic fracturing results, Haimson (1981) concluded that there was good agreement among the stress results. In particular, both gave the same relative stress magnitudes (i.e., $\sigma_v > \sigma_{hmax} > \sigma_{hmin}$) and the inclination of the principal axes as determined by the overcoring measurements were within 30^o of the hydraulic fracture axes (i.e., vertical and horizontal). Figure 2.8 presents a comparison of the hydraulic fracture and overcoring stress data for various sites discussed by Haimson (1981). The differences in the σ_{hmax} values ranged up to 100%, but Haimson (1981) suggested that the overcoring stress magnitudes were overestimated because laboratory determined rock deformation moduli were used rather than field values. Further comparisons were provided by Haimson (1983, 1984) for the Nevada Test Site. Haimson's conclusion was that "...the hydrofracturing technique yielded reliable, repeatable and accurate results which underwent rigorous verification by use of other methods and independently run hydrofracturing."

Similar studies have been performed in Sweden and China. Doe *et. al.* (1983) compared hydraulic fracture measurements with four other methods, the Luleä triaxial gauge, the CSIRO gauge, the Swedish State Power Board - Leeman triaxial gauge and the USBM deformation gauge, at the Stripa Mine. The correspondence for the σ_{hmax} orientation was excellent, but the horizontal stress magnitudes were less agreeable which may be attributed to the limited number of tests run. Overall the measurements of horizontal stress magnitude and orientation were consistent. Li Fang-Quan *et al.* (1983) reported the results of overcoring and hydraulic fracture stress tests for five regions in China. There was very good agreement among the σ_{hmin} magnitudes, but a poor correlation for horizontal stress orientation.

Another verification method is comprised of comparisons between hydraulic fracture stress data with indirect in situ stress indicators. Bredehoeft *et al.* (1976) observed a parallel trend between hydraulic fracture orientation and surface fracture pattern trends and normal fault trends. Lindner and Halpern (1978) and McGarr and Gay (1978) both prepared stress compilations for different areas which incorporated hydraulic fracture stress measurement data, thereby implying the acceptance of the hydraulic fracture method. Gay (1980) observed in his compilation an agreement between σ_v derived from hydraulic fracture data and the calculated overburden values within ± 20%. Haimson and Voight (1977) reported the concurrence between overcoring and hydraulic stress measurement results. However, these were both substantially different from the earthquake focal mechanism solutions.

Although stress measurement data has been reported for depths down to 5100 m and stress magnitudes up to 150 MPa, Hast (1979) reasoned that stress measurements may be limited to depths less than 1200 m and stresses less than 150 MPa. Only very strong and competent rock would be capable of withstanding the shear stresses generated by the stress concentration around the borehole. Pre-fractured rock would violate the assumptions used in hydraulic fracture theory. In fact, shear failure around boreholes has been postulated as a mechanism responsible for borehole breakouts.

Wellbore breakouts should be noted here because they have been proposed as a further technique for estimating in situ stress orientation (Bell and Gough 1983). Bell and Gough suggested that the wellbore stress concentration results in borehole shearing and spalling in the region of the highest compressive stress. Subsequent research (Hickman *et al.* 1985) has revealed a good correspondence between the azimuth of the maximum horizontal compression derived from study of wellbore breakouts and the σ_{hmax} orientation derived from hydraulic fracturing. Although the phenomena of wellbore breakouts provides further information regarding the stress orientations, it also prevents hydraulic fracturing tests from being conducted in zones in which it occurs.

Progress in other stress measurement techniques, such as differential strain curve analysis (DSCA) and the inelastic strain recovery method, has led to further stress data. In the 1980's the hydraulic fracture stress measurement technique has been widely adopted because of the mounting data supporting it. For many researchers and practitioners, this is the only viable method for in situ stress determination and,subsequently, it has become a standard for other stress measurement techiques. For example, Teufel (1985) evaluated stress measurements obtained from the inelastic strain recovery method and observed them to be "...not as reliable in comparison to hydraulic fracture stress measurements."

2.3 Further Developments

Successive hydraulic fracture field tests have proven the validity of hydraulic fracture stress measurements. It is now a widely accepted technique for shallow and deep borehole stress measurements in rock (but it remains largely ignored for soil stress measurement studies). As a result of these tests, and the additional laboratory and analytical research, the limitations of the techique have become well known. These limitations are the violation of the assumptions on which hydraulic fracture theories are predicated and they occur because of unanticipated underground conditions and variations in test

procedure. In some cases the limitations are not too restrictive or can be adequately handled by simplified analyses, while in other cases the limitations may invalidate hydraulic fracturing for in situ stress measurement.

The factors and conditions which limit the validity of theory are discussed in the following categories in section 2.3.1 Complications in Hydraulic Fracture Behaviour: (i) borehole condition; (ii) in situ stress orientation; (iii) geologic structure; (iv) material behaviour; and (v) packers.

Many researchers have argued that borehole pressurization results in failure modes other than tensile failure. Due to pervasive nature of pre-existing flaws and micro-cracks in geologic materials, fracture mechanics theory has been used to predict the propagation of these flaws during fluid injection Alternatively, shear failure, occuring in either localized brittle rupture or ductile rupture modes, and rock creep are other failure modes that have been proposed to explain unusual behaviour. Such behaviour totally violates hydraulic fracture theory and, therefore, is treated separately in section 2.3.2 Alternate Failure Mechanisms.

2.3.1 Complications in Hydraulic Fracture Behaviour

2.3.1.1 Wellbore Condition

Hydraulic fracture theory assumes that a smooth, circular open borehole penetrates the rock formation. In many boreholes, however, a combination of high in situ stresses and low rock strength may lead to borehole instability. This is normally remedied by borehole casing which is common in the petroleum industry. Access to the rock is through perforations created by explosive charges or casing guns (King 1987). The presence of the casing and the cement job, and the effect of the perforations all have an unquantified effect on hydraulic fracture tests conducted in cased wells.

The effect of casing on hydraulic fracture stress measurements was first studied by Daneshy (1973). His laboratory hydraulic fracture tests showed that the breakdown pressure was affected by the casing. More specifically,

breakdown pressure was a function of the number of perforations and their spatial arrangement (perforation pattern). Fracture initiation occurred at the perforations and the fracture propagated normal to the minimum horizontal principal stress. Horizontal fracture initiation at the borehole was uncommon, but when the vertical stress was the minimum principal stress, vertical fractures initiated at the borehole would gradually rotate in order to become horizontal (i.e., normal to σ_3) as dictated by the prevailing stress conditions.

Warpinski (1983) studied the reliability of hydraulic fracture tests performed in perforated, cased boreholes for in situ stress determination in mineback experiments. A typical hydraulic fracturing downhole tool arrangement for perforated cased boreholes is shown in Figure 2.9. Breakdown pressure was found to be dependent on the casing, cement annulus, the explosive perforation damage, and the perforation pattern. These effects cannot be quantified, therefore, breakdown pressure can no longer be used to calculate σ_{hmax}. Fortunately, his study showed that σ_{hmin} can still be determined from cased borehole test. From his data, Warpinski concluded that if the difference between injection pressure (i.e., propagation pressure), and shut-in pressure exceeded 3500 kPa, the σ_{hmin} value was probably unreliable. The mineback experiments revealed that fractures usually began at the perforations and sometimes occurred as multiple, parallel fractures.

Wellbore stability has undergone intense scrutiny in the petroleum industry because of its potential detrimental effects on production. Cheatham (1984) has reviewed the problem from the petroleum industry's perspective. One of the potential sources of wellbore instability is failure in compression (i.e., shear yield). As discussed in section 2.2.4, shear failure has been proposed to explain wellbore breakouts which result in elliptical wellbores. Attempts have been made to develop this shear failure theory in order to predict in situ stress magnitudes and directions (e.g., Bell and Gough 1979; Zoback *et al.* 1985). Recent developments in the application of poroelastic theory by Detournay and Cheng (1988) have revealed the possibility of shear failure associated with previously unexpected poroelastic effects on the stresses induced around the wellbore. Obviously theories concerning wellbore

stability must be investigated to check the integrity of the wellbore prior to hydraulic fracture tests. Such an analysis for oil sands is conducted in chapter 3.

In summary, open boreholes are subject to various distortional processes manifesting themselves in borehole spalling, breakouts, and sand influx which violate the assumption of perfectly smooth, circular boreholes in hydraulic fracture theory. Ususally caliper logs, if not borehole televiewer logs, are run prior to hydraulic fracture tests in order to avoid damaged borehole zones. Unfortunately such precautions are not always viable or effective. Fracture mechanics theory suggests that many materials are characterized by small microscopic flaws or cracks which affect the stress-deformation behaviour of these materials. Many researchers have recognized that geologic materials cannot really be considered homogeneous, isotropic materials, and therefore, have attempted to apply fracture mechanics theory in order to predict hydraulic fracture initiation. Under certain conditions, it may be possible to assume borehole defects and attempt to analyze hydraulic fracture initiation for these conditions based on fracture mechanics theory. This lies beyond the scope of this section and will be discussed in section 2.3.2.1.

2.3.1.2 Stress Orientation

The hydraulic fracture theories discussed in section 2.2 assume that the in situ stresses are oriented such that one of the principal stresses is aligned parallel to the vertical borehole axis with the remaining two principal stresses in a horizontal plane normal to the borehole axis. This assumption is thought to be valid for flat lying areas unaffected by local geologic structures, such as buried valleys or igneous dikes. Although this assumption has been criticized, it greatly simplifies the theory and practice of hydraulic fracture tests and, therefore, is hard to resist. In situ stress comparisons with other stress measurements which do not involve this assumption have often confirmed its validity. For example, Gay's (1980) collection of stress data showed a ± 20%

agreement between the vertical stress calculated from hydraulic fracture data and the overburden stress based on weight. However, in more general treatments of hydraulic fracture stress measurement theory, some researchers have elected not to use this assumption.

Pine *et al.* (1983) adjusted hydraulic fracture theory to account for inclined boreholes. Boreholes which deviate from the vertical are not uncommon and so this development is useful.

Cornet and Valette (1984), as noted earlier, developed a general hydraulic fracture stress measurement theory based on the measurement of the normal stress supported by pre-existing fractures intersecting the borehole. In the case where there are no assumptions made about the in situ stresses, twelve unknowns, the six components of in situ stress tensor and their orientation, are involved requiring six hydraulic fracture tests where the reopening pressures and normal stresses are measured. The number of unknowns and number of required tests are reduced when assumptions about the vertical stress are made.

Kuriyagawa *et al.* (1985) also developed a more general stress measurement theory. They did not assume any principal stress to be aligned with the borehole axis. Under such conditions, their test procedure required hydraulic fracture tests in three non-colinear boreholes in order that the complete in situ stress tensor be determined.

Warren (1983) recommended using a spherically shaped cavity because this shape does not require an assumption regarding the principal stress orientations. Since the spherical cavity has no preferred orientation, Warren's theoretical analysis shows fracture initiation occuring along a diametric plane normal to σ_3. The test procedure and analysis are similar to the classic hydraulic fracture method.

Studies have shown that the assumption of a principal stress aligned with the vertical axis and equivalent to the overburden stress is acceptable in areas or depths of simple geologic structure. In potential test areas where such an assumption is thought to be unreasonable, the other hydraulic

fracture theories may be applicable. However, such tests usually involve more complicated testing procedures and theories containing more unknowns.

2.3.1.3 Geologic Structure

Underground rock masses are routinely intersected by geologic discontinuities, such as jointing, bedding and faulting. Although attempts are made to select borehole zones for hydraulic fracture tests that are relatively homogeneous and isotropic, the propagating fracture may intercept a geologic discontinuity away from the borehole. In the petroleum industry it is crucial that controlled, massive hydraulic fracture operations result in improved petroleum recovery. This requires adequate predictions of hydraulic fracture behaviour in reserviors that are normally characterized by numerous geologic discontinuities (Nelson 1986). Most importantly the large hydraulic fracture must be contained within the payzone.

Teufel and Warpinski (1987) state that geologic discontinuities will affect these large volume fracture treatments in oil recovery schemes by (i) arresting vertical fracture growth in layered formations, (ii) by eventually limiting fracture propagation through fracture propagation into zones, demarcated by faults, or of higher in situ stress, or (iii) by limiting fracture length through increased fluid leakoff. The implications for small volume hydraulic fracture stress measurement tests are not as clear, but there are definite effects on the interpretation of in situ stress.

The bulk of the research conducted into investigating the role of geologic discontinuities has arisen from fracture containment studies. Various investigators (Simonsen *et al.* 1978; Teufel 1979; Warpinski *et al.* 1982; Teufel and Warpinski 1983; Teufel and Clark 1984) have conducted laboratory, theoretical and mineback studies of the factors controlling vertical fracture containment in layered rock. Bedding contrasts in the minimum principal stress have been reported to be the dominant factor controlling fracture containment, while contrasting material properties and the presence of unbonded or weak interfaces are thought to be of lesser importance. Teufel

and Warpinski (1983) proved the dominance of in situ stress as a control in fracture containment in mineback observations. Fractures were stopped at interfaces when approaching zones of higher σ_{hmin} (as determined from hydraulic fracturing and overcoring). They concluded that "...an evaluation of the economic success of potential fracture treatments, prior to stimulation, can be made by determining the in situ stress state in the reservoir-fracture interval as well as in the bounding layers."

In addition to stress contrasts, the weak interfacial shear strength of bedding layers can also inhibit/contain vertical growth of hydraulic fractures (Teufel and Clark 1984). Laboratory tests showed that an interfacial layer of low shear strength, through either low normal stress or low tensile strength, can inhibit vertical fracture growth. They concluded that in situ stress contrasts proved to be more effective in fracture confinement at greater depths while the interfacial shear strength was more important for shallow depths. The influence of the mechanical properties of the rock are important not in their ability to prevent fracture growth, but in their role in the distribution of in situ stress.

Teufel and Warpinski (1987) summarized experimental and mineback observations of the effect of geologic discontinuities on large volume hydraulic fractures. Among their mineback results, they observed that fractures propagating into rock masses characterized by frequent geologic discontinuities could be better described as zones of multiple fracturing. Faults either acted as barriers or caused changes in fracture direction, while bedding planes, through a combination of increased stresses and low interfacial shear strength, prevented further propagation. Their laboratory tests on the effect of pre-existing joints on fracture propagation showed that fracture arrest occurred by shear slippage along the joint at high differential stress ($\sigma_{hmax} - \sigma_{hmin}$) and small angles of approach. Fractures did not cross the joints under other conditions because the there was sufficient fluid pressure in the fracture to open the fracture and divert flow along the joints.

Any attempt to analyze the interaction of hydraulic fractures and geologic discontinuities is difficult because it would have to consider all of the

following parameters: permeability of the joints, etc.; rock frictional properties; in situ stress state (deviatoric stresses, $(\sigma_1 - \sigma_3)$ and normal stresses, σ_{ii}); joint spacing and orientation with respect to the stress state; treatment pressure; and fluid viscosity. Teufel and Warpinski (1987) performed a simplified analysis of the effect of some of these factors on fractures intersecting pre-existing joints. It considered the effect of permeability on leakoff, the effect of leakoff on the stress state, shear slippage along the joint, and the changes in the in situ stress state due to the presence of the hydraulic fracture.

What effect geologic discontinuities will have upon the interpretation of hydraulic fracture in situ stress test results is unclear. McLennan and Roegiers (1982, 1983) have identified several factors which can alter the pressure versus time response of stress tests and make it difficult to derive the in situ stresses. A more detailed discussion will follow in chapter 4, but some immediate observations can be made. Basically there are concerns that geologic discontinuities can lead to increased leakoff and the creation of multiple fractures. McLennan (1980) noted that pre-existing discontinuities resulted in an indefinite breakdown pressure and unusual pressure-time curves that lead to erroneous in situ stresses calculations.

Some laboratory research has been performed on the problem of creating hydraulic fractures unaffected by the presence of geologic discontinuities (Haimson and Avasthi 1975; Avasthi 1980; Zoback *et al.* 1977). Haimson and Avasthi (1975) observed that fracture orientation was a function of the foliation orientation in extremely foliated gneiss. When boreholes were lined in order to prevent fluid penetration into the foliated gneiss, fracture orientation became independent of foliation and was normal to σ_3. Zoback *et al.* (1977) stated that lined boreholes were impractical for actual field tests. They suggested using viscous drilling mud in inducing hydraulic fractures in fractured rock. At low injection rates, a new hydraulically induced fracture was created normal to σ_3 while the pre-existing fractures remained closed and did not propagate.

Prospective test zones characterized by geologic discontinuities should be avoided. However, this may not always be possible. These cases will require test procedures minimizing the effect of the geologic discontinuities and possible special interpretation methods. The role of geologic discontinuties in hydraulic fracture stress intrepretation and measures to account for their effects on stress results are included in the analysis in chapter 4.

2.3.1.4 Material Behaviour

Any geomechanics theory which employs the theory of linear elasticity is immediately restrained by the fact that geologic materials approaching failure usually cannot be considered to be linear elastic. Additionally the assumptions of homogenity and isotropy of the mechanical behaviour of geologic materials are also suspect. Except for hydraulic fracture initiation theory for plastically strained materials as outlined in section 2.3.2.3, every hydraulic fracture theory assumes linear elasticity until fracture initiation. The previous discussion on geologic structure outlines some of the concerns with the assumption of material homogeneity. Further study has been reported on the role of anisotropic behaviour.

Komar and Frohne (1973) studied the directional nature of sonic velocities (compression and shear), dynamic elastic constants, permeability and tensile strength of sandstone. They concluded that the directional properties were related to the σ_{hmax} since both are a result of the diagensis of the sand deposit and the imposed post consolidation stress.

Cleary (1979) proposed a general hydraulic fracture initiation equation (for vertical fracture through tensile failure) which incorporated the effect of anisotropic material properties on the stress distribution around a borehole:

$$\sigma'_{\theta\theta} = \sigma_t = \alpha_3 p_f - \alpha_4 p_o - \alpha_1 \sigma'_{hmin} + \alpha_2 \sigma'_{hmax} \qquad [2.14]$$

where $\alpha_1 = 3$ and $\alpha_2 = \alpha_3 = 1$ for linear elastic isotropic homogenous material and $\alpha_4 = 1$ for effective stress and impermeable rock. This equation is identical with the classic equation [2.2] for non-fluid diffusion conditions. However,

Cleary (1979) suggested that these factors deviated from their classical values for conditions leading to material yielding and stress transfer.

Logan (1983) even suggested that the rock fabric was the controlling factor in hydraulic fracture initiation direction. Based on a study of the directional properties of core, induced fracture (i.e., point load test, Brazilian tests and compression tests) and fabric (grain axes), Logan compared the orientation of hydraulic fractures. He concluded that the results "...clearly demonstrate the correspondence of the rock fabric and the orientation of induced hydraulic fracture...." In situ stress only appears to control fracture orientation in relation to the correspondence between fabric and the maximum compressive stress in relatively simple tectonically stressed areas. His radical conclusion is that hydraulic fracture stress measurement theory is valid only if the strain relaxation coincides with the current stress field, otherwise, the fractures only reflect the fabric's directional properties.

2.3.1.5 Packers

In order to pressurize a particular interval of open borehole, packers are required to isolate the proposed test section. Several studies have been conducted in order to study the effect of the packers on the stresses near the wellbore.

Haimson and Fairhurst (1970) reasoned that Kehle's (1964) model of the packers as a rigid assembly was not accurate for inflatable rubber packers. Kehle's analysis showed that induced axial stresses (σ_{zz}) occurred at the packers (Figure 2.5), thus allowing the possibility of horizontal fractures at the packers. Rubber packers do not meet Kehle's criteria because they act as a "liquid-solid elastomer" (Haimson 1968). Upon inflation these packers apply a radial load to the rock, but the axial stresses at the packers are reduced, as compared with rigid packers, and no horizontal fractures can occur. Laboratory experiments confirmed that no horizontal fractures were initiated under these conditions.

Roegiers (1974) conducted a finite element analysis of rigid and rubber packers which confirmed Haimson and Fairhurst's (1970) results. As packer flexibility increases, the axial stress becomes reduced, precluding the development of horizontal fractures due to packers. A steel mandril connecting the two packers further decreases the axial stresses and it also shifts the position of maximum tangential stress away from the packer towards the center of the interval. Roegiers concluded that it was important to consider the packer properties, but their influence was limited to fracture initiation.

The effect of the difference between packer pressure and fracture initiation pressure ($P_{pk} - P_f$) on the induced wellbore stresses was investigated by Warren (1981). When this effect becomes significant it can affect the determination of σ_{hmax}. Analysis of the axial and tangential stresses created by the packer's normal pressure, which was neglected in Kehle's (1964) analysis, reveals the tensile nature of both these stresses in the pressurized region of the borehole. His analysis shows that the breakdown pressure is lower than that predicted by the classic analysis.

Warren also suggested that the shut-in pressure may also be affected by the packer induced stresses. He explained that the induced stresses can alter the fracture angle at the borehole, therefore, closure of the fracture at the wellbore would then occur at a higher pressure than that required to keep the fracture open. Fracture initiation at or near the packers is an indication of the influence of the packer stresses. This could provide a means of assessing the quality of the stress results once the fracture location was determined after completion of the test.

2.3.2 Alternate Failure Mechanisms

2.3.2.1 Fracture Mechanics

The theory of fracture mechanics began with the pioneering work of Griffith who attempted to explain the discrepancy between the theoretical

tensile strength of materials and the laboratory tensile strength. In essence his theory was based on the existence of pre-existing micro-cracks or flaws which developed stress concentrations near their tips resulting in localized failure even though the applied loads were below the classical failure criteria. Fifty years later, Abou-Sayed *et al.* (1978) developed a hydraulic fracture initiation theory based on linear elastic fracture mechanics in order to account for the existence of pre-existing natural fractures which negated the classic hydraulic fracture theory. A good introduction to fracture mechanics can be found in Lawn and Wilshaw (1975) while its application to geomechanics problems, including hydraulic fracturing, is given by Atkinson (1987). Linear elastic fracture mechanics explains some of the breakdown pressure anomalies observed in laboratory hydraulic fracture experiments.

Problems with pre-existing flaws were noted by Haimson (1968) in his laboratory experiments in hydraulic fracturing. He suggested that these flaws affected the determination of the tensile strength, which is dependent on the sample size and shape, loading rate and test method. In order to replicate the hydraulic fracturing stress path, he determined tensile strength from hydraulic fracture tests on unconfined specimens. Haimson found that as the pressurization rate increased, breakdown pressure decreased which he believed to indicate the opening of microcracks with the increase in loading. Additionally, the role of pre-existing cracks also served as an explanation for the breakdown pressure increases observed with increasing borehole diameter.

Other investigators have noted the effect of pre-existing cracks and have made various observations. Komar and Frohne (1973) suggested that under near uniform stress conditions, fracture orientation under high injection rates was predominantly affected by geologic discontinuities. Zoback *et al.* (1977), in a laboratory investigation of hydraulic fracturing, were apparently successful in their attempts to minimize the effect of pre-existing cracks by using viscous drilling muds as the injected fluid. Viscous fluids exert a fluid pressure only at the borehole wall because the pressure drops in

any pre-existing fractures prevent them from being pressurized entirely along their length.

The classic tensile failure approach used for the interpretation of hydraulic fracture tests for in situ stress measurements does not accurately consider the mechanisms of fracture initiation and propagation. Abou-Sayed *et al.* (1978) analyzed these mechanisms according to the linear elastic fracture mechanics theory (LEFM). The difference between the two approaches is that LEFM incorporates crack geometry (i.e., fracture length) and the loading of pre-existing cracks. Their plane strain analysis also reaffirmed that the fracture propagated in a plane normal to the minimum in situ principal stress in order to maximize the energy release rate. For sufficiently long fractures, the fracture pressure at which fracture propagation is imminent is equivalent to σ_3 and is independent of the fracture length and the mechanical properties of the rock.

The following equation was derived for tensile (Mode I) fracture initiation based on the following conditions: the assumption of linear elastic homogeneous isotropic media; the critical crack is pressurized along its entire length (providing it is open); the crack intersects the borehole in a radial plane normal to σ_3; and fluid diffusion is negligible (i.e., no poroelastic effects):

$$\sigma_1 = \frac{K_{IC}}{(\pi L)^{1/2}(G^* - F^*)} - \frac{F^*}{G^* - F^*} P_f - \frac{G^*}{G^* - F^*} P_s \qquad [2.15]$$

where K_{IC} = critical stress intensity factor for tensile (Mode I) failure; L = 1/2 of the fracture length; F *(L/a) and G* (L/a) are dimensionless stress intensity factors and P_f and P_s are as defined previously.

Equation [2.13] can be modified to consider vertical fracture initiation under plane strain conditions for L/a << 1 (ratio of fracture length to borehole radius) where $G^* \equiv 1.5\ F^*$ and $G^* - F^* \equiv 1.0$, and by substituting $\sigma_3 = P_s$ and and solving for σ_{hmax}:

$$\sigma_{hmax} = 3P_s - 2P_f + \frac{K_{IC}}{0.6(\pi L)^{1/2}} \qquad [2.16]$$

While the use of P_s and P_f is the same as in the hydraulic fracture initiation analysis, two additional parameters, K_{IC} and L, replace the rock tensile strength term. The critical stress intensity factor, the resistance of a material to fracture extension, is determined experimentally in tests comprised of subjecting a prenotched thick-walled cylinder to an internal pressure in the borehole until the fracture propagates. About-Sayed *et al.* (1978) based their value of the pre-existing crack length L on observations from rock core. Furthermore, it was argued that the dimensionless stress intensity factors F* and G* should be reduced because the actual cracks are not plane strain cracks and they arrived at a reduction factor of 40%.

Recalling the classic equation [2.1] and solving it for σ_{hmax},

$$\sigma_{hmax} = 3P_s - P_f + \sigma_t - P_o \qquad [2.17]$$

it is apparent that the LEFM equation, when the critical stress intensity factor is the same as the tensile strength, predicts a lower σ_{hmax} by the amount of P_f. The LEFM treatment considers the two equal effects of (i) the circumferential tensile stress induced by internal pressurization and (ii) the pressure acting on the crack face. The discrepancy lies in that the second effect is not considered in the classic analysis.

Two other differences in the two approaches are revealed in the treatment of tensile strength and pore pressure. Abou-Sayed *et al.* (1978) argue that the tensile strength term in the classic equation is inaccurate for two reasons: (i) the tensile strength is evaluated in thick walled cylinder tests where the burst pressure is generally not comparable to the breakdown pressure; (ii) the tensile strength does not consider size effects (i.e., crack length) realistically because of the probable disparity between the laboratory critical crack length and the field critical crack length. Finally, the LEFM equation does not have a pore pressure term because K_{IC} for a given geometry and loading is independent of the superposition of a uniform hydrostatic

pressure. The total stress parameters can be replaced by the effective stress parameters with P_o not appearing explicitly as in the classic equation.

Zoback and Pollard (1978) investigated the effect of fracture loading, as controlled by fracture fluid viscosity, on hydraulic fracture propagation. Their two dimensional slit model had two degrees of fracture loading: (i) a point load loading inferring stable fracture propagation; and (ii) a full crack length loading inferring unstable fracture propagation. Their analysis showed that actual fracture loading exists somewhere between these two extremes.

A comprehensive analytical treatment of the application of linear elastic fracture mechanics was presented by Cleary (1979). His analysis of fracture initiation incorporated pressurization rate effects (time dependency) through linear elastic fracture mechanics. In order to account for the multitude of variables responsible for the wellbore stress concentration and then fracture initiation upon fluid injection, he recommended a proper accounting of the rupture mechanism. The classic theory is inadequate in this respect because it does not explain the smooth transition of the solutions among the varying degrees of fluid diffusion given by Rice and Cleary (1976). An examination of the time-dependent extension of a pre-existing flaw or potential initiation site at (or near) the wellbore would account for this smooth transition.

Three models for representing the pressurization of a borehole intersected by a pre-existing flaw were examined: (i) a healed crack; (ii) transmissive open flaw; and (iii) the gradual linking of micro-flaws. For the healed crack model, the crack is assumed to reinitiate and propagate when the alteration of the stresses on its faces produce a critical energy release rate at the tip. This model is adequate for most cases except at short times where an open flaw is subjected to fluid pressurization and the transmissive open flaw model is appropriate. Finally, when no macroscopic cracks are evident, the third model characterized by mechanisms causing the linking of micro-flaws becomes operative. Cleary (1979) describes this third model as the gradual formation of larger cracks through the linking of micro-cracks (or micro-

structural damage) at potential fracture initiation sites. Cleary's analytical results are plotted with some laboratory data in Figure 2.10 and seem to explain the time dependency of the fracture initiation pressure.

Cleary (1979) also provided some simplifed poroelastic analyses of the short term deformation-diffusion response around the borehole based on previous work of Rice and Cleary (1976). These short term solutions were developed to account for the effect of fluid penetration near the borehole wall on the propagation of near wellbore micro-cracks with respect to the three specific wellbore micro-crack models.

McLennan (1980) attempted to apply fracture mechanics theory to the interpretation of hydraulic fracture tests for in situ stress measurements. He noted that pre-existing cracks can result in a lack of definite breakdown pressures, anomalous pressure-time records and misleading stress calculations when classic theory is assumed. The limitations of fracture mechanics theories were: (i) most assume symmetrical bimodal fractures, (ii) they require the orientation of σ_{hmax} with respect to the microcrack, (iii) they assume uniform pressure distributions, (iv) they require a critical micro-crack length, (v) they assume planar cracks and (vi) no standardized procedure for K_{IC} evaluation exists. Abou-Sayed *et al.* (1978) realized that "... more accurate determination of the maximum principal stress can be achieved if better information is obtained on the size and shape of the dominant well bore crack and on the value of K_{IC} under field conditions."

2.3.2.2 Shear Failure

Results from an experimental hydraulic fracture program reported by Lockner and Byerlee (1977) suggested that under certain conditions, shear failure could occur prior to tensile failure. They performed triaxial cell hydraulic fracture tests in order to test the effect of varying the injection rate and deviatoric stress level on the breakdown pressure and failure mode. The results from these tests are plotted in Figure 2.11 with deviatoric stress ($\sigma_1 - \sigma_3$) versus the effective breakdown pressure, p_f. At the lower injection rates,

shear failure was found to occur (to the right of the effective pressure of -100 bars or 10 MPa) and this was attributed to the pore pressure distribution in the region surrounding the wellbore. In simplified terms, the lower injection rates allow the pore pressure to build up sufficiently to reduce the effective stresses locally until the compressive strength of the rock is exceeded prior to tensile failure. Apparently this effect is magnified as the deviatoric stress level increases (Figure 2.11).

In order to understand this phenomena, Lockner and Byerlee (1977) modelled the pore pressure development in their hydraulic fracturing experiments. Figure 2.12 shows the radial pore pressure distribution for three small sample tests at increasing injection rates and for one large sample test; all tests failed in shear. This is evident in Figure 2.12 in which the pore pressure distributions are within the compressive strength of the samples as defined by the dashed lines. However, as the injection rates are increased, the pore pressure gradient increases. They argued that eventually the increased pore pressure gradients would cause the tensile strength of the sample to be exceeded prior to shear failure. It is also apparent that the predicted pore pressure distribution in samples experiencing shear failure differs from ones experiencing tensile failure.

Further experimental work by Solberg *et al.* (1977) on oil shale and low permeability granite corroborated with the findings of Lockner and Byerlee (1977). The role of deviatoric stress was investigated and it was found that as deviatoric stress increased (for their tests, σ_3 = 1 kbar = 100 MPa) shear failure was the failure mode, while tensile failure occured at lower deviatoric stress levels ($\Delta\sigma$ < 2 kbars = 200 MPa). Figure 2.13 shows the decrease in breakdown pressure (and change in failure mode) at a fixed injection rate while $\Delta\sigma$ ranges from 1 to 6.9 kbars (100 to 690 MPa). The explanation for this behaviour again was based on the role of pore pressure development in the sample prior to failure. A high deviatoric stress level causes the opening of dilatant micro-cracks which result in higher permeabilities. An increased overall permeability favours the possibility of shear failure by the development of increased pore pressures which reduce the effective stresses

until shear failure occurs. Even though the samples were thought to be relatively impermeable, fluid diffusion took place in all cases and affected both shear and tensile failure development.

Additional testing was conducted on Westerly granite at elevated temperatures with acoustic emission monitoring by Solberg *et al.* (1980). Acoustic monitoring revealed two other possible behaviour modes associated with hydraulic fracturing: (i) no deformation; and (ii) deformation associated with no apparent macroscopic fractures (Figure 2.14). At low deviatoric stress levels and injection rates (and high temperatures) no deformation occurs and steady state radial flow is evident but with no apparent acoustic emissions. At intermediate deviatoric stress levels and injection rates (and high temperatures), no macroscopic fractures are visible, but low acoustic emissions were recorded and the rock radial permeability increased 10× the initial value. Tensile failure was characterized by a sudden peak acoustic emission value at failure and the breakdown pressure increased with increasing injection rate and increasing temperature. Acoustic emission records indicate that shear failure occurs immediately after the peak injection pressure. The breakdown pressure for shear failure is proportional to the injection rate and temperature, but is inversely proportional to the deviatoric stress level. These four behaviour modes are shown in Figure 2.15 as a function of temperature, deviatoric stress and injection rate and it summarizes the effects of these variables on hydraulic fracture behaviour mode.

Obviously the breakdown pressure recorded in a hydraulic fracture test cannot be related to the in situ stresses, based on the tensile failure mode assumed by classic and linear elastic fracture mechanics theories, if tensile failure is not the case. Lockner and Byerlee (1977) were surprised to find that the possibility of shear failure in hydraulic fracture tests had not been previously considered. Solberg *et al.* (1977) suggest that even though field tests use injection rates high enough to cause tensile failure, fluid leakoff from the fracture faces may cause shear failure in tectonically active areas (i.e., $\Delta\sigma$ is high). Also for tests conducted at great depths where in situ

temperatures are great, or in hydraulic fracture treatments with heated fluids (e.g. steam), thermal effects on failure mode cannot be ignored.

In recognition of the possibility of shear failure, Callanan (1983) proposed an analysis of the stress state around a wellbore at failure during hydraulic fracturing based on the Mohr-Coulomb failure criterion. His analysis consists of predicting fracture initiation by shear for vertical fractures (Figure 2.16) in a uniform horizontal stress field with no fluid diffusion and while $\sigma_{\theta\theta}$ remains compressive. Tensile failure may prevail once the fluid penetrates the propagating fracture. The analysis is for two cases of relative initial stress magnitudes. A stress analysis incorporating a Mohr-Coulomb failure criteria allowed him to calculate the stresses at the wellbore once the rock has failed under shear when $\sigma'_r = p_w$.(wellbore pressure). The horizontal principal stress is derived from the instantaneous shut-in pressure as in the classical analysis. This assumes that the orientation of the shear failure surface is normal to the horizontal principal stress. The analysis itself is restricted to conditions of hydrostatic horizontal stresses and where the Mohr-Coulomb strength parameters of the rock are known.

2.3.2.3 Plastic Material

With respect to hydraulic fracturing, it has been shown it is necessary to evaluate the condition of the material around the wellbore. Based on the classic elastic analysis of the stresses surrounding a wellbore, Risnes *et al.* (1982) concluded that for poorly consolidated sand, a plastic zone around the uncased borehole would exist. Employing a simplified 3D model of elastic state of stress, the theories of elasticity and plasticity were used to derive analytical expressions for all three stress components. Under non- fluid diffusion conditions, the material cohesive strength is the major factor controlling the extent of the plastic zone, with the plastic zone size decreasing with increasing cohesive strength. Their model of a cased borehole suggested that the stress level will increase, thereby reducing the plastic zone, but not necessarily eliminating it.

This work was extended to an analysis of hydraulic fracture inititation pressures in permeable poorly consolidated sands by Horsrud *et al.* (1982). They analyzed the development of stresses around a wellbore in this material as the injection pressure increased to the point of fracture initiation when $\sigma_{\theta\theta} = p_w$. Depending on the Poisson's ratio and uniaxial compressive strength of the rock and the initial in situ stresses, the plastic zone was found to either increase or decrease with injection pressure and the fracture initiation pressure could be either lesser or greater than that predicted by the classic theory. Although the plastic zone can decrease under certain injection schemes, the fracture will always be initiated in plastically strained material. For typical material properties and in situ conditions, plastic theory predicted a 10% decrease in the fracture initiation pressure as compared to classic theory. The wellbore stress distribution predicted by their theory suggests that the fracture propagation pressure will be greater than the fracture initiation pressure because once the fracture has propagated from the plastic zone into the elastic zone, the in situ stresses controlling propagation will be at their original values.

2.4 Hydraulic Fracturing in Soil

2.4.1 Hydraulic Fracture Theory for Soil

Hydraulic fracturing theory for soil was developed once it was recongnized as a mechanism responsible for some problems encountered in civil engineering practice. Morgenstern and Vaughan (1963) developed criteria for allowable grouting pressures in order to avoid hydraulic fracturing. Bjerrum *et al.* (1972) observed anomalous permeability values derived from constant head tests in clays and attributed them to hydraulic fracturing. There are also concerns that hydraulic fracturing can cause excessive leakage in dams.

Bjerrum and Andersen (1972) proposed hydraulic fracturing as a means for measuring in situ stress in soils. The mechanics of hydraulic fracturing in

soil has been developed theoretically and tested in the laboratory and in the field as part of the investigation into the above problems as well as to determine in situ stresses.

The first major analysis of hydraulic fracturing in soils arose from field studies that indicated that serious errors could be found when estimating the permeability of clay in constant head tests (Bjerrum *et al.* 1972). Permeability differences of up to three magnitudes were noted between constant head tests conducted in unfractured and fractured clays. The excess water pressure required to fracture the clays was observed to be less than the effective overburden pressure and to be as low as 0.2 times the effective overburden pressure (σ'_v). Haimson's (1968) hydraulic fracture initiation theory for rock was found to be inappropriate because it did not consider the stress changes caused by the emplacement of the piezometer. Morgenstern and Vaughan's (1963) hydraulic fracturing theory for predicting the excess pressure necessary for active failure (plastic flow toward the piezometer) was also determined to be inappropriate.

For their particular case, Bjerrum *et al.* (1972) developed their own theory which considered: (1) the initial stress state and pore water pressure; (2) stress changes caused by the piezometer and any other installation disturbance ; (3) pressure head and its variation with time; (4) deformation properties and the degree of soil homogeneity around the piezometer; and (5) the geometry of the piezometer tip. Their solution, based on the assumptions of isotropic, homogeneous fully saturated soils, identifies two possible responses to injection: (1) "blowoff" in which a water filled cavity is created around the piezometer when the effective radial stress (σ'_r) becomes zero in the soil next to the piezometer at an excess pore pressure of $\Delta u = (1+\beta^*)\ K_o\ \sigma'_v$ where β^* = stress factor, $K_o\ \sigma'_v$ = horizontal effective stress; and (2) vertical hydraulic fracturing occuring when $\sigma'_\theta = \sigma'_t$, so that

$$\Delta u/\sigma'_v = [(1/\nu) - 1)][(1 - \alpha^*)K_o + \sigma_t/\sigma'_v] \qquad [2.18]$$

where ν = Poisson's ratio, α^* = stress factor, K_o = ratio of effective horizontal stress to the effective vertical stress.

This equation predicts the pressure at which vertical hydraulic fractures are initiated, assuming fracturing precedes the "blowout" pressure, which propagate radially away from the borehole. Bjerrum *et al.* (1972) recognized the possiblity of horizontal fracture initiation at an excess pore pressure of $\Delta u = \sigma'_v$. They urged that all three potential responses to excess pore pressure be checked in order to verify the actual soil response.

Bjerrum and Anderson (1972) tested the possibility of using this technique to measure the in situ horizontal stress. Based on the theory of Bjerrum *et al.* (1972), Bjerrum and Anderson (1972) suggested it was possible to calculate the horizontal principal stresses in the case of vertical fracturing. Their triaxial cell tests indicated that (fracture) closure pressure (P_c) selected from graphs of pressure versus flow rate could be used as a reliable measure of the horizontal stress. Over-consolidated soils underwent horizontal fracturing.

Massarsch (1978) offered an alternate theory based on Vesic's concept of cylindrical cavity expansion. Instead of fracturing occurring immediately, an elastic-plastic zone would develop around the cavity as the internal pressure was raised until fracture initiation. He argued that vertical fractures would be created independent of the coefficient of the lateral earth pressure (K_o).

A review of laboratory simulated hydraulic fracture experiments by Nobari *et al.* (1973) as reported by Jaworski (1979), and by Jaworski *et al.* (1981) and by Widjaja *et al.* (1981) revealed two common characteristics of hydraulic fracture behavior in soils:

(1) Hydraulic fracturing occurs when the tangential effective stress reduces to the soil tensile strength on the plane of maximum tensile stress and P_f is primarily a function of the induced in situ stresses, soil tensile strength, and the ambient pore pressure.

(2) Fractures are perpendicular to the minimum principal stress when the in situ stresses are non-hydrostatic.

Studies reported by Jaworski (1979), Jaworski *et al.* (1981), and Widjaja *et al.* (1984) concluded that for hydraulic fracturing to occur, some form of soil discontinuity (i.e., borehole, soil/concrete interface) that allowed a wedging action was necessary. Widjaja *et al.* (1984) also stipulated that the tested material must possess tensile strength (cohesion), in order for a fracture to be created, otherwise $\sigma'_{\theta\theta}$ would be reduced to the minimum active earth pressure state where the soils would deform plastically. For cohesive soils under conditions of non-hydrostatic stress, hydraulic fracturing would initiate at one point of low effective stress and gradually propagate along points where the effective stress has been reduced to the tensile strength of the soil. This stable fracture propagation is unlike the rapid crack propagation in brittle materials such as rock and glass. Jaworski (1979) suggested that stable crack propagation can be attributed to pressure losses in the fracture which inhibits the buildup of fracture tip pressure. Propagation occurs when the crack widens and allows the crack tip pressures to reach the propagation pressure. Hydraulic fracture behaviour in soil seems to be very similar to hydraulic fracture behaviour in rock when accounting for differences in confining pressures and the extent of cementation or cohesion (i.e., similar to sedimentary rocks).

As with hydraulic fracturing tests in rock, tests in soils have been found to be affected by injection rate (time dependency), permeability, mechanical properties of the soil (ν, E) and the test parameters (e.g., borehole diameter). Widjaja *et al.*'s (1984) work also included a laboratory program to test the effect of some of these factors on fracture initiation pressure. Fracture initiation pressure was highly dependent on the horizontal stress and ν, but only marginally affected by borehole diameter, injection rate, soil permeability, and soil tensile strength. Research conducted in rock hydraulic fracturing has indicated that fluid diffusion affects fracture initiation pressure substantially. This has been observed in pressurization rate experiments and has been explained by time dependent fluid diffusion into the surrounding material controlled through pressurization rate, material permeability and disturbance, viscous pressure losses, etc.

2.4.2 Field Test Verification

Massarsch *et al.* (1975) reported a comparison of horizontal stress measurements from hydraulic fracturing tests and modified Glötzl earth pressure cells. The Glötzl cell measurements proved to be more precise than the hydraulic fracture results. These shallow stress measurements (i.e., <17 m) indicated a disappointing correspondence between the two methods with the differences ranging up to 250 per cent. One major complication they noted was that fracture orientation was controlled by geologic factors (e.g., varves, bedding, fissures, etc.). From the errors involved in stress determination, they recommended that a range of K_o values should be provided for geotechnical analyses.

Tavenas *et al.* (1975) arrived at a similar conclusion based on horizontal stress measurements derived from hydraulic fracture tests, total stress cells, and pressuremeter tests. Their findings showed good agreement for the hydraulic fracture and total stress cell measurements while the pressuremeter results were characteristically lower. Despite the good hydraulic fracture results, they indicated three problems associated with these tests: (1) interpretation of the closure pressure; (2) time dependent soil disturbance surrounding the piezometer; and (3) borehole dilation (pressuremeter effect).

Piezometer installation caused an apparent time dependent soil disturbance that was evident in the increases in the horizontal stresses observed around the borehole which eventually stabilized after one hundred days. Additionally, borehole dilation during pressurization, a phenomenom recognized previously by Bjerrum *et al.* (1972), was thought to be causing reductions in the tangential stress near the wellbore. The lower clay permeability measurements obtained during the latter stages of the test were also attributed to borehole dilation. Despite the recognized effects of the time dependent disturbance associated with piezometer installation and stress changes caused by borehole dilation, Tavenas *et al.* (1975) concluded that the

stress measurements were reasonable because these two effects tended to cancel each other.

More recently, Lefebvre *et al.* (1981) suggested that some hydraulic fracture tests could induce multiple fractures near the piezometer and such tests would overestimate the horizontal principal stress. By studying block samples in which had been hydraulically fractured, a vertical fracture system and an additional inverted cone shaped fracture system (20^o - 30^o from the horizontal) were both observed.

Chan (1986) considered the hydraulic fracture method for determining the in situ stresses in Genesse clay. However in his review of the method, the conflicting evidence for the reliability of the method led him to adopt the self-boring pressuremeter as the main method for lateral stress determination.

2.5 Summary

Although it may not have been necessary to review hydraulic fracture theory in such detail to meet the objectives of the thesis, the amount of research and actual practice that has occurred since the work of Hubbert and Willis in 1957 presents a difficult task of information synthesis. In this chapter, some areas have received either a superficial treatment, as in actual field tests in the disciplines of petroleum, civil engineering and geophysics, or have not been cited at all, as in the case of the petroleum engineer's development of hydraulic fracture models because they were beyond the scope of this work. This final section first presents a brief summary of hydraulic fracture theory relevant to in situ stress determination. Secondly, it states some conclusions regarding the application of hydraulic fracture theory for the interpretation of in situ stress.

The classic theory of hydraulic fracture initiation developed for predicting fracture initiation in open boreholes for non-fluid diffusion conditions continues to be the most widely used approach for analyzing hydraulic fracture stress tests. The theory has been adapted in order to account for coupled deformation-diffusion effects associated with hydraulic

fracturing of fluid saturated porous material that were observed in laboratory tests. These poroelastic effects manifested themselves in time dependent fracture initiation pressures and failure modes other than tensile fracture.

Additional research has delineated the limits of the applicability of hydraulic fracture theory for in situ stress determination. The wellbore condition, as reflected by the presence of casing, wellbore integrity and the state of the material around the wellbore, has a profound effect on hydraulic fracture initiation. Geologic structure, encompassing geologic discontinuites and the relevant sedimentary/igneous/metamorphic rock structures, affects both hydraulic fracture initiation and propagation. Simplifying assumptions regarding the in situ stress state and the behaviour of the material may be significantly violated under actual test conditions. The influence of the packers on the plane strain assumption of classic theory, which negates the creation of horizontal fractures, has to be critically examined. It is essential that a proposed field stress measurement program be arranged in conjunction with knowledge of the influence of these complicating factors.

Several researchers have proposed alternate hydraulic fracture theories in recognition of failure mechanisms other than tensile failure. Fracture mechanics theory has been applied to the problem of a pressurized borehole characterized by micro-cracks or flaws. Experimental research has suggested that shear failure may be occurring prior to tensile fracturing, depending on the pore pressures induced during fluid injection. In some materials, the introduction of the borehole would induce a stress concentration causing plastic failure around the borehole. A complicated hydraulic fracture initiation analysis was reported in order to predict fracture initiation pressures in plastic material around the borehole. However, none of these alternate theories has been widely used because they are invariably more complex and require a more difficult test procedure or stress analysis.

A somewhat parallel development of hydraulic fracture theory and practice for soil in civil engineering showed that the same fundamentals of hydraulic fracture initiation and propagation hold for both soil and rock. However, different test procedures, the lower confining pressures, and

different material properties of soil were the major details that precluded a completely duplicate analysis. The application of the hydraulic fracture stress measurement test for soil is not as widely practiced and seems to have become less popular in the 1980's.

The hydraulic fracture stress measurement test has become a widely accepted in situ stress measurement method in reservoir engineering, geophysics research and civil engineering. This chapter has shown that in order to credibly apply this method a broad understanding of the theory and test procedure, and a recognition of the limits of the method are necessary. To aid the examination of hydraulic fracture theory, Table 2.1 summarizes the factors which may affect hydraulic fracture initiation and Table 2.2 states the basic concepts of hydraulic fracture propagation.

Table 2.1 Factors which may affect hydraulic fracture initiation.

1. STRESS-STRAIN BEHAVIOUR
   - Linear Elasticity
   - Homogeneity
   - Stress Path

2. MATERIAL STRENGTH
   - Tensile Strength
   - Shear Strength
   - Stress Path

3. POROELASTIC PARAMETERS
   - Drained vs Undrained Behaviour
   - Permeability

4. WELLBORE CONDITION
   - Perforated Casing
   - Pre-existing Cracks
   - Unstable (Failed or Yielded) Material

5. IN SITU STRESS
   - Vertical Stress Assumption
   - Hydrostatic Stresses

6. GEOLOGIC DISCONTINUITIES

7. TEST PROCEDURES
   - Injection Rate
   - Fracture Fluid Viscosity

Table 2.2 Basic concepts of hydraulic fracture propagation.

(1) IN SITU STRESS STATE

1.1 NON-HYDROSTATIC IN SITU STRESS STATE

1.1.1 For $\sigma_{hmin} = \sigma_3$, the fracture propagates in a plane normal to the minimum horizontal principal stress.

1.1.2 For $\sigma_v = \sigma_3$, the fracture will begin at the wellbore in a vertical plane but will gradually rotate in order to become normal to σ_v.

1.2 NEAR HYDROSTATIC IN SITU STRESS STATE

1.2.1 Fracture propagation is no longer strictly controlled by the in situ stress state. The material fabric or geologic discontinuities may exert a predominant influence on fracture propagation.

1.2.2 If the fracture is deflected from the plane normal to σ_3, shear stresses will develop adjacent to the fracture. Fracture propagation is no longer only Mode I (tensile failure).

(2) FRACTURE PROPAGATION CRITERIA

2.1 Linear elastic fracture mechanics based on Mode I (tensile) fracturing.

2.1.1 Two common fracture mechanics models exist which are based on different assumptions on fracture geometry.

2.1.2 Models couple fracture growth with injected fluid volume.

2.2 Mixed mode fracture mechanics analyses which consider shearing along with tensile failure.

2.3 Criteria is coupled with fluid flow.

2.3.1 Considers leakoff from the fracture into the formation.

2.3.2 Interaction of fracture and formation fluid flow.

2.3.3 Poroelastic effects which cause increases in closure stress.

(3) GEOLOGIC DISCONTINUITIES

3.1 Geologic discontinuities can manifest their influence on fracture propagation through:

3.1.1 Vertical fracture containment;

3.1.2 Limiting lateral propagation;

3.1.3 Multiple fracture systems.

(4) FRACTURE MORPHOLOGY

4.1 Planar fractures with two wings extending away from the borehole are assumed.

4.2 Effects of geologic discontinuities and fluid-fracture interaction on fracture orientation, dimensions and width.

4.2.1 Vertical fractures propagating in *en echelon* manner.

4.2.2 Horizontal fracture propagation in offsets.

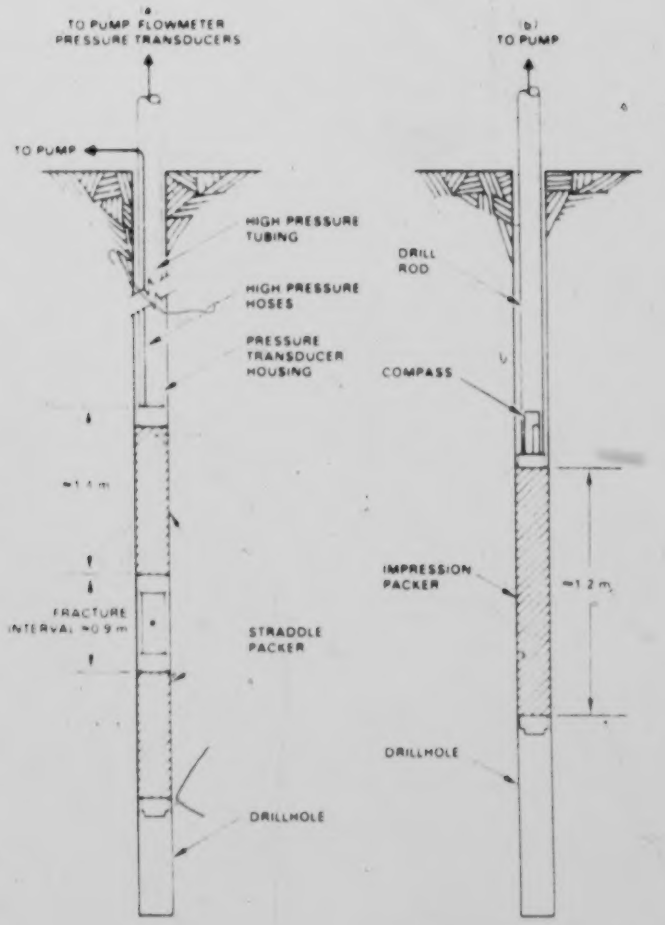

(Modified after ISRM 1987)

Figure 2.1 Schematic representations of (a) an openhole hydraulic fracturing tool and (b) an inflatable impression packer.

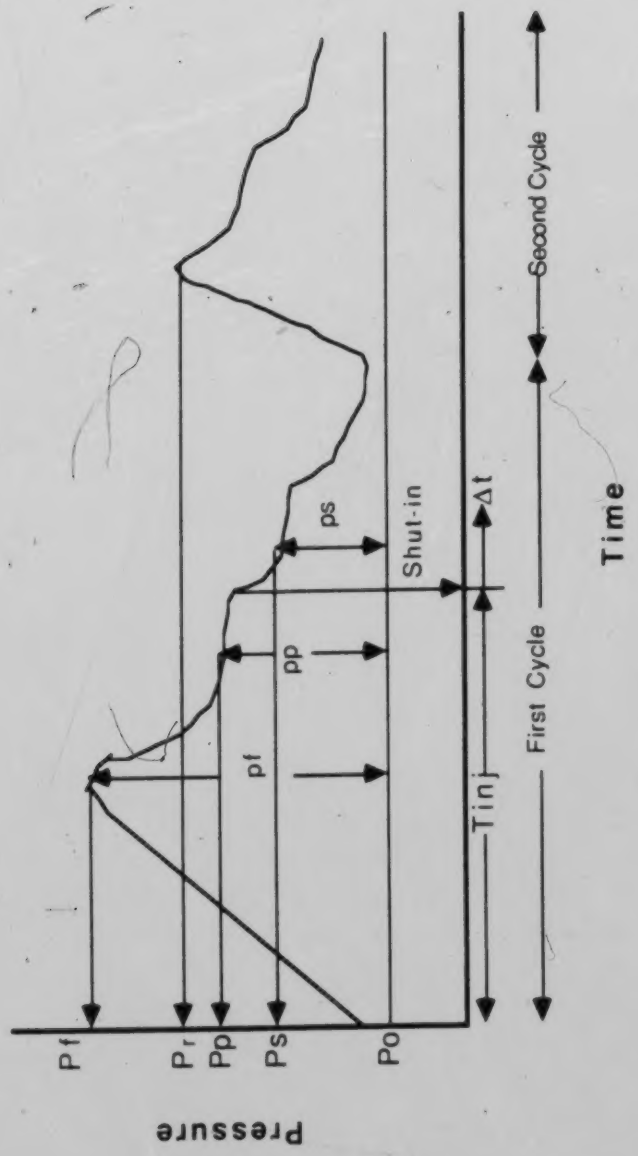

Figure 2.2 Schematic drawing of a hydraulic fracture stress measurement pressure-time record which defines the nomenclature used in the thesis.

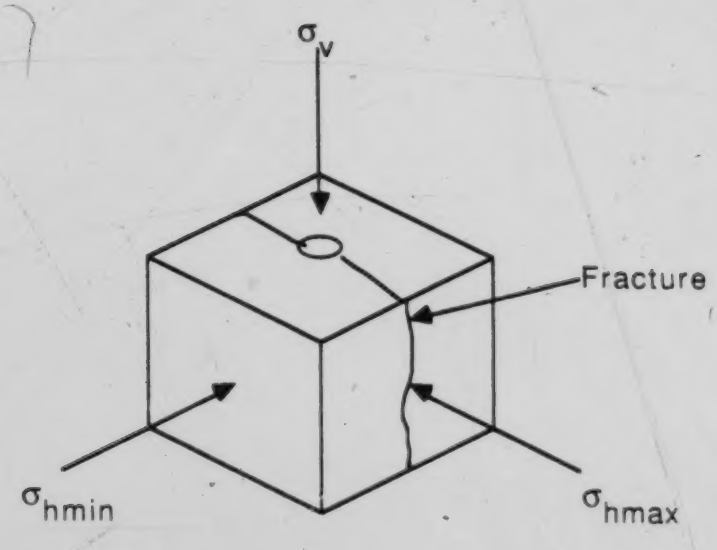

Figure 2.3 Relationship between the principal stresses and fracture orientation for the classic vertical fracture analysis.

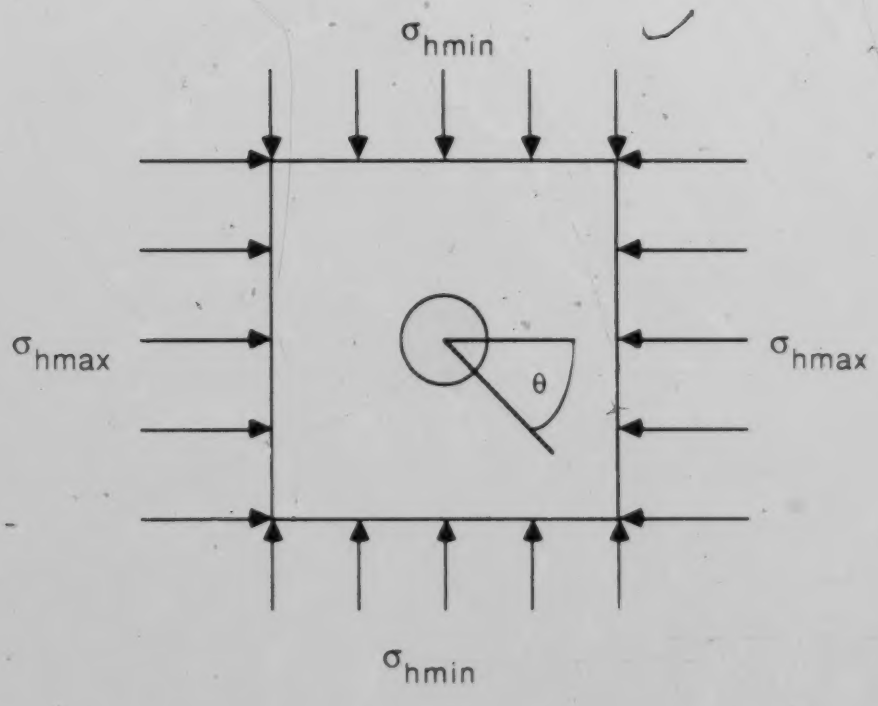

Figure 2.4 Plane strain model of a circular hole in a externally loaded plate (Kirsch's model).

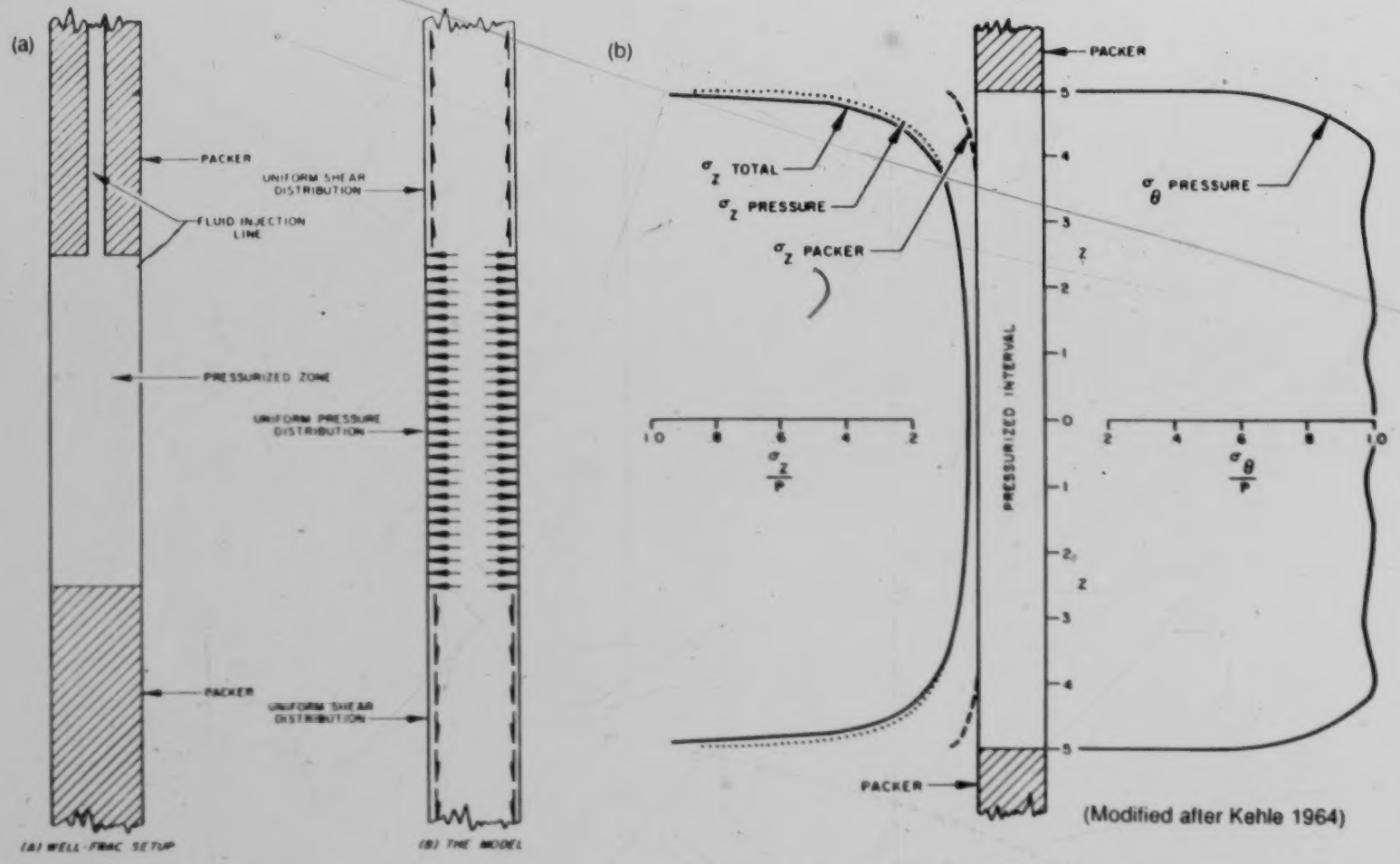

Figure 2.5 The influence of rigid packers in a hydraulic fracture test: (a) model of the pressurized zone and packers and (b) the tangential and vertical stresses induced during borehole pressurization (fluid injection).

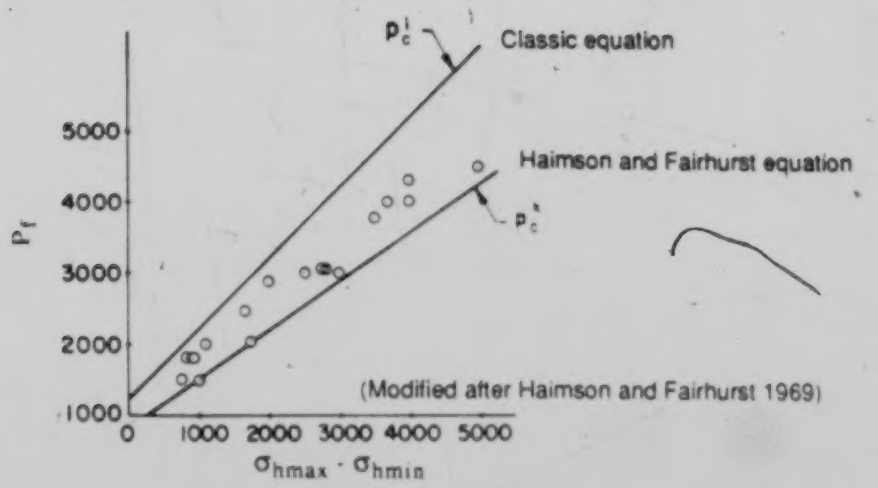

Figure 2.6 Comparison of experimental fracture initiation pressure data and theoretical calculations (classic and Haimson and Fairhurst equations).

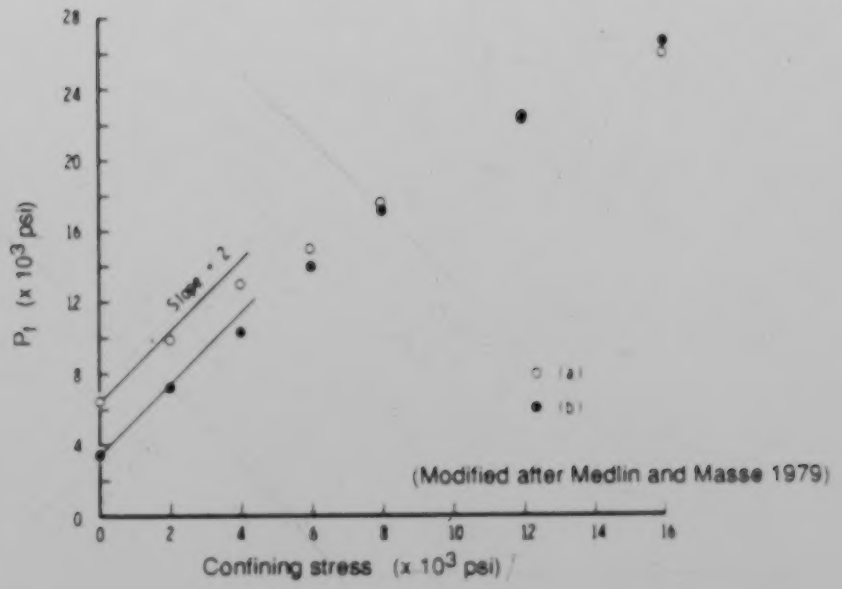

Figure 2.7 Comparison of the fracture initiation pressure data for (a) non-penetrating fluid (heavy grease) and (b) penetrating fluid (vacuum pump oil).

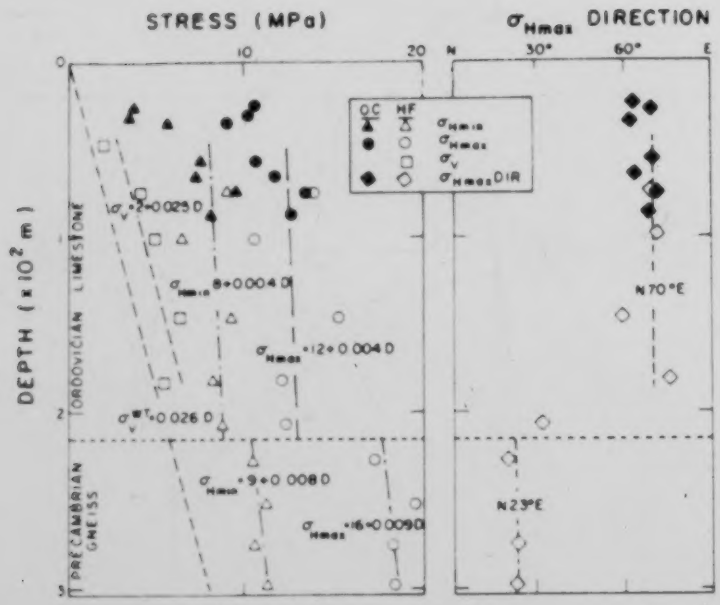

(a) Darlington, Ontario

(Modified after Haimson 1981)

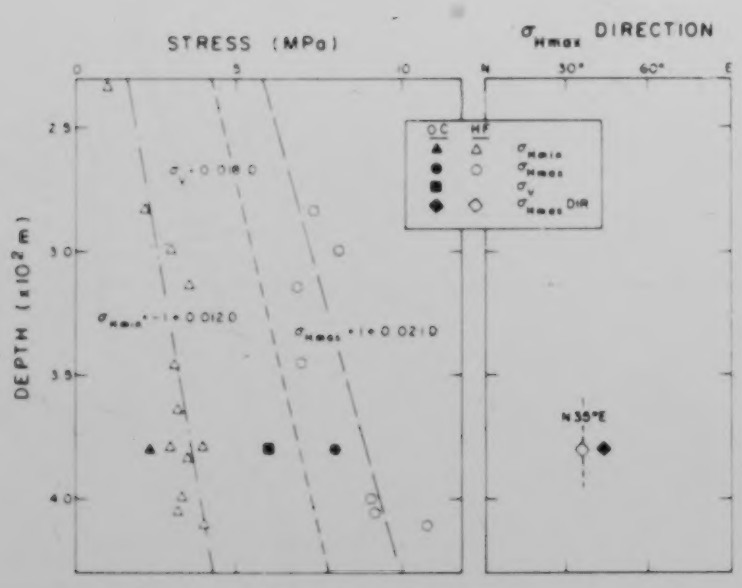

(b) Nevada Test Site

(Modified after Haimson 1981)

Figure 2.8 Comparison of hydraulic fracture stress measurement data and overcoring stress measurment data for two sites.

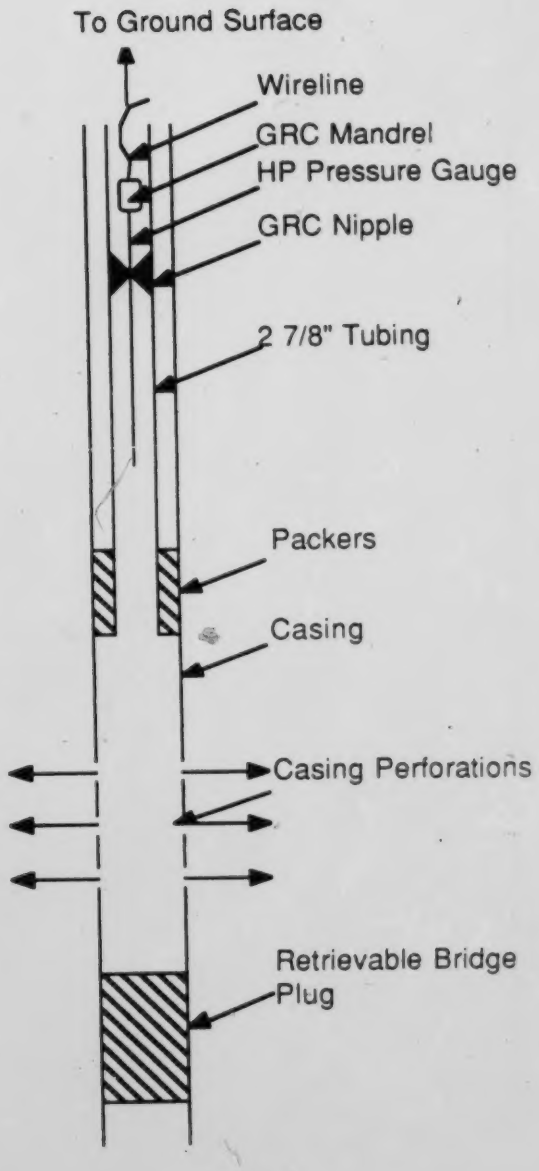

Figure 2.9 Schematic drawing of a downhole hydraulic fracture tool assembly used in perforated cased boreholes.

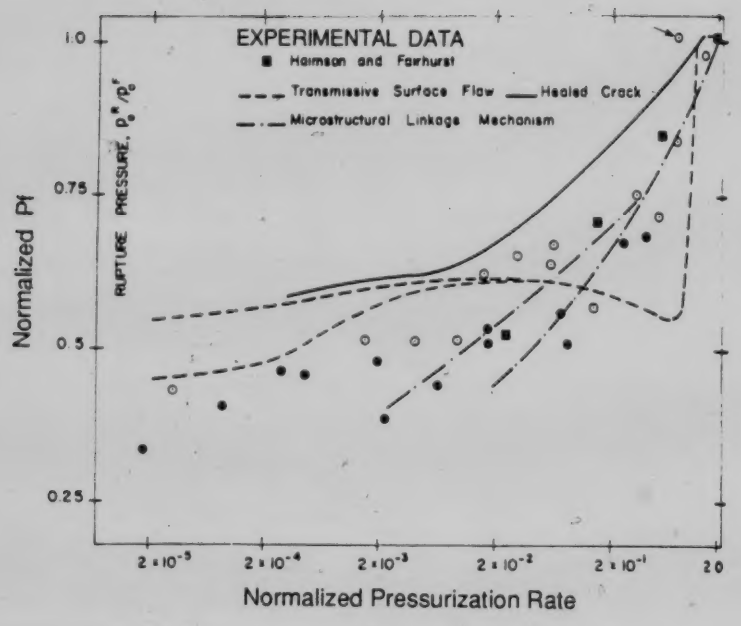

(Modified after Cleary 1979)

Figure 2.10 Comparison between experimental data and linear elastic fracture mechanics model predictions of fracture initiation pressure for varying pressurization rates.

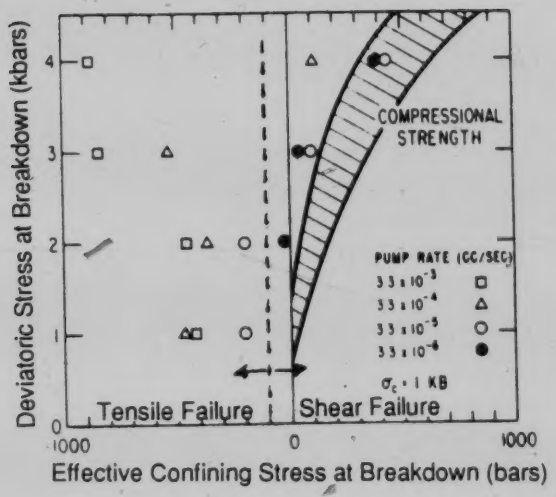

(Modified after Lockner and Byerlee 1977)

Figure 2.11 Laboratory results of deviatoric stress vs effective confining stress at fracture initiation indicating either tensile or shear failure.

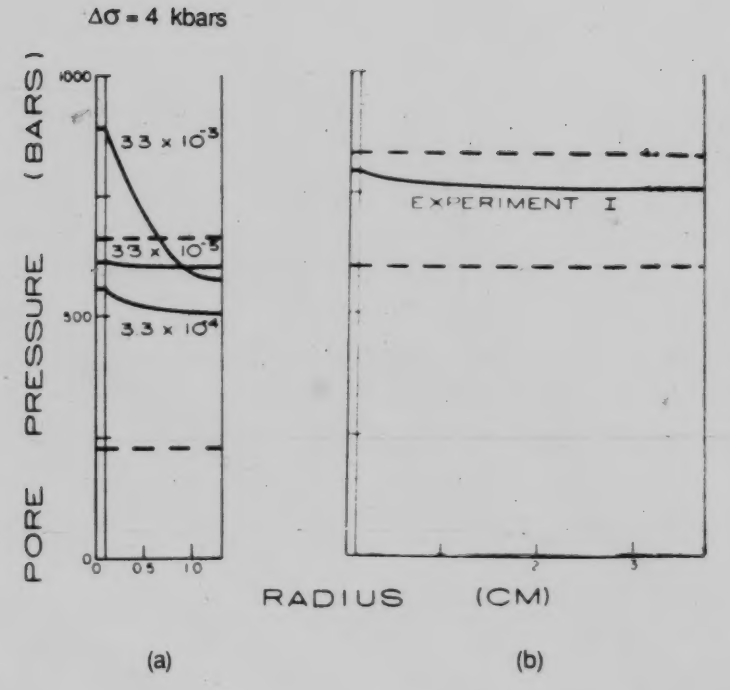

(Modified after Lockner and Byerlee 1977)

Figure 2.12 Theoretical radial pore pressure distribution for laboratory samples all experiencing shear failure at varying injection rates: (a) small samples and (b) large sample.

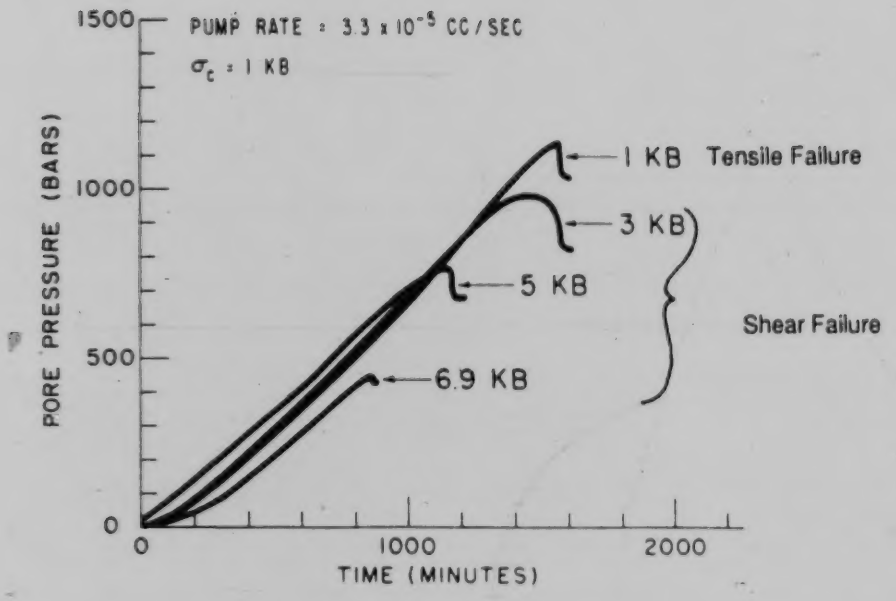

(Modified after Solberg *et al.* 1977)

Figure 2.13 Hydraulic fracture initiation curves for experiments with varying deviatoric stress values resulting in two different failure modes.

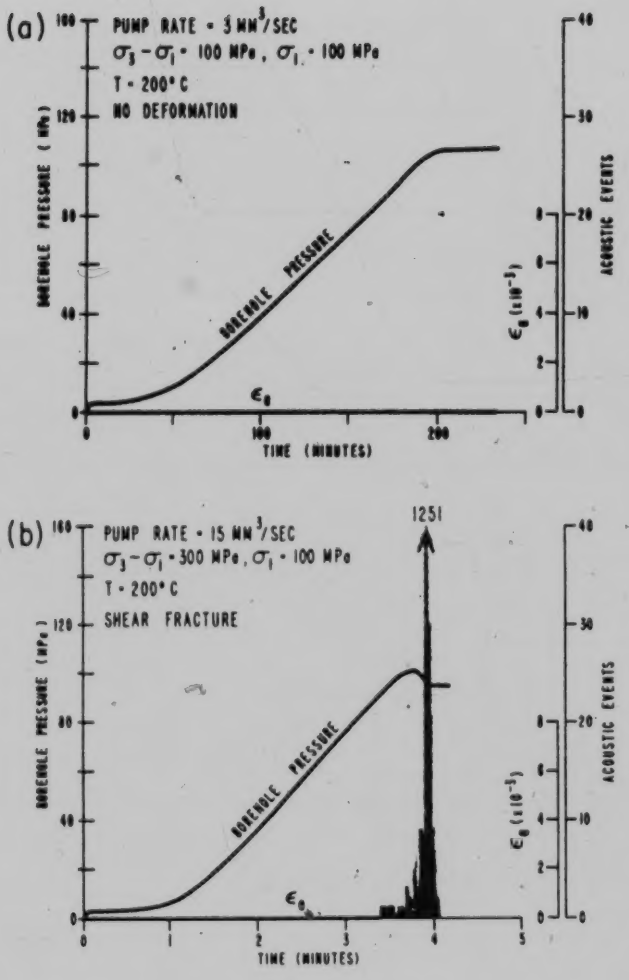

(Modified after Solberg *et al.* 1980)

Figure 2.14 Laboratory fracture initiation curves with the associated acoustic emission records suggesting four possible failure modes.

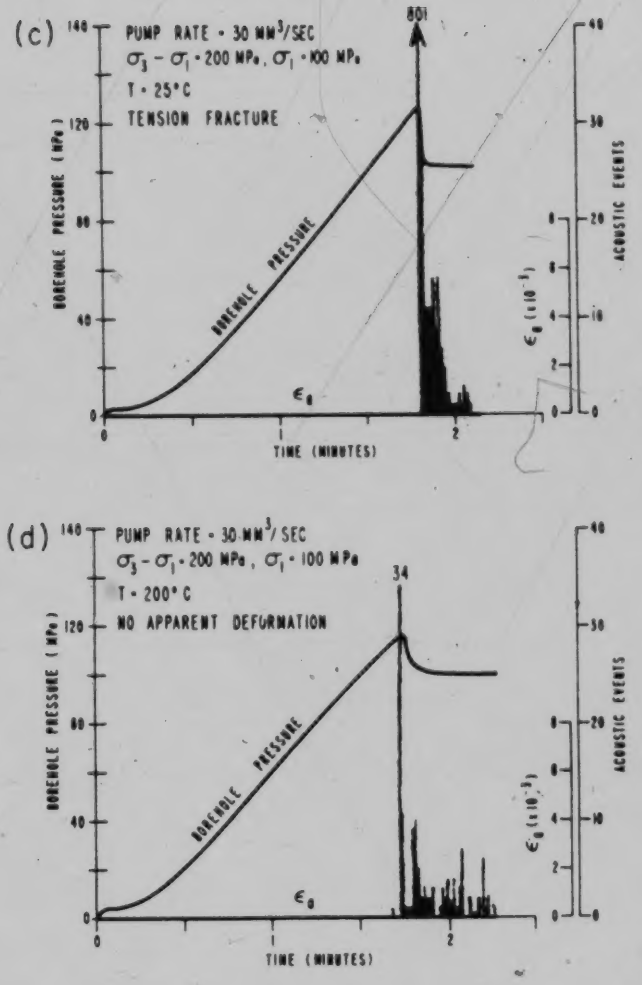

(Modified after Solberg *et al.* 1980)

Figure 2.14 Continued from previous page..

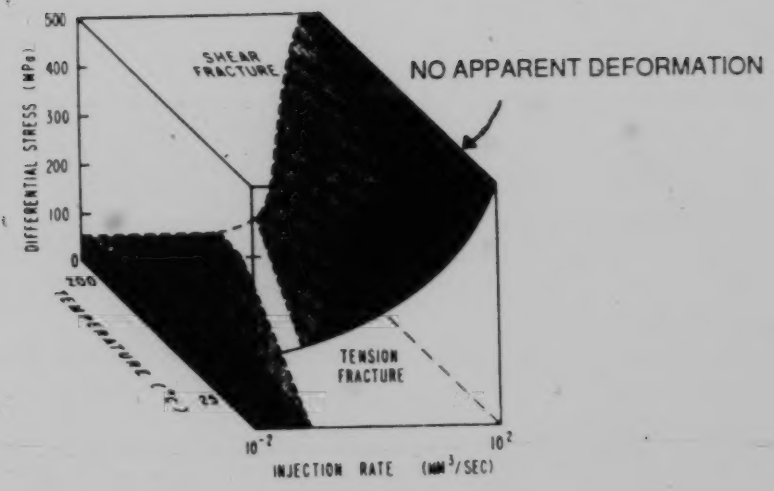

(Modified after Solberg *et al.* 1980)

Figure 2.15 Four possible failure modes as a function of injection rate, temperature and differential (deviatoric) stress.

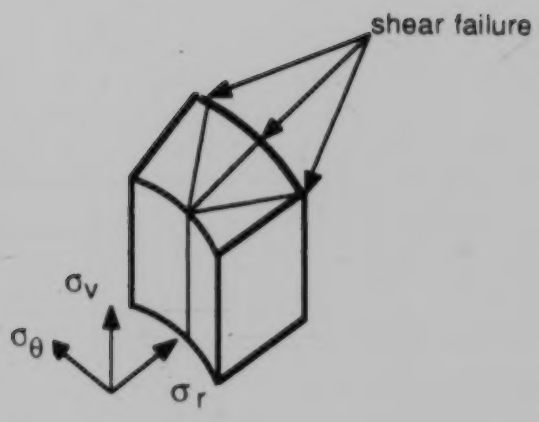

a) $\sigma_\theta \leq \sigma_v \leq \sigma_r$

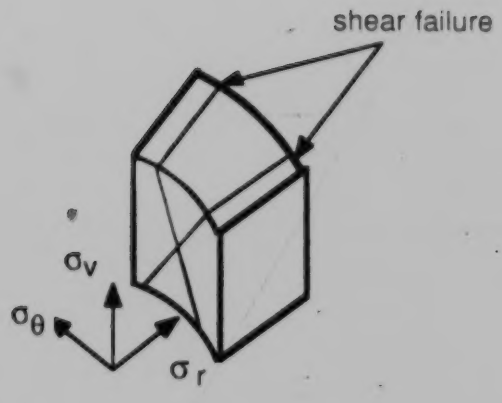

(b) $\sigma_\theta \leq \sigma_r \leq \sigma_v$

Figure 2.16 Possible vertical fracture orientations associated with shear failure.

3. HYDRAULIC FRACTURING IN OIL SANDS

3.1 Introduction

Hydraulic fracture theory and practice have been used extensively in the design of enhanced bitumen recovery schemes for oil sands. Due to the unique geomechanical properties of oil sands, the complex formation stratigraphy, and the high bitumen viscosity characteristic of oil sand deposits, in situ recovery methods have to rely on reducing the bitumen viscosity and enhancing the formation permeability in order to economically extract the bitumen. Cyclic steam stimulation is currently the most common bitumen heating and recovery technique. Steam injection heats the bitumen and reduces its viscosity and it create zones of enhanced permeability within the oil sands Settari and Raisbeck (1978) suggest that the creation of initial flow paths within the oil sands by hydraulic fracturing are a necessary precursor for successful application of recovery methods.

In situ stress is a required input parameter for hydraulic fracture models, commonly numerical simulators, that are designed to predict the behaviour of large hydraulic fracture field programs used in enhanced bitumen recovery schemes. As with conventional hydrocarbon reservoirs, the hydraulic fracture stress measurement method is normally the only reliable technique available to determine the in situ stress state in oil sand deposits. It is important, therefore, to evaluate the various aspects of hydraulic fracture behaviour identified in chapter 2 with respect to the specific geological and geomechanical properties of Alberta oil sand deposits .

The modelling of classic hydraulic fracture initiation and propagation involves understanding the coupled deformation-diffusion effects of borehole pressurization in a non-hydrostatic stress field of porous linear elastic material. Geomechanics is concerned with the prediction of the stresses and strains induced in geologic materials subject to loading or unloading. Therefore, the geomechanical properties of the geologic material as well as

the strength and fluid-flow properties are needed for the assessment and prediction of hydraulic fracture behaviour.

In order to investigate the impact of oil sand geomechanics on hydraulic fracture theory, the unique geomechanical properties of oil sand pertinent to hydraulic fracture theory will be reviewed.

In situ stress data for Alberta oil sand deposits suggest that hydrostatic stress conditions exist for depths between 250 and 400 m (Chhina and Agar 1985). Hydraulic fractures in in situ stress regimes approaching hydrostatic conditions are no longer strictly controlled by in situ stress. Geologic structure or discontinuities become important in predicting hydraulic fracture behaviour. We can conclude, therefore, that hydraulic fracturing in shallow oil sand deposits (e.g., the Athabasca deposit) will be affected by the bedding and any other geologic discontinuities found in these deposits.

Theoretical and laboratory research and field studies of hydraulic fracturing in Alberta oil sand deposits are reviewed in this chapter in order to identify the unusual characteristics of hydraulic fracturing in oil sand. Theoretical research can be divided into the numercial modelling of large scale hydraulic fracture treatments and the conceptual geomechanical model proposed by Dusseault (1980a,b,c). Limited laboratory work is also reported. Case histories of hydraulic fracturing in oil sand, not only for stress measurement but also for reservoir engineering analysis, test the validity of hydraulic fracture theory.

Chapter 3 concludes with a discussion of the impact of oil sand geomechanics and geology, hydraulic fracture theory and case studies on the viabililty of the hydraulic fracture stress measurement method for oil sand deposits.

3.2 Geomechanical Behaviour of Oil Sands

The geomechanical behaviour of oil sands is examined here because its unique geomechanical properties have important effects on hydraulic fracture stress measurement theories. The stress-strain, strength and fluid

flow properties (along with the reservoir properties) of oil sands are also required input parameters for hydraulic fracture models.

3.2.1 General Description

Oil sand deposits of Alberta (Figure 3.1) may be generally described as overconsolidated, cohesionless sand deposits characterized by dense, interpenetrative fabrics with pore space inhabited by viscous bitumen, water and dissolved gas. These deposits are Cretaceous in age and have experienced varying degrees of post depositional diagenesis in terms of subsequent burial, erosion and glacial loading and unloading. The three major deposits in Alberta, Athabasca, Cold Lake and Peace River (Figure 3.1), each have unique post-depositional histories resulting in oil sand formations of varying geologic and geotechnical properties.

The geotechnical behaviour and properties of Alberta oil sand has been extensively studied at the University of Alberta in the past ten years by a number of investigators (Dusseault 1977a; Dusseault and Morgenstern 1978; Barnes 1980; Au 1984; Agar 1984; Agar *et al.* 1987, 1989; Kosar *et al.* 1987; Plewes 1987, Kosar 1989). Research has concentrated on the geotechnical testing of Athabasca oil sand (mainly surface accessible Saline Creek samples, fairly shallow Syncrude samples and, moderately deep AOSTRA Underground Test Facility samples), with some tests performed on deep Cold Lake samples. Very little information exists for the geotechnical properties of Peace River deposit oil sands. Based on summaries of the geotechnical properties of oil sands published by Dusseault (1980a, 1980b) and Bawden (1983), four general comments can be made concerning Alberta (primarily Athabasca deposit data) oil sands' geotechanical behaviour:

(i) Oil sands has a dense, interpenetrative (locked) fabric consisting of water- wet sand grains (and minor fines) and a pore space comprised of viscous bitumen (density > 1.0 g/cm^3), water and dissolved gas. Stress-strain behaviour is nonlinear, brittle and is post-peak strain-softening. It exhibits a curvilinear failure envelope (Figure 3.2) and undergoes

substantial dilation during shear, which are both related to the interlocked fabric.

(ii) Oil sands are essentially cohesionless. No cementation exists and the bitumen is immobile under in situ conditions.

(iii) Although the absolute permeability of oil sands is high (8000 md, similar to that of a dense sand) due to its high porosity (n=35 %) and lack of cement, the effective permeability to water is low (10 md). The viscous bitumen inhabiting the pore space impedes fluid flow and the bitumen viscosity is highly temperature dependent.

(iv) There is a variable amount of dissolved gas, predominantly methane, in the bitumen for undisturbed oil sands. When the confining stresses are relieved, such as in sample extraction, the gas comes out of solution and disturbs the interpenetrative fabric. The resulting sample disturbance has important implications for the laboratory evaluation of the geotechnical and fluid-flow behaviour of the oil sands.

Although four general comments about Alberta oil sand geotechanical behaviour have been made, detailed description of an overall oil sand behaviour is prevented by the lithologic and stratigraphic variability between and within individual deposits. The stratigraphic differences and geotechnical variation between oil sands deposits has been well documented. Mossop (1978) has suggested that the extreme lithologic variability within the McMurray Formation of the Athabasca deposit due to shale layers alternating with oil sand layers presents areal and regional variations in geotechnical properties. Variations in the geotechnical behaviour within the Athabasca deposit are related to the formation stratigraphy and variations in bitumen and fines content (Dusseault 1980b and Kosar 1989). Although the Cold Lake oil sand deposit is located at a greater depth and has experienced a different geologic history, stratigraphic and lithologic studies show a similar formation variability.

Recent geotechnical studies (Agar 1984; Plewes 1987; Kosar 1989) have shown that the geotechnical properties of oil sands, in addition to being deposit/site specific and confining stress dependent, are also stress path

dependent. However, it is only recently that the stress path dependency of oil sands geotechnical properties has been adequately studied. Plewes (1987) compared triaxial extension tests with triaxial compression tests while Kosar (1989) reported geotechnical properties from five different stress paths. He stressed the fundamental importance of testing oil sands samples according to stress paths similar to the anticipated field stress path.

An additional concern is the effect of sample disturbance due to gas evolution upon unloading on the geotechnical properties of oil sands. Numerous studies have shown that gas evolution disrupts the interpenetrative oil sands fabric which drastically alters the geotechanical properties. Dusseault (1977) attempted to minimize sample disturbance through downhole freezing and created the index of disturbance criterion in order to quantify sample disturbance for comparison purposes. Since then other researchers have used this disturbance index to evaluate their samples and to provide a method for comparing oil sand geomechanical data. McKay (1988) has developed an alternate technique for oil sands sampling based on a triple tube core barrel. Preliminary evidence suggests that this technique provides less disturbed samples than obtained previously.

While attempts can be made to generalize oil sand geomechanical properties, the following factors must be considered when evaluating the geotechnical behaviour of a particular oil sands sample: (i) specific deposit and sample location in order to account for the characteristic geological and geotechanical properties, (ii) in situ stresses or confining stresses which may be characterized by sample location depth, (iii) stress path which most closely replicates the stress-strains associated with the particular problem being examined, and (iv) desired sample quality.

3.2.2 Implications for Hydraulic Fracture Theory

An examination of the geomechanical behaviour of oil sands in conjunction with the basic principles of the classic hydraulic fracture theory reviewed in chapter 2 (Table 2.1) is essential to evaluating the current

practice of hydraulic fracturing in oil sands. The findings of this examination can be summarized in three categories: (i) classic assumptions of linear elastic homogeneous isotropic media; (ii) oil sand tensile strength; and (iii) fluid diffusion (i.e., partially drained behaviour during wellbore drilling and fluid injection). Indirectly related to this examination were the influence of stress path and wellbore condition on hydraulic fracturing. Implications arising from these findings on classic hydraulic fracture theory for stress measurement purposes in oil sand are discussed below.

3.2.2.1 Classic Assumptions

The classic assumptions of linear elastic homogeneous isotropic media is fundamental to the analysis of many soil and rock mechanics problems. However, only when exceptional geologic conditions exist can this assumption provide adequate predictions of stresses and strains arising from a particular loading in soil or rock. Ordinarily the geological processes involved in the continuing formation of soil and rock deposits result in complex deposits that are not amenable to analyses borrowed from material science. Oil sand deposits are no exception.

Agar *et al.* (1987) identified three significant departures of the stress-strain behaviour of oil sand from linear elastic theory: (i) strain is not a linear function of stress; (ii) oil sands is stress path dependent; (iii) shear stresses cause not only shear strains but also volumetric strains (dilatant or contractant behaviour). They suggested modelling the non-linear stress-strain behaviour of oil sand by a hyperbolic relationship derived from empirical techniques.

Because of the considerable local and regional variability of the McMurray formation, Dusseault (1980b) recommended that detailed stratigraphic and lithologic studies be conducted for each specific site. Besides recognizing the variability of the McMurray Formation and the interbedded nature of most oil sand deposits, no other conclusions have been drawn regarding the homogeneity of the oil sand deposits. Like all sedimentary

deposits, the degree of material heterogeneity is related depositional/stratigraphic features (Nelson 1986).

Agar *et al.* (1987) note that no studies of the anisotropy ~~of the stress~~-strain properties of oil sands has been conducted.

3.2.2.2 Oil Sands Tensile Strength

Dusseault (1978) stated that Athabasca oil sands has no stress-independent cohesion and that the failure envelope can be extended to the origin because (i) microscopic studies showed that no cementing agent exists, (ii) slaking tests indicate the absence of cohesion, (iii) oil sands readily remoulds in the hand and (iv) triaxial data trend towards zero shear strength at low confining stresses. Plewes (1987) reported that McRoberts performed Brazilian tensile strength tests at room temperature on oil sands and found tensile strength values of 8.1 to 17.1 kPa.

Plewes (1987) performed drained and undrained triaxial extension tests at low confining stresses between 32 and 80 kPa on Syncrude oil sands samples. The results had to be corrected for membrane effects because at low confining stresses (< 100 kPa), the membrane could offer a significant contribution to the measured strength. Test procedures prevented the possible observation of the "conical cup and cone" characteristic of tensile fracturing. Based on the results presented in a p-q' plot in Figure 3.3, Plewes found no evidence for oil sands tensile strength.

Three unconfined triaxial extension tests were also conducted by Plewes (1987) and revealed a very low tensile strength of 2 to 3 kPa. Plewes suggested that it was possible for rich oil sands to mobilize short term tensile strength due to bitumen viscosity and negative pore pressures. In total stress terms, a significant apparent tensile strength may be mobilized during undrained unloading due to the generation the negative pore pressures.

3.2.2.3 Fluid Diffusion

The potential influence of fluid diffusion and poroelastic effects on hydraulic fracture behaviour was summarized in chapter 2. This section briefly investigates the relevant oil sands poroelastic properties to determine if there are any significant poroelastic effects possible in oil sand microfracs. The fluid flow properties of oil sands are also noted in relation to fluid leakoff.

The poroelastic behaviour of oil sands needs to evaluated for its possible effects in hydraulic fracturing. The development of poroelastic effects are dependent on B ($\propto$ Kf/K) and α ($\propto$ K/Ks). It was observed that with an infinitely compressible fluid (i.e., gas), B=0, thus solid (matrix) deformation does not result in any excess pore pressure and the pore pressures are governed by the homogeneous diffusion equation. Except for the occluded gas bubbles, the water and bitumen pore phases are not considered infinitely compressible fluids and B values should be greater than zero. Plewes (1987) measured B values between 0.5 and 1.0 which are plotted as a function of oil sands compressibility in Figure 3.4. It is evident that undrained loading of oil sands will produce an excess pore pressure.

The poroelastic coefficient α can be evaluated based on a typical bulk modulus value of 500 MPa and a solid (quartz grain) bulk modulus of 37 GPa (Mitchell 1976); essentially $\alpha \equiv 1.0$. This infers that the simplified effective stress law $\sigma' = \sigma - P_o$ holds for oil sands and that oil sands is a porous material with the volumetric deformation controlled by σ'. Furthermore, the K parameter in Haimson and Fairhurst's equation [2.6] can be calculated in order to arrive at a steady-state fracture initiation equation. Assuming $\nu = 0.25$, $K = 4/3$ and equation [2.6] becomes:

$$P_f = \frac{3}{4}[\sigma_t + 3\sigma_{hmin} - \sigma_{hmax} - \frac{2}{3}P_o] \qquad [3.1]$$

Consequently, it appears that at long-time or for steady-state fluid leakoff conditions (where induced pore pressures have dissipated), the hydraulic

fracture initiation pressure is reduced from the classic (non-fluid diffusion) equation.

Although permeability does not appear explicitly in the poroelastic hydraulic fracture initiation equation for short-time at r = a, it does appears in a generalized consolidation coefficient as defined by Detournay and Cheng (1988). Poroelastic considerations in fracture initiation and fracture propagation are assessed in relation to the comparative time frames of the poroelastic processes, as dictated, in part, by the permeability, and by the test procedure (i.e., injected fluid viscosity). Permeability is used to estimate the duration of the transient pore pressure period and also to calculate the steady-state fluid flow capacity (injectivity) of the oil sands formation once the transient effects have ended. The time dependency of the poroelastic effects in borehole stability and in fracture propagation are discussed in section 3.2.2.5 and in chapter 4, respectively.

The last remaining aspect of fluid diffusion is the role of fluid leakoff on fracture dimensions. Numerical modelling work by Settari *et al.* (1989) suggested that the difference between injection pressure and ambient pore pressure (P_p - P_o), the absolute permeability, k, the fluid mobilities (bitumen, water and gas) and the total compressiblity (or bulk modulus) were the dominant parameters controlling fluid leakoff effects on fracture dimensions.

The fluid flow properties of oil sand deposits have been studied primarily for assessing the feasibility of various in situ production recovery schemes. Agar *et al.* (1989) presented laboratory test results for fluid flow properties of Athabasca oil sand and summarized publicly available permeability data for Alberta oil sands as shown in Table 3.1.

Since hydraulic fracture stress measurement tests in oil sands use water as the injection fluid, the effective permeability of oil sands to water is the pertinent fluid flow parameter controlling leakoff. Agar *et al.* (1987) found that their effective permeability values for undisturbed oil-rich Athabasca oil sands compared well with the hydraulic conductivity values determined by Hackbarth and Natasa (1979) for McMurray Formation oil sands in the Athabasca deposit. Based on the range of these values of 1 to 1000 md, Agar *et*

al. (1989) conclude that "Initial water permeabilities of this magnitude indicate that substantial rates of fluid leak-off may be expected during hydraulic fracturing of oil rich Athabasca oil sand with either water or steam."

3.2.2.4 Stress Path

In the theory of elasticity, elastic deformations depend only on the final state of stress and so are independent of stress path. Plastic deformations, however, depend on the stress history and the stress-strain relations are generally nonlinear. Agar *et al.* (1987) showed that shear strength and the stress-strain behaviour of oil sand is dependent on the loading and unloading history. Other researchers have observed similar behaviour (Plewes 1987; Kosar *et al.* 1987; Scott and Morgenstern 1987) and Kosar (1989) stressed the importance of replicating, in geotechnical laboratory tests, the anticipated field stress path of oil recovery schemes.

The effect of stress path on the strength and stress-strain properties of oil sands can be observed by comparing results derived from the variety of stress paths used in triaxial tests. By manipulating the principal effective stresses during the test, the triaxial test is capable of simulating field stress paths. Figure 3.5a shows four common triaxial stress paths on a principal stress space graph of σ_1 versus $\sqrt{2}\,\sigma_3$: (i) isotropic compression where $K_o = 1$ to the initial condition; (ii) confined drained compression; (iii) confined undrained compression; and (iv) confined compression for $0 < K_o < 1$.

Kosar *et al.* (1987) and Kosar (1989) summarized the effect of undrained versus drained triaxial stress paths on Athabasca and Cold Lake oil sands behaviour, specifically the stress-strain properties, such as Young's modulus (E), isotropic (C_i) and confined (C_c) compressibility, and the strength-stress-strain properties, such as strain to failure, ε_f, maximum deviatoric stress, $(\sigma'_1 - \sigma'_3)_{max}$, and maximum stress ratio, $(\sigma'_1/\sigma'_3)_{max}$. Tables 3.2 and 3.3 summarize their findings. They concluded that (i) the stress path has a significant effect on the initial tangent (Young's) modulus for Athabasca oil sands, but a smaller effect for Cold Lake oil sands; (ii) $(\sigma'_1 - \sigma'_3)_{max}$ is greatly affected by stress

path for oil sand, where undrained strength is lower than drained strength for Athabasca oil sands, and is higher for the Cold Lake oil sands; (iii) the strain to failure, ε_f, is highly stress path dependent for Athabasca oil sands, but less so for Cold Lake oil sands; and (iv) the compressibility of both Athabasca and Cold Lake oil sands vary when comparing confined compression (C_c) and isotropic compression (C_i).

Plewes (1987) conducted undrained compression and extension triaxial tests on Saline Creek oil sand samples of varying degrees of sample disturbance. The undrained shear strength at $(\sigma'_1/\sigma'_3)_{max}$ decreases nonlinearly with the effective normal stress. Plewes found a correspondence between undrained and drained shear strength envelopes when corrections for volume change according to Rowe's stress dilatancy theory were applied to the drained tests (Figure 3.6). Triaxial extension tests were also conducted and are shown in Figure 3.7 with $c' = 0$ and $\phi' = 68^o$ with the effective stress paths for both undrained and drained extension tests being consistently bounded by this Mohr-Coulomb failure envelope. The extension tests exhibited an overall maximum increase of 5 to 13% in the angle of shearing resistance above the compression tests.

Scott and Morgenstern (1987) reported additional geotechnical data for oil sand based on further stress path testing. Besides the conventional stress paths mentioned previously, they also tested McMurray Formation oil sand according to J_1 ($J_1 = \sigma_{ii} = \sigma_{11} + \sigma_{22} + \sigma_{33}$) constant drained compression and extension stress paths and the active compression (σ_1 = constant while σ_3 decreases) stress path (Figure 3.5b). Their results further supported the stress path dependency of oil sand which is particularly evident in the initial Young's modulus. The variability of ε_f shows that shear strength mobilization depends on the stress path. To ensure appropriate geotechnical input for engineering design of bitumen recovery schemes, it is important to recognize that stress path is a function of the initial stress state, stress unloading, thermal recovery strategy, and the drainage characteristics.

A vertical wellbore in a hydrostatic stress field ($\sigma_{hmax} = \sigma_{hmin}$) will create near wellbore response in the formation in which a decrease in one

horizontal normal stress occurs simultaneously with a corresponding increase in the other horizontal normal stress. Scott and Morgenstern (1987) suggested that this stress path can be modelled in the triaxial cell by a J_1 constant stress path as shown in Figure 3.5b. However, the assumption of a uniform horizontal stress field is restrictive and it is usually not the case for most in situ stress states.

Anticipated stress paths replicating undrained oil sands response to borehole drilling and pressurization are shown in Figure 3.8 for a in situ stress state typical for most Alberta oil sands payzones. The stress paths start at the initial given stress state then follows the stresses created by the instantaneous drilling of the borehole as given by Kirsch's solution. The final stage is the stress response caused by instantaneous borehole pressurization in drained material with no fluid diffusion. It is important to consider the vertical stress in the stress path graphs because it is apparent that the induced stresses cause a rotation of the minimum principal stress as the horizontal principal stress magnitudes change and the vertical stress remains fixed. A true triaxial device is required to simulate fully independent stress states since the stress paths are no longer confined to the σ'_1 versus $\sqrt{2}\ \sigma'_3$ plane.

3.2.2.5 Wellbore Condition

The conditon of the formation around the wellbore (i.e., wellbore stability) is an important consideration when conducting small volume hydraulic fracture tests. Stress interpretation theory assumes that the wellbore is circular and that the formation remains linear elastic. Therefore, the possibility of wellbore damage, wellbore breakouts and plastically strained material around the wellbore are factors which must be assessed prior to a hydraulic fracture test. Bawden (1983) has suggested that the uncertain effects of gas evolution and fabric disturbance on the wellbore condition need to be examined; in fact, without such an examination, the applicability of classical elastic analyses are in doubt.

Wellbore stability must also be considered in the drilling and production of oil and gas wells because the shape and direction of the borehole during drilling needs to be maintained and hole collapse and solid particle influx have to be prevented (Cheatham 1984). This involves an analysis of the uncontrollable factors: in situ stress, rock strength and formation pore pressure; and the analysis of controllable factors: wellbore fluid pressure and drilling mud chemistry. The four main mechanisms behind wellbore instability are summarized as (i) hydration of swelling shales, (ii) tensile failure due to hydraulic fracturing, (iii) wellbore failure in compression (shear failure), and (iv) solid particle influx (e.g., sand production). Since we are concerned with the mechanical response of an oil sand wellbore to borehole drilling (prior to borehole pressurization), the emphasis of this section is on the role of shear failure.

The phenomena of wellbore breakouts has been investigated in the last decade by a number of researchers (Gough and Bell 1982; Bell and Gough 1983; Hickman *et al.* 1985; Zoback *et al.* 1985; Kaiser and Maloney 1987; Kaiser 1987,1988). This work centers on the study of breakout initiation, orientation and size by calculating the induced stresses through Kirsch's solution and then applying an appropriate Mohr-Coulomb yield criterion to determine the breakout behaviour. Bell and Gough (1983) observed that breakouts were spalled regions on either side of the wellbore and were centered at the azimuth of σ_{hmin} where the compressive stress concentration was the greatest. The breakout was concluded to be the result of a localized compressive shear failure which resulted in a triangular shaped breakout enclosed by flat conjugate shear planes orientated at a constant angle to the azimuth of the far field principal stresses (Figure 3.9).

In a more detailed analysis, Zoback *et al.* (1985) found that near the wellbore, the stress concentration resulted in curved potential shear failure surfaces (Figure 3.10). Equations were developed to predict the size and shape of the breakouts in terms of the formation strength (c' ϕ') and the in situ stresses. A positive excess wellbore pressure was found to decrease the breakout size while a negative excess wellbore pressure increased it. Both

responses were related to the changes in effective normal stress on the potential failure surfaces.

Additional studies reported by Kaiser and Maloney (1987) and Kaiser (1987, 1988) confirm many of these conclusions. Four possible borehole rupture modes, three shear and one tensile mode, were observed (Figure 3.11). The results were generally consistent with the prediction of the Mohr-Coulomb yield criterion and the shape of the yield surfaces indicated that shear was the dominant failure mechanism. As noted by Zoback *et al.* (1985), borehole breakout (rupture) propagation is a time dependent process, possibly related to sub-critical crack growth, and the analysis cannot be applied to excessively yielding conditions. Further tests conducted in rock samples with planes of weaknesses showed that the areal extent of the failure zone was significantly enlarged and that non-symmetrical breakout zones for hydrostatic lateral stresses were possible.

Detournay and Cheng (1988), based on their complete poroelastic stress analysis of a borehole in porous medium, proposed a mechanism for delayed borehole instability. It was noted previously that the deviatoric loading component of Detournay and Cheng's model introduced time dependency in the stress distribution around a wellbore. Figure 3.12 shows a plot of maximum shear stress $[1/2\sqrt{((\sigma_{\theta\theta} - \sigma_{rr})^2 - 4\sigma_{r\theta}^2)}]$ vs the mean normal stress $[-1/2\ \sigma_{\theta\theta} + \sigma_{rr})]$, both normalized to the far-field deviatoric stress, along a radial direction perpendicular to σ_3 for various times t^* for deviatoric loading mode. Except at the right side of the graph, approaching the borehole wall, the relationship between shear stress and normal stress is time independent. However, as shown in Figure 3.13, when the graph is in terms of effective stress, the curves for various time periods t^* are substantially different owing to the time dependent pore pressure. Figure 3.13 also shows that significant shear stresses can develop away from the borehole wall (at the right side of the diagram).

Detournay and Cheng (1988) extended these results in a test case for evaluating wellbore stability with respect to the poroelastic effects resulting from the superposition of hydrostatic loading and deviatoric loading (no

initial pore pressure assumed). The resulting stress distributions for various times t* are plotted along with a Mohr-Coulomb failure criteria in Figure 3.14 in terms of the variables of Figure 3.13. When the Mohr-Coulomb failure envelope is adjusted so that incipient failure occurs at the borehole wall, the isochrones for $t^* = 10^{-4}$ and 10^{-5} infer that the shear strength has already been exceeded in the material away from the borehole wall. The poroelastic analysis reveals that shear failure may not necessarily occur first at the borehole wall as predicted by elastic analysis.

A simplified (drained) analysis of the near wellbore condition of an oil sands formation around a wellbore is reported here. Employing the elastic Kirsch's solution for calculating the stress induced around a borehole in a biaxially stressed plate, the critical effective stresses induced at the borehole, for drained conditions, in a typical oil sands can be determined. The induced $\sigma'_{\theta\theta}$ and σ'_{rr} and σ'_{v} are used to determined the maximum shear stresses generated at the borehole wall. These are then compared with appropriate shear strength envelopes for oil sands in order to evaluate shear failure.

Figure 3.15 shows the most critical stress states around a wellbore plotted on a p'-q plot for (a) two typical Athabasca deposit stress states and (b) one Cold Lake deposit stress state. It is readily apparent that for these three typical cases, the induced shear stresses around the wellbore exceed the shear strength of the oil sands. The oil sands around the wellbore can react to induced shear stresses in two ways: (i) plastic deformation or (ii) brittle rupture resulting in distinct shear surfaces. The actual oil sands response is governed by stress-strain response of the oil sands under in situ conditions and by the geologic structure.

Kaiser (1987) identified two categories of underground opening behaviour: stable behaviour where the deformations are limited and acceptable, and unstable behaviour where the deformations are large and unacceptable for engineering design. Figure 3.16 shows that the unstable modes can be divided into brittle rupture and ductile rupture modes. Geologic materials usually exhibit a transition from strain-softening behaviour at low confining stresses to elastic-plastic behaviour at higher stresses (Goodman

1980). While all previous triaxial tests show strain softening behaviour for Athabasca oil sands, Plewes (1987) observed general yielding at high confining stress for tests using frictionless platens. Figure 3.17 (Scott and Morgenstern 1987) shows elastic-plastic oil sands behaviour in the Athabasca Clearwater Formation. It is possible, therefore, that typical Athabasca oil sands payzones, with effective confining stresses exceeding 3.4 MPa, may behave in elastic-plastic manner. Alternately, global yielding may be the rupture (yield) mode for the oil sands around a wellbore. Localized shearing or yielding is also possible for heterogeneous oil sands or extremely shale interbedded oil sands.

Although wellbore stability is a prime concern in conventional oil recovery, few field studies and theoretical analyses of oil sands wellbore stability have been reported. Vaziri (1987) proposed a coupled diffusion-deformation formulation, solved by the finite element method, developed for predicting the extent of oil sands failure, in tensile and shear yield modes, due to stress relief caused by well drilling and subsequent fluid production. His model incorporates many of the features of oil sands geomechanics, such as nonlinear stress-strain behaviour, unsaturated flow characteristics, and gas evolution. Vaziri's finite element formulation is based on Risnes *et al.* (1982) analytical model for investigating wellbore stability in poorly consolidated materials. Vaziri's model predicts that for zero cohesion, instability occurs when the wellbore pressure becomes less than the formation pore pressure and fluid flows toward the well. In a producing well, instability is characterized by the creation of a tensile zone immediately around the wellbore (where the minimum normal stress is zero) which grades into a plastic oil sand zone, then into a non-linear elastic zone and evenutally into undisturbed oil sands. The development of these zones results from the seepage forces as fluid flows to the well. The formation cohesion and the pressure reduction gradient (dp/dr) are the main factors controlling wellbore stability.

As discussed earlier, the relevant poroelastic properties of oil sands (B, G, K, α, and k) imply that poroelastic effects would be evident during hydraulic

fracture tests in oil sands. A poroelastic analysis of wellbore stability along the lines provided by Detournay and Cheng (1988) would be a valuable exercise, but it remains beyond the scope of this thesis.

3.3 Hydraulic Fracture Studies in Oil Sands

There have been few published studies of hydraulic fracturing in oil sands. These studies can be divided into (a) theoretical, (b) laboratory, and (c) field. Theoretical studies have followed along two routes, one being the conceptual geomechanical model of oil sands hydraulic fracturing proposed by Dusseault (1980a,b, c) and the other being numerical modelling efforts of Settari and Raisbeck (1978, 1981) and Settari *et al.* (1989). Only one case of laboratory experiments of hydraulic fracturing in oil sand have been reported (Raisbeck and Currie 1981). Such testing, however, has proven to be valuable in hydraulic fracture studies in other materials. Field studies (Holzhausen *et al.* 1980; Bawden 1983; Chhina and Agar 1985; Chhina *et al.* 1987) are more numerous and have provided further insight into hydraulic fracture behaviour in oil sands.

The results from these studies, in conjunction with the implications from the review of oil sands geomechanics, provide a basis for evaluating the hydraulic fracture theories discussed in chapter 2 and the subsequent formulation of a hydraulic fracture theory suited for oil sands. This section reviews previous observations of hydraulic fracture behaviour in oil sands.

3.3.1 Theoretical Studies

Theoretical studies have centered on attempts to model hydraulic fractures induced during enhanced recovery operations, typically cyclic steam stimulation. Hydraulic fracture stress measurements are discussed in terms of providing input data for simulation studies (Settari and Raisbeck 1981). Such studies have indirectly supplied insight into the relationship between hydraulic fracturing and in situ stress. Two approaches are reviewed: the numerical modelling of Settari and Raisbeck (1978, 1981) and

Settari *et al.* (1989) and the conceptual geomechanical model of Dusseault (1980 a,b,c).

3.3.1.1 Numerical Modelling

The continuing refinement of the numerical modelling of cyclic steam stimulation by Settari and Raisbeck (1978,1981) and Settari *et al.* (1989) has produced information about hydraulic fracture behaviour in oil sands. Their model attempts to incorporate the following mechanisms: (i) fracture propagation kinematics and their dependence on elastic properties, injection rate and leakoff; (ii) two-phase flow in the formation with thermal and relative permeability effects; and (iii) fluid and heat transport in the fracture. Hydraulic fracturing for stress measurement purposes in oil sands involves a more simplified analysis of the mechanisms. It does not consider two-phase flow and or thermal effects.

The major components of Settari and Raisbeck's (1978,1981) model is as follows. Oil sands is assumed to be in a state of elastic stress and it behaves, under in situ conditions, like cemented rock (e.g., a soft sandstone). Consequently, it fails by brittle fracture. Fracture initiation and propagation, therefore, can be treated in terms of linear elastic fracture mechanics. Because there is some uncertainity regarding the drainage conditions, both non-fluid diffusion and fluid diffusion conditions (i.e. poroelastic) equations are given.

In their 1981 paper, Settari and Raisbeck note some of limitations of oil sands behaviour. They state that oil sands behaviour is distinctly nonlinear, even under initial in situ conditions. This problem is averted by using equivalent secant moduli corresponding to the loading conditions. While oil sands tensile strength is very low, it does not necessarily have a low specific surface energy (i.e., low fracture toughness). In fact, due to plastic straining at the fracture tip, the propagation energy may be unusually high. These factors affect the applicability of linear elastic fracture mechanics to an analysis of oil sands hydraulic fracturing.

A major source of uncertainity in their model is that while fracture propagation is primarily stress controlled, lithologic and stratigraphic variations can alter the actual fracture shape and orientation. This predicament is compounded by the presence of hydrostatic stress states at the depths usually associated with in situ recovery in the Athabasca deposit. Because of the predominant influence of in situ stress on fracture behaviour, it is imperative that the in situ stress state be known in order to predict hydraulic fracture behaviour. Fracture behaviour can be argued to be unique for each site, depending on the in situ stress state, formation properties and stratigraphy.

The next step in the modelling of oil sands hydraulic fracturing were the efforts of Settari *et al.* (1989) to incorporate important facets of oil sands geotechnical behaviour. Their model attempted to represent the conditions present during isothermal leakoff from the fracture face by coupling the fluid flow behaviour with the relevant oil sands mechanical properties. Their model was then checked against field observations from cyclic steam injection tests at Esso's Cold Lake site.

They began with a conceptual view of oil sands hydraulic fracturing in order to provide a framework for analyzing oil sands tests. First, the injection pressure increases until the in situ stress is overcome and fracturing takes place at a pressure slightly exceeding the total minimum principal stress. Second, during fluid injection, leakoff reduces the effective stresses near the fracture face which leads to shear failure. Shear failure is accompanied by dilation which results in a zone of enhanced porosity and permeability. The actual leakoff zone extends beyond the shear zone and is characterized by increased compressibility and permeability in areas of reduced effective stress. Third, their parametric studies showed that non-linear compressibility and shear failure were the main factors controlling injectivity (the formation's ability to accept injected fluid) or leakoff. The relationship between leakoff and fracture volume controlled the fracture dimensions. The mechanical properties, E, ν and K_{IC}, had little effect on fracture leakoff and, therefore, on fracture length.

Settari *et al.* (1989) also incorporated in their model the effective confining stress dependent properties E and K, dilatant shear failure adjacent to the fracture, fluid mobility, water saturation and the pressure distribution. The mechanical properties E and K were especially variable at low confining stresses. These properties were also affected by the dilatant effects of shear failure. Shear failure also affected the permeability, but Settari *et al.* (1989) proposed two simplified permeability models. Prior to shear failure, their model uses local values for the mechanical properties and permeability. When shear failure is detected the mechanical properties are adjusted along with the permeability in order to account for the increased porosity. Plastic deformation after failure is not included thereby implying that post-failure deformation does is assumed not to affect the porosity.

Settari *et al.* (1989) tested the model against actual Cold Lake steam injection data, but the results are reviewed later under field studies.

3.3.1.2 Conceptual Modelling

In a series of papers in 1980, Dusseault (1980a,b,c) proposed a conceptual geomechanical model to explain hydraulic fracture behaviour in Athabasca oil sands and to serve as a prediction tool for large volume hydraulic fracture treatments connected with steam injection. The basic features of this model are outlined below.

Starting with the mechanics of hydraulic fracture, Dusseault argued that since oil sand possesses no tensile strength, conventional fracture mechanics theory is inapplicable for oil sands. Fracturing infers the breaking of bonds between particles resulting in a permanent discontinuity. In oil sands, only a minimal amount of energy is necessary to overcome interparticle penetration to create a physical parting between grains. No true discontinuity will remain after injection stops except a possible zone of increased porosity. For small volume hydraulic fracture tests in oil sands, this explains the similarity between breakdown, propagation and shut-in pressures cited by Dusseault.

Hydraulic fracture propagation is a function of energy minimization, therefore, for a non-hydrostatic stress field in a homogeneous isotropic formation, a fracture extends normal to the minimum principal stress. Under in situ stress conditions approaching hydrostatic, vertical and especially horizontal fractures will tend to climb (in order to minimize work) since the minimum principal stress normally decreases upward in the formation. The presence of geologic discontinuities, such as bedding, joints, and fractures, will have definite effects on vertical and horizontal fracture containment and orientation. If horizontal fractures intersect geologic discontinuities, they will be deflected or pass through according to work minimization principles. Vertical fractures will grow both laterally and vertically, but will be confined vertically if the fracture intercepts a bed of higher cohesive strength. The shaley silt beds found in the Athabasca deposit inhibit vertical fracture growth because the fracture requires additional energy to cross them. In some cases, the bounding beds may also experience pore pressure reduction in advance of the propagating fracture as the fracture causes shear failure and associated dilation. Decreased pore pressures will increase the effective stresses and the formation's resistance to shear and fracture. This is valid for low viscosity fluids injected at moderate rates so that pressure losses in the fracture are minimal.

As a result of fracture climbing, shear stresses will develop along the fracture because it is no longer normal to σ_3. These stresses are relieved by shear strains expressed as lateral displacements across the fracture plane and in advance of the propagating fracture. Shear distortion is accompanied by a narrow plane of elastic dilation.

Dusseault also noted the many poroelastic effects evident during fracturing. Extensive fluid leakoff occurs despite attempts to limit leakoff through the use of viscous fluids and high injection rates. Fluid leakoff raises the pore pressure, reduces the effective stresses and increases the possibility of shear failure. Shear dilation accompanies fracturing and reduces the pore pressure, but gas evolution due to stress unloading will tend to maintain the pore pressures. At the time, the inadequate knowledge of the relative

permeability to water and the compressibility of oil sand prevented Dusseault from predicting these pore pressure changes.

Extensive remoulding of the oil sands in the vicinity of the borehole occurs during hydraulic fracturing with high injection rates and heated fluids. The strength and stiffness are reduced and the fracture/parting will reheal under the action of the formation stresses when injection stops. Subsequent fluid injection will probably result in plastic deformation rather than brittle fracture.

Fluid flow in the induced fractures is not possible after shut-in because the fractures will reheal. Formation fluid flow will predominate only after shut-in, while fracture fluid flow will dominate during fluid injection.

3.3.2 Laboratory Observations

Although laboratory studies of hydraulic fracturing under controlled conditions have been quite valuable in understanding this phenomena, only one such study for oil sands is publicly available.

Raisbeck and Currie (1981) performed laboratory simulated hydraulic fracture tests on rich oil sands core. The samples were obtained by conventional coring techniques and although they experienced reductions in bulk density, radiograph examination of the samples suggested that the disturbance was not great. The 5.3 cm x 2.5 cm cylindrical samples were subjected to triaxial stress states with the axial load independently controlled (σ'_3 = 3.8 MPa and σ_v = 4.2 MPa). During fluid injection, the pressure rose quickly to 6.5 MPa and then declined slowly to a final value of 1.6 MPa. Radiograph examination of the samples showed that a discrete fracture was created. "There is evidence (from radiographs and visual inspection) that fluid injected into the wellbore first permeates outward into the sand, then gradually creates a narrow path of enhanced injectivity (fracture) by inter-granular adjustment among grains and groups of grains which propagates progressively outward towards the sample margin." Material dilation in the injected zone appeared to accompany fracturing.

Preliminary injection tests were conducted at the University of Alberta in 1986 (Morgenstern and Scott 1986). The sample consisted of compacted oil sand with a bulk density of 2.00 g/cm^3, a porosity of 37% and a fluid saturation of 92.5%. After two injection cycles the sample was sectioned and a wedge shaped zone of fracture fluid penetration at the borehole midheight was found (Figure 3.18). No discrete fracture was found.

Such experimental evidence is provocative. Obviously more rigorous experimental programs, along the lines performed by other investigators for other geologic materials, are necessary in order to test hydraulic fracture models for oil sands and to better understand the mechanisms involved.

3.3.3 Field Studies

Field studies of hydraulic fracturing have been reported by Holzhausen *et al.* (1980), Bawden (1983), Chhina and Agar (1985), Gronseth (1988) and Settari *et al.* (1989). These particular studies are reviewed because they provide valuable information concerning hydraulic fracture behaviour with respect to in situ stress measurements. Field studies of cyclic steam stimulation induced hydraulic fractures are not included because they involve factors not relevant to hydraulic fracture stress measurement tests.

Holzhausen *et al.* (1980) conducted a cold water minifrac test and one cycle of steam stimulation, in which the ground deformation was monitored, in the Athabasca oil sands deposit at a depth of 310 m. The initial cold water test in a perforated interval (308-317 m) had a breakdown pressure of 9300 kPa, and a propagation pressure and shut-in pressure of 5600 kPa. They concluded that a vertical fracture was created because the shut-in pressure (5600 kPa) was less than the total vertical stress (6500 KPa). The substantial difference between breakdown and shut-in pressures suggests a significant fracture resistance existed around the borehole which is possibly related to the casing.

The steam injection response suggested that steam and hot water entered the formation in discrete events rather than in a continuous manner. "The pressure, flow, and ground responses during the events bear a strong

resemblance to those observed during cold-water hydraulic fracturing, suggesting that planar, fracture-like structures were forming and serving to conduct hot water and steam laterally away from the wellbore." Although planar hydraulic fractures have been found in brittle consolidated materials, Holzhausen *et al.* (1980) argued that since planar fractures have been found in plastic clays, such features are possible in inelastic oil sands subjected to steam injection.

Based on the observed surface deformation patterns, they proposed that horizontal fractures had been created. The difference between the cold water test vertical fractures and the steam stimulation test horizontal fractures was attributed to the possible modification of the in situ stress regime during the two weeks of steam injection. Such a mechanism has been analyzed by Dusseault and Simmons (1982) and noted by Chhina and Agar (1985).

Holzhausen *et al.* (1980) applied linear elastic fracture mechanics in order to analyze the observed fracture propagation behaviour. They argued that such an analysis was reasonable for crack propagation in unheated oil sands, but inappropriate when the crack tip was in the heated oil sands. In linear elastic fracture mechanic theory, sharp crack tips are capable of developing high tip stresses without the development of significant process zones (plastic zones characterized by permanent deformation). For materials prone to inelastic or plastic deformation, such as heated oil sands, a significant process zone can develop ahead of the crack tip. Consequently, the blunted crack tip experiences reduced stress concentrations which inhibit fracture propagation. This process is manifested in small pressure drops when fracture breakthrough does occurs. Holzhausen *et al.* (1980) suggest that this fracture mechanics approach may explain the variable pressure drops recorded during the treatment, with large drops associated with unstable fracture propagation in unheated oil sand and with small drops attributed to fracturing in inelastic, heated oil sands.

Bawden (1983) provided a summary of hydraulic fracturing in oil sands He stated that the small volume hydraulic fracture tests he had analyzed showed a substantial difference between the breakdown, propagation and

shut-in pressures. From these findings he inferred that boreholes in oil sands were capable of withstanding the stress concentration induced around the borehole. He did not think this was due to an unexpected oil sands tensile strength. He recommended that further study of the effects of oil sands expansion, due to gas evolution and elastic unloading, on wellbore damage was required in order to address this problem Although oil sands possess an interlocked fabric leading to strength behaviour similar to that of a soft sandstone, the potential effects of wellbore damage should be evaluated.

Chhina and Agar (1985) and Chhina *et al.* (1987) provide the most comprehensive hydraulic fracture data for oil sands based primarily on hydraulic fracture stress measurement tests. Two case histories of hydraulic fracturing in oil sands are particularly interesting.

In the first case (Chhina and Agar 1985), a hydraulic fracture stress measurement test conducted at 342 m depth was observed to initially create a horizontal fracture because the injected fluid was "...confined between two closely spaced shale stringers." As the fracture broke through the confining layers, indicated by a sudden drop in the propagation pressure, the fracture became vertical.

In the second case (Chhina *et al*, 1987), a series of hydraulic fracture tests were conducted at the Athabasca deposit in the McMurray Formation (305 m and 365 m.). A hot gelled water test was first performed at 352 m and gave P_f = 8740 kPa and P_s = 4600 kPa. Subsequently, coloured grout was injected at a depth of 352 m (P_f = 7710 kPa and P_s = 7020 kPa) and of 306 m (P_f = 6070 kPa and P_s = 5980). A coloured grout filled fracture was observed at an inclination of 85° to the horizontal in a post-test core well drilled 7.6 m from the injection well. It was concluded that the initial fracture was horizontal, but it climbed upwards at 40° from the horizontal and gradually became vertical a short distance away from the injection well. Furthermore, discrete horizontal fracture fingers were observed rather than a single planar fracture.

The observations of Chhina and Agar (1985) and Chhina *et al.* (1987) can be combined to form some conclusions regarding fracture propagation in oil sands. First, shear stresses can develop near and in advance of the

propagating fracture. Shear failure may be the predominant failure mode when fracture propagation is no longer restricted to a plane normal to σ_3. This can occur under two conditions: (i) when in situ stress conditions are hydrostatic and geologic discontinuities begin to control fracture propagation, and (ii) when in situ stress conditions dictate horizontal fractures (which have a tendency to climb and be deflected by geologic discontinuities). Under such circumstances, when fracture propagation is not normal to σ_3, shear stresses develop near and ahead of the propagating fracture. Fluid leakoff, by raising the local pore pressures, enhances the conditions for shear failure.

Second, it was also concluded that for shallow conditions (low confining stresses), shear failure will be accompanied by dilation on a number of sub-parallel and/or intersecting planes beyond the fracture tip. This was realized in the discrete fracture fingers observed in the Athabasca deposit test. Further evidence consisted of pore pressure decreases observed in adjacent wells suggesting dilatancy during shear deformation as a possible mechanism. Surface heave monitored at several in situ projects cannot be adequately explained solely in terms of pressure and temperature effects, therefore, it may be explained by deformation associated with shear dilatancy of the formation.

Third, tensile fracture is not an appropriate description of mechanism involved in hydraulic fracturing. The concept of a parting is more appropriate when confronted with (i) the absence of oil sands tensile strength, (ii) the anomalous pressure responses in observation wells and (iii) the lack of discrete planar fractures in the field.

Settari *et al.* (1989) stated four common observations of hydraulic fracture behaviour in oil sands which they attempted to model by incorporating oil sand geomechanics in their numerical simulator. These four observations were: (i) the comparatively small fracture dimensions and large fracture widths; (ii) an unexpectedly high injectivity; (iii) the quick fracture closure times due to large fluid leakoff; and (iv) the rapid pressure responses seen in observation wells.

Settari *et al.* (1989) also reported the results of comparison between observed pressure responses from two Cold Lake hydraulic fracture field tests and their model predictions. For both the vertical and horizontal fracture cases, incorporation of dilatant shear failure and non-linear stress-strain behaviour reduced the volume of injected fluid and, therefore, the induced fracture lengths. Results of field pressure matching indicated that these factors should be considered in order to predict the smaller fractures associated with oil sands hydraulic fracturing.

Chhina (1988) conducted openhole hydraulic fracture stress measurement tests at shallow depths at the UTF site. Openhole tests in oil sands are rare and, theoretically, the fracture initiation pressure can be used to determine the maximum horizontal principal stress. However, the interpretation of the oil sands tests suggested that fracturing was predominantly horizontal, thereby negating the use of the classic hydraulic fracture initiation analysis. Tests conducted in the underlying Devonian limestone gave closure stress values greater than the vertical stress implying that the minimum horizontal stress exceeded the vertical stress. This contravenes current Alberta oil sands in situ stress data which are discussed in chapter 5.

3.4 Summary

The geomechanical behaviour of oil sands and its most important effects on hydraulic fracture theory and practice have been reviewed. Previous oil sands hydraulic fracture theory, laboratory and field investigations have provided insight into oil sands hydraulic fracture behaviour. Table 3.4 summarizes the various oil sands factors affecting hydraulic fracture theory. Table 3.5 summarizes the influence of oil sands factors on hydraulic fracture propagation.

Oil sands behaviour affects the hydraulic fracture initiation theories to varying degrees. An adequate evaluation of the three tensile fracture theories has been limited because most field tests occur in perforated cased boreholes.

Fracture mechanics has received special attention in the oil industry because of its incorporation in many fracture simulators, but, as outlined in chapter 2, many practical considerations have prevented its use in oil sands stress measurements. Meanwhile shear failure theory and plastic failure theory have only recently been proposed and very little experimental research has been conducted on their behalf. Any assessment of the influence of the oil sands hydraulic fracture factors on these two theories, therefore, remains speculative. Oil sand possesses many unique geomechanical properties previously unconsidered in hydraulic fracture theory. Laboratory hydraulic fracture stress measurement tests along with controlled field tests are needed to investigate these oil sands properties.

The limited review of hydraulic fracture theory conducted here leads the author to conclude that only openhole tests will allow a conclusive evaluation of hydraulic fracture initiation. When such conditions do exist, the temptation is to use the simplest theory because the knowledge of the pertinent geomechnical, geological and fluid-flow properties necessary for the more sophisticated analyses is usually incomplete. Hydraulic fracture initiation analysis is contingent on the knowledge of these properties.

For the majority of field hydraulic fracture stress measurement tests, which are conducted in perforated cased boreholes with only pressure data being recorded, a hydraulic fracture initiation analysis is questionable. What remains important is an understanding of the factors that affect hydraulic fracture propagation in oil sands and the interpretation of the minimum principal stress from these tests.

Some researchers, most notably Dusseault (1980a,b,c) have argued that hydraulic fracturing does not create discrete tensile fractures. Instead, materials with no stress independent tensile strength, such as oil sand, fail by "parting" in hydraulic fracturing tests. Raisbeck and Currie's (1981) laboratory test on disturbed oil sand tends to confirm this concept. The field evidence of Chhina and Agar (1985) and Chhina *et al.* (1987) also refutes the notion of discrete planar fractures. The complex fracture geometries which may result currently cannot be handled by numerical fracture models which

use idealized fracture geometries and fracture propagation criteria. Fortunately, identification of the appropriate failure mode is more critical to hydraulic fracture initiation. Hydraulic fracture propagation in oil sands is affected to a greater extent by other factors.

Oil sands geomechanics and previous hydraulic fracture studies in oil sands were reviewed in order to determine the factors affecting hydraulic fracture propagation (Table 3.5). The geomechanical behaviour of oil sands reveals the potential influence of fluid leakoff, poroelastic effects, failure mode, and wellbore condition on aspects of fracture propagation. Theoretical, laboratory, and field studies of oil sands hydraulic fracturing emphasize the importance of geologic discontinuities, climbing fractures and the in situ stress state on hydraulic fracture propagation.

Some of these factors, such as geologic discontinuites and fluid leakoff, have been observed in hydraulic fracture tests in other rock types (e.g., granite, shale and sandstone). Often the determination of the minimum principal stress from these tests is difficult because the shut-in pressure response is distorted and is very different from the classic response. Subsequently, many hydraulic fracture practitioners have proposed various methods for interpreting these complicated shut-in pressure responses. These methods are discussed in chapter 4.

Table 3.1 Reported permeability values for Alberta oil sands.

Permeability Value	Reference	Comments
10 md	Hackbarth and Natasa (1979)	An effective permeability to water derived from in situ pump tests conducted in the Athabasca deposit (range in values of 1 to 1000 md).
9 to 12 md	Agar (1984)	Laboratory effective permeability of Athabasca oil sand to water at room temperature.
17.7 md	Sufi and Thompson (1988)	Falling head test at 240 m depth in the Athabasca deposit.
22.4 md	"	Pressure fall off test at 240 m depth.
8.6 md	"	Falling head test.
10.4 to 10.6 md	"	Pressure build-up test.
31.1 to 115.7 md·m	Chhina (1988)	Transmissivity to water from microfrac tests.

Note: 1 md = 9.869×10^{-16} m^2

Table 3.2 Effect of confined drained and unconfined drained stress path tests on the stress strain properties of Athabasca and Cold Lake oil sands (after Kosar *et al.* 1987).

	Athabasca		Cold Lake	
Stress Path	CD	CU	CD	CD
Property				
σ_3	4.0 MPa	2.0 MPa	4.0 MPa	2.0 MPa
E_i	2200 MPa	276 MPa	677 MPa	570 MPa
ν	0.22	----	0.27	-----
$\left(\frac{\sigma'_1}{\sigma'_3}\right)_{max}$	5.2 MPa	4.7 MPa	2.8 MPa	5.4 MPa
$(\sigma_1-\sigma_3)_{peak}$	16.9 MPa	10.7 MPa	6.9 MPa	6.0 MPa
$(\varepsilon)_{max.\ ratio}$	1.1%	1.6 %	2.5%	1.1%
$(\varepsilon)_{peak}$	1.1%	8.7%	2.5%	2.0%

Notes
CD denotes confined drained stress path.
CU denotes confined undrained stress path.

Table 3.3 Effect of stress path on the isotropic compressibility (K) and the confined compressibility (D) of Athabasca and Cold Lake oil sands (data from Kosar 1989).

Stress Path	Athabasca D (MPa)	Athabasca K (MPa)	Cold Lake D (MPa)	Cold Lake K (MPa)
Confined Compression	693 [1.6-3.3]	429[a] [1.0-2.0]	813 [4.0-12.0]	503[a] [2.5-7.4]
	941 [2.0-3.9]	583[a] [1.2-2.4]		
Isotropic Compression	693[b] [4.8-8.2]	429 [3.0-5.1]	1187-2460[b] [8.1-14.5]	735-1523 [5.0-9.0]
	997[b] [14.9-19.7]	617 [9.2-12.2]		

Notes

Range in confining stresses is given in brackets below the compressibility value.

All tests were conducted at 20 °C and the compressibility values are based on the second loading cycle.

[a] For the confined compression tests, the bulk modulus K was calculated according to the relationship $K = \frac{D(1+\nu)}{3(1-\nu)}$ for $\nu = 0.3$.

[b] For the isotropic compression tests, the constrained modulus D was calculated according to the relationship $D = \frac{3K(1-\nu)}{(1+\nu)}$ for $\nu = 0.3$.

Table 3.4 Oil sands factors affecting hydraulic fracture initiation theories.

THEORY / FACTORS	CLASSIC	HAIMSON & FAIRHURST	PORO-ELASTIC	LEFM	SHEAR FAILURE	PLASTIC FAILURE
STRESS-STRAIN BEHAVIOUR						
Linear Elasticity	significant	significant	significant	significant	significant	N/A
Homogeneity	significant	significant	significant	significant	significant	significant
Isotropy	significant	significant	intermediate	significant	significant	signiicant
Stress Path	significant	significant	significant	uncertain	uncertain	uncertain
MATERIAL STRENGTH						
Tensile Strength	intermediate	intermediate	intermediate	N/A	N/A	intermediate
Shear Strength	uncertain	uncertain	uncertain	uncertain	significant	significant
Stress Path	uncertain	uncertain	uncertain	uncertain	uncertain	uncertain
POROELASTIC PARAMETERS						
Drained vs Undrained	N/A	N/A	significant	uncertain	uncertain	uncertain
Permeability	N/A	N/A	intermediate	N/A	N/A	N/A
WELLBORE CONDITION						
Perforated Casing	invalidates	invalidates	invalidates	uncertain	uncertain	intermediate
Pre-existing Cracks	significant	significant	significant	low	significant	uncertain
Unstable Material	invalidates	invalidates	invalidates	uncertain	uncertain	uncertain
IN SITU STRESS						
Vertical Stress Assumption	significant	significant	significant	significant	significant	significant
Hydrostatic Stresses	low	low	low	low	significant	uncertain
GEOLOGIC DISCONTINUITIES	invalidates	invalidates	invalidates	intermediate	uncertain	uncertain
TEST PROCEDURES						
Injection Rate	intermediate	significant	low	low	uncertain	uncertain
Fracture Fluid Viscosity	low	intermediate	low	low	uncertain	uncertain

Table 3.4 Continued.

KEY TO ASSESSMENT GRADES IN TABLE 3.4

significant: either has a significant effect on hydraulic fracture initiation or it may even invalidate the theory in some cases.

intermediate: either has an intermediate effect on hydraulic fracture initiation or it may even invalidate the theory in a few cases.

low: variation in this factor will not generally affect fracture initiation.

uncertain: subject to conjecture but generally unknown effects.

invalidates: presence of this factor invalidates the theory.

Table 3.5 Oil sands factors affecting hydraulic fracture propagation.

1. **Fluid Leakoff**
   - influences fracture dimensions
   - induces pore pressure response which may affect shear failure

2. **Poroelastic Effects**
   -poroelastic properties of oil sands suggest that induced pore pressure may affect local total stress state
   -induced pore pressures may affect shear failure

3. **Failure Mode**
   - possibility of shear failure adjacent and ahead of the propagating fracture may alter fracture orientation
   - shear failure in oil sands has been found to cause dilation which may affect other factors (i.e., fluid leakoff, poroelastic parameters)

4. **Climbing Fractures**
   - climbing horizontal fractures deviate from the principal stress plane causing the development of shear stresses along the fracture (see 3)

5. **In Situ Stress State**
   - a major portion of oil sands payzones in the Athabasca deposit are located at intermediate depths where the in situ stress state is hydrostatic and the in situ stress no longer dominates fracture propagation (see 6)

6. **Geologic Discontinuities**
   - oil sands geologic discontinuities, in the form of interbedded oil sands-shale layers and cross bedding, can deflect propagating fractures
   - increased fluid leakoff may occur when fractures intersect geologic discontinuities resulting in smaller fractures (see 1)
   - cause multiple fracturing

7. **Wellbore Condition**
   - presence of perforated casing may introduce fluid flow restrictions at the wellbore entrance

(after Morgenstern *et al.* 1988)

Figure 3.1 Oil sands deposits of Alberta.

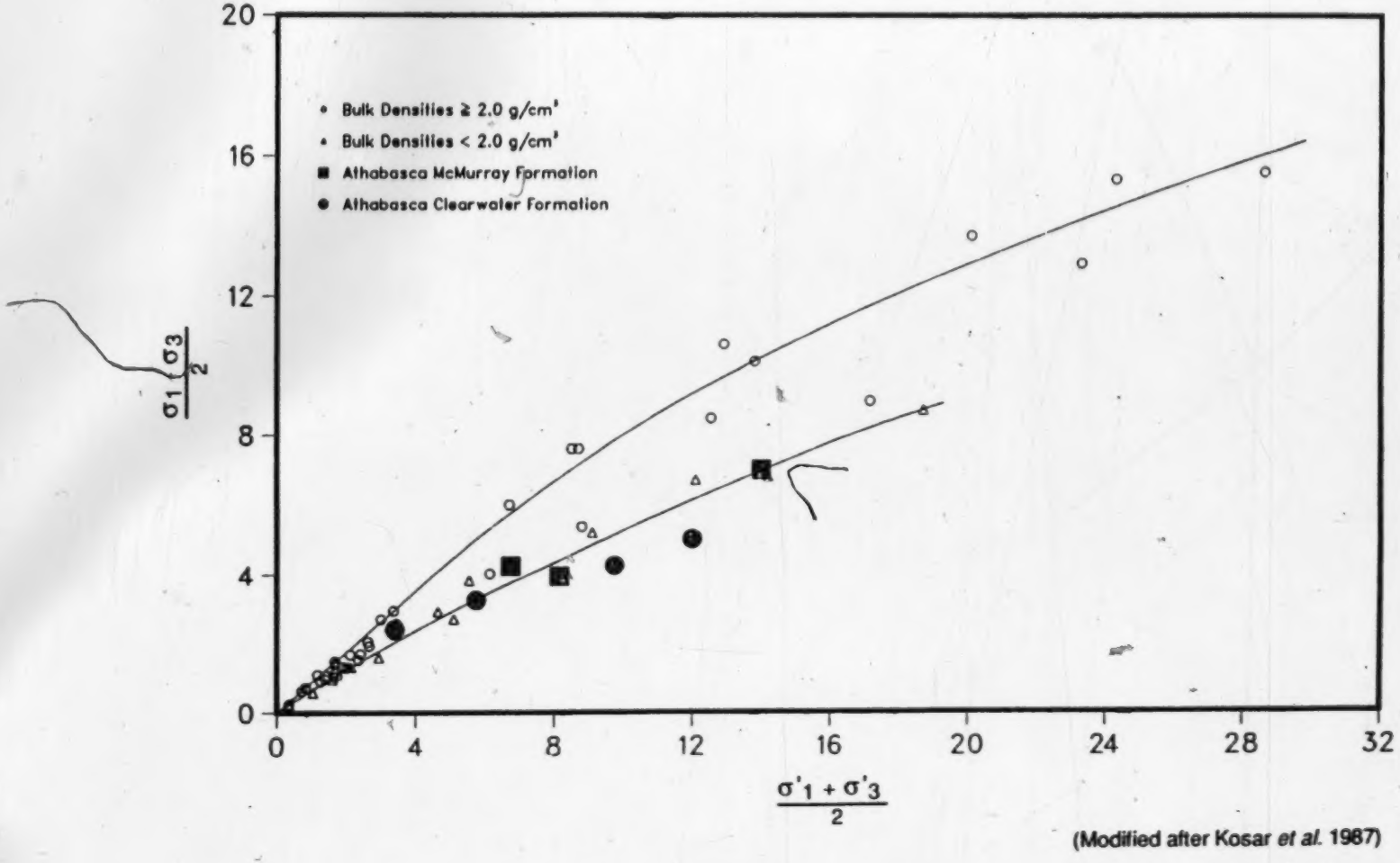

Figure 3.2 Typical shear strength envelope for Athabasca oil sands.

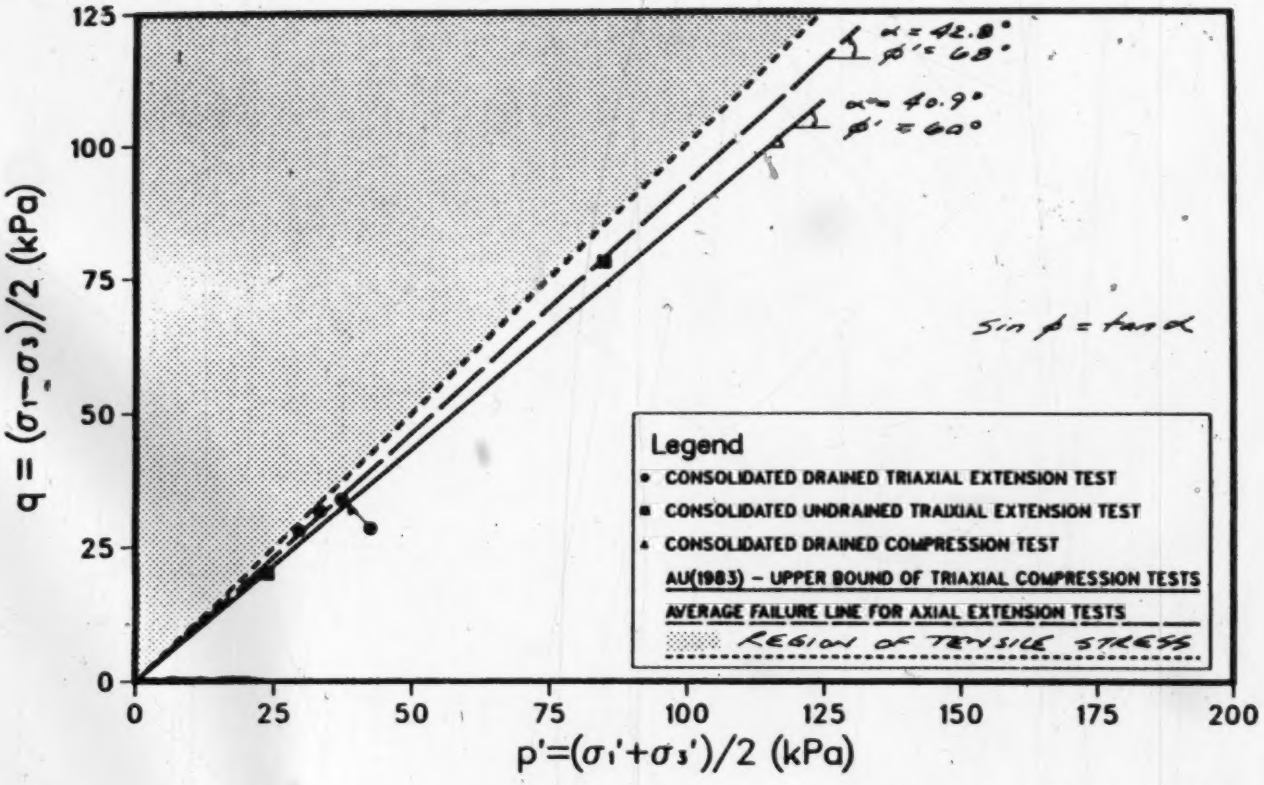

(After Plewes 1987)

Figure 3.3 Drained and undrained triaxial extension test results.

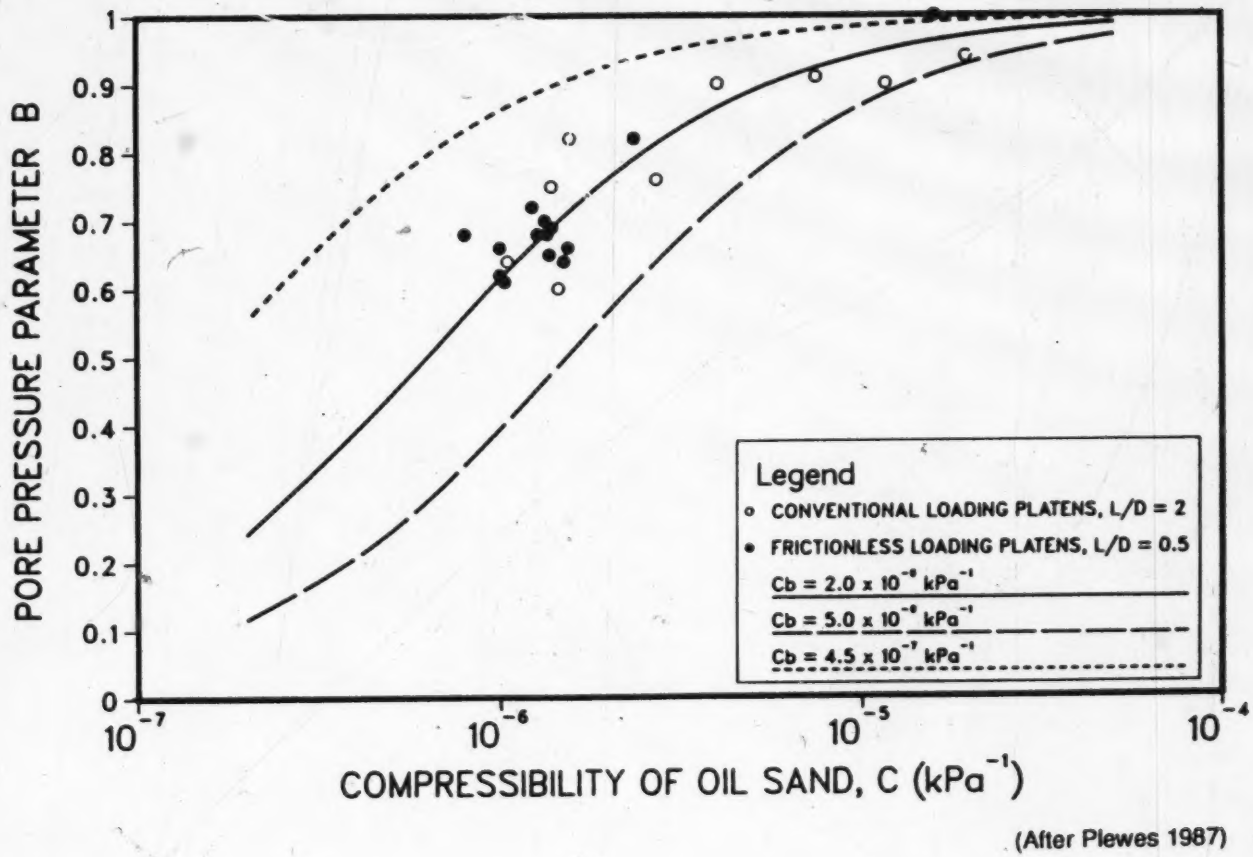

Figure 3.4 Relationship between pore pressure parameter B and oil sands compressibility.

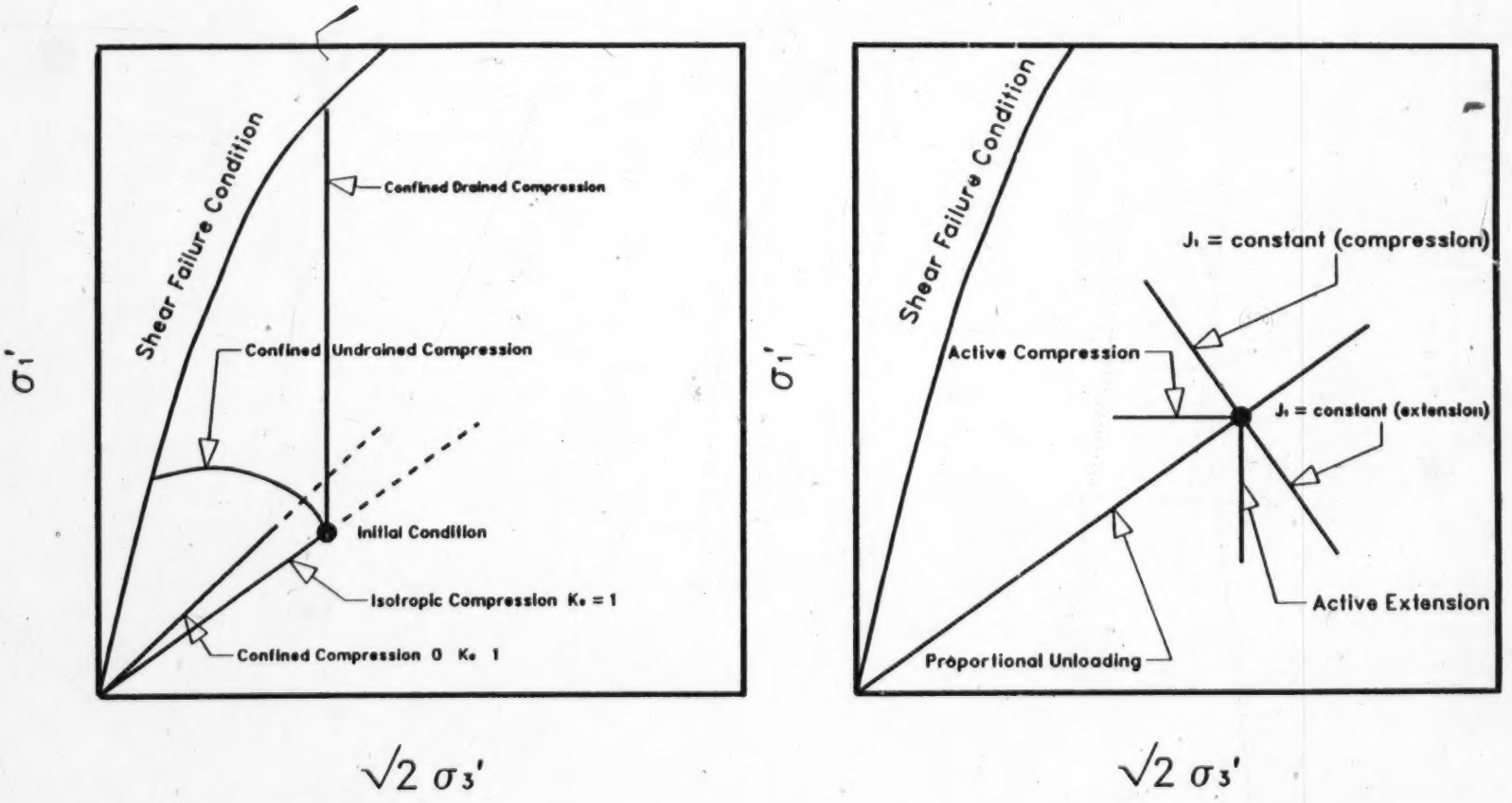

Figure 3.5 Stress paths used in geomechanics tests.

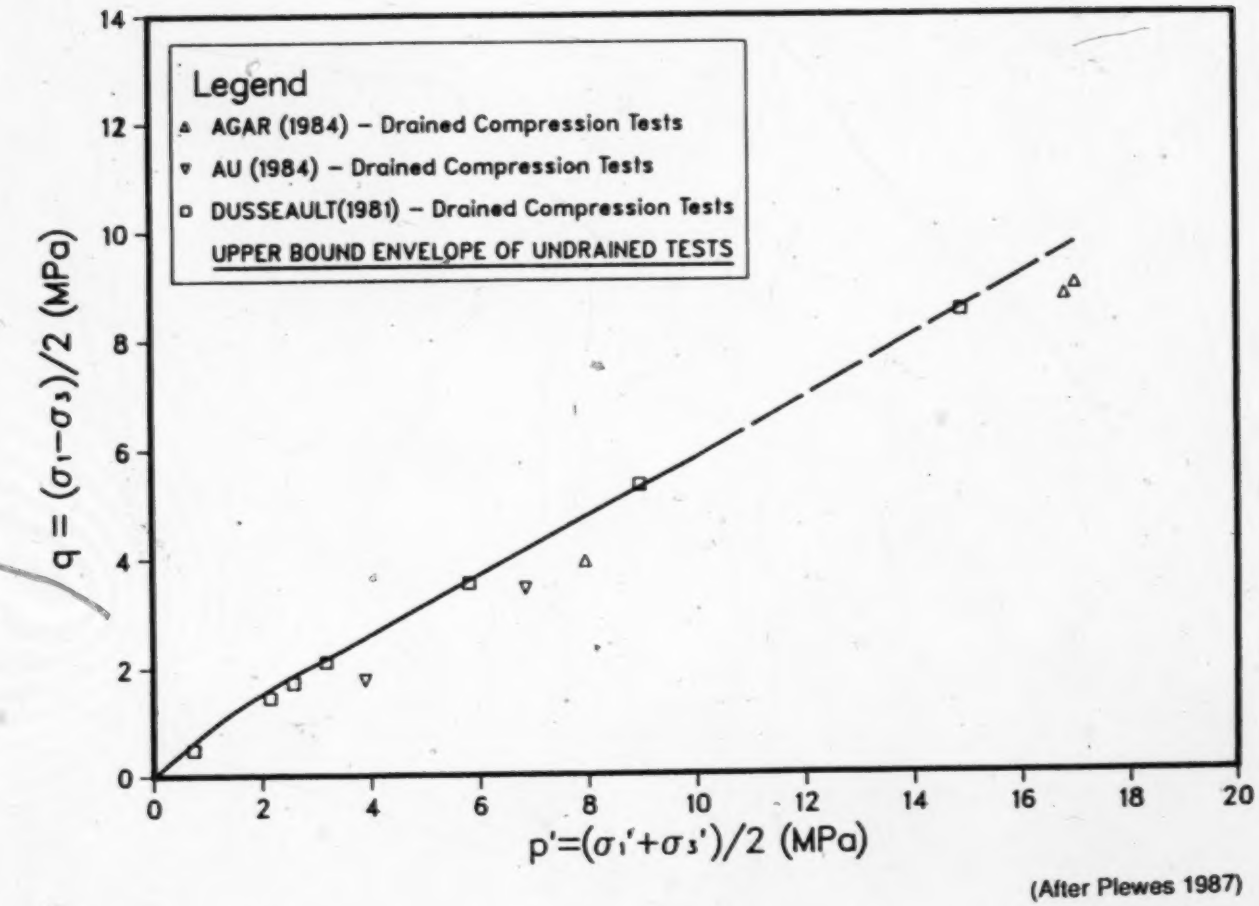

Figure 3.6 Comparison of undrained and drained shear strength data for oil sands.

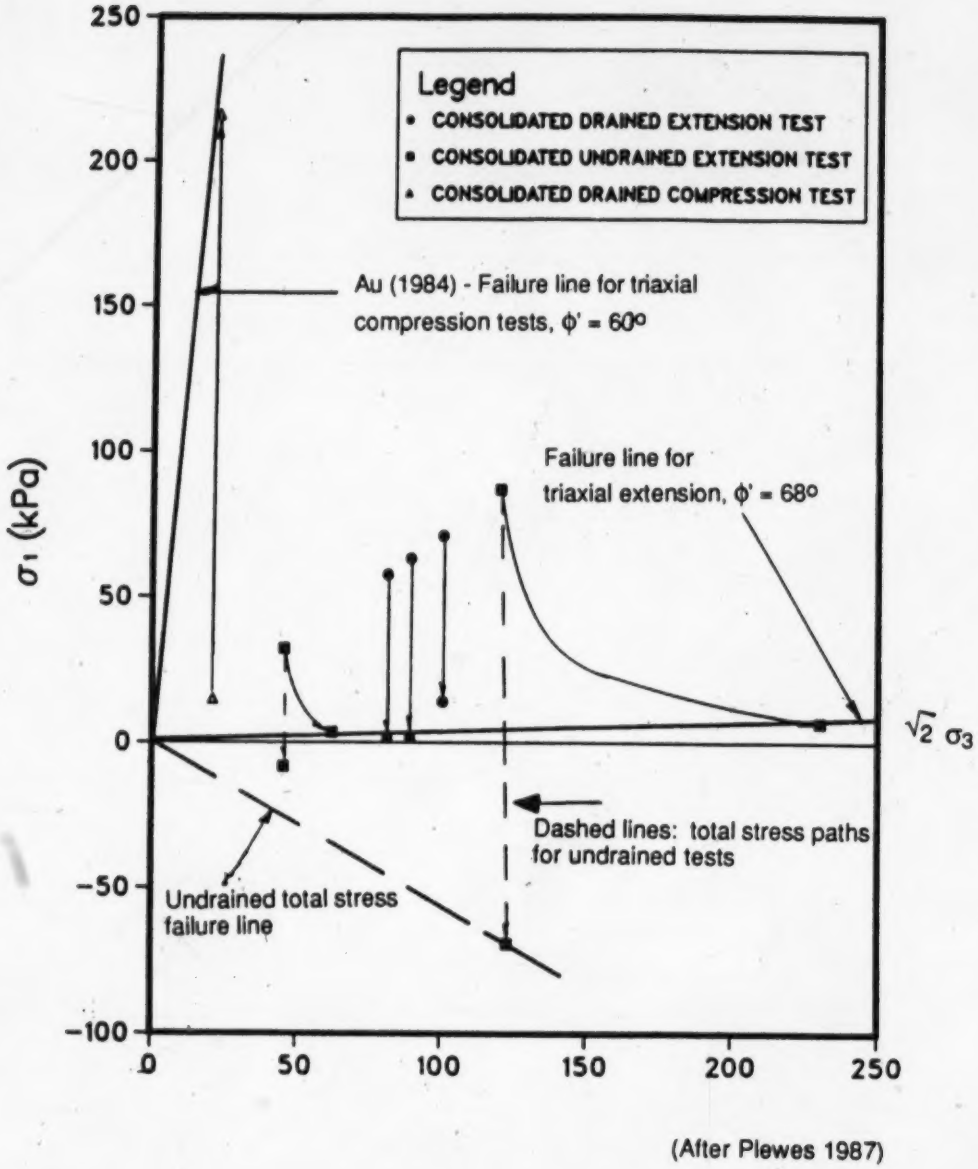

Figure 3.7 Stress paths to failure in triaxial stress space for triaxial tests on Syncrude oil sands.

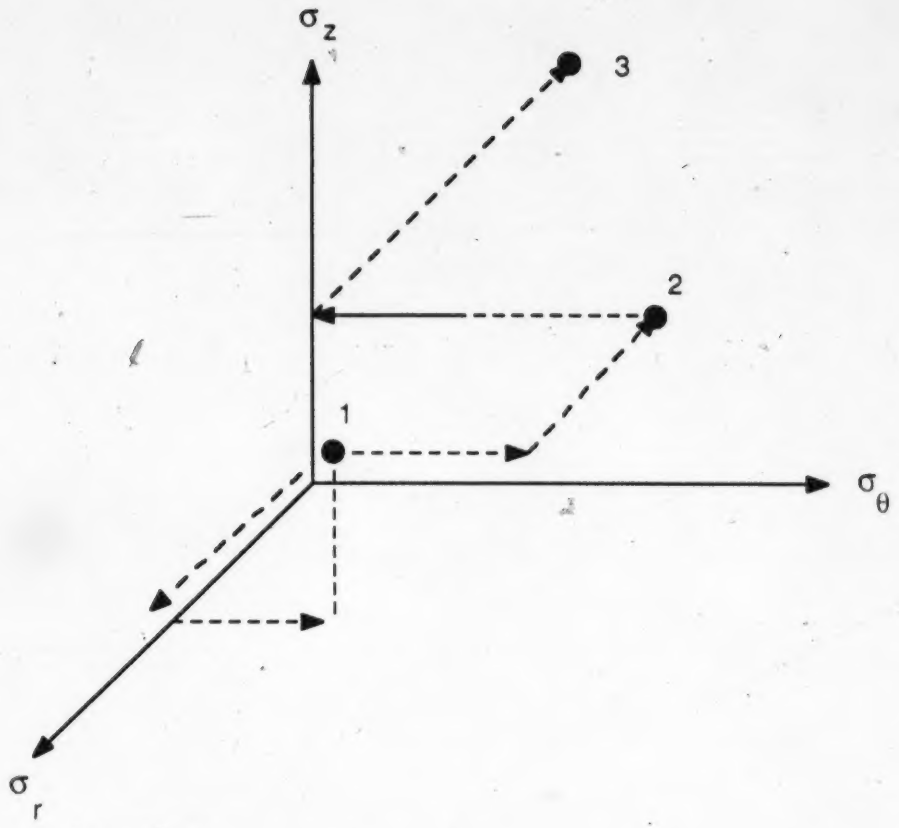

(1) Initial Conditions: $\sigma_\theta = \sigma_r = \sigma_z$

(2) Stresses at the borehole wall for hydrostatic conditions.

(3) Stresses induced by borehole pressurization.

Figure 3.8 Possible stress path for oil sands at depth which undergoes a drained response to borehole drilling and pressurization.

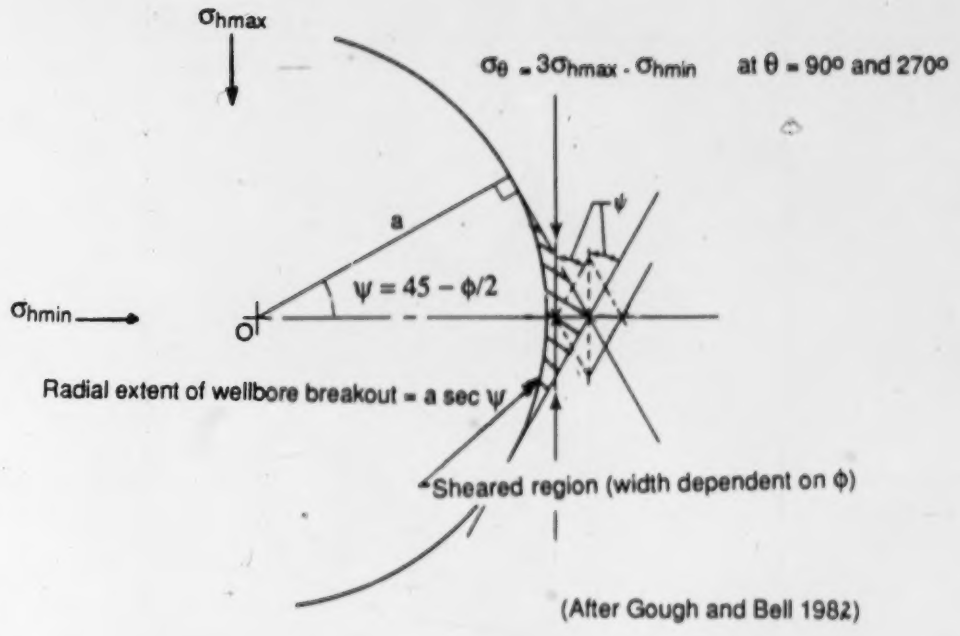
σhmax
σθ = 3σhmax - σhmin at θ = 90° and 270°
a
ψ
ψ = 45 − φ/2
σhmin
O
Radial extent of wellbore breakout = a sec ψ
Sheared region (width dependent on φ)
(After Gough and Bell 1982)

Figure 3.9 Localized shear failure around a wellbore leading to a wellbore breakout.

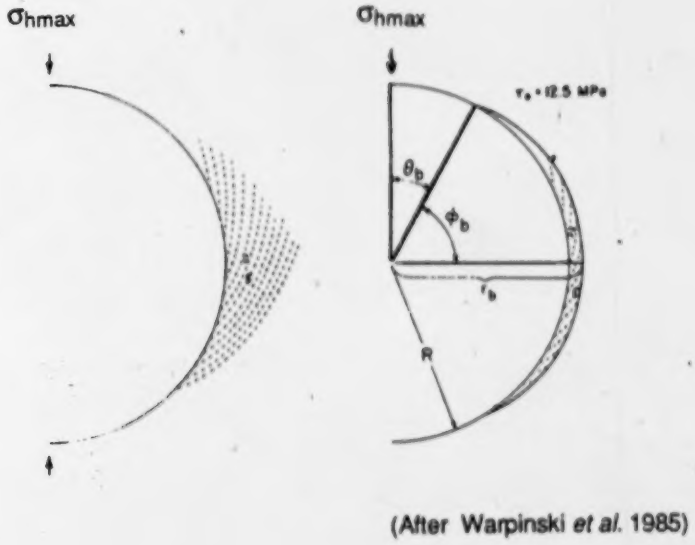

Figure 3.10 Potential shear failure surfaces around a wellbore based on a Mohr-Coulomb failure criteria.

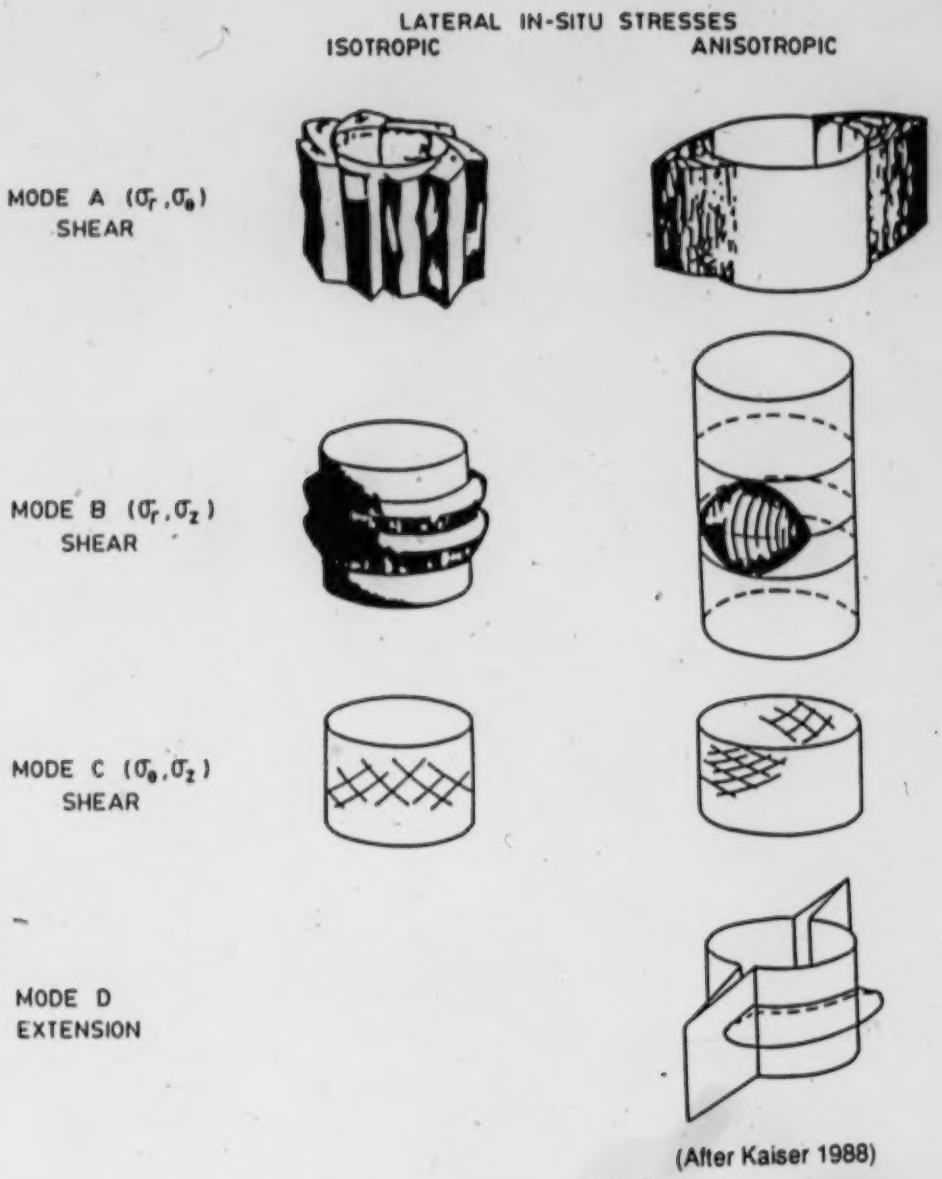

Figure 3.11 Possible borehole rupture modes.

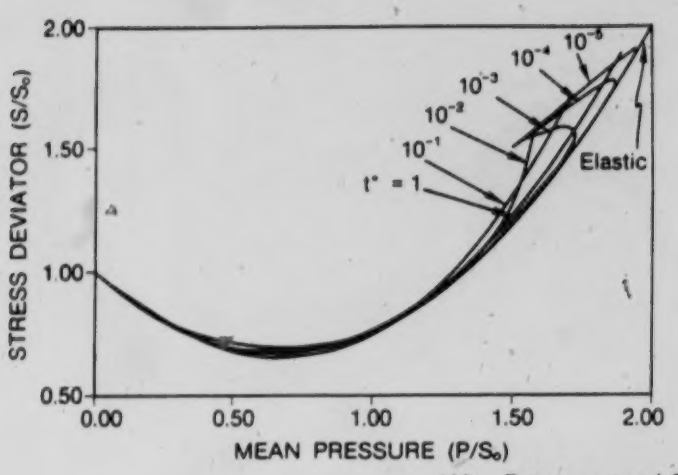

(After Detournay and Cheng 1988)

Figure 3.12 Total stresses developed around a borehole along a radial direction normal to the minimum principal stress calculated using poroelastic theory (deviatoric loading mode only).

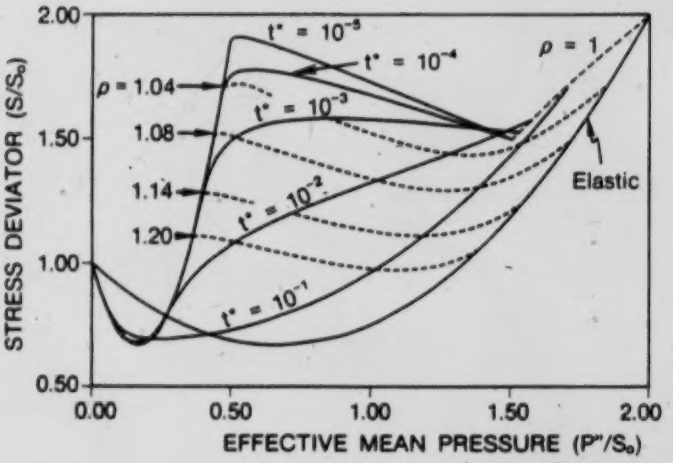

(After Detournay and Cheng 1988)

Figure 3.13 Effective stresses developed around a borehole along a radial direction normal to the minimum principal stress and calculated using poroelastic theory (deviatoric loading mode only).

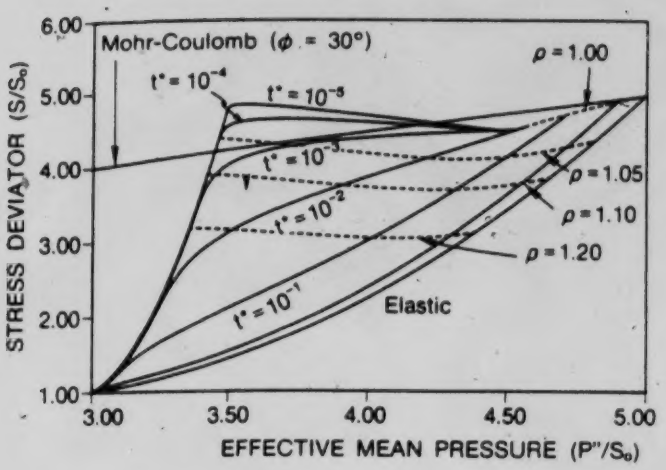

(After Detournay and Cheng 1988)

Figure 3.14 Evaluation of shear failure around a borehole based on poroelastic theory (for hydrostatic and deviatoric loading modes).

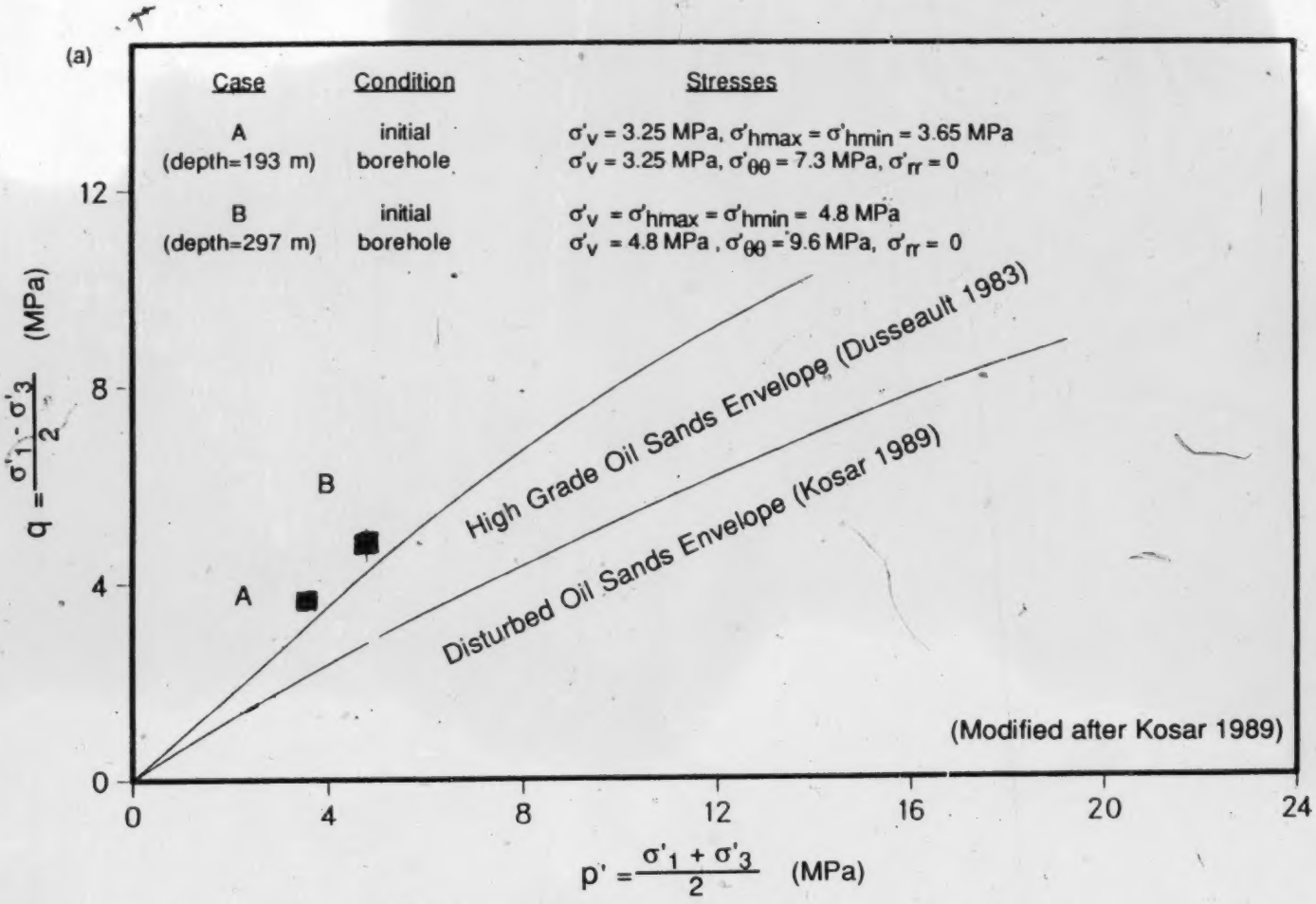

Figure 3.15 Elastic stress evaluation of possible shear failure around a borehole for (a) two Athabasca oil sands stress states and (b) a Cold Lake oil sands stress state.

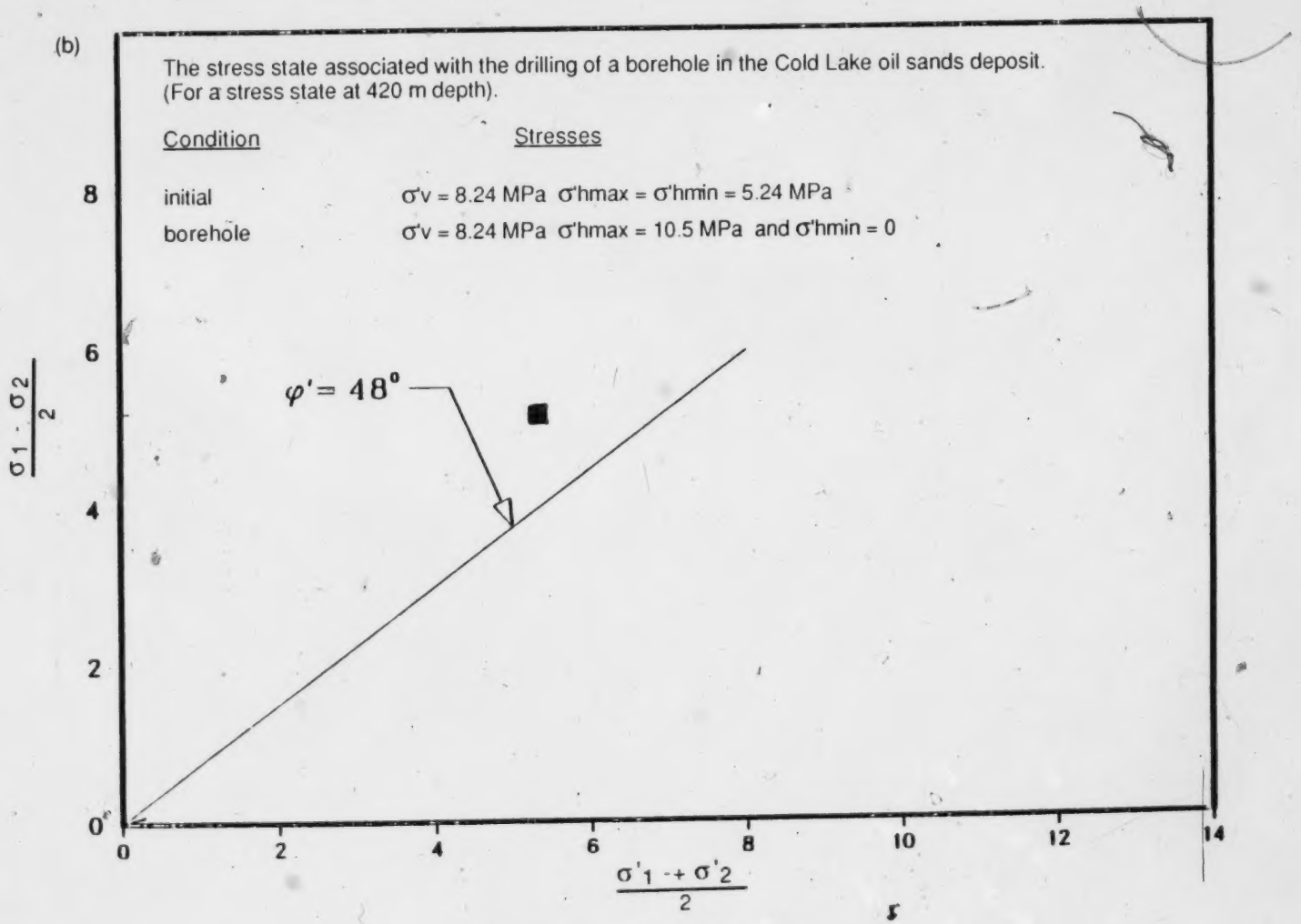

Figure 3.15 Continued

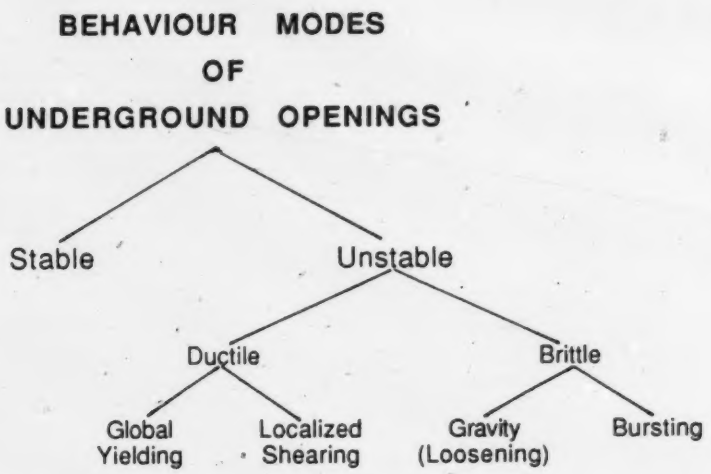

Figure 3.16 Unstable rupture modes for underground openings.

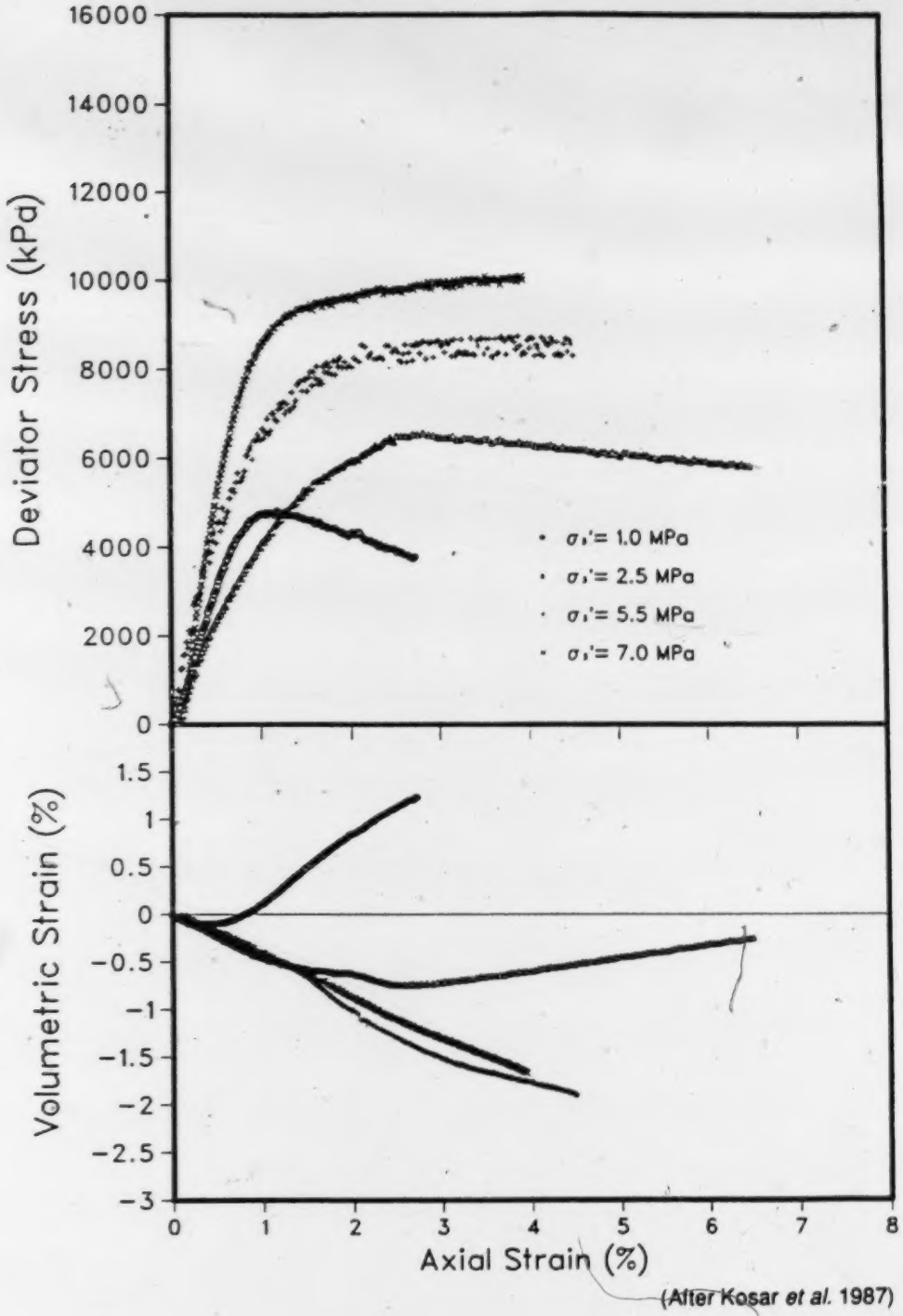

Figure 3.17 Stress-strain curves for Athabasca Clearwater Formation oil sands.

Figure 3.18 Sectioned oil sands sample indicating fluid penetration which occurred during a hydraulic fracture experiment: (a) photograph of the sample and (b) schematic drawing of the sample (modified after Scott and Morgenstern 1986).

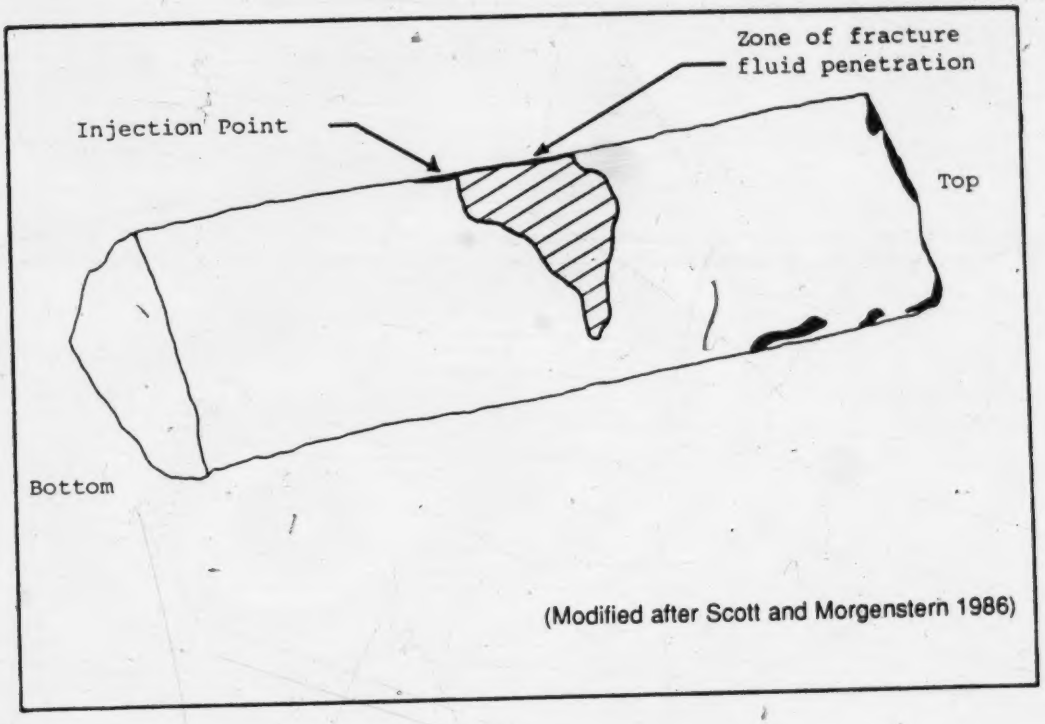

Figure 3.18 continued.

4. MINIMUM PRINCIPAL STRESS INTERPRETATION IN OIL SANDS MICROFRAC TESTS

4.1 Introduction

After reviewing hydraulic fracture stress measurement theory in chapter 2, the effect of oil sands behaviour on hydraulic fracure theory, considering the geomechanical properties and previous oil sands hydraulic fracture studies, was discussed in chapter 3. Two significant conclusions were made: (i) hydraulic fracture initiation theory generally cannot be used to determine the maximum horizontal principal stress because most oil sands wells are cased, and (ii) oil sands factors often distort the shut-in pressure response thereby complicating the determination of the minimum principal stress. Most oil sands hydraulic fracture tests, therefore, are limited to an estimation of the minimum principal stress and are difficult to interpret.

Research and field practice outside of oil sands practice has shown that many hydraulic fracture tests are plagued by material and test factors which affect the shut-in pressure response. Consequently, many techniques have been theoretically or experimentally derived for the interpretation of the minimum principal stress from complicated shut-in pressure responses. Oil sands shut-in pressure responses are often affected by many of these same factors. It seems plausible to examine the interpretation techniques developed outside oil sands practice to determine techniques most suited to oil sands behaviour. This chapter combines the findings of the previous two chapters with a review of hydraulic fracture in situ stress interpretation theory and practice.

The development of an interpretation method or technique was based on an examination of current theory and practice in analyzing hydraulic fracture shut-in pressure data. Chapter 4 pursues this objective in three parts: (i) a summation of current problems in the interpretation of hydraulic fracture shut-in pressure data, (ii) a review of laboratory, empirical and

experimental shut-in pressure interpretation techniques; and (iii) a proposed method for interpreting oil sands shut-in pressure data.

In the literature on shut-in pressure interpretation, two terms, instantaneous shut-in pressure (ISIP or P_s) and closure pressure (P_c), are encountered when determining the minimum principal stress. The following section explains the differences between these two terms.

4.2 Determination of the Minimum Principal Stress

4.2.1 Relationship Between ISIP and the Minimum Principal Stress

According to the classic analysis, the minimum horizontal principal stress can be equated to the instantaneous shut-in pressure, P_s. Zoback and Haimson's (1982) summary paper of the 1st Workshop on Hydraulic Fracturing Stress Measurements concluded that there existed three types of shut-in responses other than the classic response: (i) indistinct P_s; (ii) distinct, multiple P_s; and (iii) decrease/increase in P_s with injected fluid volume. These complicated shut-in pressures responses are due to a variety of factors which violate the assumptions of the classical method, such as fluid leakoff, incomplete fracture closure, equipment problems and so on. As a result, various methods have been proposed (e.g., Aggson and Kim 1987) for the identification of the instantaneous shut-in pressure from shut-in pressure data. Some researchers (McLennan and Roegiers 1982, 1983) have noted, however, that the instantaneous shut-in pressure may not be an accurate representation of the minimum principal stress. This finding requires a brief examination of instantaneous shut-in pressure.

In the classic analysis, the instantaneous shut-in pressure is an equilibrium pressure in the fracture equivalent to the total stress acting normal to the fracture plus the negligible effects of the pressure necessary to keep the fracture open and any friction pressure losses in the fracture (Warpinski *et al.* 1985). This may be expressed by the equation:

$$P_s = \sigma_3 + P_{open} + P_L \qquad [4.1]$$

where P_{open} = pressure necessary to keep the fracture open, P_L = friction pressure losses in the fracture and P_s and σ_3 are as defined previously. Hickman and Zoback (1983) argued that P_s approaches σ_3 through successive injection-shut-in cycles as P_{open} and P_L are reduced. They explained that P_{open} approaches zero as the fracture lengthens because, according to linear elastic fracture mechanics theory, minimal excess pressure is required for further fracture propagation. Friction pressure losses in the fracture are reduced as the fracture widens through successive injection cycles. Therefore, the validity of equating P_s and σ_3 is restricted to the classic conditions and adequate fracture dimensions. However, the effects of fluid diffusion often complicate the shut-in pressure response. As noted earlier, the effects of fluid diffusion on the shut-in pressure response can be divided into two categories: (i) the relationship between fluid leakoff and fracture volume and (ii) poroelastic effects on local in situ stresses.

The first effect is when fracture volume decreases due to fluid leakoff during shut-in thereby introducing the concept of fracture closure. Under these conditions, some researchers have replaced the instantaneous shut-in pressure with the fracture closure pressure, P_c, (Smith 1985) as being representative of the minimum total principal stress. McLennan and Roegiers (1982) reported two definitions of the fracture closure pressure: "...(1) as the pressure required to hold the fracture open after initiation, or (2) as pressure required to keep the fracture from just closing." Neither one of these two definitions appears to be substantially different from the instantaneous shut-in pressure definition. However, additional research has shown that relationship between the minimum principal stress and P_s or P_c is often quite complicated.

For example, Medlin and Massé (1984) have proposed two different mechanisms associated with fracture closure during shut-in. In laboratory hydraulic fracture propagation experiments, they observed: "Fracture closure measurements after shut-in showed an initial period of leakoff-controlled closure and a final period of creep-controlled closure." Through comparison

with actual field records, Medlin and Massé postulated that the transition between leakoff-controlled closure and creep-controlled closure could be equated with the instantaneous shut-in pressures for in field tests. Since this transition pressure does not reflect complete fracture closure, it was reasoned that the instantaneous shut-in pressure overestimated the minimum principal stress up to twenty per cent. Fluid leakoff-controlled closure was primarily dependent on the fluid efficiency (ratio of fluid leakoff volume to total injected fluid volume). The following period of creep-controlled closure was primarily controlled by the creep properties of the rock.

The second effect of fluid diffusion is related to the poroelastic effects on the local in situ stress as outlined by Detournay and Cheng (1988) and Detournay *et al.* (1988). Detournay *et al.* (1988) explained that poroelastic mechanisms can influence the closure pressure. In an analysis similar to the one for the poroelastic effects on hydraulic fracture initiation, they found that the local in situ stresses will have increased if injection period exceeds the characteristic time for the poroelastic mechanisms to develop. Detournay *et al.* 's (1988) analysis is a general analysis of the concept of "back stresses" introduced by Cleary (1979) and Smith (1985). The long-time increase of the local in situ stresses, defined as the "back stresses", σ_b, can be calculated according to the simplified equation:

$$\sigma_b = \eta\ (P_p - P_o) \qquad [4.2]$$

where $\eta = \alpha[(1 - 2\nu)/(2 - 2\nu)]$ and α, P_p and P_o have been defined previously. The poroelastic parameters i.e., k, B, G, α, and K, must be known in order to check for the development of time dependent back stresses by evaluating the induced pore pressure and its dissipation rate. The magnitude of the stress increase is primarily a function of the difference between propagation pressure and reservoir pressure.

The ISRM's suggested method for rock stress determination using the hydraulic fracturing technique (ISRM 1987) does not consider the difference between instantaneous shut-in pressure and fracture closure pressure. The

proceedings of the 2nd International Workshop on Hydraulic Fracturing Stress Measurements show that it is mainly practitioners from the oil industry who have considered the fracture closure pressure to be a superior estimate of the minimum total principal stress. This is probably related to that industry's tendency of employing larger volume hydraulic fracture tests (i.e., minifracs) in order to evaluate the in situ stresses. As shown previously, larger volumes are more likely to violate the assumptions of the classic theory. It is hoped that the ISRM's survey of hydraulic fracturing interpretation methods will eventually lead to a consensus on the performance and analysis of hydraulic fracture tests.

In summary, for ideal hydraulic fracture test conditions, the instantaneous shut-in pressure will give a reliable estimate of the minimum principal stress. Furthermore, the instantaneous shut-in pressure and the fracture closure pressure appear to be identical for ideal test conditions. However, when fluid diffusion is not negligible, it may be difficult to identify the instantaneous shut-in pressure. Depending on the creep properties of the rock, instantaneous shut-in pressure and fracture closure pressure may differ and the latter will more accurately represent the minimum total principal stress as shown by Medlin and Massé (1984). The poroelastic effects of fluid diffusion on the local in situ stress, as discussed by Smith (1985) and Detournay *et al.* (1988), should be assessed prior to shut-in pressure interpretation.

4.2.2 Oil Sands Behaviour and Shut-In Pressure Response

Table 3.5 summarizes the effect of oil sands behaviour on the basic concepts of hydraulic fracture propagation. As was shown earlier, there is a relationship between fracture propagation and the minimum principal stress. Therefore, this table can be used to summarize the various factors found to affect the shut-in pressure response in oil sands hydraulic fracture tests. Although other researchers have observed some of these factors to affect the shut-in pressure response for their materials, this section outlines the

relevant oil sands factors, such as fluid diffusion, in situ stress state, geologic discontinuities and wellbore condition.

The most important factor appears to be the effect of fluid diffusion because of its relationship with the other factors, such as poroelastic effects and shear failure. Fluid diffusion can affect the fracture dimensions, and through poroelastic mechanisms, can alter the in situ stress state. The likelihood of shear failure is increased because fluid leakoff will cause increased pore pressures and reduced effective stresses. Since shear failure in oil sands is accompanied by dilation, the porosity is increased locally, thereby increasing the oil sands permeability. These factors serve to affect the shut-in fracture behaviour which increases the difficulty in reliably determining the minimum principal stress.

The relationship between the principal stresses is also important. Dusseault (1980a) has suggested that horizontal fractures in oil sands will tend to climb because of the decrease in vertical stress higher in the formation. Once the fracture deviates from a plane normal to the minimum principal stress, significant shear stresses are generated around the fracture. Also, P_s is no longer equivalent to the minimum principal stress. A large portion of the Athabasca deposit oil sands payzone is located at intermediate depths (200 to 400 m) where the in situ stresses are hydrostatic. Under hydrostatic conditions, geologic discontinuities can override in situ stress as being the predominant control on fracture orientation.

The oil sands-shale interbedding along with minor cross bedding are apparently the major geologic discontinuities that exist in oil sand deposits (i.e., minor jointing or extensive faulting has been observed). Depending on the site lithology, the oil sands-shale interbedding can play a major role in controlling fracture propagation. However, it is difficult to include geologic discontinuities in an analysis of fracture propagation because of the inherent interdependence among all the mechanisms involved (Teufel and Warpinski 1987). The major effect of geologic discontinuities is their role in enhancing fluid leakoff when they are intercepted by the propagating fracture. Bedding

layers would affect vertical fracture containment and the lateral propagation of climbing horizontal fractures.

Since oil sand wells are usually cased, the influence of casing, cement and perforation damage on the wellbore condition should be assessed. Warpinski (1983, 1988) observed that once any minor wellbore flow restrictions due to casing effects have been removed by repeated injection cycles, the resulting minimum principal stress determinations are usually reliable. He assessed the extent of wellbore damage based on the difference between the propagation pressure and the shut-in pressure. If this difference exceeded 3500 kPa, he found the minimum principal stress determination to be inaccurate.

All of these factors have some effect on the shut-in pressure response curve. The following section groups the oil sands factors affecting the shut-in response according to their effects on the determination of the minimum principal stress.

4.2.3 Shut-in Pressure Response Models

By grouping the factors which may affect the shut-in pressure response according to their effects on the shut-in pressure curves, a simple but useful tool for assesing microfrac shut-in pressure data is provided. Most of the factors affecting the interpretation of the minimum principal stress from pressure-time response were summarized by McLennan and Roegiers (1982). These factors included (i) fluid leakoff from the fracture; (ii) inclined fractures; (iii) fracture orientation changes; (iv) geologic discontinuities; (v) incomplete fracture closure; (vi) propagation pressure; (vii) pore pressure effects; and (viii) equipment and test procedure.

It is now possible to make some qualitative conclusions about the character of the shut-in pressure curves for each of the above eight factors which may complicate the determination of the minimum principal stress. The shut-in pressure-curves can be separated into three groups: (i) false shut-in pressure responses; (ii) changes in shut-in pressure with injected

fluid volume giving multiple shut-in pressure responses; and (iii) indistinct shut-in pressure responses.

4.2.2.1 False Shut-In Pressure Response Model

There are a number of situations where the analysis of the shut-in response will lead to a false or misleading minimum principal stress for the actual test depth. These can be classified according to influence of geologic discontinuities, improper test procedure or equipment, and incomplete fracture closure.

Previous discussion has indicated that under certain circumstances, especially under hydrostatic in situ stresses, fracture propagation will be controlled by geologic discontinuities (i.e. bedding jointing, faults, etc). Misleading minimum principal stress values can result from geologic discontinuities in three ways. In two related ways, geologic conditions may dictate that (i) a climbing fracture, not normal to the vertical principal stress, be pressurized or (ii) that a pre-existing inclined discontinuity be pressurized. Either case will result in an inclined fracture with the P_s value being some combination of the in situ stresses as in Figure 4.1. In the third case, geologic discontinuities may deflect a propagating fracture as the fracture approaches and intercepts a discontinuity. Teufel and Warpinski (1987) observed in mineback experiments that geologic discontinuties caused multiple fracturing and enhanced fluid leakoff. Inevitably the shut-in pressure response may be affected by these other mechanisms and cannot be relied on giving an accurate minimum principal stress.

The selection of proper equipment and the employment of the proper test procedures have an important effect on hydraulic fracture tests. If equipment and test procedure are not selected to provide test conditions approaching those assumed in theory, the extraneous factors will cause minimum principal stress interpretation problems. For example, the influence of fluid leakoff and pre-existing discontinuities can be minimized by employing the proper fracture fluid and injection rates (Zoback *et al.* 1977

and Lockner and Byerlee 1977). Poor seating of the inflatable straddle packers in open borehole tests may allow fluid leakoff past the packers, thereby causing fracture initiation outside the test zone. Fracture initiation outside the test zone has also been seen in cased boreholes where a poor cement bond allowed fluid leakoff outside the test zone. In both instances, the interpreted minimum principal stress would be for a zone other than test zone.

When fracture closure is occurring during the shut-in pressure response, the prevention of complete fracture closure could lead to erroneous minimum principal stress values. Incomplete fracture closure may be caused by inelastic deformation, slippage at fracture boundaries and the presence of proppant (McLennan and Roegiers 1982).

4.2.2.2 Multiple Shut-In Pressure Response Model

Decreases in P_s have been attributed to two possible mechanisms. For stress conditions where $\sigma_v = \sigma_3$, it has been found that vertical fractures initiated at the wellbore rotate to become horizontal as they propagate away from the near wellbore stess state. As shown in Figure 4.2, the first two or three cycle P_s values would reflect σ_{hmin}, and as more fluid is injected and the fracture propagates, P_s would eventually reflect σ_v as the fracture became horizontal.

The second mechanism is that as a fracture is extended, it also widens, therefore reducing the viscous pressure losses in the fracture (Hickman and Zoback 1983). With each additional cycle, the fracture is lengthened and P_s approaches σ_3 as the pressure losses are reduced.

Poroelastic effects associated with fluid diffusion and its effects on the local total in situ stresses along a propagating fracture have been proposed to cause changes in the minimum principal stress for sequential cycles. According to Detournay *et al.* (1988) the development of the poroelastic effects depends on a sufficient injection period as compared with the mechanism's characteristic time $t_c = L^2/c$. Since the characteristic time is a function of the square of the fracture length, longer fractures will less likely experience an

increase in the "back stresses" for a given injection period. In actual field tests, an estimate of the characteristic time and the possible increase in back stresses can be made if the poroelastic parameters of the material are known.

4.2.2.3 Indistinct Shut-In Pressure Response Model

Depending on the formation permeability, the injected fluid properties and the injection rates, fluid leakoff from the fracture and wellbore during shut-in period may be substantial. Fluid leakoff results in shut-in pressure curves which usually have no distinct P_S (Figure 4.3). The pressure response during shut-in reflects some combination of fracture closure and fluid flow in the fracture and the formation. In well test theory and practice, petroleum reservoir engineers have developed extensive analytical and numerical models of fluid flow in wells intercepted by horizontal and vertical fractures (Earlougher 1977). Some researchers have noted the analogy between injection well tests and hydraulic fracture stress measurement tests. McLennan and Roegiers (1982) recommended adopting appropriate well test analysis techniques for the analysis of shut-in pressure data. If shut-in pressure response is controlled by fluid leakoff, identification of the fluid flow periods expected for the particular circumstances, by well test techniques, may aid the determination of the minimum principal stress.

4.3 Shut-In Pressure Interpretation Methodology

Many factors can complicate the interpretation of the minimum principal stress from hydraulic fracture shut-in pressure data. When an open borehole test in low permeability, unfractured homogeneous rock is conducted according to the classic test procedure (ISRM 1987), a clear P_S is readily obtained. For tests afflicted by complicating factors, the P_S value is not readily identifiable. Zoback and Haimson (1982) have summarized different methods used in identifying P_S from complicated shut-in pressure responses. Many of these methods are based on adapting well testing techniques to the interpretation of hydraulic fracture pressure data. However, they reported

that none of the methods have been either adequately tested or theoretically verified.

Since Zoback and Haimson's 1982 paper, additional methods have been proposed for minimum principal stress determination. These methods are either based on laboratory hydraulic fracture experiments (Gronseth and Kry 1983) or simple well test theory (Aamodt and Kuriyagawa 1983). The recent proceedings of the 2nd International Workshop on Hydraulic Fracturing Stress Measurements revealed additional research and field work performed in this area. More importantly, theoretical analyses based on numerical models were reported which gave a stronger theoretical basis for shut-in data analysis.

A review of the shut-in pressure response interpretation methodology developed in the last fifteen years is divided into (i) laboratory, (ii) theoretical and (iii) empirical analyses.

4.3.1 Laboratory Analyses

Very little laboratory experimental work on the interpretation of shut-in pressure data has been published. This section is limited to a discussion of three published studies of controlled laboratory tests on the correlation between applied loads and the minimum principal stress determined from shut-in pressure data.

Gronseth and Kry (1983) reported experimental verification for using the inflection point method for determining P_S. Biaxially loaded cubic specimens of granite were hydraulically fractured and the pressures monitored throughout the injection and shut-in periods. Their "simple graphical technique" consists of drawing a tangent line on the pressure-time curve immediately after shut-in and defining the point at which the curve departs the line as P_s (Figure 4.4). The correlation between the interpreted P_s and the applied stress (normal to the fracture) was very good except at lower stress values (Figure 4.5). Currently this method seems to be the most widely accepted interpretation technique.

McLennan and Roegiers (1982) adapted well test techniques to the analysis of shut-in pressure data collected from laboratory hydraulic fracture tests on polyaxially stressed cubic samples. Some of the three sample types tested, plexiglass, granite and mortar blocks, exhibited leakoff behaviour. These tests allowed them to examine the interaction between fracture closure and fluid leakoff. The interpretion of the principal stresses from the shut-in pressure data proved to be difficult.

McLennan and Roegiers also noted the similarity between the analysis of hydraulic fracture stress measurement tests and well tests in hydraulically fractured wells. They suggested that proven graphical well test analyses be used to interpret the shut-in pressure data. These graphical well tests analyses included the log pressure versus log Δt (Δt is the time since shut-in) and Horner plots of pressure versus log $[(t_{inj} + \Delta t)/\Delta t]$ (t_{inj} is injection period). They found that the Horner plot appeared to be the best method for determining the stresses normal to the induced fracture plane (Figure 4.6). Based on their experimental analyses, McLennan and Roegiers (1983) suggested that all features of the shut-in pressure response should be considered because they may be relevant to the stress analysis. For example, in some cases, the analysis revealed that mechanisms other than fracture closure were also evident.

Data from laboratory experiments on polyaxially stressed cubic samples of Niagara dolomite provided some contradictory evidence for determining the minimum principal stress (Cheung and Haimson 1988). Cheung and Haimson found that the inflection point method of Gronseth and Kry (1983) and the pressure versus log Δt method (similar to the Horner method) did not adequately predict P_s. Instead, they adopted an exponential decay model (Lee and Haimson 1988) that is based on the radial flow theory developed by Muscat. By fitting the exponential decay model to the shut-in pressure data using a non-linear regression method, they obtained two points, P_u and P_l, representing upper and lower limits on the normal stress as seen in Figure 4.7 The lower pressure, P_l, represents the point at which the fracture closes and radial flow dominates the pressure response. The upper limit, P_u, is the

extrapolation of the exponential line to zero shut-in time and is the pressure required to sustain radial flow at shut-in. The P_u values compared well with the applied normal stress (± 5%) while the P_l values underestimated the normal stress.

Cheung and Haimson (1988) also investigated the pressure decay rate method (dP/dt vs pressure) for determining the minimum principal stress. This method is based on fitting two different exponential functions representing (i) open fracture flow and (ii) closed fracture-formation radial flow (Tunbridge 1988). An accuracy comparable to the exponential decay model method for predicting the applied normal stress was observed.

4.3.2 Theoretical Analyses

Modelling the shut-in pressure response of a hydraulically fractured well is complex because it must consider the inter-related effects of a number of factors: fracture geometry, fracture propagation criteria, coupling of fluid leakoff and fracture dimensions, the coupling of deformation-diffusion in terms of poroelasticity, and other mechanisms. Although a considerable number of analytical models and numercial simulators exist for predicting fluid flow in hydraulically fractured wells, very little research has gone into simulating the shut-in pressure response of hydraulic fracture tests. However, five papers presented at the 2nd International Workshop attempted to model the shut-in process in order to provide a better theoretical basis for interpreting P_s. Of the five papers, four were from researchers based in the petroleum industry, but all papers have been influenced by the theoretical efforts of researchers from this industry. This section reviews the conclusions of these papers on the interpretation of minimum principal stress from shut-in pressure data.

de Bree and Walters (1988) present a shut-in pressure analysis for microfrac and minifrac tests which specifically incorporates fluid compressibility, pressure dependent leakoff and arbitrarily shaped fractures. Fluid leakoff is related to the pressure difference (P_p - P_o) and two parameters which reflect the fluid flow properties of the reservoir and the fluid. Usually a pre or post-test leakoff test is necessary to evaluate these leakoff properties.

Fracture growth during injection, assuming constant q, uniform pressure distribution and uniform fracture width, is modelled by varying the fluid efficiency (fracture volume divided by total injected volume) of the test for limit cases (e.g., general case, negligible fluid loss case, microfrac case, etc.). The shut-in pressure response is divided into two parts, the first prior to fracture closure where fracture compliance is considered, and the second after fracture closure. The shut-in pressure response simulation is then arrived at by combining the fluid leakoff model, the fracture growth model and the equation of mass conservation. Their analysis leads to a graph of shut-in pressure vs time which consists of two straight lines representing the shut-in behaviour before and after fracture closure.

The final solution shows a relationship between the pressure difference and pressure decline function, $g(\delta)$ ($\delta = [\Delta t - tinj]/tinj$), the latter reflecting the fracture growth model. The pressure decline function for the period prior to fracture closure is different from the period after fracture closure. This results in two slopes in the pressure decline curve: "By plotting a suitable function of $(p - p_p)$ against the function $g_o(\delta)$, two straight-line portions should be obtained with a change of slope being expected at the value of $go(\delta)$ where FCP (p_c) is reached." Fracture closure pressure is equated to the minimum principal stress, while P_s is considered to related to P_p because it includes the pressure necessary to keep the fracture open.

Shlyapobersky (1988) presents a brief derivation of a mathematical model of pressure decline during shut-in for microfrac tests. He simplifies the analysis by assuming a penny shaped (i.e., circular and horizontal) crack. The differential equation for pressure decline during shut-in is combined with expressions for a time-dependent leakoff rate and fracture storage. The final equation contains two unknowns, the fluid loss coefficient and the fracture radius. Instead of determining these unknowns from a single point from a plot of shut-in pressure decline rate vs shut-in time, he advocates that the theoretical shut-in pressure decline be matched with the field pressure decline data for the entire time interval (i.e., a global match). Besides giving more accurate and objective results, it also reveals any discrepancies between the observed and theoretical behaviour. The fracture closure pressure is considered to be a better estimate of the minimum principal stress. Fracture closure is identified from the global match when the field response deviates from the predicted response because fracture closure results in zero fracture

storage. Shylapobersky's analysis, therefore, like previous well test analyses, does not directly consider fracture closure. His analysis relys on the indirect influence of fracture closure on the shut-in pressure response without considering fracture compliance.

Charlez *et al.* (1988) presents an alternative approach to analyzing the shut-in pressure response. They take the opposite solution route by globally modelling the shut-in pressure data and then, through a mathematical inversion of the solution, derive two parameters, the minimum principal stress and the fluid loss coefficient. Their model is based on the contained (fixed vertical height) Nordgren fracture model and Nolte's analysis of the coupling of fluid flow and fracture dimensions. No fracture propagation, governed by fracture mechanics theory, is assumed to occur during shut-in. Numerical results showed that in the direct problem, σ_3 significantly affected the shut-in pressure response and leakoff coefficient being less significant. The inverse problem consisted of minimizing a function, S, characterizing the difference between the experimental shut-in pressure response data and the model prediction. Their algorithm calculates the difference, S, in terms of σ_3 and the fluid leakoff coefficient, c_w, on a 3-D mesh. The solution for σ_3 and c_w (Figure 4.8) is obtained at the minimum S value.

The inversion method was applied to field data and the calculated values of σ_3 and c_w were used to derive a pressure-time response during shut-in. The comparison between the actual field data and the theoretical prediction was quite good (Figure 4.9). At fracture closure, the experimental data falls below the predicted data providing support for the hypothesis of a gradual change from a linear flow to a pseudo-radial flow response. Variation in other parameters, such as fluid viscosity, were found to result in different solutions. Therefore, their analysis provides a unique pressure curve inversion solution only when there are two parameters, i.e., the leakoff coefficient and the minimum principal stress.

In another approach to modelling the shut-in pressure response, Hayashi and Sakurai (1988) combine a linear elastic fracture mechanics analysis of fracture growth with a coupled fluid diffusion-stress analysis. The model accounts for fracture fluid leakoff, equipment compliance, partial fracture closure and fracture growth after shut-in. However, it was not a complete poroelastic analysis. Their analysis begins with the model of surface cracks on a cylindrical cavity subjected to a hydrostatic pressure in the

framework of 2D elasticity. A simple linear elastic fracture mechanics criteria of Mode I (i.e., tensile) fracturing is used to model fracture growth. These two analyses are combined to describe the initiation and propagation of hydraulically induced fractures. The shut-in pressure response considers the coupling of fracture growth, fluid leakoff from fracture and borehole and equipment compliance.

Sensitivity analyses were performed to investigate the effect of crack length, crack height, stress ratio ($\sigma_{hmax}/\sigma_{hmin}$) and fluid leakoff coefficient on the shut-in pressure response. In all cases, an immediate drop in pressure occurred briefly after shut-in which was attributed to instantaneous fracture growth at shut-in. At shut-in, the pressure losses in the fracture become very small and so the fracture tip stress intensity factor exceeds the fracture toughness until the fracture becomes sufficiently long enough to reduce the tip stresses. The shut-in pressure decline after this instantaneous drop is affected by various factors. As the stress ratio increases, so does the pressure drop (Figure 4.10). Fluid leakoff coefficient has the greatest effect on pressure drop (Figure 4.11). Crack length, crack height and equipment compliances are less significant.

Hayashi and Sakurai (1988) observed that the borehole pressure at the onset of fracture tip closure was approximately equal to σ_{hmin}. On plots of pressure vs [(tinj + Δt)/Δt], the onset of fracture tip closure occurred at the maximum point of curvature at a pressure equal to σ_3. Six interpretation methods were evaluated against their model: (i) inflection point method, (ii) maximum curvature, (iii) pressure versus log Δt, (iv) log pressure versus log Δt, (v) the Horner plot method, and (vi) the Muskat method. They concluded that methods (ii) through (v) all gave reliable indications of σ_{hmin}. The inflection point method improved as the fracture length became larger. The Muskat method produced significant errors as the fluid leakoff became larger. Apparently, their rigorous analysis shows that many of the most common interpretation techniques give reliable estimates of σ_3.

BenNaceur and Roegiers (1988) discussed some of the limitations of shut-in pressure decline models. They sought to identify the conditions under which their Nolte based curve matching model could be applied to σ_3 determination and to quantify the errors introduced by field mechanisms unaccounted by theory. Because their discussion also encompasses the modelling of large hydraulically induced fractures, involving more

complicated procedures and fluids, only the relevant points to stress measurements are mentioned here. First, the fracture is normally assumed to be confined within a well defined payzone by bounding layers of higher stresses. For complete fracture growth modelling, the bounding stresses or relevant material properties are required. Secondly, injection rate is assumed to be constant, but uncontrollable variations due to equipment problems may affect the injection rate (q) and influence the fluid leakoff. If variations are less than 20%, an average q is acceptable. Thirdly, even though fluid leakoff is known to be pressure dependent, constant leakoff coefficients are normally used in modelling.

Two other factors mentionbed by BenNaceur and Roegiers are the possibility of in situ stress variations and poroelastic effects. In situ stress can affect both the fracture compliance and the fracture geometry. Usually a constant fracture compliance is used in the analyses but lateral and vertical in situ stress variations may alter the actual fracture compliance. In situ stress contrasts also control vertical and lateral fracture propagation and this should be considered when assuming a given fracture geometry for analysis purposes. They also emphasized the importance of poroelastic effects on fracture propagation. They summarize two current treatments of the poroelastic effects: (i) fully coupled poroelastic analyses or (ii) linearized analyses treating the coupling of deformation-diffusion in a quasi-static manner.

4.3.3 Empirical Analyses

Empirical analyses have centered on adapting well test analyses methods, commonly used by reservoir engineers and groundwater engineers, to the analysis of hydraulic fracture test pressure data. Because of the similarity between well tests and hydraulic fracture stress measurement tests, many researchers have attempted to apply well test analysis methods for aiding in the determination of in situ stresses. Analytical and numerical models have been developed for wells intercepted by either a single vertical or a horizontal fracture in order to understand their influence on oil and gas production (Earlougher 1977). These analyses revealed that vertically and

horizontally fractured wells exhibit characteristic flow regimes associated with linear flow in the fracture and formation and pseudo-radial flow in the formation (once the influence of fracture fluid flow has become negligible). Most of the empirical methods correlate the transition pressure of one flow regime to another as the point of fracture closure. Many techniques, based on different models, have been proposed to identify this transition point which can be equated to the minimum principal stress.

Several empirical methods were reported at the 1st International Workshop on Hydraulic Fracturing Stress Measurements. Doe *et al.* (1983) recommended using a plot of pressure versus log Δt to select P_s, while Haimson (1983) suggested using a plot of log pressure versus log Δt. Aamodt and Kuriyagawa (1983) proposed a method based on Muskat's exponential fit of radial flow data. This method was "...an empirical method which gives a unique and repeatable pressure, Pe, which characterizes the curve and which agrees within a few percent with the fracture opening pressure as determined by other means." They reported that this technique worked well for their hydraulic fracture stress measurement tests in crystalline basement rock.

Aggson and Kim (1987) reported a comparative study of different methods for identifying the P_s value from hydraulic fracture tests conducted at the Basalt Waste Isolation Project site. They used five different methods: (i) inflection point method; (ii) pressure vs log $[(t_{inj}+\Delta t)/\Delta t]$ method; (iii) pressure versus log Δt method; (iv) log pressure versus log Δt; and (v) the Muskat method. Their results showed that ps values at the same depth for various methods could vary as much as 14% or 4.9 MPa in absolute terms. The Muskat method and the log pressure versus log Δt methods gave the highest and lowest values, respectively. Although the relative difference of 14% is not major, it may be too large in absolute terms to be of sufficient accuracy for fracture containment studies (Gronseth and Kry, 1983 and Teufel and Clark 1984).

The results reported in chapter 5 and the work of others indicate that there is a certain degree of subjectivity and scale dependency when using the graphical techniques described by Aggson and Kim (1987). Examination of the

graphs used by Aggson and Kim (1987) to determine the P_s, as in Figure 4.12, show that the lines they have drawn are subjective. Lee and Haimson (1988) counteract this problem by applying statistical techniques in the analysis of two interpretation methods: Muskat's exponential decay model and Tunbridge's (1988) shut-in pressure decay rate method. The former method consists of fitting Muskat's model of exponential decay to the shut-in pressure data by using a non-linear regression analysis. The latter portion of the shut-in curve, representing formation radial flow after the fracture has closed, is fitted iteratively in order to stabilize the root-mean-square error for the appropriate curve parameters, P_l and P_u (as defined previously). Their data suggests that P_u is a better approximation of P_s when compared with other methods.

The shut-in pressure decay rate method advocated by Tunbridge (1988) was also fitted to shut-in pressure data using similiar statistical techniques by Lee and Haimson. Non-linear regression analysis led to best fitting curves which effectively determined the transition point in the bilinear behaviour. This transition pressure, when equated with the fracture closure pressure, gave values consistent with the P_u values obtained from the previous analysis.

Baumgärtner and Zoback (1988) proposed an interactive analysis method wherein various interpretation methods are used together in order to determine by P_s. They presented a case history of hydraulic fracture tests performed in low permeability crystalline rock at depths from 108 to 1284 m. Five methods were used interactively to determine P_s: (i) expanded plots of pressure versus time; (ii) pressure versus injection rate; (iii) pressure versus shut-in pressure decay rate; (iv) shut-in pressure decay rate versus time; and (v) shut-in pressure decay rate versus log time. They concluded that the interactive analysis could identify the minimum principal stress from in indistinct shut-in pressure data.

Interactive analysis is a fundamental aspect of well test analysis which Sookprasong (1986) stressed when he considered shut-in analysis from a reservoir engineer's perspective. He recommended a well test based analysis which consisted of log pressure versus log Δt graphs, pressure vs $[(t_{inj}+\Delta t)/\Delta t]$

graphs and the tandem square root plot (pressure versus $[(t_{inj} + \Delta t)^{1/2} - \Delta t^{1/2}]$). These graphs allowed identification of the flow periods associated with shut-in in a hydraulically fractured well based on theoretical analyses relating the wellbore pressure response to the flow periods (Earlougher 1977). The flow periods were related to fracture flow, formation flow and the interaction between the two during shut-in. The normal stress acting on the induced fracture is approximated by the wellbore pressure at the time of complete fracture closure as indicated by the start of pseudo-radial flow.

Other researchers have reviewed the analytical basis for applying well test analyses to hydraulic fracture stress measurement tests (Tunbridge 1988; Whitehead *et al.* 1988; and Wooten and Elbel 1988). These reviews of the application of well test theory to shut-in pressure analysis are discussed in section 4.4.2.

4.3.4 Summary

The wide array of methods and analyses proposed for the determination of the minimum principal stress from shut-in pressure response data are summarized in Table 4.1. This table presents a brief explanation of the application of each method for the evaluation of σ_3 from hydraulic fracture test data. The reader may refer to the pertinent references for a complete description of the interpretation methods. Table 4.2 considers the laboratory, theoretical and empirical basis of each method. Of all the methods discussed, the inflection point method and the pressure decay rate method have the widest support among practitioners.

Except for the interpretation methods based on experimental data, all the methods and analyses of the interpretation of the minimum principal stress incorporate the influence of fluid flow within the fracture and in the formation. Only the more sophisticated analytical and numerical models have attempted to combine fracture geometry, fracture propagation criteria and coupled fluid diffusion-deformation in the analysis of shut-in fracture behaviour. None of the other factors, such as geologic discontinuities,

poroelastic effects, and shear failure, have been included in these analyses of shut-in pressure data.

The only factor which has been systematically studied is the role of fluid leakoff during shut-in. This has been a major component of well test theory and practice for many years. While current interpretation methods do not adequately consider the factors affecting the transient shut-in pressure behaviour, well test methods are well suited to the analysis of hydraulic fracture stress measurement tests affected by fluid leakoff. Field practice suggests that well test methods may also be useful in identifying σ_3 in shut-in pressure data influenced by other factors.

4.4 An Interpretation Method for Oil Sands Tests

The proposed method for interpreting oil sands microfrac shut-in pressure data is based on the application of well test methodology. The implications of the unique geomechnical properties of oil sands on hydraulic fracture behaviour in oil sands are only partially addressed by the methods discussed in the previous section. Most of these methods, however, attempt to consider the role of fracture fluid leakoff during shut-in. Well test theory includes the theoretical analysis of the the shut-in pressure response in hydraulically fractured wells. Although well test analyses have a limited theoretical basis, they do have a proven empirical basis for deriving the minimum principal stress from complicated pressure-time data. Their simplicity lends itself to the analysis of microfrac tests.

The implications of oil sands behaviour on hydraulic fracture tests were discussed in section 3.2.2. McLennan and Roegiers (1983) summarized the factors which affect the validity of hydraulic fracture stress measurement tests for general materials i.e., hard rock and sedimentary rock. The review of the various interpretation methods shows that they are limited to identifying σ_3 from shut-in pressure data affected by leakoff. These methods have no theoretical basis in their attempts to analyze records affected by fracture

climbing, pore pressure effects, incomplete fracture closure, well bore effects, etc.

Although the interpretation of oil sands shut-in pressure data have been shown to be influenced by other factors, fluid leakoff appears to be the most important factor. The approach adopted in this thesis for the analysis of oil sands shut-in pressure data is based on well test analysis methodology because it has been extensively developed for analyzing the influence of fracture and formation fluid flow on the shut-in pressure response.

Five methods will be used to analyze the hydraulic fracture stress measurement data presented in chapter 5. The first two methods are used to determined the instantaneous shut-in pressure, P_s: (i) the inflection point method (Gronseth and Kry, 1983); (ii) the pressure decay rate method ($\delta P/\delta t$ vs P_{avg}); and three well test graphical procedures which are used together to determine the fracture closure pressure, P_c: (iii) log ($P - P_{si}$) vs log Δt, (iv) P vs lot $[(tinj+\Delta t)/\Delta t]$, and (v) P vs $[(tinj+\Delta t)^{1/2} - (\Delta t)^{1/2}]$. If the test conditions approach the classic hydraulic fracture theory conditions, the classic instantaneous shut-in pressure, ISIP, has been included. The following section summarizes the theoretical concepts behind well test methodology as applied to hydraulically fractured wells.

4.4.1 Application of Well Test Analysis Methodology

McLennan and Roegiers (1982, 1983) have previously suggested the application of well test analysis methods to the interpretation of microfrac shut-in curves. They indicate that well test analysis methods can help in analyzing shut-in pressure response of microfracs affected by unanticipated factors and can provide a consistent means of determining σ_3. However, no theoretical basis is provided for the application of well test analysis methods to the interpretation of the shut-in pressure response. An attempt is made here to review the theory behind well test analysis of hydraulically fractured wells.

Well test analysis of fractured wells was developed in the early 1970's (Gringarten and Ramey 1974; Gringarten *et al.* 1974) in order to understand

the influence of vertical and horizontal fractures on well production behaviour. Conventional well test analyses were inapplicable to fractured wells because they displayed other types of flow during well tests (Cinco 1982). Because well test analyses have been successfully used to estimate reservoir fluid flow properties, it would be worthwhile to consider applying such analyses to microfrac tests.

Microfracs, which consist of the three stages of fracture initiation, fracture propagation (until a stable injection pressure is reached) and shut-in, are similar to the traditional pressure build-up and injectivity tests in oil reservoir engineering practice as seen in Figure 4.13. By superposing the solution for the shut-in period (i.e., Δt) on the solutions to injection pressure behaviour in fractured wells, a solution can be derived modelling hydraulic fracture stress measurement tests. Solutions for models of hydraulically fractured wells already exist and can be applied to hydraulic fracture analysis. These solutions are for models of vertically fractured wells with either an infinite conductivity, uniform flux or finite conductivity fracture and horizontally fractured wells with a uniform flux fracture.

4.4.1.1 Vertically Fractured Wells

Gringarten *et al.* (1974) present an analytical solution for the transient pressure distribution created by a well with a single, infinite conductivity vertical fracture (Figure 4.14). Their model assumed a constant production rate and no pressure losses in the fracture (i.e., infinite conductivity). The resulting transient pressure distribution could be divided into three time periods each characterized with its own flow regime (Figure 4.15): (i) formation linear flow; (ii) pseudo-radial flow; and (iii) pseudo-steady state.

At early time, the infinite conductivity model can be simplified to a uniform flux distribution model(i.e. a uniform flow rate along the fracture) The early time solution is shown to be controlled by formation linear flow and is indicated by a 1/2 slope on a log p vs log Δt graph. Later on the well exhibits a radial flow-like (pseudo-radial flow) pressure behaviour. In fact, the

solution for a vertically fractured well becomes identical to that for radial flow to a well when the fracture length becomes small and the reservoir radius becomes infinite. This pseudo-radial flow period can be detected on a plot of p vs log $[(tinj + \Delta t)^{1/2} - (\Delta t)^{1/2}]$ graph. Only reservoirs which can be considered infinite exhibit all three flow periods.

When they reported a general theory for transient flow towards a vertically fractured well, Cinco and Samaniego (1981) proposed an additional flow period, bilinear flow, which is exhibited by intermediate or low conductivity fractures of low storage capacity. Bilinear flow consists of incompressible linear flow in the fracture and compressible flow in the formation and may be identified by observing a straight line on graph of p vs $(\Delta t)^{1/4}$. The slope of this graph is inversely proportional to the square root of the fracture permeability. Bilinear flow can also be identified by a 1/4 slope line on a graph of log p vs log Δt.

Cinco (1982) concluded that four flow regimes were possible for a well intercepted by a finite conductivity vertical fracture. In addition to the formation linear flow and pseudo-radial flow, there exists fracture linear flow and bilinear flow as depicted in Figure 4.16. Fracture linear flow occurs immediately and is usually obscurred by wellbore storage and not readily apparent on the log p vs log Δt graph. Both types of linear flow can also be detected by the line observed on a graph of p vs $(tinj + \Delta t)^{1/2} - (\Delta t)^{1/2}$. Bilinear flow occurs prior to the time when the effects of fluid flow at the fracture tip have reached the wellbore.

The transient pressure analysis of a vertically fractured well may be affected by factors not included in the theoretical model. For example, wellbore storage often distorts early time data, but some efforts have been made to theoretically account for this effect (Lee 1983).

4.4.1.2 Horizontally Fractured Wells

The primary pay zone in the Athabasca deposit is the McMurray Formation and it is generally situated at depths less than 300 m. At depths less

than 300 m, the vertical stress is the minor principal stress (Dusseault 1977b), thereby dictating the creation of horizontal hydraulic fractures (Chhina and Agar 1985). It is apparent that the model for a well intersected by a horizontal fracture would be more appropriate for microfrac analyses in Athabasca oil sands deposits than vertical fracture models.

The analytical solution for the transient pressure distribution for a single uniform flux horizontal fracture model, as shown in Figure 4.17, was first proposed by Gringarten and Ramey (1974). The solution for horizontally fractured wells presents flow behaviour characterized by three flow periods as indicated in the transient pressure responses shown in Figure 4.18: (i) a storage flow period; (ii) a vertical linear flow period; and (iii) a pseudo-radial flow period. Figure 4.19 is a schematic of the three possible flow periods. Depending upon the fracture width and the fracture's vertical position within the pay zone, a storage type flow period of unit slope on a log p versus log Δt may first be observed (for non-zero fracture width). Slightly later, a period of vertical linear flow from formation to fracture follows and is indicated by a half slope on the log p versus log Δt graph. Eventually a transition period leads to the long time response of pseudo-radial flow. As in the vertical fracture case, the long time solution for the horizontally fractured well is identical with the solution for radial flow to a unfractured well (i.e., a line source well--Gringarten and Ramey 1974). Ultimately, all fractured wells will display a pseudo-radial flow period as long as the fracture length is less than one-third of the drainage radius.

4.4.4.3 Minimum Principal Stress Interpretation

The interpretation of oil sands shut-in pressure data will depend on the extent to which these data are affected by factors unrelated to the determination of the minimum principal stress. When the test conditions and shut-in pressure response suggest that the minimum principal stress is controlling the shut-in pressure response, the ISIP and inflection point methods should be reliable indicators of the minimum principal stress. When

it is apparent that the shut-in pressure response is affected by fluid leakoff, the well test analysis methods should aid the identification of the closure stress, and, hence the minimum principal stress.

Applying well test analysis methods to microfrac interpretation is based on identifying the fracture closure due to fluid leakoff during shut-in. This requires an analysis of the shut-in pressure data in order to identify the possible flow regimes. This flow regime analysis consists of:

(1) A log [P_{si} (pressure at $\Delta t=0$) - P (pressure during shut-in)] versus log Δt (shut-in time) graph is prepared in order to identify wellbore storage and storage flow (for horizontal fractures) with a unit slope, formation linear flow with a 1/2 slope, and bilinear flow with a 1/4 slope.

(2) A tandem square root plot of P versus $[(t_{inj} + \Delta t)^{1/2} - (\Delta t)^{1/2}]$ is prepared in order to identify any straight lines signifying either fracture or formation linear flow

(3) A Horner graph of P versus log $[(t_{inj} + \Delta t)/\Delta t]$ is prepared in order to identify any straight lines signifying pseudo-radial flow.

It is important to prepare the log-log graph because it will aid in the proper selection of the linear flow in the tandem square root plot and will indicate the extent of wellbore storage at early time. These well test analyses allow the identification of the flow regimes exhibited by a particular microfrac test and an assessment of wellbore storage, fracture linear flow for vertical fractures and storage flow for horizontal fractures.

When it is reasonable to assume that fluid leakoff is controlling the shut-in pressure response through fracture closure, the well test analyses may be used to identify the closure stress. Upon fracture closure, the influence of the fracture on the fluid flow is suddenly halted. While the fracture is open, fracture linear flow dominates the shut-in pressure response, with the both the formation linear flow and the pseudo-radial flow being negligible. Fracture closure infers the cessation of linear fracture flow and the shut-in pressure response is similar to that of an unfractured well exhibiting radial flow. Fracture closure pressure occurs between the pressure at which linear fracture flow ends and which pseudo-radial flow begins.

A similar use of well test analysis techniques was proposed by Whitehead *et al.* (1988) and they found it to be useful despite its limitations

4.4.2 Limitations of Well Test Analysis Methodology

Beside the factors that have been found to affect well test analyses, the main deficiency in the application of well test analysis methodology to hydraulic fracture tests is that it does not consider the influence of fracture compliance (i.e., fracture closing) on the shut-in pressure response. These well test analysis methods do not explicity consider the effects of closing fractures on the shut-in pressure response. Instead, fracture closure is interpreted through its effects on the transient pressure response and fluid leakoff. For example, Whitehead *et al.* (1988) found that rapid fracture closure and incomplete fracture closure resulted in flat log-log curves. Conversely, Wooten and Elbel (1988) stated that since fracture closure is not included explicity in the well test analyses, these analyses are only valid when changes in fracture width and length are negligible during shut-in. Meanwhile, the numerical model of Hayashi and Sakurai (1988), which explicity incorporates fracture compliance, showed that many of the commonly used interpretation techniques, including well test analysis methods, predicted the minimum principal stress quite accurately. Apparently more research is necessary to clarify the role of fracture closure on the shut-in pressure response.

The factors that affect well test analyses have been noted (Earlougher 1977 and Lee 1983). Depending on the fracture size, reservoir properties and the testing procedure, some of the flow periods may not be evident. Wellbore storage exhibits a unit slope on the log p versus log Δt plots and it obscures the early time data. Solutions have been developed in order to analyze the early time data, mainly in the form of type curves (Earlougher 1977). In light of theoretical limitations, it remains possible to analyze microfrac shut-in data.

4.5 Conclusions

This chapter has examined the problem of determining the minimum principal stress from hydraulic fracture stress measurement tests. In particular, various methods and techniques have been reviewed which have been proposed for the interpretation of shut-in pressure responses affected by extraneous factors. However, most of the factors which can affect shut-in pressure responses are not explicitly accounted for by most of these methods. Well test analysis methodology was found to be applicable in the interpretation of hydraulic fracture tests affected by fluid leakoff. The premise for the successful application of well test methodology is that fracture closure will affect the flow regimes during shut-in. Other factors, such as geologic discontinuities, poroelastic effects, and climbing fractures, are not considered explicitly by well test analyses. The limitations of any interpretation method and the possible range of factors which may affect shut-in pressure data suggest that the success of an hydraulic fracture test is not solely contingent upon the accuracy of the interpretation method.

Warpinski (1988) produced a list of test considerations, in addition to the interpretation method, which are essential to good hydraulic fracture tests. They are: (i) the selection of the test zone, (ii) the proper perforation design for cased holes, (iii) the need for a good pressure monitoring system, (iv) the appropriate fracture fluid and (v) the proper injection rates and fluid volumes. Hydraulic fracture test design, which minimizes the possible influence of extraneous test and site factors, will benefit from a review of this list.

Warpinski's recommendations are detailed below. A test zone of uniform material at least 2 m thick which is not intersected by geologic discontinuities is preferred. Proper perforation design, including perforation pattern, charge and phasing, will minimize any wellbore damage. A downhole pressure monitoring system with a pressure resolution of more than one pressure reading per second should ensure that no details of the shut-in pressure response are omitted. Although water is the preferred fracture fluid,

other fluids may be useful in reducing viscous pressure losses in the equipment and the fracture. Finally, appropriate injection rates and fluid volumes are necessary in order to ensure that the borehole is hydraulically fractured (instead of fluid leaking off into the formation) and in order to ensure adequate fracture propagation. If the injection rate is too low then only leakoff may occur and if it is too high then friction losses in the well and the fracture may be excessive. The fluid volume must be large enough that the fracture will extend beyond the influence of the wellbore, but not too large so that it extends into other geologic strata.

Table 4.1 Summary of interpretation methods for determining σ_3.

METHOD	DESCRIPTION
ISIP Methods	
(1) Classic	Instantaneous shut-in pressure (ISIP) derived from a graph of pressure versus shut-in time.
(2a) Inflection Point Method	The pressure at which the tangent line immediately after shut-in departs from the pressure versus shut-im time data (Gronseth and Kry, 1983).
(2b) dP/dt vs P plot	Plot of pressure decay rate vs average pressure which shows a bilinear behaviour representing an open and closed fracture (Tunbridge 1988).
(2c) dP/dt vs Δt plot	Variation of (2b) (Baumgärtner and Zoback, 1988)
(2d) dP/dt vs log(Δt) plot	Variation of (2b) (Baumgärtner and Zoback, 1988)
(3) Pressure vs injection rate	(Baumgärtner and Zoback, 1988)
(4) Maximum Curvature	The point of maximum curvature on a pressure versus shut-in time graph.
Well Test Analysis Methods	
(5) log p vs log Δt plot	A graph of log pressure vs log shut-in time is used to identify various flow regimes possible after shut-in which may be useful in identifying σ_3.
(6a) Horner Plot	Graph of pressure vs log $[(t_{inj} + \Delta t)/\Delta t]$ where a fitted straight line indicates radial flow and fracture closure.
(6b) p vs log Δt plot	Variation of (6a) but valid only for long injection durations as compared with the shut-in time.

Table 4.1 continued.

(7a) Tandem Square Root Plot	Graph of pressure vs $(t_{inj} + \Delta t)^{1/2} - (\Delta t)^{1/2}$ where a fitted straight line indicates formation/fracture linear flow.
(7b) p vs $(\Delta t)^{1/2}$	Variation of (7a) but valid only for long injection durations as compared with the shut-in time.
(8) Muscat Method	Employs the exponential pressure decay model proposed by Muskat (1937) in which a straight line is fitted to data plotted on log pressure versus time graph with an assumed pressure pe until a best fit is obtained (Aamodt and Kuriyagawa, 1983).
Numerical Methods	
(9) Pressure Curve Inversion	Using an appropriate fracture model, match theoretical data with the transient shut-in pressure data until a minimum difference is reached through manipulation of the analytical input data (Charlez *et al.* 1988).

Table 4.2 Summary of the experimental, theoretical and empirical evidence for the σ_3 interpretation methods.

EVIDENCE / Method	Laboratory	Theoretical	Empirical
ISIP Methods			
(1) Classic	*	*	*
(2a) Inflection Point Method	*		*
(2b) dP/dt vs P plot			*
(2c) dP/dt vs Δt plot			*
(2d) dP/dt vs log(Δt) plot			*
(3) Pressure vs injection rate			*
(4) Maximum Curvature			*
Well Test Analysis Methods			
(5) log p vs log Δt plot			*
(6a) Horner Plot	*		*
(6b) p vs log Δt plot			*
(7a) Tandem Square-Root Plot			*
(7b) p vs $(\Delta t)^{1/2}$			*
(8) Muscat Method	*	*	*
Numerical Methods			
(9) Pressure Curve Inversion		*	*

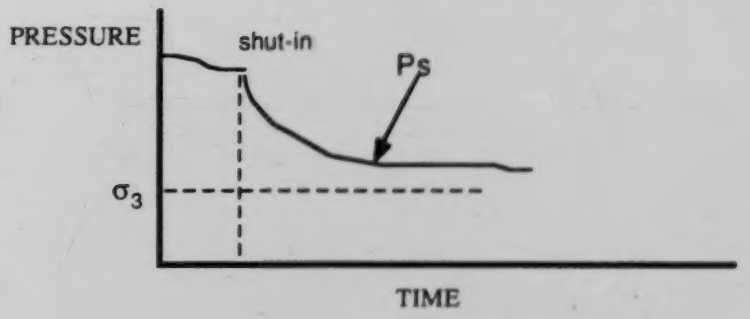

Response is influenced by:
- inclined fractures
- geologic discontinuities
- incomplete fracture closure
- equipment and test procedure
- fluid leakoff
- perforation related flow restrictions

Figure 4.1. False shut-in pressure response curve.

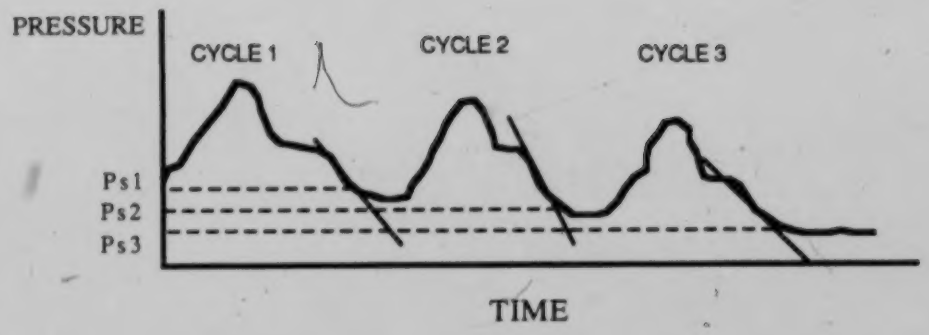

Variation in Ps values:
- fracture orientation changes with fracture lengthening
- excess fracture propagation pressure
- poroelastic effects
- removal of perforation damage
- climbing horizontal fractures
- fracture propagation into a zone of different in situ stress

Figure 4.2 Multiple shut-in pressure response curve.

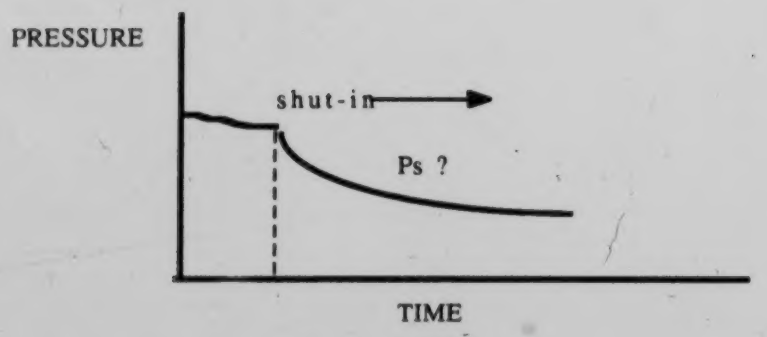

Response affected by:
- fluid leakoff from the fracture and wellbore
- equipment and test procedure
- injected fluid properties
- injection rate
- geologic discontinuities

Figure 4.3 Indistinct shut-in pressure response curve.

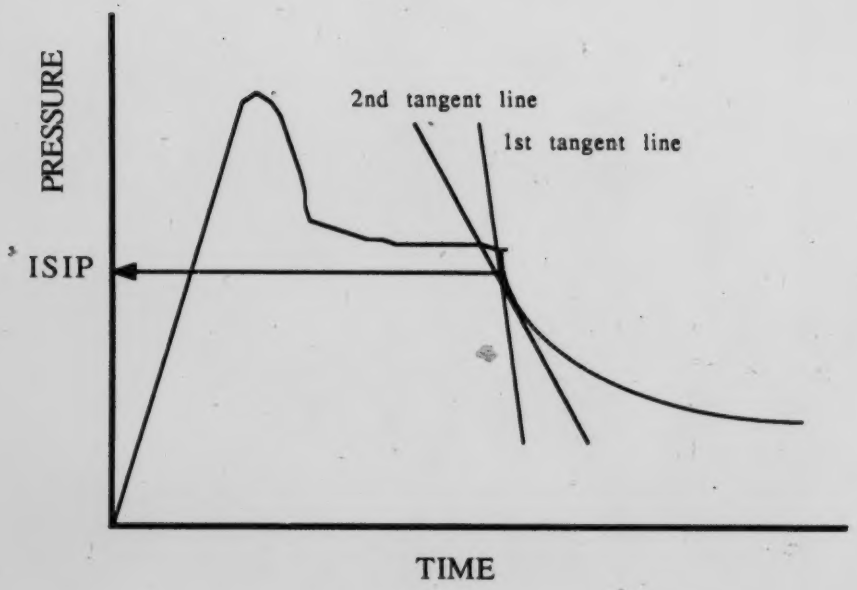

Figure 4.4 Application of the inflection point method to shut-in pressure data for the determination of the minimum principal stress.

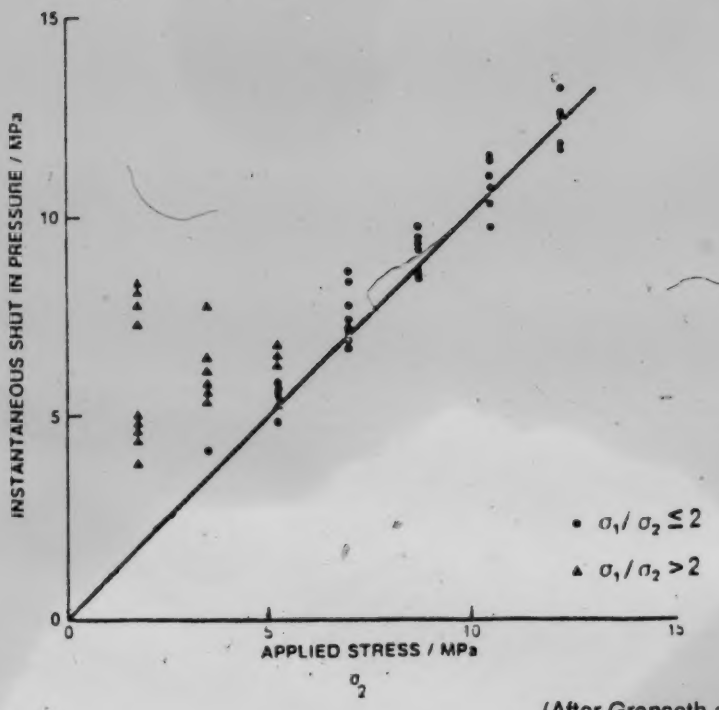

(After Gronseth and Kry 1983)

Figure 4.5 Correlation between applied load and the inflection point method interpretation of the minimum principal stress.

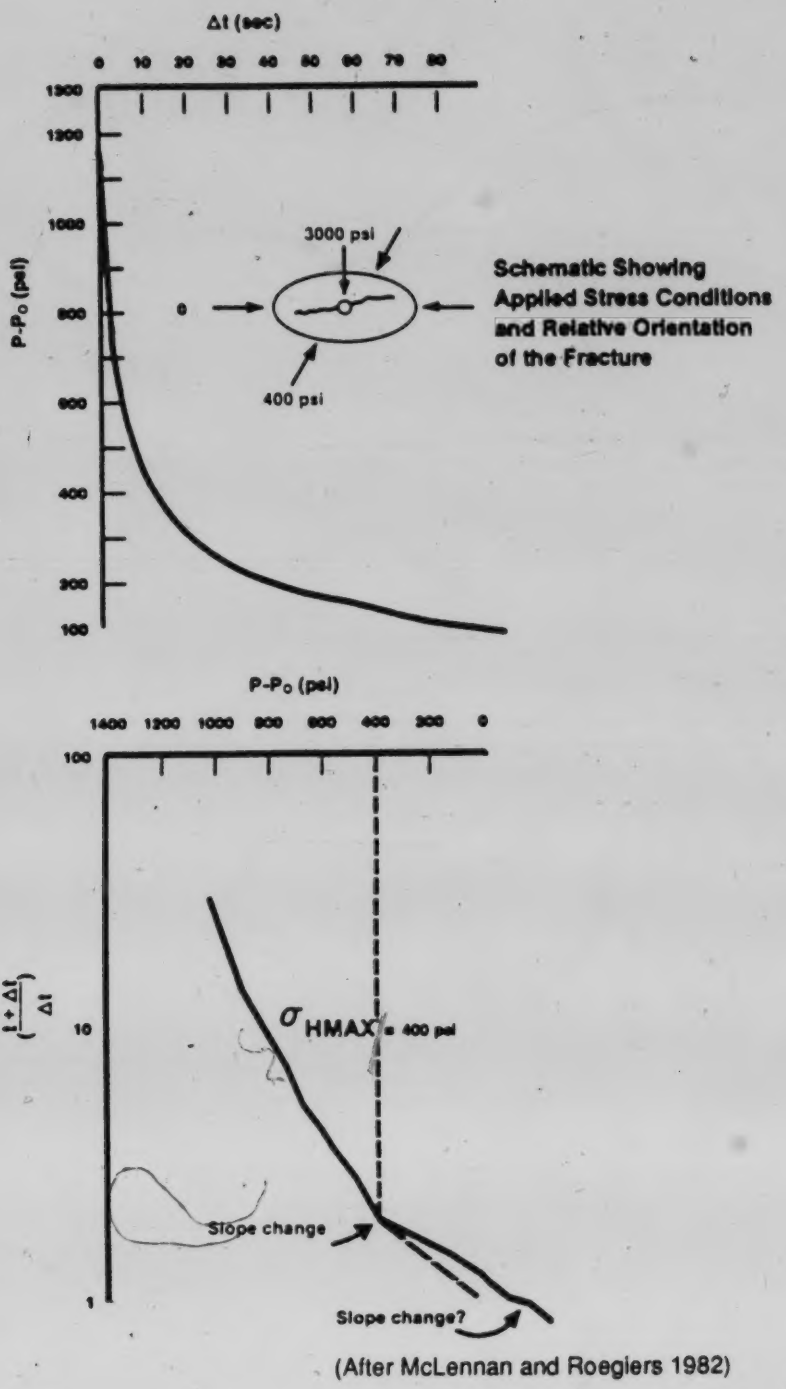

Figure 4.6 Horner analysis of the minimum principal stress from shut-in pressure data.

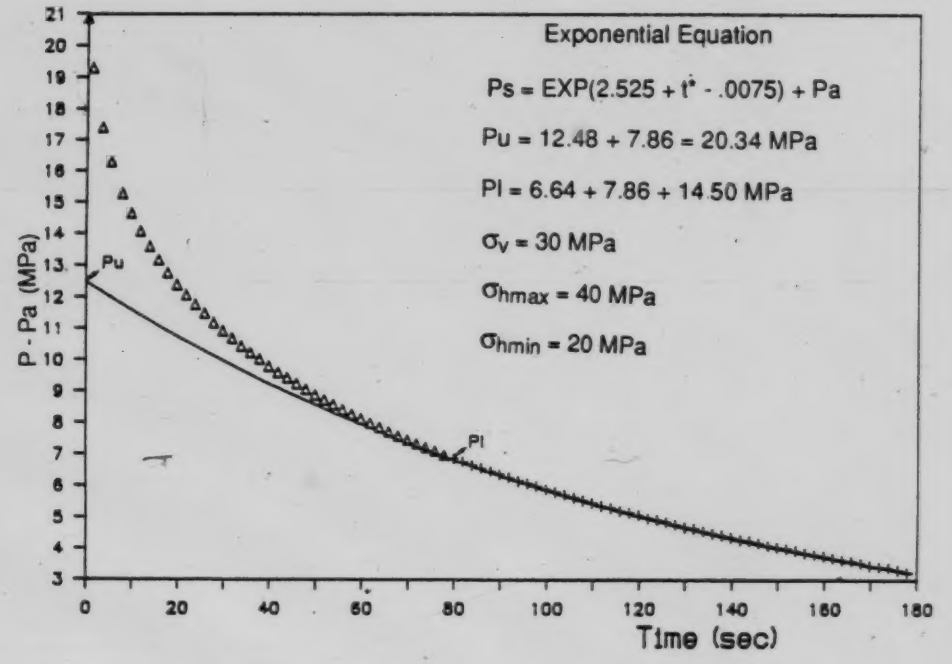

(After Cheung and Haimson 1988)

Figure 4.7 Application of the exponenetial decay model of Lee and Haimson (1988) to laboratory shut-in pressure data.

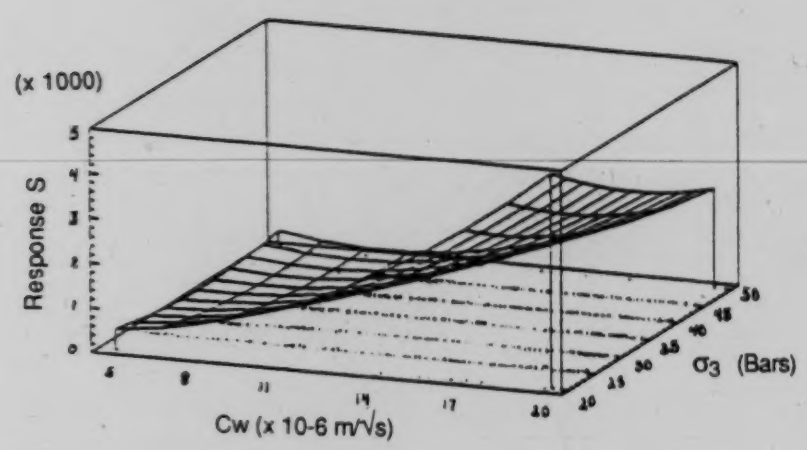

(a) 3-D Contours

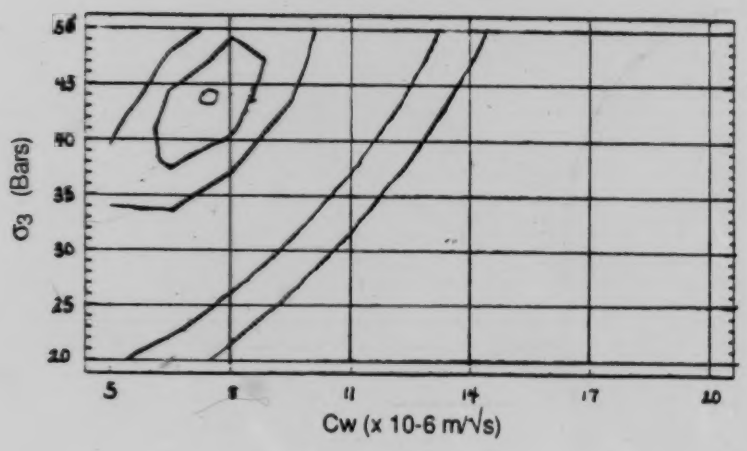

(b) Projection on the horizontal plane

(Modified after Charlez *et al.* 1988)

Figure 4.8 Schematic of the minimum principal stress contours for the application of the shut-in pressure curve inversion technique proposed by Charlez *et al.* (1988).

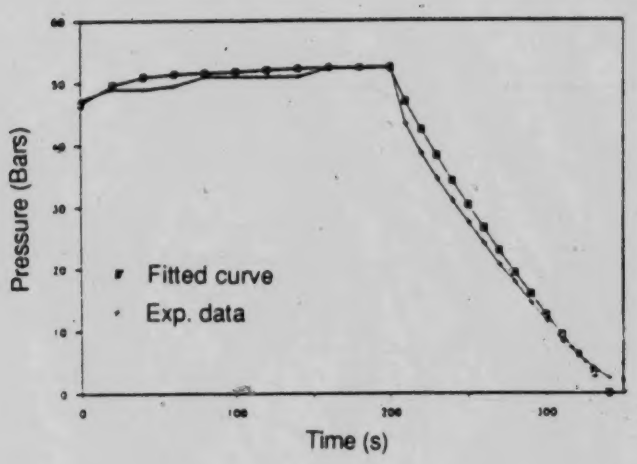

(Modified after Charlez *et al.* 1988)

Figure 4.9 Comparison of the field data and the model prediction of the shut-in pressure response.

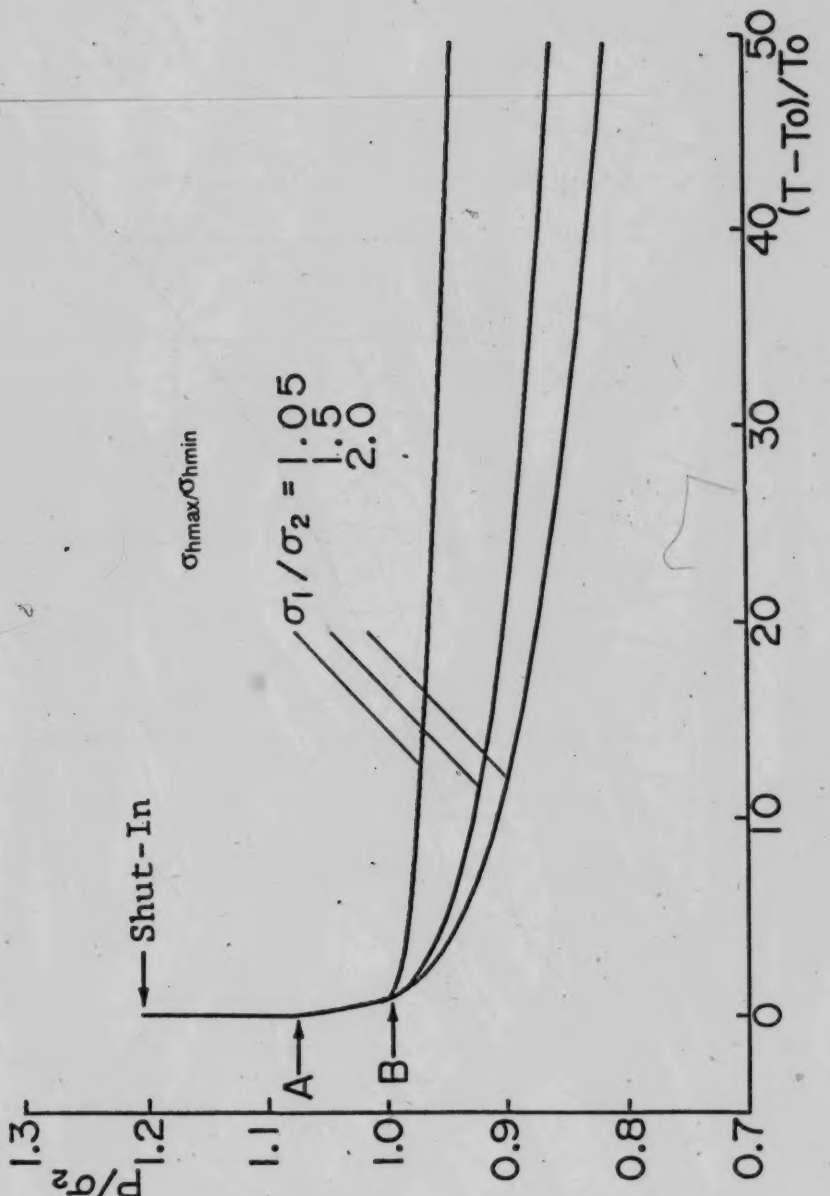

Figure 4.10 Effect of horizontal stress ratio on the predicted shut-in pressure response.

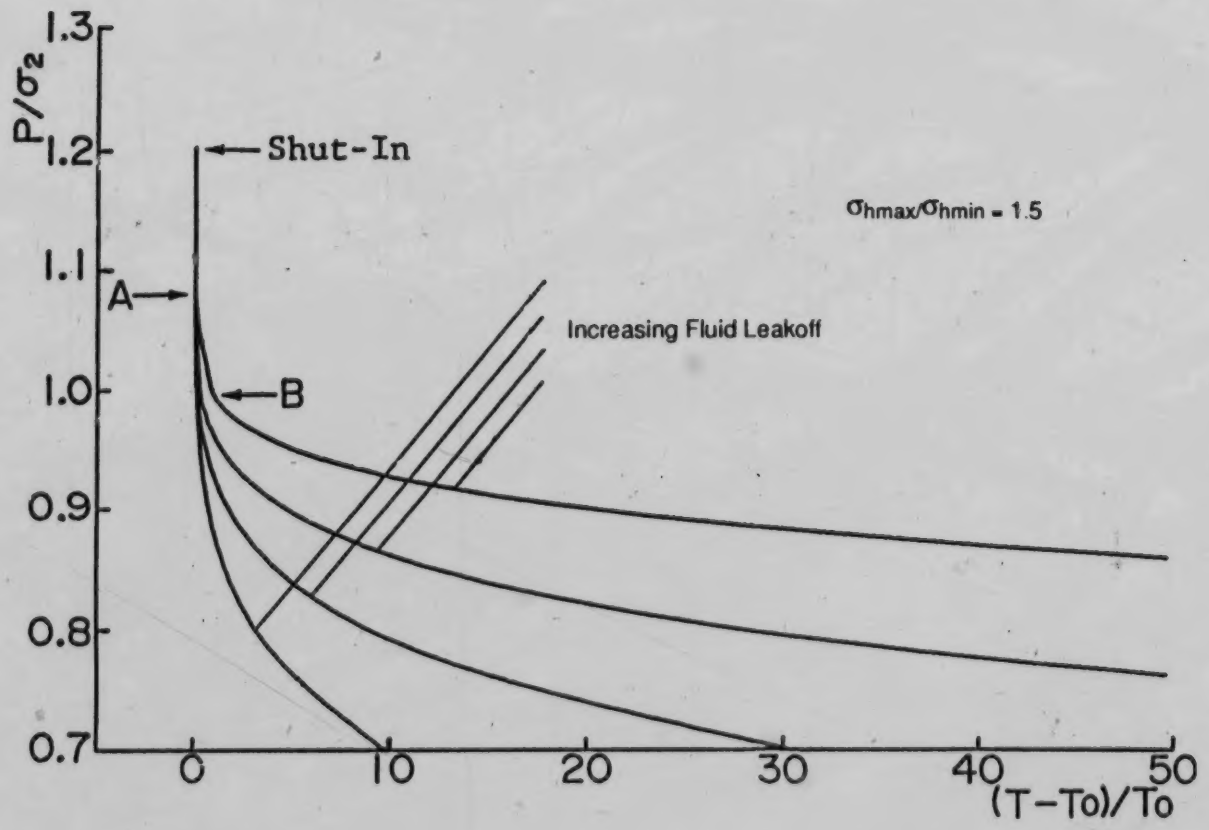

Figure 4.11 Effect of fluid leakoff coefficient on the predicted shut-in pressure response.

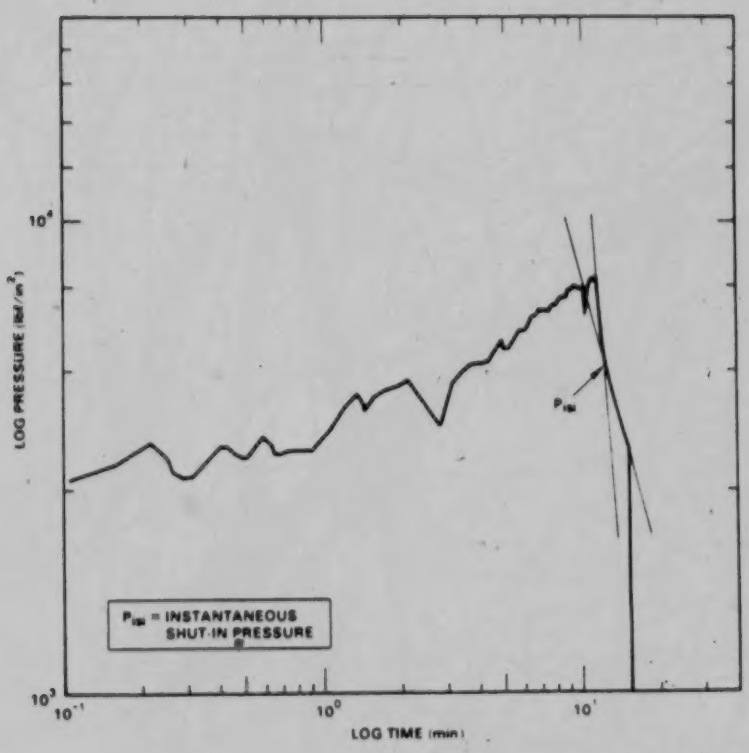

(a) Log P vs Log Δt

(Modified after Aggson and Kim 1987)

Figure 4.12 Two of the shut-in pressure response interpretation techniques employed by Aggson and Kim (1987).

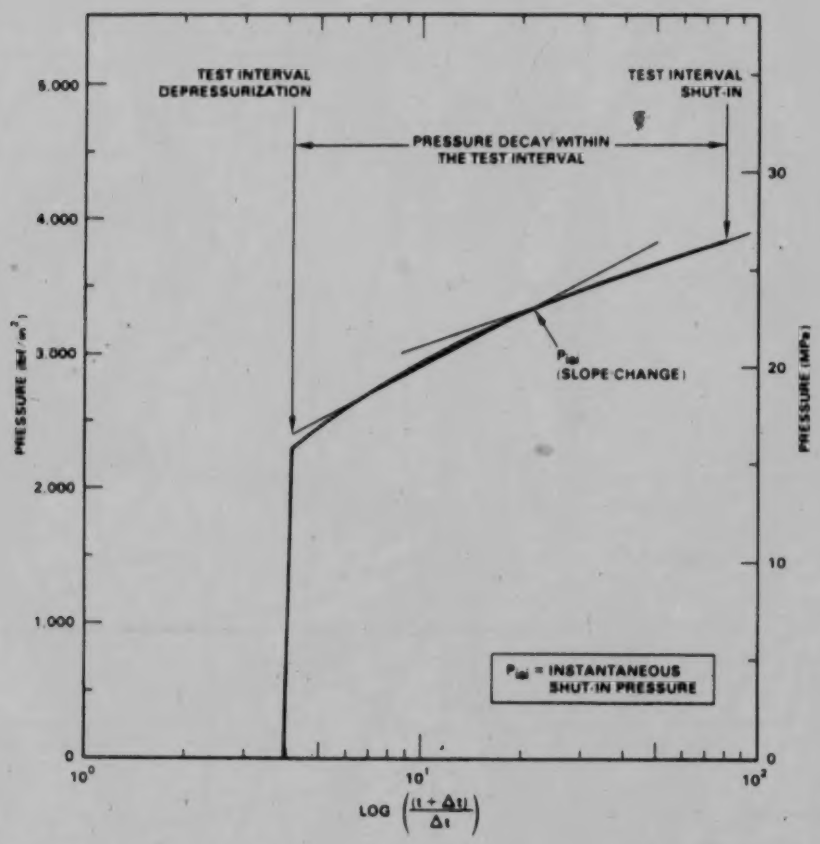

(b) P vs Log $[(t_{inj} + \Delta t)/\Delta t]$

(Modified after Aggson and Kim 1987)

Figure 4.12 continued.

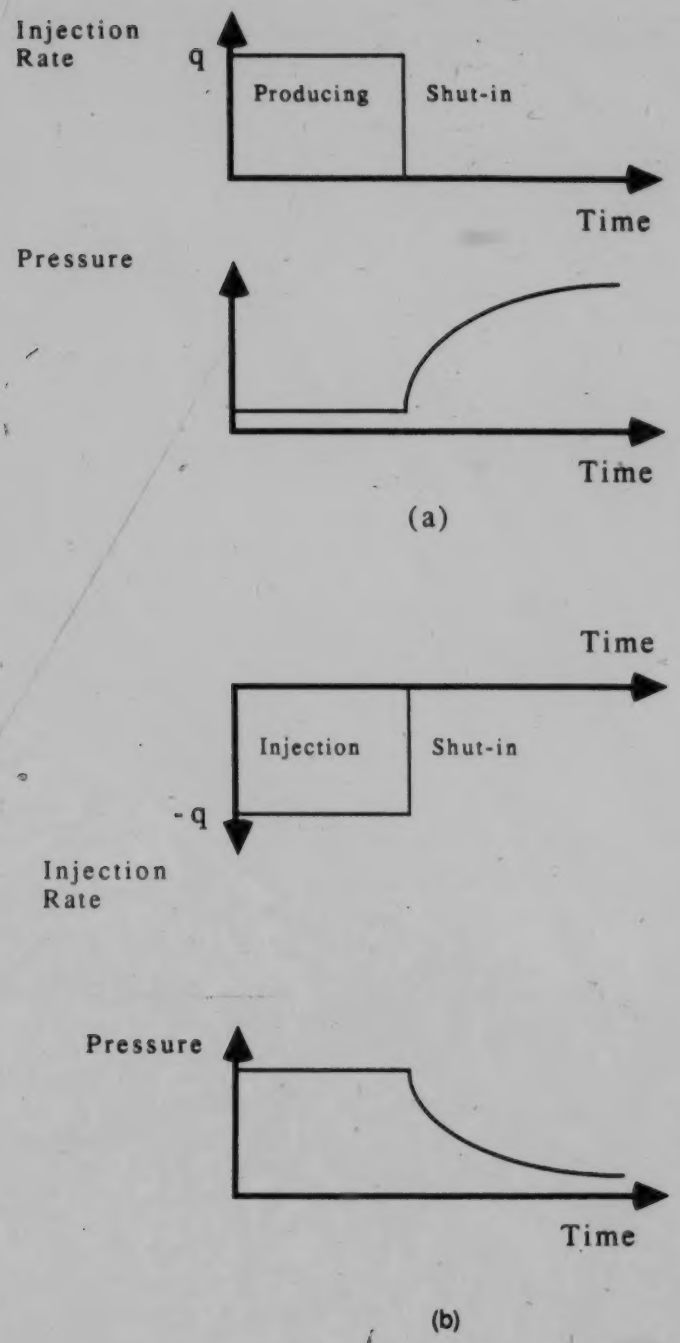

Figure 4.13 Injection rate vs time models for simulating (a) pressure build-up and (b) pressure fall-off tests.

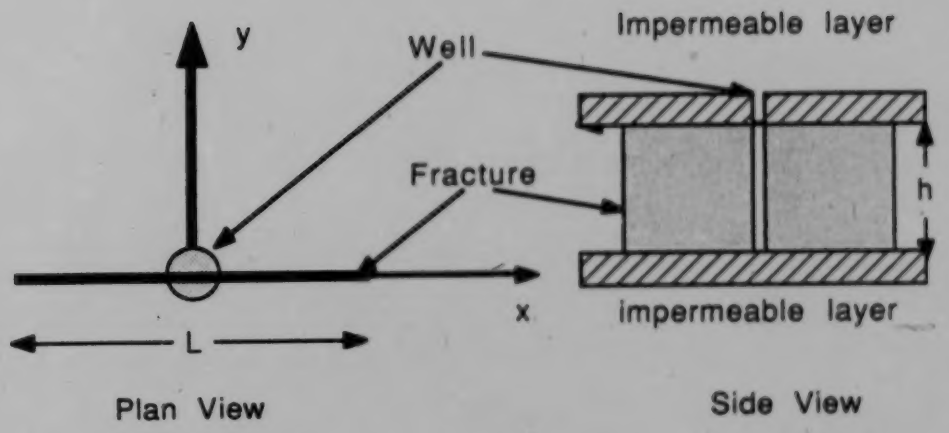

(Modified after Gringarten *et al.* 1974)

Figure 4.14 Model of a well intercepted by a single vertical fracture.

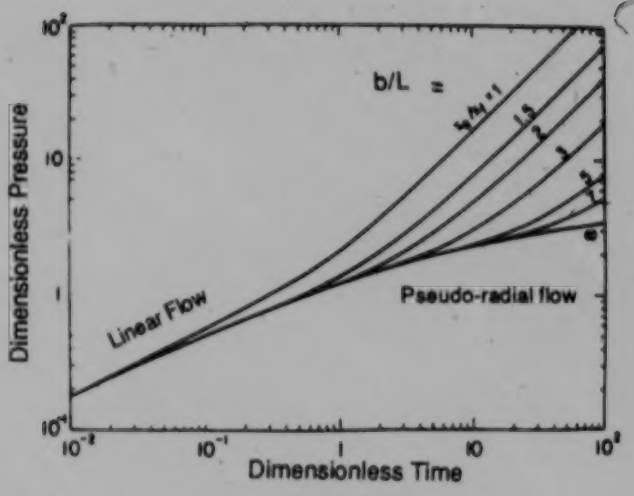

(a) Log-log graph for short time data

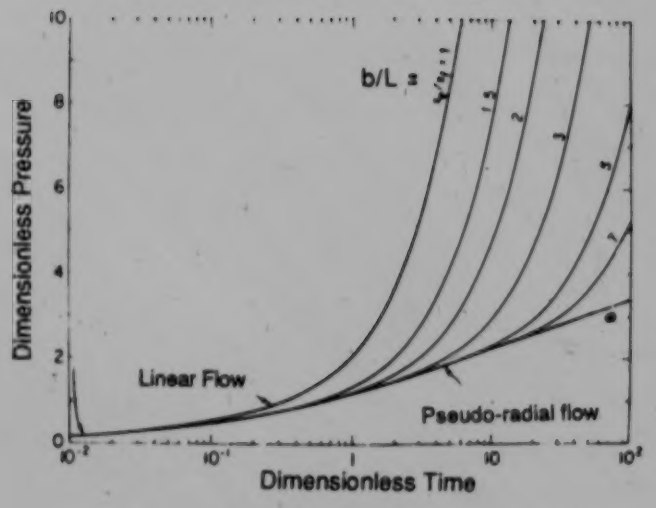

(b) Semilog graph for the long-time transient response

(Modified after Gringarten *et al.* 1974)

Figure 4.15 Characteristic pressure curves of an infinite conductivity vertical fracture for various fracture lengths.

(a) Fracture linear flow

(b) Bilinear flow

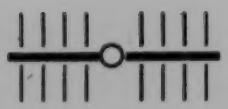

(c) Formation linear flow

(d) pseudo-radial flow

(Modified after Cinco 1981)

Figure 4.16 Four possible flow regimes exhibited by a vertically fractured well.

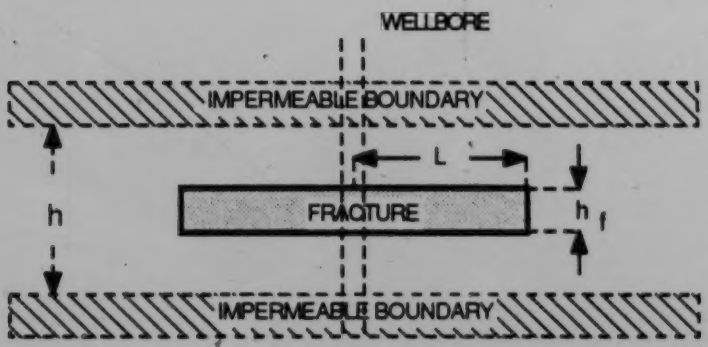

(Modified after Gringarten and Ramey 1974)

Figure 4.17 Model of a well intercepted by a single horizontal fracture.

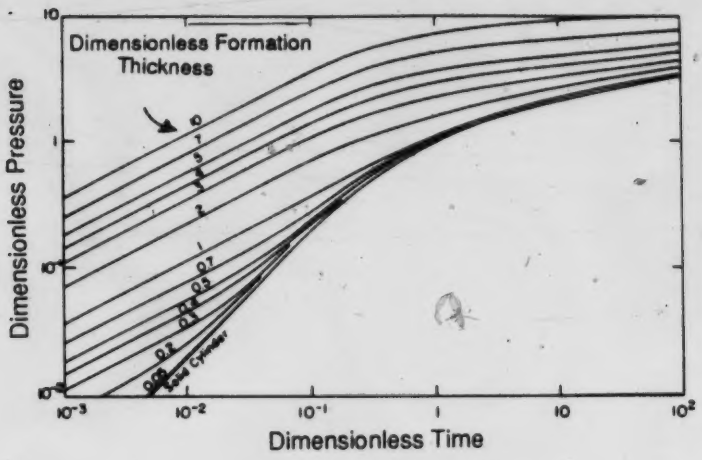

(a) Log-log graph for short time data

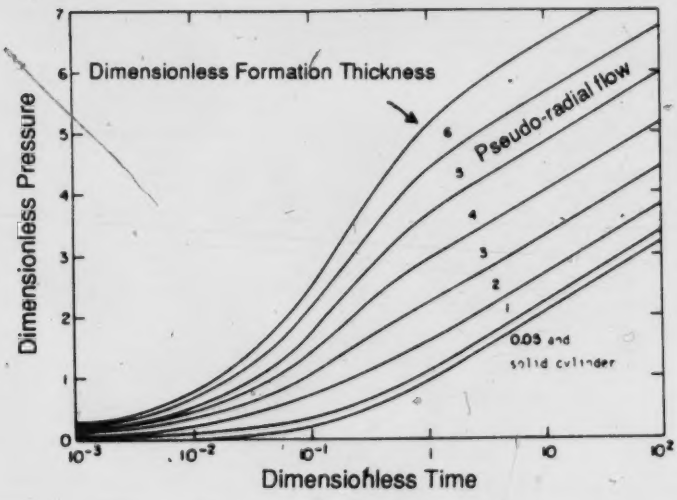

(b) Semilog graph for the long-time transient response

(After Gringarten and Ramey 1974)

Figure 4.18 Characteristic pressure curves of a uniform flux horizontal fracture centered at the borehole for various dimensionless formation thicknesses.

(a) linear storage flow

(b) vertical linear flow

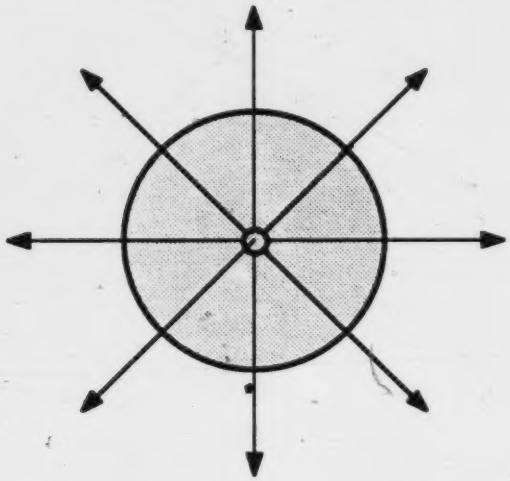

(c) pseudo-radial flow (plan view)

Figure 4.19 Three possible flow periods exhibited by a horizontally fractured well.

5. OIL SANDS MICROFRAC CASE STUDIES

5.1 Introduction

5.1.1 Background

The methodology presented in the previous chapter for the interpretation of small volume hydraulic fracture tests (microfracs) in oil sand deposits is employed in this chapter in the analysis of four oil sands microfrac case studies. The data for these case studies were obtained from AOSTRA and the tests were performed at several sites with various industrial participants. The four case studies are: (i) AOSTRA-AMOCO Gregoire Lake Pilot Project (AMOCO) tests, (ii) AOSTRA-CANTERRA TENNECO Kearl Lake Pilot Project (CANTERRA) tests, (iii) AOSTRA-BP B Unit Pilot Project (BP) tests, and (iv) AOSTRA-COLD LAKE-BOW VALLEY Pilot Project (ABC) test. The four case studies consist of one or more microfrac tests, of at least three cycles duration, in an oil sand layer. The Amoco micro-frac also consists of tests performed in the overlying shale layer and underlying limestone layer. Site locations are depicted in Figure 5.1.

Since the microfrac tests were conducted at various times for different operators, the test equipment and procedures vary from case to case. The Canterra tests were conducted in an open hole while the others were conducted in perforated cased boreholes. Test instrumentation affected the quality of the pressure-time data as seen in the difference between analog strip chart records of the ABC and the BP tests and the quartz gauge digital records of the Amoco and the Canterra tests. The ISRM guidelines recommend monitoring the injection rate with a flow meter of an accuracy of 0.3 m^3/d. Unfortunately, injection flow rate data and the injection rate monitoring methods for these tests were unavailable, therefore the quality of the injection rate data is unknown. Presumably, the injection rates given are average values over the entire injection period. Additionally, none of the four cases analysed used downhole shut-in tools and instead relied on surface shut-in.

Since the wells were not shut-in downhole at the perforation depth, the early time shut-in data is possibly affected by wellbore storage. Data collected during the wellbore storage period cannot be readily related to the reservoir properties and it also obscures the fracture linear flow response on the log-log plot at early time. Equipment and test procedure factors such as these are among the site specific factors which must be considered in the analysis of the minimum principal stress. This becomes evident later in the analysis of the case studies.

The transient pressure data during shut-in for the microfrac tests were analyzed according to the interpretation method described in chapter 4. This method consisted of a combination of: (i) inflection point method; (ii) $\delta P/\delta t$ versus p_{avg} method (pressure decay rate method); (iii) log $[P_{si} - P]$ versus log Δt method; (iv) P versus log $[(t_{inj} + \Delta t)/\Delta t]$ method (Horner method); and (v) P versus $[(t_{inj} + \Delta t)^{1/2} - (\Delta t)^{1/2}]$ method (tandem square root method). The results are summarised in tables for each microfrac case.

Some hydraulic fracture stress measurement tests include a method for determining the fracture orientation either downhole using, for example, borehole cameras or acoustic televiewers, or on the surface using, for example, tiltmeter arrays. Without such fracture monitoring, it is difficult to make definite conclusions regarding the fracture orientation. Unfortunately such a luxury was not available in any of the cases examined here. Therefore, some other method of ascertaining the induced fracture orientation was necessary in order to determine the orientation of the minimum principal stress. The only feasible method was based on the ratio of overburden stress to horizontal stress as developed by Dusseault (1980b) and used by Chhina and Agar (1985). A brief discussion on this method and in situ stress data for Alberta oil sand deposits follows in section 5.2.

Each case was analysed separately with regards to the relevant test and equipment factors, the geology/stratigraphy and the pressure-time data. Table 5.1 provides information concerning the perforation depth (or open-hole test depth), the test formation and the fluid injection data. Table 5.2 summarizes the relevant reservoir properties for the tests.

The minimum principal stresses for the microfrac cases have been analysed in terms of the interpretation method developed in chapter 4 and evaluated based on the analysis of section 5.2. The conclusions consist of a discussion of the minimum principal stress interpretation method for oil sands and the minimum principal stress results and inferred fracture orientations in the context of Alberta oil sands stress data.

5.1.2 Injection Rate Data

A major problem with the microfrac test data is that no fluid injection records were available for any of the tests, therefore, the accuracy of the injection rates and, consequently, the injected fluid volumes (Table 5.1) are unknown. This introduces additional uncertainity in the microfrac analysis because the analysis assumes constant injection rates which are high enough to ensure borehole fracturing.

An estimate of the injection rate required to cause hydraulic fracturing can be based on the steady-state fluid injection rate for the formation. The steady-state fluid flow solution for radial flow is (Lee 1983):

$$q = 2\pi \frac{kh}{\mu} \frac{(P - P_o)}{\ln (b/a)} \qquad [5.1]$$

where h = height of the confined pay zone. Fracturing will occur if the test injection rate exceeds the formation's steady-state fluid flow rate, q_{ss}, because the formation will be unable to accept all of the injected fluid. Conversely, an estimate, based on the test injection rate, can be made of the pressure difference $(P-P_o)$ (or the steady-state pressure, $P_{ss} = P$) which would cause steady-state fluid leakoff. If the actual breakdown pressure is less than the pressure required for steady-state fluid flow, it may be argued that a fracture has been induced in order to accomodate the test injection rate.

An analysis of the steady-state fluid leakoff for each of the microfrac tests was conducted in order to check that fracturing did occur in these tests.

Table 5.3 compares the steady-state injection rate and pressure for each test with the actual injection rate and the fracture initiation pressure. In summary, the results show that, except for the Canterra BP1 microfrac, all tests resulted in fracturing. However, two points must be noted about the steady-state calculations using equation 5.1. First, the transmissibility values, kh, were derived from a Horner analysis of the long-time shut-in pressure data of each microfrac (Earlougher 1977; Lee 1983) assuming that the influence of the induced fracture on the formation fluid flow was negligible. These results (Table 5.3) are comparable with other oil sands permeability measurements (Table 3.1), but the effect of the induced fractures on these results is unknown. Second, the steady-state drawdown radius, b, used in the calculations was assumed to be 50 m (borehole radius of a = 0.089 m was also used). Fortunately, the q_{ss} and P_{ss} calculations are not too sensitive to changes in b (i.e., for b = 100 m, q_{ss} would be reduced by 11%).

5.2 Alberta Oil Sands Stress Data

The basic concept of hydraulic fracture propagation is that a fracture will propagate in a plane normal to the minimum in situ principal stress (Abou-Sayed *et al.* 1978). When no direct observation of fracture orientation is available for small volume hydraulic fracture tests (i.e., microfracs), this concept may be used to derive the induced fracture orientation (i.e., horizontal, vertical or inclined). This is done by comparing the instantaneous shut-in pressure, P_s, with σ_v (the overburden or vertical stress). When the calculated overburden stress is less than P_s, a fracture initiated at the wellbore would be horizontal in order to be normal to the minimum principal stress, σ_v. Likewise, when the calculated vertical stress is greater than P_s, the fracture orientation is vertical and in a plane normal to minimum horizontal principal stress. Chhina and Agar (1985) expressed this relationship in the following equation:

$$\frac{\sigma_v}{P_s} \leq 1, \text{ for horizontal fractures} \qquad [5.2]$$

This method can be validated against previously reported oil sand hydaulic fracture test stress measurement data as well as existing theories for the distribution of in situ stress in Alberta oil sand deposits (the emphasis is on the Athabasca and Cold Lake deposits). Since most in situ stress measurement tests in oil sand deposits are performed for the oil industry, only a limited amount of data is publically available. Hydraulic fracture stress measurement data has been compiled from the literature and are presented in Table 5.4 and are plotted against depth in Figures 5.2 for the Cold Lake deposit and 5.3 for the Athabasca deposit. Some comments are necessary to explain this in situ stress compilation.

In the Cold Lake oil sand deposit, the most important payzone is located in the Clearwater Formation, which is located at depths that vary from 400 to 450 m (Figure 5.2). Based on stress data available to him, Dusseault (1980a) concluded that vertical fractures with a NE-SW trend would be generated in hydraulic fracturing operations in the Clearwater Formation. The in situ stress data in table 5.4 confirms this in that values of the σ_v/P_s ratio, with one exception, range from 1.04 to 1.93, thereby indicating a preference for vertical fractures. In situ stress data reported by Gronseth (1988) suggests that at least at Esso's Leming site, the minimum horizontal principal stress is approximately the same as the overburden stress at 454 m depth. Of the twenty wells tested, over half were interpreted as vertical fractures while the remainder were either horizontal fractures or fractures that rotated from a vertical to a horizontal orientation. Although Gronseth (1988) states that the in situ stress state dictates horizontal fractures ($0.89 \leq \sigma_v/P_s \leq 1.0$), the majority were vertical at the wellbore and allowed an evaluation of the minimum horizontal principal stress.

The in situ stress data for the Athabasca deposit presents a more complicated picture because of the greater variability in the depth of the payzone across the deposit (Figure 5.3). Dusseault (1980a) suggested that for the Athabasca deposit, at depths less than 250 m σ_3 was oriented vertically ($\sigma_3 = \sigma_v$) inferring the creation of horizontal fractures. At depths greater than 400

m, σ_3 was in the horizontal plane inferring the creation of vertical fractures. The in situ stress data for the Athabasca deposit presented in table 5.4 seems to follow these guidelines. It is apparent that at intermediate depths, where σ_v/σ_3 approaches unity, in situ stress no longer predominantly controls fracture orientation. Geologic discontinuities identified in oil sands deposits, such as the shale-oil sand interbedding and sand cross bedding, will exert some control over fracture orientation as noted in chapters 3 and 4.

The simple models proposed here for predicting hydraulic fracture orientation for the Cold Lake and Athabasca deposits, based on Chhina and Agar's equation and the limited oil sands in situ stress database, are, at present, the only route available for the determination of hydraulic fracture orientation when actual downhole or surface inferred measurements are unavailable. Although it is possible to theoretically calculate the in situ stress state in a deposit (e.g., Dusseault 1977b) based on simple gravitational loading, these models do not accurately account for tectonic, sedimentologic, and diagenetic factors which act during the formation of the deposit Cleary 1988). In addition to an accurate knowledge of the overburden stress (e.g., derived from density logs), this route requires that an experienced hydraulic fracture practitioner analyse the results because of the inherent complications involved in the data interpretation.

The analysis of hydraulic fracturing stress measurement technique should not be contingent upon a previous knowledge of the in situ stress state. Unfortunately, present oil sands hydraulic fracture stress measurement practice requires an *a priori* assumption on the induced fracture direction or previous in situ stress data for the test site in order for the pressure data to meaningfully interpreted. In general, it is essential that in hydraulic fracture stress measurement tests where the induced fracture orientation is uncertain, some means of determining the induced fracture orientation should be included.

5.3 AOSTRA-AMOCO Gregoire Lake Pilot Project Tests

5.3.1 Test and Site Description

5.3.1.1 General Description

Three series of microfrac stress measurement tests conducted in the Athabasca oil sands deposit were analyzed. Each series of tests consists of three or four cycles of injection and shut-in. The test data is summarised in Table 5.1. The digital pressure-time data was plotted and analyzed according to the interpretation scheme presented in chapter 4. The limestone and shale microfrac tests were performed in the H1 well and these tests provide in situ stress data for the strata that confine the McMurray Formation oil sands. The oil sands microfrac tests were performed in the H3 well.

The test procedure for all of the tests conform to standard small volume hydraulic fracture stress measurement (microfrac) practice. Table 5.1 shows that the total injected fluid volumes fall within the 0.004 to 1.0 m^3 guidelines of Warpinski *et al.* (1985). The injected fluid was KCl water and it was injected at rates that were less than the 72 m^3/d upper limit recommendation of Gronseth and Kry (1983). Since the only injection rate record is that shown in Table 5.1, the accuracy of q and V_{inj} is unknown.

The tests were performed in perforated cased boreholes as is the normal practice with oil wells in unconsolidated formations. Accordingly, breakdown pressure cannot be used to estimate σ_{hmax} due to the unquantifiable effect of the casing, cement job and perforation damage. Table 5.5 shows that the difference between propagation pressure and shut-in pressure did not exceed the 3500 kPa limit recommended by Warpinski (1983). This suggests that the relationship between P_s and σ_3 was not affected by the perforation or casing related factors.

The early time shut-in data is affected by wellbore storage because these tests were not shut-in downhole. Log-log graphs were prepared in order to assess the extent of wellbore storage.

The limestone and shale microfrac tests were both conducted in the H1 well, while the oil sands tests were performed in the H3 well. Figures 5.4 and 5.5 depict the lithology for both wells. The microfrac tests at the perforation depth of 240-241 m in the H1 well were performed in the Devonian limestone which underlies the Lower McMurray member. Very little has been published about the Devonian limestone. Higher up in the H1 well, in the Wabiskaw member of the Clearwater Formation, the well casing was perforated at 187-188 m depth. Logs indicate that the perforations are located in one of the alternating shale layers characteristic of this member. The Wabiskaw is generally a glauconitic sand or sandy shale, but the stratigraphy is comprised of a complex interbedded lithology of variable layer thicknesses (1 cm to 1 m). The sediments are usually highly bioturbated and the sands can be considered very fine grained and argillaceous. A dark grey marine shale overlies the Wabiskaw and serves as a marker bed.

The microfrac perforations in the H3 well are located at 235-238 m depth in the McMurray oil sand formation.

5.3.1.2 Limestone Tests

This test series consists of four cycles of fluid injection and well shut-in performed in the Upper Devonian Waterways Formation (Table 5.6). For some reason, the cycle 1 and 2 injection periods were stopped before a breakdown pressure was reached (Figure 5.6). It is concluded that no fracture was created in these two cycles. The following two cycles experience breakdown at 10900 and 8300 kPa respectively and have stable propagation pressures prior to shut-in. The difference between the third and fourth cycle breakdown pressure of 2600 kPa indicates a substantial formation fracture resistance. The steady-state fluid flow analysis (Table 5.3) confirms that the injection rates were sufficient to cause fracturing. Also, the pressure calculations using this analysis indicate that fracturing occurred.

Because the first two cycles did not experience fracture initiation, there remain only two cycles of shut-in data for analyzing σ_3. Table 5.6 shows that

all five methods gave P_s = 6000 kPa for cycle 3 because the shut-in interpretation was rather unambiguous. Cycle 4 shut-in analysis shows a poorer agreement among the various interpretation methods. The three closure pressure methods give P_s = 5680 kPa and the inflection point method gives P_s = 5250 kPa. The reduction in P_s observed with the subsequent injection of a further 0.068 m^3 of fluid in cycle 4 may be due to one of mechanisms postulated in chapter 4.

5.3.1.3 Shale Tests

As with the limestone tests, the first injection cycle was stopped before a breakdown pressure was reached, therefore no fracture was created in this cycle (Figure 5.7). However, the steady-state fluid flow analysis (Table 5.3) suggests that the injection rates were sufficient to cause fracturing. Also, the pressure calculations using this analysis indicate that fracturing occurred. In the second cycle, the injection rate was raised to 19.3 m^3/d and it resulted in a clear breakdown pressure at 4400 kPa. After breakdown the injection pressure decreased steadily until a sudden drop to 4000 kPa occurred approximately 190 s after injection began. The pressure gradually recovered to an injection pressure of 4400 kPa. Such behaviour can be explained by the propagating fracture experiencing some variable choke or flow restriction. The third cycle injection, with a slightly lower injection rate of 17.3 m^3/d, had a break in the injection curve at 4400 kPa, but the pressure continued to increase to a level of 4900 kPa, whereupon it leveled off until shut-in, with a few minor fluctuations of 50 kPa. The initial fracture created in cycle 2 was possibly re-opened at 4400 kPa, but the higher injection pressures indicate some other mechanism at work. The fourth cycle injection rate was increased to 27.9 m^3/d and the breakdown occurred at 5100 kPa, with the injection pressure at approximately 5000 kPa, but it was plagued by erratic spikes of ± 250 kPa. The last cycle's increased P_f and P_p values may be due to the 60% increase in the injection rate from the previous cycle, or it may be related to

the mechanism responsible for a similar increase observed in the previous cycle.

The shut-in response for the first cycle was not because no fracture was thought to be initiated in this cycle. The pressure-time graph indicates that no sustained injection pressure was maintained and the breakdown pressure is significantly lower than the later cycles (Table 5.6). It is concluded that the first cycle of the microfrac is instead a pressure falloff injection test which may reveal some information about the reservoir's fluid flow properties.

The second cycle shut-in pressure analysis reveals that well test plots along with the inflection point method and the pressure decay rate graph all give 3500 kPa as the approximate σ_3. Once wellbore storage is complete, two linear flow lines eventually change into a pseudo-radial period at the very end the of shut-in data. The third cycle shut-in response is very similar except it gives a higher value of σ_3 as 4200 kPa. The shut-in response of the fourth cycle is different from that of the previous two cycle and is more difficult to explain. There is no apparent wellbore storage and a minor linear flow period at the start, but the data then behaves in neither a linear nor a pseudo-radial flow manner. A value of 4600 kPa for σ_3 was tentatively derived, but this is approximately 400 kPa higher than the previous value. The increase in the minimum principal stress is shown in Figure 5.8.

5.3.1.4 Oil Sands Test

This test series consisted of three cycles of fluid injection/well shut-in performed in the oil sands of the McMurray Formation (Table 5.1). The steady-state fluid flow analysis (Table 5.3) suggests that the injection rates were sufficient to cause fracturing. Also, the pressure calculations using this analysis indicate that fracturing occurred. The pressure versus time records in Figure 5.9 exhibit a response similar to that proposed by Dusseault (1980). In this case, the breakdown pressure, fracture propagation pressure and the instantaneous shut-in pressure are all very close (maximum difference of 400 kPa) as shown in Table 5.6. Although cycles 1 and 2 have no clear breakdown

pressure, they both have an inflection point at approximately 5000 kPa which is succeeded by a gradual increase in injection pressure to 5300 kPa prior to shut-in. The final cycle has a slightly different response where there is a breakdown pressure of 4800 kPa and then the propagation pressure falls slightly and then gradually recovers to 5000 kPa prior to shut-in. The breakdown behaviour may be affected by initial perforation induced wellbore damage. The lack of a definitive P_f value in the first two cycles is possibly due to initial wellbore flow restrictions which were eventually removed by subsequent fluid injection.

Analysis of the shut-in curves reveals that there are two characteristic points. As seen in Table 5.6 the inflection point method gives a P_s value of 4900 - 5300 kPa, while the other three well test methods identify a consistent point between 3200 - 3600 kPa. Curiously, the slope change analysis agrees with the well test analyses. The substantial difference between these two points on the shut-in curve (1300 - 1700 kPa) suggests that they represent two different fracture-formation responses rather than a difference in interpretation methods.

5.3.2 Interpretation of Microfrac Data

Examination of the microfrac results show that while the interpretation methods identify similar σ_3 values for each cycle in the limestone and shale microfracs, there are substantial differences for oil sand microfracs. The limestone tests have a substantial breakdown pressure which differs from the propagation and shut-in pressure, whereas the oil sands and shale tests exhibit breakdown pressures similar to the propagation pressures. This preliminary analysis seems to suggest that there are some common hydraulic fracture characteristics as well as some significant differences for the three GLISP microfracs.

5.3.2.1 Limestone Tests

Unlike the oil sands and shale zones, the limestone observed in these tests apparently possesses a substantial tensile strength of approximately 2600 kPa. Chhina (1988) also observed high tensile strength of approximately 14,000 kPa in this limestone formation at the UTF site. His data also suggested that higher injection rates (> 20 m^3/d) and longer injection durations (1700 s) were necessary in order to overcome this tensile strength and rupture wellbore. Cycle 3 and 4 data were obtained by increased injection rates and injection durations which seemed to result in fracture initiation.

The minimum principal stress interpretation for cycle 3 was unambiguous and indicated σ_3 = 6000 kPa. The vertical stress-instantaneous shut-in pressure ratio for this cycle is less than 1 (Table 5.3) suggesting horizontal fractures are preferred. Although the minimum principal stress interpretation for cycle 4 was not as precise, the range in σ_3 also gives a vertical stress-instantaneous shut-in pressure ratio approaching 1. In contrast, the limestone results of Chhina (1988) exhibit ratios of 0.44 to 0.72. Although the test depth for Chhina's microfrac data would suggest the creation of horizontal fractures giving $\sigma_3 = \sigma_v$, the interpreted stress data infers the creation of vertical fractures at the wellbore.

The actual minimum principal stress interpretation is limited to the analysis of data of two shut-in cycles. While the shut-in data was well defined and was not markedly affected by wellbore storage, the disparity in cycle 4 interpretation methods shows how difficult it is to obtain an agreement within 1000 kPa. Furthermore, the reduction in the P_s values of approximately 320 to 750 kPa from cycle 3 to 4 may or may not be significant depending on the measurement and interpretation error. Other practitioners have observed a similar phenomena and many factors, such as fracture widening, geologic discontinuities and horizontal fracture climbing, have been proposed to explain these stress decreases. Because we are restricted to limited data from only two cycles, no conclusion can be made about this decrease.

5.3.2.2 Shale Test

The injection pressure behaviour for the shale tests presents valuable information useful for interpretation of the minimum principal stress. Previous hydraulic fracture data showed that breakdown pressure normally decreased with each added cycle, but the opposite trend is observed here. Evidently fluid injection of the first cycle was discontinued prior to fracture initiation . By roughly doubling the injection rate for cycle 2, a fracture was initiated at a pressure of 4400 kPa. The third cycle breakdown pressure response suggests that the initial fracture was re-opened at 4400 kPa, but the pressure continued to rise until 4900 kPa. Such behaviour suggests that either some flow restriction existed around the borehole or that a second fracture was pressurized during the third cycle. The further increase in P_f and P_p in cycle 4 may be related to either one of these two hypotheses or it could be related to the effect of injection rate on fracturing pressure. A similar trend in the P_s values was also observed as shown in Figure 5.8.

The in situ stress data for this depth and the vertical stress/minimum principal stress ratio (Table 5.5) support the creation of horizontal fractures. The σ_3 interpretations for cycle 2 were uniform and gave a stress ratio of approximately 1. While the second cycle σ_3 interpretations are also relatively uniform, the increased breakdown pressure and P_s values indicate a different fracture response. Furthermore, the cycle 4 response continues the trend. There are a number of possible explanations:

(i) a horizontal fracture propagating into a strata with increased stress;

(ii) multiple fracturing related to the increased injection rates;

(iii) poroelastic effects increasing the local in situ stresses.

However without further knowledge of the fracture orientation and the geologic structure away around the borehole, it is difficult to identify the actual physical explanation(s). The safest conclusion is that the second cycle test created a single horizontal fracture with $P_s = \sigma_3 = \sigma_v$.

5.3.2.3 Oil Sands Test

Review of the fracture initiation and propagation behaviour as indicated by the pressure-time records (Figure 5.9) suggests that the oil sands behaves in manner similar to that predicted by Dusseault's (1980a,b,c) conceptual geomechanical model. Oil sand's geomechanical behaviour implies that the fracture initiation pressure should be approximately the same as the propagation pressure and the shut-in pressure. All three cycles exhibit such a response as shown in Table 5.6. Under these circumstances, the instantaneous shut-in pressure should give a definitive value of σ_3 as confirmed by the fracture initiation and fracture propagation pressure. However, the minimum principle stress interpretation from the other four interpretation graphs all identify a consistently lower P_s value (Figure 5.10 and Table 5.6).

Like the limestone and shale tests, horizontal fractures were expected for these depths. The vertical stress/instantaneous shut-in pressure ratio for the higher P_s values is near 1 (Table 5.5) confirming this initial conjecture. On the other hand, the vertical stress/instantaneous shut-in pressure ratio for the other four interpretation methods infers the creation of vertical fractures. Chapter 4 provides a number of possible explanations for this conundrum:

(i) Two fractures could have been created at two different locations as reflected in the two different shut-in pressures caused by the closure of these two fractures;

(ii) As observed by Medlin and Masse (1985), there could be two mechanisms controlling fracture closure: first leakoff and, second, creep controlled closure.

(iii) fracture orientation changes in which a horizontal fracture becomes vertical if the fracture propagates into strata where $\sigma_3 = \sigma_v$.

(iv) The second P_s value may be related to some other mechanism unrelated to fracture closure (e.g., shear failure, perforated casing).

The phenomena of dual closure stresses has been observed before (Warpinski *et al.* 1985) and it could be responsible for the observed behaviour.

The second P_s value of 3500 kPa is a good approximation of the vertical stress at a depth of 169 m, where a shale layer exists capping the oil sands formation (Figure 5.5). Past experience with casing in oil sands has suggested that a poor bond exists between the cement and the oil sand, while the bond is quite tight at the shale cap (Chhina 1988). It is possible that fracture fluid not only initiated a fracture at the perforations in the oil sand, but it also leaked past the cement and rose along the cement-oil sands interface until the shale cap was encountered. The propagation pressure indicates the fracture pressure in the oil sands fracture according to Dusseault's conceptual model, but at shut-in this fracture closes immediately and the shut-in response is controlled by the fracture at the shale cap. This interpretation of the microfrac data gives the unexpected result of supplying a value of σ_v at the shale-oil sands interface.

The second hypothesis lies in Medlin and Masse's (1982) observations in carefully monitored laboratory hydraulic fracture tests of two points on the shut-in curve. The traditional P_s value represents leakoff dominated fracture closure, while the second point, P_c, represents rock controlled closure. Early closure is controlled by fluid leakoff, but full fracture closure is controlled by residual strain where the creep properties of the rock become important. Medlin and Masse (1982) suggest that the true σ_3 may be overestimated by up to 20% by selecting the leakoff controlled P_s. This may be a possible explanation for the two points observed in the shut-in response. While the initial P_s value of 5000 kPa agrees with the vertical stress, the second P_c value of 3500 kPa does not fit in with current in situ stress data for 235 m depth. This disagreement with the in situ stress data, along with the substantial difference between P_s and P_c of 43%, seems to refute the second hypothesis. Additional work on the leakoff and the creep properties of oil sands is necessary to better evaluate this hypothesis.

The third hypothesis is based on the fracture orientation changes associated with the fracture extending beyond the near wellbore rock where an altered stress state may exist and into rock where the original in situ stress state exists and the fracture rotates in response to the this change. It may be

possible to detect this occurrence in multiple cycle tests where the P_s changes with each cycle (Zoback and Haimson 1982).

Finally, as the fourth hypothesis, the second point identified by the interpretation methods may be indicating an unknown mechanism unrelated to fracture closure. For larger hydraulic fracture treatments, shearing adjacent and in advance of the fracture due to fluid leakoff has been proposed. Although the injection rates and fluid volumes are low in these tests, it is possible that shearing may be occurring at some critical location and is affecting the shut-in pressure response. Alternatively there may be some variable choke mechanism caused by the perforation damage which has not been removed throughout the test. Despite the possible influence of these secondary mechanisms on the shut-in pressure response, the P_s interpretation suggests horizontal fracturing.

5.4 AOSTRA-CANTERRA TENNECO Kearl Lake Pilot Project Tests

5.4.1 Test and Site Description

5.4.1.1 General Description

The only openhole microfrac tests analysed were the BP1 and the BP4 tests performed at the Kearl Lake project in the Cold Lake oil sands deposit. The lower oil sand of the McMurray Formation was the object of both tests. Table 5.1 summarizes the information regarding test depth, injected fluid volumes and injection rates. The digital pressure-time data were plotted and analyzed according to the interpretation procedure described in chapter 4.

Openhole microfrac tests in oil sand formations are rare because wellbore stability and production considerations normally require that the wellbore be cased. Apparently the BP1 and BP4 wells were in oil sands material sufficiently competent so that casing was not necessary. Without the perforated casing, the BP1 and BP4 wells better approximate the conditions assumed in classical hydraulic fracture theory. This means it is now possible to use a hydraulic fracture initiation equation to calculate σ_{hmax}. However,

there remain two assumptions necessary for such a conclusion which may not apply to the BP1 and BP4 microfrac tests: (i) a circular borehole in linear elastic homogenous isotropic material and (ii) vertical fracture initiation.

The test procedure is fairly similar to those of the previous case histories. Unfortunately, there were no injection rate-time records except those shown in Table 5.1. The injection rates, which vary between 225 to 572 m^3/d, are 2 to 60 times higher than the other tests (Table 5.1) and exceed Gronseth and Kry's (1983) recommendation of 72 m^3/d. While the injection times are fairly small and the injected fluid volumes are not significantly greater than the other case histories, the high injection rates may introduce certain rate effects, such as increased breakdown pressure and excessive friction losses in the fracture and the tubing. Pressures were measured downhole by quartz crystal gauges at a rate of 1 per 2-3 seconds. Shut-in occurred at the surface and so early time data is probably affected by wellbore storage.

Lithologic logs for wells BP1 and BP4 are shown in Figure 5.11. The test interval for BP1 is located in a fluvial channel deposited oil sand layer of the McMurray Formation which is underlain by the Devonian limestone. This oil sand layer is characterized by high angle planar bedding and by minor cross bedding and graded bedding. Overlying this layer is an 3 m thick upper tidal flat deposit of dark grey mud that is poorly laminated, homogeneous (bioturbated in some locations) with thin, irregular lenses or laminae of sand and silt. The BP4 test interval is found in tidal channel deposit that overlies the Devonian limestone. This tidal channel layer is fairly well-sorted clean quartz sand, usually homogeneous but with some small scale bedding. The upper tidal channel deposit also overlies this tidal channel deposit. In both wells it is thought that the Devonian limestone and the shaley upper tidal flat layers act as permeability barriers.

5.4.1.2 BP 1 Test

The first two pressure-time graphs complement each other while the third cycle appears to be distinct from the previous two (Figure 5.12). The steady-state fluid flow analysis in Table 5.3 suggests that the injection rates were too low to cause borehole rupture. This is also confirmed by the steady-state pressure. However, the steady-state fluid flow analysis is based on unusually high transmissibility values (Table 5.3). These high values may be due to influence of the induced fracture on the steady-state flow period in the Horner plot which assumes formation pseudo-radial flow. Transmissibility values similar to those of the other tests infer that the injection rates were high enough to cause fracturing. The first cycle suggests classic hydraulic fracture initiation behaviour with breakdown at 5900 kPa followed by fracture propagation at pressures between 4950 and 5150 kPa. Repressurization of this fracture occurs in the second cycle at a secondary breakdown pressure of 5100 kPa which suggests that some oil sand fracture resistance remains. The propagation pressure response shows that some form of flow restriction prevents a steady propagation pressure. By the third cycle, no abrupt fracture breakdown is evident and it appears that the fracture reopens at 4300 kPa. Like the previous two cycles, the third cycle propagation pressure increases during injection. The injection behaviour for this test can be explained by the fracture initiation in the first cycle and subsequent repressurization of this fracture in the last two cycles.

Examination of Table 5.7 reveals that, except for the instantaneous shut-in pressure, the minimum principal stress interpretation methods give uniform values for each cycle. The log-log plots indicate that unit slopes are evident in the early time data indicating the presence of wellbore storage. The first and third cycle log-log plots show poorly developed 1/2 or 1/4 slopes which are representative of linear flow. There is evidence of linear flow in the tandem square root plots immediately following shut-in. The Horner plots and the pressure decay rate plots suggest that fracture closure occurred immediately after shut-in (i.e., less that 20 seconds).

5.4.1.3 BP 4 Test

The first injection cycle (Figure 5.13) experiences a high breakdown pressure of 6200 kPa followed by an immediate 2000 kPa drop during fracture propagation where the pressure increases from 4200 to 4800 kPa at shut-in. While the steady-state fluid flow analysis of Table 5.3 suggests that the injection rates were too low to cause fracturing, the steady-state pressure indicates otherwise. As with the BP1 tests, perhaps the transmissibility value derived from the Horner analysis of the shut-in data was affected by the induced fracture. Prior to breakdown there is a brief period where the pressure levels off at 3000 kPa. During the second cycle injection period, fracture reopening appears to take place at 4700 kPa after which the pressure continues to rise to 5100 kPa where it levels off until shut-in. Fracture reopening seems to occur at 4700 kPa in cycle 3 and the propagation pressure decreases to 4600 kPa just before shut-in. Like the BP1 well, the oil sands offers substantial resistance to fracturing in the first cycle. This fracture resistance is reduced in the following two cycles. The injection behaviour of these three cycles possibly indicates multiple fracture initiation.

As with the interpretation of the BP1 data, Table 5.8 shows a reasonable agreement among the results for each cycle except for the instantaneous shut-in pressure. All three shut-in shut-in responses are affected by wellbore storage and indicate rapid, if not instantaneous, fracture closure. The immediate shut-in data for the first cycle has a slope greater than one on the log-log graph which may be indicative of the instantaneous drop in shut-in pressure associated with the classic response. Linear flow at early time is evident in the tandem square root plot. The cycle 2 log-log graph (Figure 5.14) presents anomalous behaviour because an early time unit slope is followed by a steeper slope. The other flow plots do not readily delineate their respective flow periods for this cycle. The third cycle shut-in period is similar to the first cycle and the interpretative graphs identify a lower minimum principal stress value than the previous two cycles (Table 5.8).

5.4.2 Interpretation of BP1 and BP4 Microfrac Data

For openhole hydraulic fracture tests, the classical analysis states that the existing boundary conditions would dictate the initiation of vertical fractures at the wellbore. Because current in situ stress data for the Athabasca deposit for this depth indicates that the vertical stress is the minimum principal stress, we could expect that vertical fractures would rotate once away from the wellbore stress concentration in order to become normal to σ_v as noted in chapter 4. This hypothesis has two implications for in situ stress interpretation of the BP1 and BP4 tests: (i) breakdown pressure (or secondary breakdown pressure) may be used to determine the maximum horizontal principal stress based on an appropriate hydraulic fracture initiation equation, and (ii) the shut-in pressure analysis should be affected by the change in the fracture orientation.

The fracture initiation behaviour observed in these tests gives some indication of the applicability of hydraulic fracture theory to oil sands. Dusseault (1980) postulated that oil sands hydraulic fracture tests would not exhibit a breakdown pressure or propagation pressure much greater than the minimum principal stress. Examination of the first cycle BP1 and BP4 data in Tables 5.7 and 5.8 shows that there is an initial 850 to 1500 kPa fracture resistance. Since oil sands are essentially cohesionless, some mechanism or property, other than tensile strength, is responsible for this first cycle fracture resistance. Bawden (1983) presented microfrac test data which implied that some open wellbores in oil sands can withstand the borehole stress concentration and provide substantive breakdown pressures. More open hole tests are needed to investigate this problem, but the geotechnical behaviour of oil sands, contrary to Bawden's suggestion, implys that open boreholes in oil sands would undergo shear/plastic failure. Alternatively, the higher injection rates used in these tests may have caused excessive pressure losses in the wellbore and the fracture resulting in anomalous breakdown pressures. Rate effects in hydraulic fracture initiation have been observed by

other practitioners (see chapter 2). Hydraulic fracture initiation analysis of oil sands, therefore, should consider this factor as well as the other factors which may affect fracture initiation (e.g., geologic discontinuities, poroelastic effects).

Review of the vertical stress-instantaneous shut-in pressure ratio in Table 5.9 indicates ratios between 0.95 and 1.27. These stress ratio data and previous in situ stress data for Athabasca deposits at 210 m depth support the predominance of horizontal fractures. The classic hydraulic fracture assumptions dictate vertical fracturing at the borehole. For these conditions, it is possible that fracture rotation may have occurred once sufficient fracture propagation had taken place. However, the classic reduction in the P_s values in multicycle tests (preferably more than 5 cycles) is not evident in the data presented here.

Analysis of the BP4 pressure response during injection and shut-in provides an argument for multiple fracturing. After fracture initiation in the first cycle, the bend in the injection curve at 4700 kPa in the second cycle suggests fracture reopening, but the steady increase in pressure to 5100 kPa may be indicative of propagation of a second fracture. Minimum principal stress interpretation gives a higher P_s value of 5000 kPa as compared to the first and third cycle values of 4400 and 4500 kPa. Multiple fracturing may be related to vertical fracture rotation, the propagation of a pre-existing crack or the initiation of a new fracture. There are insufficient data in order to confirm fracture orientation.

Analysis of the shut-in pressure response according to the methodolgy described in chapter 4 confirmed that some unusual fracture behaviour was occurring. The BP4 cycle 2 analysis led to the hypothesis that a second fracture was being pressurized because of the unusual shut-in response as compared with cycle 1 and 3. It also shows the need for additional information fracture initiation at the wellbore.

The fracture initiation and propagation data along with the minimum principal stress interpretation provides evidence for the initiation of a fracture with subsequent propagation in cycles 2 and 3. Although previous

hydraulic fracturing tests in perforated cased boreholes have resulted in horizontal fractures, theoretical considerations for openhole conditions support vertical fracturing. Without additional fracture orientation data, the orientation is inconclusive. While the orientation of σ_3 is indeterminate, the magnitude is known to be between 4300 and 5100 kPa.

It is possible that under uniform stress conditions where the minimum horizontal principal stress is equivalent to the vertical stress the stress values measured can be indicative of either horizontal or vertical fracturing. The decreasing trend in the σ_3 values with each cycle in BP1 can be explained by reduction in pressure losses in the propagating fracturing as it is widened with each cycle. Alternatively, horizontal fracture climbing could also result in such a trend. Without more detailed analysis or additional data, such as downhole fracture detection, the interpretation cannot be more conclusive.

The benefits of data recording equipment and detailed interpretation analysis are indicated by the additional information revealed in the shut-in pressure analysis. While this additional information may reveal a complicated hydraulic fracture behaviour, the results emphasize the importance of considering the factors which may affect the analysis.

5.5 AOSTRA-BP B Unit Pilot Project Tests

5.5.1 Test and Site Description

5.5.1.1 General Description

Two series of micro-frac tests were conducted in perforated cased boreholes in boreholes OB-B01 and OB-B02 at the Marguerite Lake site in the Cold Lake oil sand deposit. The tests were conducted in the Lower Grand Rapids member which overlies the Clearwater Formation. Both series consisted of three cycles of injection and shut-in which were followed by three further cycles after additional casing perforations at different locations were made. The analog pressure-time records were digitized and the data analyzed according to the interpretation procedure of chapter 4. The actual records are

not included because of the poor reproducability of the strip chart. The test data, including perforation interval depth and phasing, the test formation and injection data are summarized in Table 5.1.

As with the GLISP tests, the test procedure for all of the tests conform to small volume hydraulic fracture stress measurement practice. No more than 0.269 m^3 of fracture fluid was injected in one cycle, but injection rates of 130 m^3/d exceed the recommended 72 m^3/d reported by Gronseth and Kry (1983). No injected fluid volume records were available except that shown in Table 5.3.

Both boreholes were cased and perforated for the first three cycles as indicated in Table 5.1. In borehole OB-B01 the casing was reperforated at three different intervals (435-436 m, 437-438 m, and 441-443 m.) at 2 shots/0.3 m at 120° phasing prior to an injectivity test and the final three cycles of the micro-frac test. Similarily, borehole OB-B02 was reperforated at two intervals (435-438 m. and 439.5-444 m) with the same perforation arrangement. This has important implications regarding whether a new or pre-existing fracture is pressurized in the last three cycles.

Cased boreholes micro-frac tests cannot be analysed to relate the breakdown pressure to the stress concentration around the borehole due to the unknown effects of the casing. Warpinski's (1983) recommendation that the difference between propagation pressure and shut-in pressure not exceed 3500 kPa to ensure reliable σ_3 values was checked for this case (Table 5.10).

The pressure-time data was recorded by an analog strip chart which did not provide very good data resolution for the minimum principal stress interpretation analysis. The actual transient pressure data does not have more than two pressure readings during the first minute of shut-in and thereafter, pressure was recorded every minute. The Amoco data, however, suggests that a pressure recording frequency of 2-3 seconds provides the necessary detail to observe most of the behaviour exhibited during the early part of shut-in. Warpinski *et al.* (1985) recommended a pressure recording frequency of more than 1/second in order that all the features of the fracture-fluid pressure interaction could be observed.

Both test series were conducted in the Lower Grand Rapids member of the Upper Manville Formation. This member is up to 50 m thick and consists mainly of interbedded sand and shale layers. Figure 5.15 provides a lithologic log of the wells at the test depth. At the test depth (435 -445 m), the perforations are located predominantly within the B-10 sand, which is separated from the B-8 unit at 430 m by a 1 m thick competent shale layer and is underlain by the B-11 unit, an interbedded bitumen and water sand layer at 446 m. Due to the variability of the interbedded oil sand, perforations may have intersected shale streaks as well as sand layers. Additionally, the close proximity of the underlying bitumen and water bearing layer may be a sink zone for the injected fluid.

5.5.1.2 OB-B01 Tests

The first three cycles in the OB-B01 well were conducted through a perforated casing at a depth of 439.5-440.5 m. The steady-state fluid flow analysis (Table 5.3) suggest that the injection rates were adequate to cause fracturing. This was confirmed by the steady-state pressure analysis. Table 5.11 shows that a distinct breakdown pressure of 9200 kPa was reached on the first cycle, but this was reduced to 7200 and 6950 kPa on the next two cycles. This is probably an indication that some of the initial near wellbore damage, causing fluid flow restriction, was reduced in the following two cycles. The injection data is unclear as to whether a stable injection pressure was reached, but the first cycle pressure difference (P_p-P_s) gives a value of 2000 kPa (Table 5.10) which seems to suggest that the P_s values were not affected by excessive perforation damage.

The shut-in behaviour is quite uniform throughout the three cycles. The poor resolution of the shut-in data prevents an early time analysis of the data (i.e., less than 30 sec) where, apparently, fracture closure occurs (Figure 5.16). The log(P_{si}-P) vs. log(dt) plots indicate either the very end of linear flow or do not show it at all. However, all the minimum principal stress interpretation methods consistently identify the same P_s value. P_s increases

with each cycle, as shown in Figure 5.17, but this can be explained by various mechanisms.

The final three cycles were conducted after the casing was reperforated and an injectivity test was performed (Table 5.11). Because three new perforated zones were created over a 5.5 m length of casing, it is not known whether a new fracture was created or if the fracture created in the previous three cycles was repressurised. The P_f values for these three cycles were inconclusive and suggest that either the previous fracture was repressurized or that a new fracture was created in a strata of either lower stress or reduced perforation damage.

The shut-in pressure responses of the final three cycles are similar to those of the first three cycles. The σ_3 values of the final three cycles, 5490 kPa, 5750 kPa and 5785 kPa, respectively, have increased up to 250 kPa over their corresponding values in the previous three cycles. As with the first three cycles, fracture closure appears to take place immediately after shut-in and is not adequately resolved by the shut-in data. The trend of increasing P_s values with each cycle is also continued (Figure 5.17).

5.5.1.3 OB-B02 Tests

The first three cycles in the OB-B02 well were performed in a cased borehole with planar perforations at 441.5 m depth (Table 5.11). The steady-state fluid flow analysis (Table 5.3) suggest that the injection rates were adequate to cause fracturing. This was confirmed by the steady-state pressure analysis. The initial breakdown pressure of 10,000 kPa is slightly higher than the corresponding OB-B01 value, but it is reduced to 7050 kPa and 6800 kPa on the second and third cycles. As in the previous tests, this decrease in breakdown pressure is most likely an indication of near wellbore perforation restrictions being eliminated with each additional injection cycle. The maximum (P_p - P_s) difference of 1200 kPa (Table 5.10) is less than the 3500 kPa limit advocated by Warpinski *et al.* (1985) that ensures reliable σ_3 determinations. The first cycle (P_f - P_p) difference of 3650 kPa is significant,

but it is reduced to 550 and 350 kPa in the following two cycles. This implies that substantial perforation damage exists in the first cycle, but it appears that it is reduced by further injection cycles, therefore, the P_s values should be reliable.

As with the OB-B01 shut-in data, the poor resolution of the OB-B02 data prevents a detailed analysis of the fracture behaviour at the start of shut-in. The log(Psi-P) vs log(dt) graph, as in Figure 5.18, shows that fracture closure occurs immediately after shut-in and early fracture closure is not recorded adequately by the pressure recording system. In spite of this limitation, the stress interpretation methodology was able to consistently identify the minimum principal stress for each cycle. As observed in the OB-B01 data, the minimum principal stress seems to be increasing with each additional injection cycle as shown in Figure 5.19.

Testing was stopped after cycle 3 and the casing was reperforated at depth intervals of 435-438 m and 439.5-444 m prior to the restarting of the test. The fourth cycle breakdown pressure of 7800 kPa is 2200 kPa lower than that of the first cycle and is only 850-1000 kPa higher than the secondary breakdown pressures in cycles 2 and 3. Because the new perforations extend over a 9 m length of casing, it is possible that either the initial fracture was repressurised or a new fracture was initiated at a point of lower fracture resistance. The pressure response of cycles 4 and 5 suggest that perforation damage had a minimal influence on these final two cycles.

The shut-in pressure response was probably unaffected by perforation damage since the first cycle (P_p - P_s) difference of 900 kPa is not significant. The shut-in behaviour exhibited by the final three cycles is very similar to that of previous BP"B" Unit data. The first cycle P_s value of 5810 kPa is approximately 150 kPa higher than that of cycle 3 (i.e., prior to reperforating the casing). This value increases to 5900 kPa and then 5960 kPa in cycles 2 and 3 (Figure 5.19), respectively suggesting that some mechanism is responsible for the apparent increase in the minimum principal stress.

5.5.2 Interpretation of the OB-B01 and OB-B02 Microfrac Data

The two sets of microfrac tests for each of the OB-B01 and OB-B02 wells behave similarily and have three common characteristics: (i) the first cycle breakdown pressure is quite high and it is reduced in the second and third injection cycles, (ii) the interpretation methods give similar $\sigma 3$ values, and (iii) the $\sigma 3$ values increase with each injection cycle by roughly 100 to 200 kPa. Because of the similarity between the OB-B01 and OB-B02 microfracs, their interpretations are discussed together. Based on the minimum prinicipal stress interpretation and in comparison with other Cold Lake stress data, it is believed that the best explanation of the observed behaviour is the initiation of a vertical fracture at the perforations with the early shut-in response indicative of fluid leakoff-controlled rapid fracture closure.

The high P_f values observed in the first cycle along with the gradual decrease in secondary breakdown pressure in the additional two cycles, suggests that the first cycle injection had to overcome substantial fracture resistance at the wellbore. Since these are perforated cased borehole tests, this fracture resistance can be attributed to effects of perforation damage, casing, and cement. If this is true, there are legitimate concerns about the effects of perforated casing on the minimum principal stress values. However, if Warpinski's $(P_f - P_s)$ guideline is accurate, the minimum principal stress results are unaffected by wellbore damage (Table 5.10). While this damage apparently affects the initial breakdown pressure, the decrease in secondary breakdown pressures implies that the damage has been reduced with successive injection cycles.

Although the minimum prinicipal stress interpretation analysis was limited by the resolution of the pressure data, the stress results suggest the creation of vertical fractures. Table 5.10 shows that the vertical stress-instantaneous shut-in pressure ratio varies between 1.70 and 1.91 which infers that the minimum principal stress is in the horizontal plane. This finding is consistent with previous in situ stress data for Cold Lake.

The interpretation analysis also shows that fracture closure is rapid and occurs less than 30 seconds after shut-in. The log-log graphs all lack an early linear flow period, thereby indicating that linear fracture flow has ended because of fracture closure. Such rapid fracture closure is normally associated with substantial fluid leakoff. The tandem square root and Horner graphs confirm that leakoff is a predominant factor even after fracture closure. Whitehead *et al.* (1988) also observed rapid fracture closure and believed it be representative of either very low conductivity fractures or choked fractures.

In both of the OB-B01 and OB-B02 tests, the interpreted minimum principal stress increases 400 to 600 kPa from the first cycle value to the sixth cycle value. It is difficult to determine whether or not this is a statistically significant variation owing to the uncertainity in calculating the error of these interpreted measurements. For example, is it valid to determine the average σ_3 value from various interpretations of the same shut-in pressure data? If these minimum principal stress increases are real, there exist two hypotheses capable of explaining these stress increases:

(i) adequate development of poroelastic effects which cause an increase in the local total stress along the fracture;

(ii) propagation of fracture(s) into strata of increased in situ stress.

According to Detournay *et al.*'s (1988) analysis of poroelastic effects during fracture propagation, the increase in in situ stresses due to the development of backstresses for this case can be as high as 1300 kPa for $\alpha = 1$ as long as the fluid injection period exceeds the characteristic time necessary for the development of these effects. Poroelastic theory, therefore, does predict increases in σ_3 within the realm of the observed increases.

The impact of fracture propagation into different stress zones is more difficult to quantify. If the in situ stress state of the strata which may be traversed by the propagating fracture are known, it may be possible to predict the increase in stress as the fracture propagated. Unfortunately this information is rarely known.

A certain irony exists in that despite the poor resolution of the pressure data wherein that details of the fracture shut-in behaviour were lost, the

minimum principal stress interpretation was much simpler and more precise. In some cases it may be preferrable not to deal with high resolution pressure readings if proper data analysis precautions are not followed (e.g., data filtering).

5.6 AOSTRA-COLD LAKE-BOW VALLEY Pilot Project Test

5.6.1 Test and Site Description

5.6.1.1 General Description

A microfrac test consisting of three cycles of injection and shut-in was performed in the ABC Ch#3 well in the Cold Lake deposit. The cased well was perforated at 440 m depth in the Clearwater Formation. The shut-in pressure data was obtained by digitizing the analog pressure records. These data were analyzed according to the interpretation procedure of chapter 4. The microfrac data is summarized in Table 5.1.

The test injection rates were approximately 270 m^3/d which greatly exceeds the 72 m^3/d recommendation of Gronseth and Kry (1983). A nitrogen conductivity test was conducted prior to the microfrac test and it gave a formation injectivity of 1.7 m^3/d. A Lynes DSR-300 and SP380 wellhead pressure transducer were used to record the microfrac pressure response. The wellhead pressures were converted to bottomhole pressures by adding the hydrostatic head of 3925 kPa resulting from the column of fluid in the wellbore while friction pressure losses were assumed to be negligible. No records of the injected fluid volumes were available except that shown in Table 5.3. A 2% KCl-water solution was used as the fracturing fluid.

Since the microfrac test results were obtained from perforated cased boreholes, the breakdown pressure cannot be related to any of the in situ stresses. A check of the (P_p - P_s) pressure difference (Table 5.12) shows that the first cycle value of 2575 kPa is below the 3500 kPa recommended by Warpinski (1983), thereby impling that the P_s values were not affected by perforation damage.

The effect of poor data resolution on in situ stress determination has been mentioned for the BP microfracs. Because an analog pressure recorder was used, the pressure data was digitized at 10 second intervals for the purpose of shut-in pressure analysis. The previous microfrac tests suggest that such data may be of insufficient detail. For example, since the well was shut-in at the surface, the early shut-in data was expected to be affected by wellbore storage. However, the log(P_{si}-P) vs log (Δt) plots for these data do not show the unit slope characteristic of wellbore storage. If the pressure data is insensitive to wellbore storage, the poor data resolution may also affect the interpretation of the minimum principal stress

The well was perforated at a depth of 439.8 m to 441.5 m with a perforation schedule of 13 shots/m at the bottom of the C-2 zone of the Clearwater Formation (Figure 5.20). The C-2 zone is a very fine to fine grained oil sands formation with good oil saturation and is relatively free of shale at the top, but contains shale laminae near the bottom. Overlying the C-2 zone is a bioturbated shale less than a metre thick. At the bottom of this zone is a 1 m thick calcium carbonate cemented sandstone which contains no oil. The perforation interval is located partially in this cemented sandstone, as shown in Figure 5.20.

5.6.1.2 ABC CH#3 Test

The injection and shut-in behaviour summarized in Table 5.13 indicates that oil sands does offer substantial fracture resistance. The steady-state fluid flow analysis (Table 5.3) suggests that the injection rates were sufficient to ensure fracturing. This was confirmed by the steady-state pressure analysis. The first cycle pressure-time response rises very rapidly to a breakdown pressure of 10,900 kPa followed by an erratic decline to 7,100 kPa prior to shut-in as shown in Figure 5.21. The pressure difference (P_p-P_s) of 2,575 kPa is fairly large, but is less than Warpinski's recommended 3,500 kPa for tests in perforated cased boreholes. In the second cycle, refracturing pressure of 8,235 kPa is followed by a pressure decline to the propagation pressure of 6,900

kPa. The 2,665 kPa pressure drop between the first and second cycle breakdown pressures suggests the oil sands exhibits a substantial fracture resistance possibly related to perforation damage. By the third cycle, once the refracturing pressure of 7900 kPa is surpassed, a steady injection pressure of 6600 kPa is maintained. The difference between secondary breakdown and propagation pressure decreases from 3700 in the first cycle to 1335 kPa and 1300 kPa in the second and third cycles. The initial fracture resistance evident in the first cycle appears to be reduced by the third cycle.

The shut-in pressure interpretation analysis (Figure 5.22) reveals that various methods give consistent minimum principal stress results for each cycle, but the interpreted P_s value increases with the cumulative injected volume. The $\log(P_{si}-P)$ vs $\log(\Delta t)$ graphs for all three cycles indicate that no linear flow exists after the first shut-in pressure value at 10 seconds, suggesting that linear flow may be occurring prior to this pressure. The tandem square root graphs confirms the large pressure drop between shut-in and the first pressure value 10 seconds later which is possibly related to fracture closure. Linear flow may also be evident but the lack of early time shut-in pressure data prevents a conclusive analysis. Since the Horner graph cannot incorporate the initial shut-in value at 0 seconds, this graph completely misses the crucial first 10 seconds of pressure data thereby affecting the interpreted σ_3 values.

The shut-in pressure response of all three cycles are similar and the average σ_3 values for each cycle are 5730 kPa, 5840 kPa and 5930 kPa. This increase with cumulative injected fracture fluid (Figure 5.23) has been observed with some of other microfrac cases. The possible mechanisms responsible for this behaviour are discussed in the following section.

If instantaneous fracture closure at shut-in is assumed, then the ISIP values would be equivalent to the final propagation pressures. Such an assumption would lead to significantly higher interpreted σ_3 values.

5.6.2 Interpretation of the Microfrac Data

Analysis of the BVI-CH #3 hydraulic fracture data leads to the same three characteristics observed in the BP tests: (i) a very high first cycle breakdown pressure which is substantially reduced in the following cycles, (ii) good agreement among the interpretation analysis of the minimum principal stress, and (iii) an apparent increase in the σ_3 values with each cycle by approximately 100 to 200 kPa. Like the BP data, the ABC pressure data is limited by the poor data resolution given by the analog pressure records. Finally, the vertical stress-minimum principal stress ratio (Table 5.13) favours the creation of vertical fractures with σ_3 equivalent to the minimum horizontal principal stress.

The first cycle breakdown pressure of 10,900 kPa implies that there was some initial fracture resistance offered by the oil sands related to perforation damage. Warpinski (1983) has stated that perforation damage can inhibit fracture initiation and propagation by restricting fluid flow in the fracture. The (P_p - P_s) pressure difference of 2575 kPa supports his argument of restricted fluid flow in the fracture. Furthermore, Warpinski (1988) has attributed the fluctuation in propagation pressure as an indicative of variable flow restriction within the fracture.

Examination of the borehole geology reveals that the 1.7 m long perforated zone is located in both a highly saturated oil sands layer and an underlying calcium carbonate cemented sandstone with no oil saturation (Figure 5.20). A vertical fracture interacting with this cemented sandstone may exhibit a substantial breakdown pressure related to its inherent tensile strength. The subsequent reduction in the secondary breakdown pressures can be explained by either a reduction in perforation damage or fracture propagation in the oil sands. It is considered more likely that the fracture was in the oil sands because of the likelihood of higher horizontal stresses in the sandstone.

The interpretation analysis of the minimum principal stress differs from Dusseault's argument for the agreement between P_p and P_s. If fracture

propagation is only slightly in excess of the minimum principal stress, fracture closure should be instantaneous at shut-in. The interpretation analysis suggests fracture closure occcurring slightly later at a pressure substantially lower (600 to 1200 kPa) than the instantaneous shut-in pressure. The log-log and tandem square root graphs, in spite of the poor pressure resolution, suggest that fracture closure occurs with 10 seconds of shut-in. Even though fracture closure is rapid, the significant pressure drop associated with closure requires an adequate pressure monitoring during shut-in. Such rapid fracture closure is usually associated with fluid leakoff from the fracture. This interpretation shows the importance of performing a proper minimum principal stress analysis which considers fluid leakoff. Otherwise, overestimates of the minimum principal stress of up to 1200 kPa are possible.

The interpreted minimum principal stress values increase by approximately 100 kPa with each further injection-shut in cycle. The limited amount of data prevents a meaningful statistical analysis to determine if this increase is statiscally valid. The approximate error in the σ_3 determinations is not really known. If this stress increase is real, a number of hypotheses have been discussed previously. The interpretation of the BP data showed that poroelastic effects and fracture propagation into zones of increased in situ stress are the most plausible. What is necessary, however, is that an adequate number of injection-shut-in cycles be run in order to properly establish the minimum principal stress and define any trends in pressure response.

Previous in situ stress data and observed fracture behaviour provide evidence for the creation of vertical fractures. Because the perforations were located in the bottom of the 9 m thick C-2 zone, the fracture could have extended outside this zone upward through the C-2 zone and, to a lesser degree, downward in the C-3 zone. Fracture growth through such boundaries is controlled predominantly by the minimum principal horizontal stress and also by the rock's fracture toughness and mechanical properties (Warpinski *et al.* 1982). The injection and shut-in pressures would reflect the overall effect of vertical and horizontal fracture growth into zones of varying properties.

5.7 Review of the Microfrac Results

5.7.1 In Situ Stress Results

The in situ stress data obtained from the analysis of the hydraulic fracture case histories are compared with previous in situ stress data in Figure 5.24 for the Cold Lake deposit and in Figure 5.25 for the Athabasca deposit. The Cold Lake graph shows two possible horizontal principal stress magnitudes, one at 5500 kPa and the other between 8000 and 10700 kPa. No vertical fracture orientations were obtained in the case histories in order to confirm the NE-SW trend of minimum principal stress orientation observed in previous measurements. The Athabasca deposit in situ stress measurements from this thesis are close to the vertical stress trend. All the previous in situ stress data in these graphs were obtained by hydraulic fracturing.

Such an exercise enables one to assess the validity of the in situ stress measurements. The relative agreement among the results tends to confirm the case history stress measurements and to reaffirm the validity of the in situ stress database, but this evaluation is limited by the restrictions imposed by the data base. Review of in situ stress compilations shows that in situ stresses are variable in regional extent, dependent on lithology, tectonic history, and geomorphological processes. Stresses have been shown to vary as much as 3 to 4 MPa over of 3 to 4 m thick bedding. Furthermore, there are no reported oil sands in situ stress measurements derived from other stress measurement methods to confirm the hydraulic fracture measurements. Confidence in this chapter's in situ stress measurements, therefore, is limited to the validity of comparing it with in situ stress data obtained from the literature.

5.7.2 Hydraulic Fracture Initiation

All tests, except the Canterra tests, were performed in perforated cased boreholes, thereby preventing a complete analysis of hydraulic fracture initiation theory. The major observation in the cased hole tests was the existence of substantial resistance to fracture initiation in the first cycle,

which was subsequently reduced in the later cycles. This finding may be related to the unquantifiable effects of perforation damage, casing and cement in perforated cased boreholes. Meanwhile, the open hole Canterra tests indicated that an open borehole in oil sands may give a unexpectedly high breakdown pressures. This may be attributed to excessive pressure losses, both in the wellbore and the fracture, associated with high injection rates. More open hole tests are needed to investigate this problem.

The various factors outlined in chapters 2 and 3 which could affect hydraulic fracture initiation were not rigorously investigated. Test and procedural limitations prevented an investigation of the effect of pre-existing fractures, geologic discontinuities and poroelastic effects on hydraulic fracture initiation.

It is essential that the injection rate or the injection fluid volume be monitored during a microfrac test. This would ensure that the test is being performed properly and it would also be useful in the analysis of the pressure-time data.

5.7.3 Minimum Principal Stress Interpretation

An assessment of these microfrac results is based on an examination of the integrity of the test methods and equipment, the validity of the theory used to interpret the results, and verification based on a comparison with independently obtained stress results. The limitations of the theory have been outlined in chapters 2 through 4, focusing on the validity of applying hydraulic fracture theory to oil sands deposits and the ability to interpret the distorted shut-in pressure data. Test methods and equipment are evaluated based on how closely they fulfil the assumptions of the theory and how well they meet the required test specifications. These aspects have been outlined as they pertain to each analysed case. Finally the in situ stress data base for oil sands deposits is limited and is founded entirely on hydraulic fracture test results, with no contributions from other methods.

Table 5.1 Microfrac case data summary.

Operator /Well	Cycle	Formation	Depth (mKB)*	q (m^3/d)	t_{inj} (s)	V_{inj} (m^3)
Amoco						
H1-Zone 4	1	McMurray	187-188	9.30	262	0.0282
(shale)	2			19.30	305	0.0681
	3			17.30	684	0.137
	4			27.90	371	0.12
H1-Zone 1	1	Woodbend	240-241	10.70	211	0.0261
(limestone)	2			9.50	120	0.0132
	3			14.30	412	0.0682
	4			14.30	394	0.0652
H3	1	McMurray	235-238	27.10	1164	0.365
(oil sands)	2			27.10	1303	0.408
	3			27.10	1140	0.357
Canterra						
BP4	1	McMurray	211.6-214.6	405	532	2.49
	2			565	291	1.90
	3			571	378	2.53
BP1	1		205.9-208.9	292	681	2.30
	2			300	462	1.60
	3			225	539	1.40
BP						
OB-B01	1	Grand	439.5-440.5	129	180	0.269
	2	Rapids		130	156	0.235
	3			127	144	0.212
	4		435.0-443.0	128	156	0.231
	5			127	150	0.22
	6			132	132	0.201
OB-B02	1	Grand	441.5	128	156	0.231
	2	Rapids		128	120	0.178
	3			130	144	0.216
	4		435.0-444.0	128	156	0.231
	5			128	156	0.231
	6			128	138	0.204
ABC						
CH#3	1	Clearwater	439.8-441.5	271	230	0.721
	2			264	180	0.549
	3			264	240	0.732

Note
*Depths below kelly bushing (KB).

Table 5.2 Microfrac case reservoir data.

Operator /Well	P_o (kPa)	T (°C)	n (%)	S_w (%)
Amoco				
H1 and H3	900	15	35	15
Canterra				
BP1 and BP4	800	12	35	20
BP				
OB-B01 and OB-B02	2700	15	35	23
ABC				
CH#3	3450	15	35	25

Table 5.3 Steady-state fluid flow parameters.

Operator /Well	kh* (md·m)	q (m^3/d)	q_{ss} (m^3/d)	P_f (MPa)	P_{ss} (MPa)
AMOCO					
H1-limestone	2-14	9.5-14.3	1-6	9-11	18-26
H1-shale	12	9.3-27.9	3-9	3.6-5.1	12-34
H3-oil sands	32-50	27.1	10-16	5-5.3	8-12
CANTERRA					
BP1	1400-2100	225-300	380-390	4.3-5.9	2.8-3.4
BP4	1300	405-570	375	4.7-6.2	5.2-6.9
BP					
OB-B01	50	130	17	6.7-9.2	39
OB-B02	20	130	7	6.8-10	86
ABC					
CH#3	80-120	265	18-25	7.9-11	33-48

Note:

*The transmissibility values, kh, were calculated from the pseudo-radial flow period in the microfrac tests using the Horner analysis (Lee 1983). This assumes that the effect of the fracture on the fluid flow during shut-in eventually becomes negligible as pseudo-radial flow develops at long time.

Table 5.4 Hydraulic fracture stress measurement data for Alberta oil sand deposits.

Location	Formation/ Rock Type	Depth (m)	σ_v (MPa)	σ_3 (MPa)	σ_{hmin} (MPa)	σ_v/σ_3	P_o (MPa)	Reference
UTF	McMurray oil sands	156	3.23	2.81-3.36	----	0.96-1.15	0.600	Chhina (1988)
UTF	Devonian limestone	171	3.6	4.69-8.24	----	0.44-0.77	0.750	"
Athabasca	McMurray	193	3.9	4.3	----	0.91	0.650	Chhina and Agar (1985)
Athabasca	McMurray	216	4.380	4.99	----	0.88	0.800	Chhina and Agar (1985)
Athabasca	McMurray	236	4.83	4.97	----	0.97	1.060	"
Athabasca	McMurray	239	----	4.49-5.07	----	----	----	Kular *et al.* (1988)
Wabasca	Grand Rapids	240	5.8-6.1	----	6.4-7.7	----	1.350	Settari and Raisbeck (1978)
Athabasca	McMurray	297	6.07	5.04	----	1.20	1.200	Chhina and Agar (1985)
GLISP	McMurray	317	6.7	----	5.60	----	----	Holzhausen *et al.* (1980)
Athabasca	McMurray	325	6.66	5.66	----	1.18	1.52	Chhina and Agar (1985)
Athabasca	Lower Grand Rapids	342	7.71	6.165	----	1.25	3.12	"
Athabasca	"	352	7.91	6.25	----	1.27	3.12	"
Athabasca	Wabiskaw	364	8.37	8.30	----	1.01	----	"

Table 5.4 continued.

Location	Formation or Rock Type	Depth (m)	σ_v (MPa)	σ_3 (MPa)	σ_{hmin} (MPa)	σ_v/σ_3	P_o (MPa)	Reference
Cold Lake	oil sands	417	10.40	----	9.80	----	3.26	Settari and Raisbeck (1978)
Cold Lake	oil sands	420	11.1-12.1	----	7.90-9.10	----	3.26	"
Cold Lake	Clearwater	454	9.50	9.50-12.00	----	0.89-1.0	----	Gronseth (1988)
Cold Lake	----	457	11.25	----	9.00	----	----	Bell and Babcock (1986)
Peace River	Bullhead	576	12.585	11.515	----	1.09	3.65	Chhina and Agar (1985)

Table 5.5 Pressure difference and stress ratio data for the Amoco tests.

Borehole	Cycle	$P_p - P_s$ (kPa)	σ_v/P_s	σ'_v/σ'_3
H1 (limestone)	1	----	----	----
	2	----	----	----
	3	700	0.80-0.92	0.77-0.91
	4	1920-2350	0.85-1.05	0.82-1.06
H1 (shale)	1	----	----	----
	2	400-1000	1.03-1.26	1.05-1.36
	3	600-700	0.95-1.05	0.86-1.06
	4	50-850	0.78-1.01	0.73-1.02
H3 (oil sand)	1	30-1900	1.33-1.54 (0.96)	1.07-1.33 (0.79)
	2	0-1800	1.31-1.57 (0.96)	1.06-1.31 (0.79)
	3	10-1700	1.37-1.66 (1.02)	1.11-1.39 (0.84)

Table 5.6 Summary of minimum principal stress determinations: Amoco shale, oil sands, and limestone tests.

Zone	CYCLE	q (m^3/day)	P_f (kPa)	P_p (kPa)	Minimum Principal Stress (kPa) ISIP	PDR	Log-Log	Horner	TSR
H1-Z4-Shale	1*	9.3	3560	----	----	----	----	----	----
187-188 m	2	19.3	4400	4000-4400	3400	3500	3500	3600	3600
depth	3	17.3	4930	4800	4200	4150	4100	4200	4200
	4	27.9	5100	4850-5100	4500	4250	4800	4700	4700
H1-Z1-Limestone	1*	10.7	9060	----	----	----	----	----	----
240-241 m	2*	9.5	9400	----	----	----	----	----	----
depth	3	14.3	10900	6700	6000	6000	6000	6000	6000
	4	14.3	8300	7600	5250	5500	5680	5680	5680
H3-Oil Sands	1	27.1	5300	5300	5270	3500	3400	3540	3540
235-236 m	2	27.1	5290	5250	5250	3450	3500	3600	3450
depth	3	27.1	4980	4950	4940	3250	3440	3440	3300

* Fracturing did not occur during this injection period.

Table 5.7 Minimum principal stress analysis for the CANTERRA BP1 test.

CYCLE	q (m^3/d)	P_f (kPa)	P_p (kPa)	ISIP	Minimum Principal Stress (kPa) PDR	Log-Log	Horner	TSR
1	292	5900	4950-5150	5150	4425	>3500	4425-4860	4400-4800
2	300	5050	4600-5100	4650	4100	>3900	4400	4400
3	225	4300	4300-4950	4840	4650	>3400	4300	4300

Table 5.8 Minimum principal stress analysis for the CANTERRA BP4 test.

CYCLE	q (m^3/d)	P_f (kPa)	P_p (kPa)	ISIP	Minimum Principal Stress (kPa) PDR	Log-Log	Horner	TSR
1	405	6200	4200-4800	4790	4280	4400	4400	4400
2	565	4700	4700-5100	5000	4100	>4900	5000	5000
3	572	4850	4700-4800	4650	3770	?	3760-4550	4500

Table 5.9 Pressure and stress ratio data for the CANTERRA tests.

Borehole	Cycle	$P_p - P_s$ (kPa)	σ_v/P_s	σ'_v/σ'_3
BP 1	1	750	0.95-1.11	0.94-1.14
	2	1000	1.05-1.11	1.07-1.24
	3	650	1.01-1.14	1.02-1.17
BP 4	1	520	1.00-1.17	1.00-1.15
	2	1000	0.96-1.17	0.95-1.21
	3	1040	1.03-1.27	1.04-1.35

Table 5.10 Pressure and stress ratio data for the BP tests.

Borehole	Cycle	$P_p - P_s$ (kPa)	σ_v/P_s	σ'_v/σ'_3
OB-B01	1	2000	1.91	3.61
	2	1700	1.84	3.25
	3	1350	1.81	3.10
	4	1900	1.84	3.25
	5	1300	1.76	2.90
	6	950	1.52	2.84
OB-B02	1	1000	1.89	3.51
	2	1200	1.84	3.25
	3	900	1.81	3.10
	4	900	1.73	2.78
	5	1050	1.72	2.72
	6	850	1.70	2.67

Table 5.11 Minimum principal stress analysis for the BP tests.

Borehole	CYCLE	q (m^3/d)	P_f (kPa)	P_p (kPa)	ISIP	Minimum Principal Stress (kPa) PDR	Log-Log#	Horner	TSR
OB-B01	1*	130	9200	7300	5400	5450		5300	5300
	2	131	7200	6950-7200	5500	5500		5500	5500
	3	128	6950	6550-6950	5600	5600		5600	5600
	4**	128	7950	6800-7400	5500	5450		5500	5500
	5	127	7050	6400-7050	5750	5750		5750	5750
	6	133	6750	6350-6750	5800	5800		5725	5800
OB-B02	1+	128	10000	6350	5325	5325		5350	5400
	2	128	7050	6500-6700	5600	5550		5500	5600
	3	130	6800	6450-6550	5650	5625		5650	5700
	4++	128	7800	6750	5850	5825		5725	5840
	5	128	6950	6550-6950	5925	5900		5850	5925
	6	128	6800	6500-6800	5950	5950		5925	6000

Notes

*Perforation interval of 439.5 to 440.5 m depth for cycles 1 to 3.
** Reperforated the casing at 435 to 436 m, 437 to 439 m and 439.5 to 440.5 m depth for cycles 4 to 6.
+ Planar perforated interval at 441.5 m depth for cycles 1 to 3.
++Reperforated the casing at 435 to 438 m and 439.5 to 444 m. depth for cycles 4 to 6.
Insufficient data resolution for log-log analysis.

Table 5.12 Pressure difference and stress ratio data for the ABC test.

Borehole	Cycle	$P_p - P_s$ (kPa)	σ_v/P_s	σ'_v/σ'_3
CH #3	1	2575	1.76	2.94
	2	1150	1.72	2.78
	3	760	1.69	2.68

Table 5.13 Minimum principal stress analysis for the ABC test.

CYCLE	q (m^3/d)	P_f (kPa)	P_p (kPa)	Minimum Principal Stress (kPa) ISIP	PDR	Log-Log	Horner	TSR
1	270	10900	7200-8235	5660 (7070)*	5730	≥5750	5660	5800
2	264	8235	6940	5800 (6855)	5850	≥5870	5790	5870
3	263	7890	6640	5880 (6600)	5945	≥5955	5880	5965

Notes:

The pressures were originally analog records of surface pressures and have been converted to bottomhole pressures by adding the hydrostatic head in the tubing (3925 kPa) and assuming that pressure losses in the tubing are negligible.
*The values in brackets are instantaneous shut-in pressures assuming instantaneous fracture closure, thus, are equal to the final propagation pressure prior to shut-in.

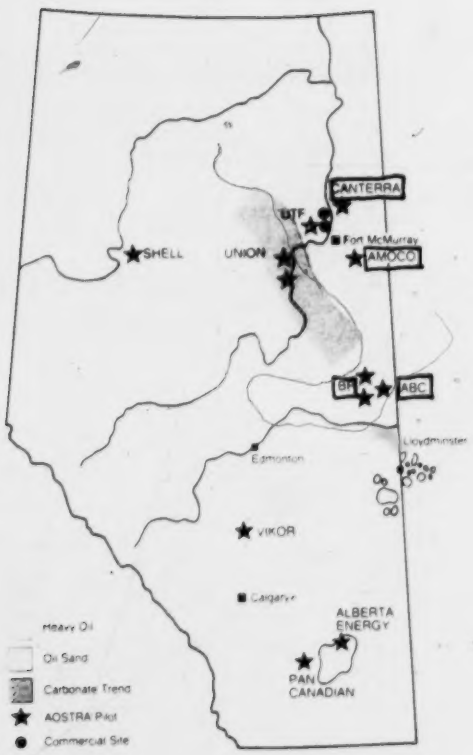

(Modified after AOSTRA 1987)

Figure 5.1 Location of the microfrac test sites.

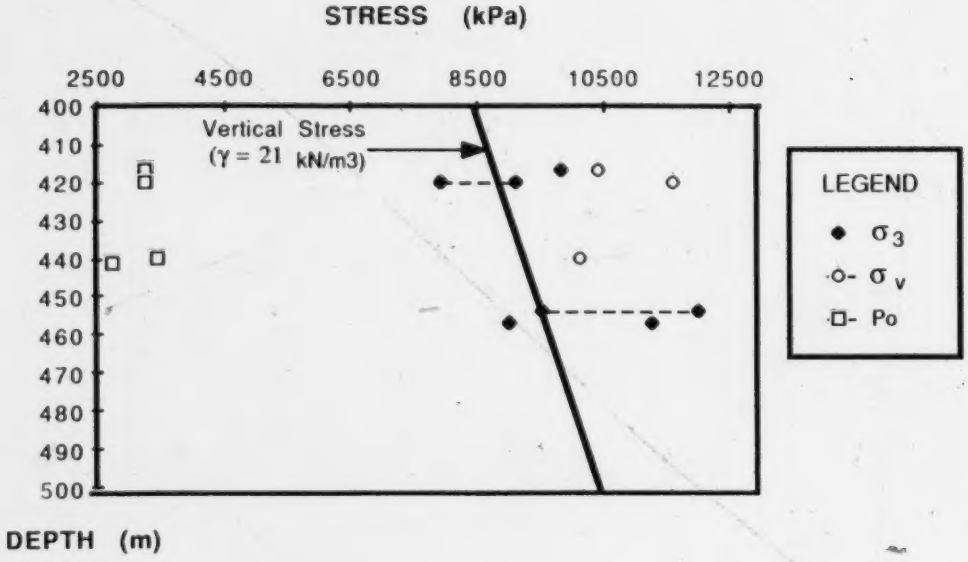

Figure 5.2 Hydraulic fracture in situ stress data for the Cold Lake deposit.

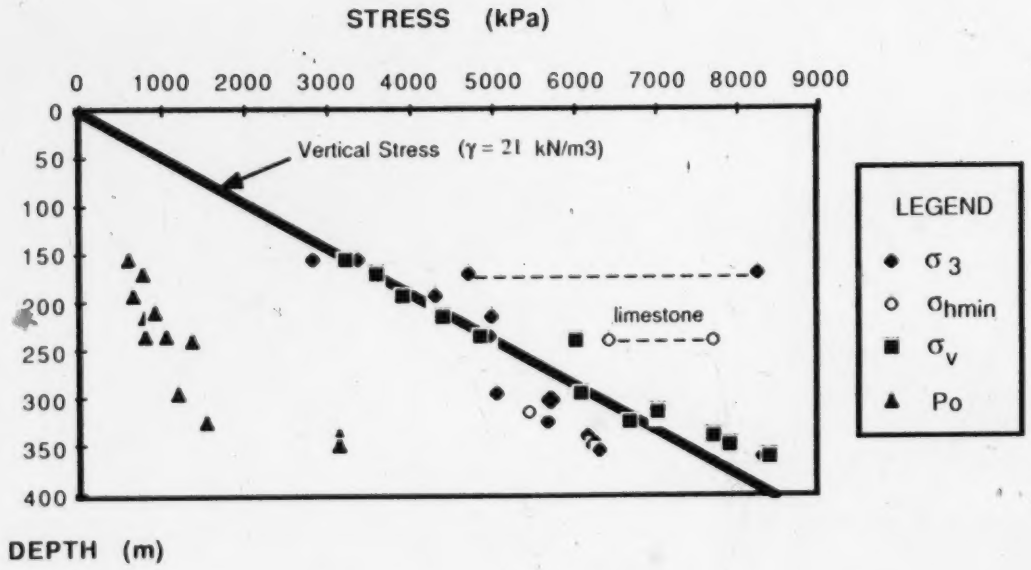

Figure 5.3 Hydraulic fracture in situ stress data for the Athabasca deposit.

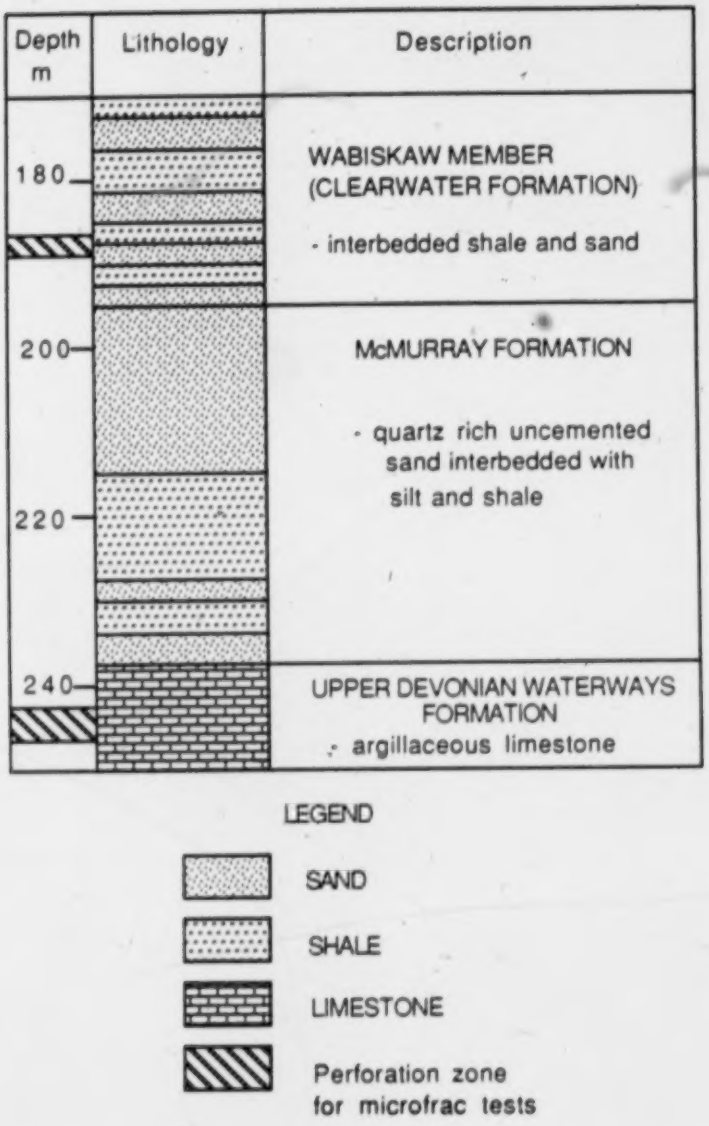

Figure 5.4 Lithologic log of the Amoco H1 well (shale and limestone tests).

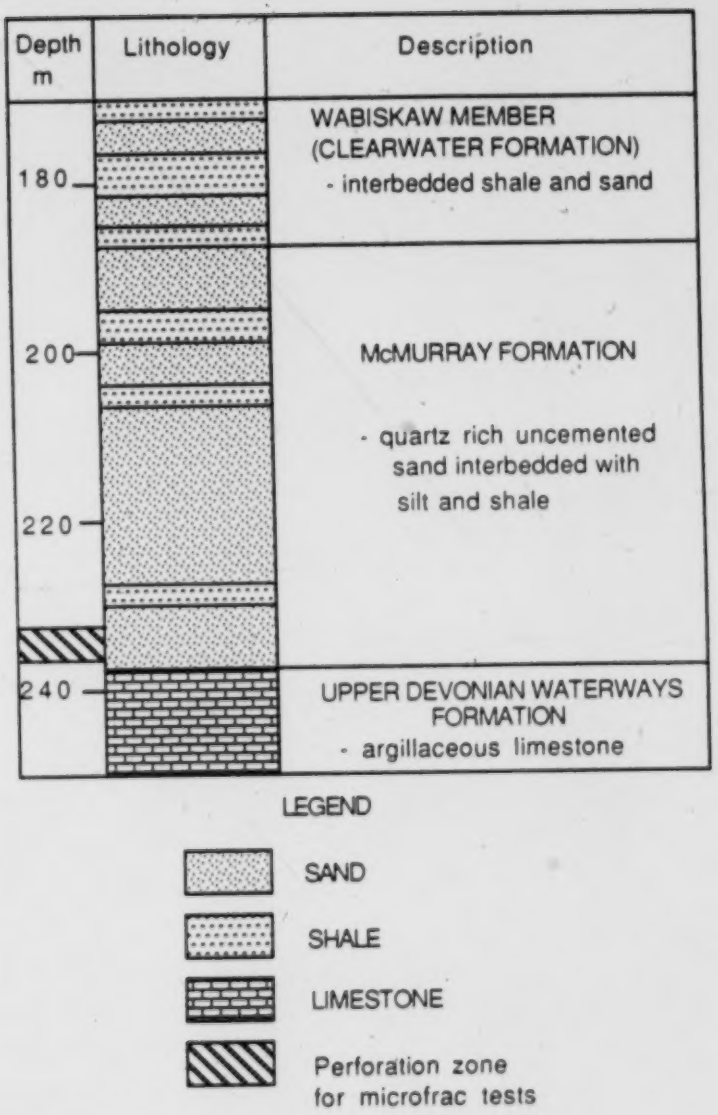

Figure 5.5 Lithologic log of the Amoco H3 well (oil sands test).

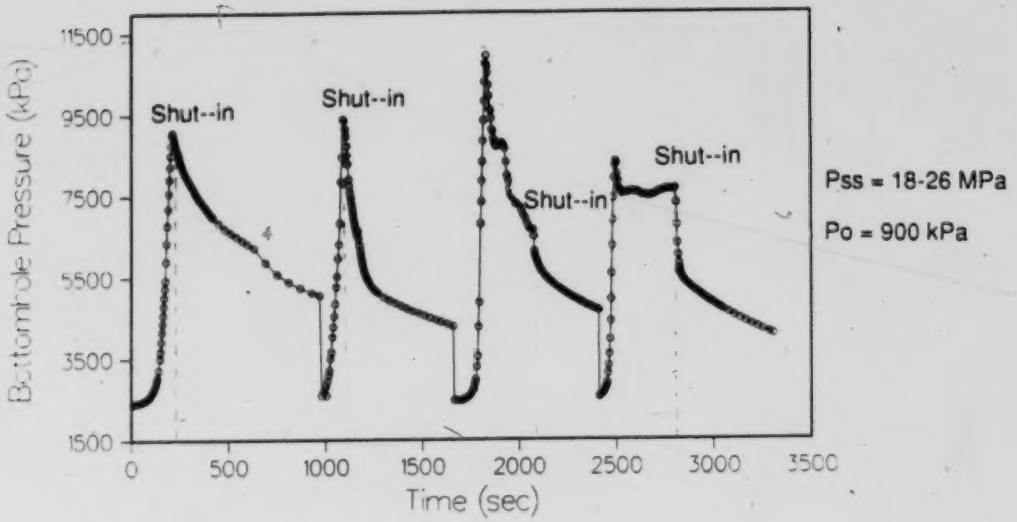

Figure 5.6 Pressure-time graph for the Amoco H1 well limestone microfrac test consisting of four injection/shut-in cycles.

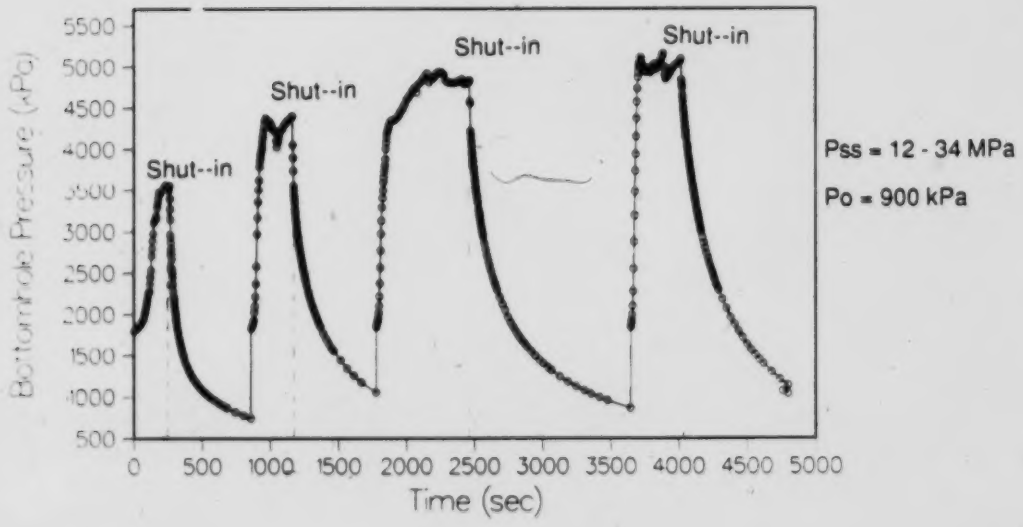

Figure 5.7 Pressure-time graph for the Amoco H1 well shale microfrac test consisting of four injection/shut-in cycles.

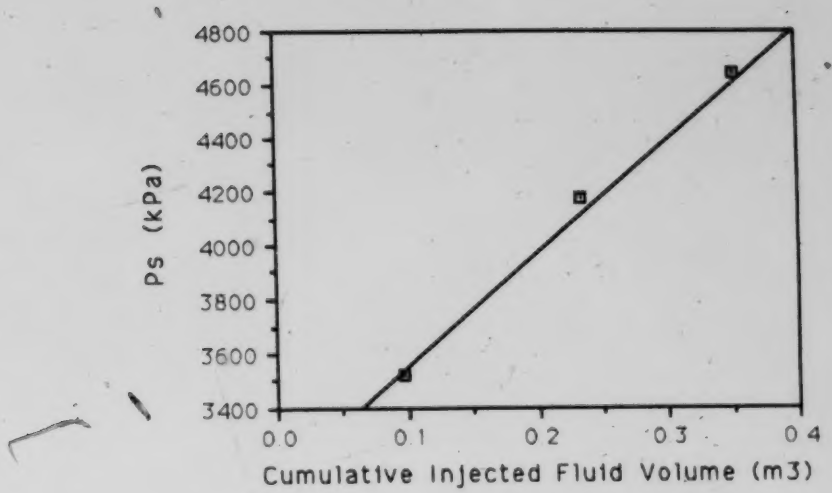

Figure 5.8 Variation in the minimum principal stress for the Amoco H1 shale microfrac test.

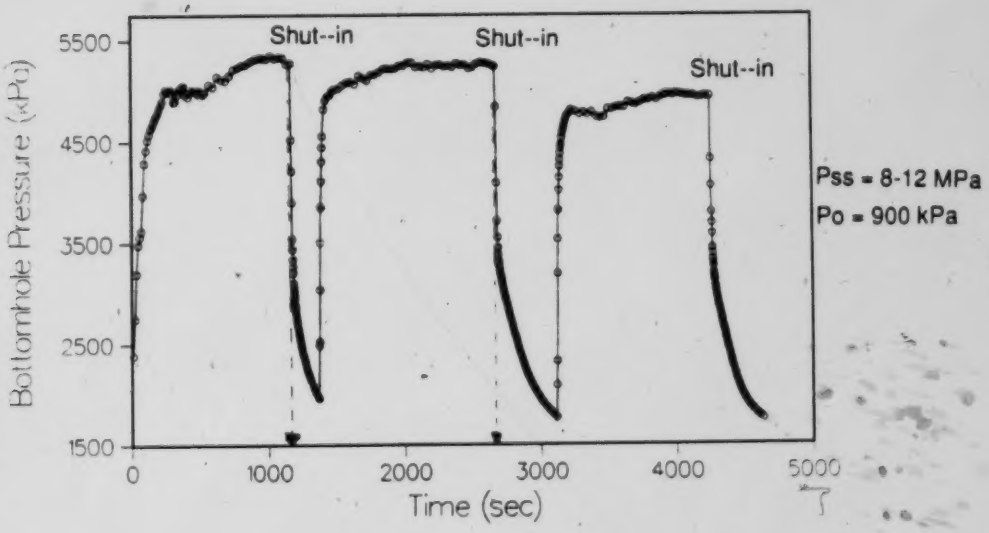

Figure 5.9 Pressure-time graph for the Amoco H3 well oil sands microfrac test consisting of three injection/shut-in cycles.

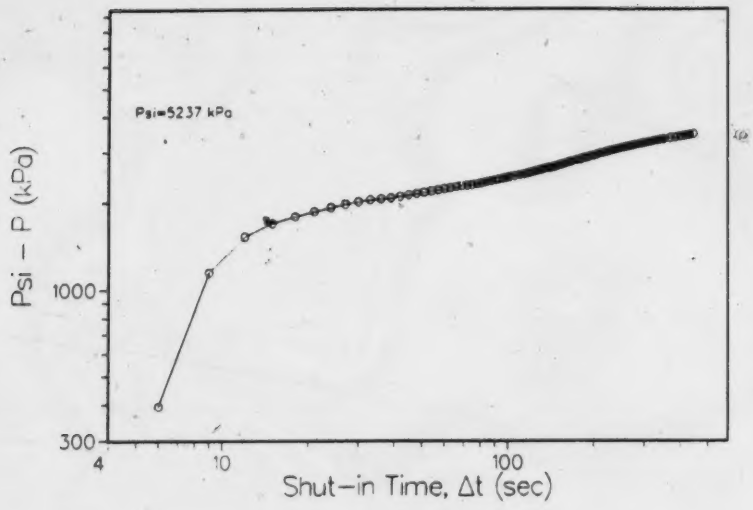

(a) Pressure-shut-in time graph.

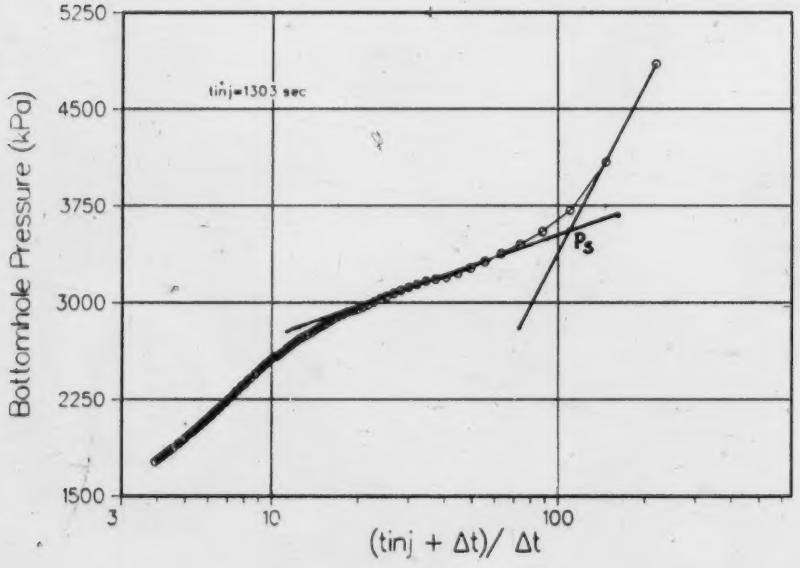

(b) Horner graph.

Figure 5.10 Shut-in pressure interpretation graphs for the Amoco H3 well oil sands microfrac-cycle 1.

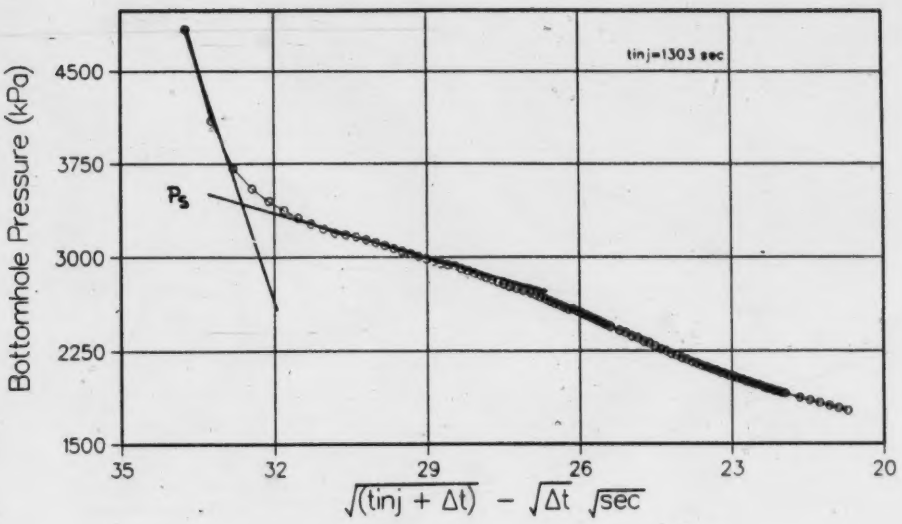

(c) Tandem square root graph

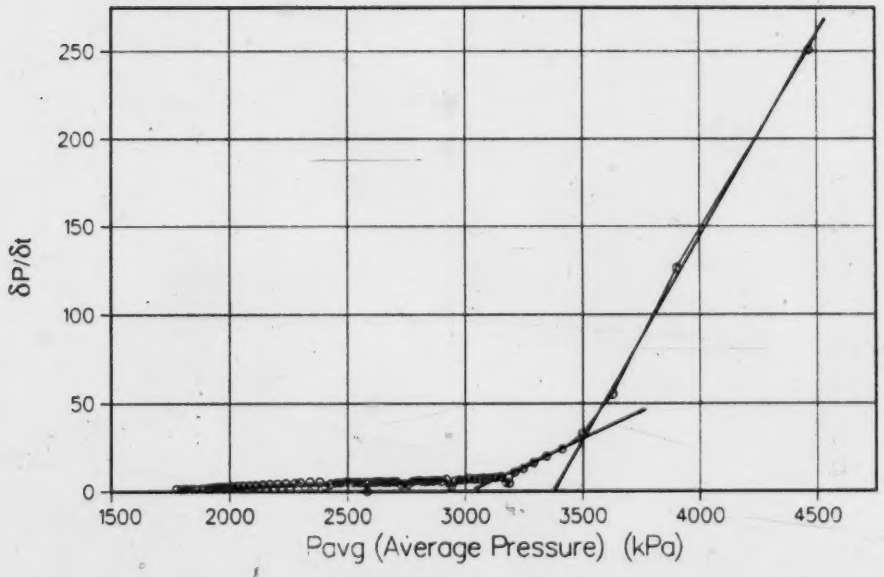

(d) Pressure decay rate graph

Figure 5.10 continued

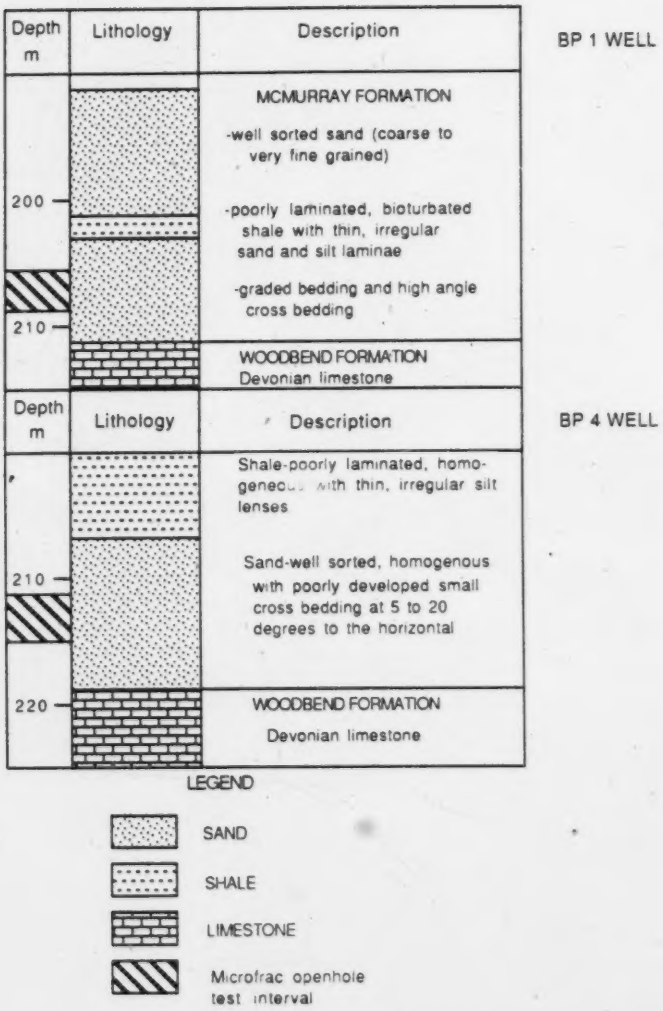

Figure 5.11 Lithologic logs of the Canterra BP 1 and BP 4 wells.

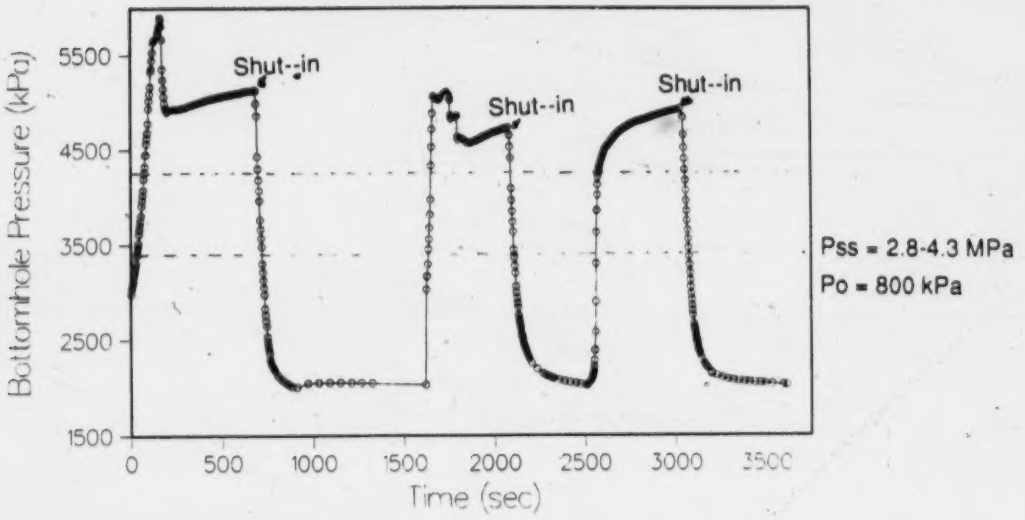

Figure 5.12 Pressure-time graph for the Canterra BP 1 well microfrac test consisting of three injection/shut-in cycles.

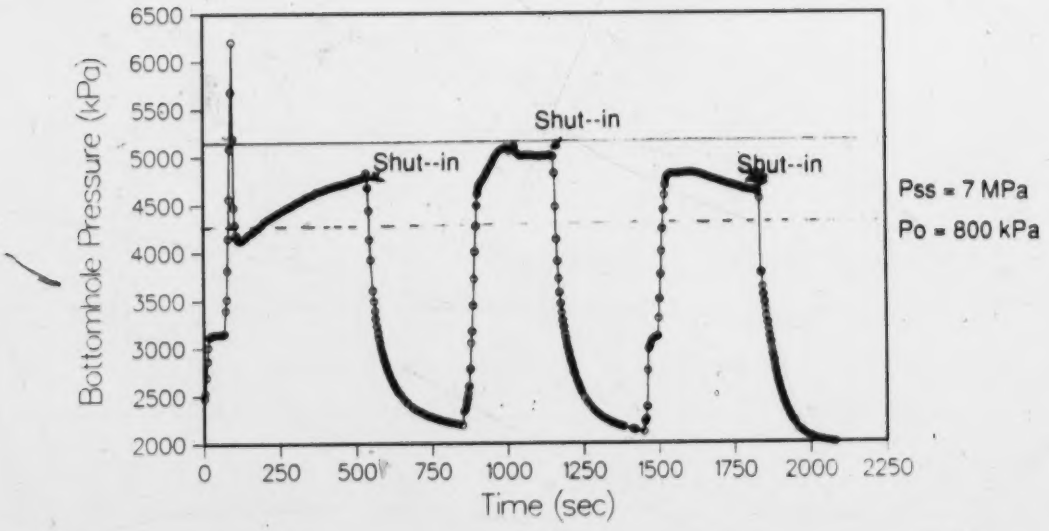

Figure 5.13 Pressure-time graph for the Canterra BP 4 well microfrac test consisting of three injection/shut-in cycles.

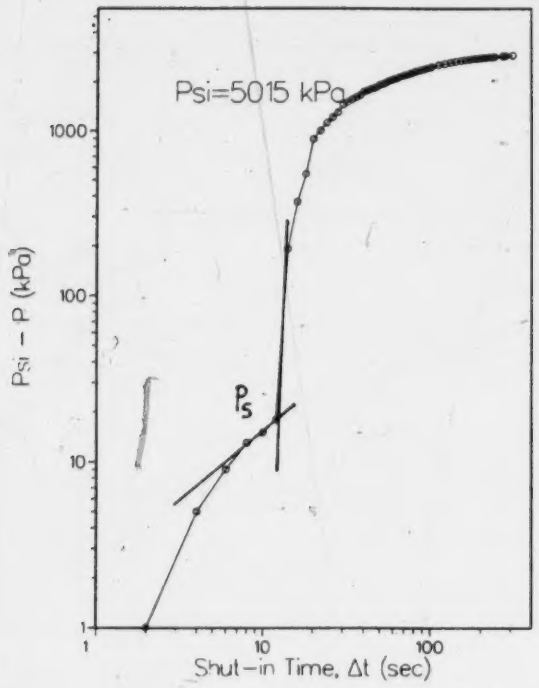

(a) Log-log graph

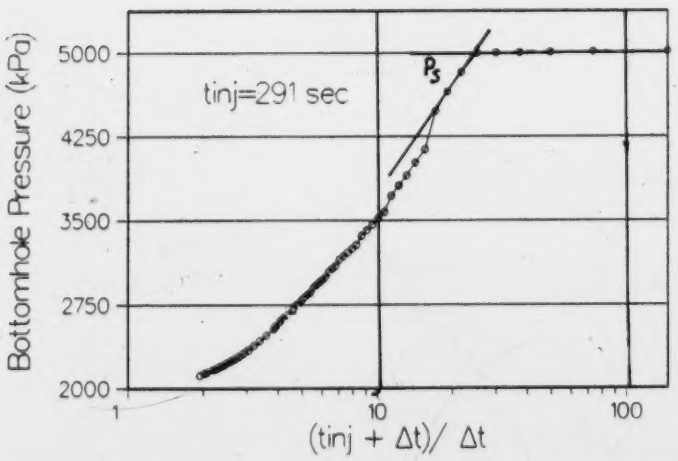

(b) Horner graph

Figure 5.14 Shut-in pressure interpretation graphs for the Canterra BP 4 well microfrac-cycle 2.

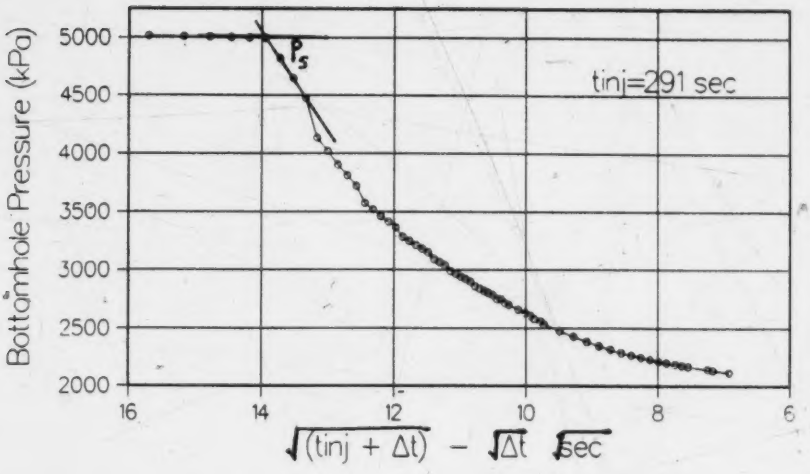

(c) Tandem square root graph

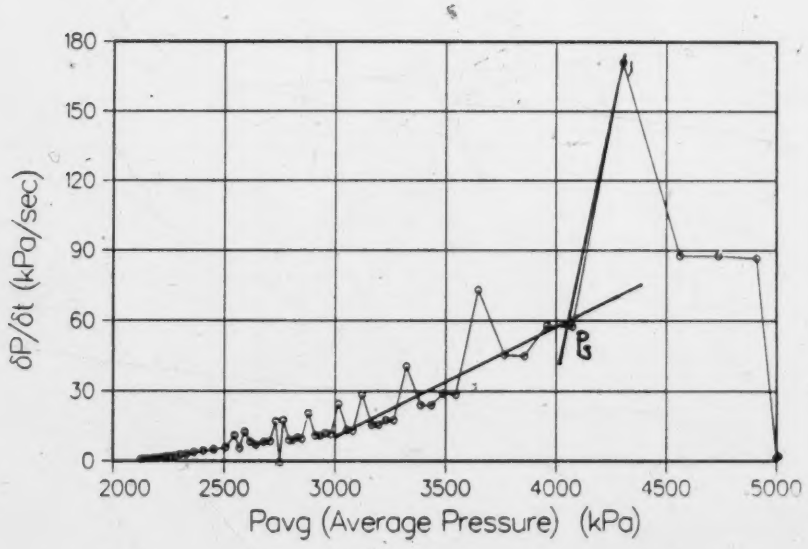

(d) Pressure decay rate graph

Figure 5.14 continued

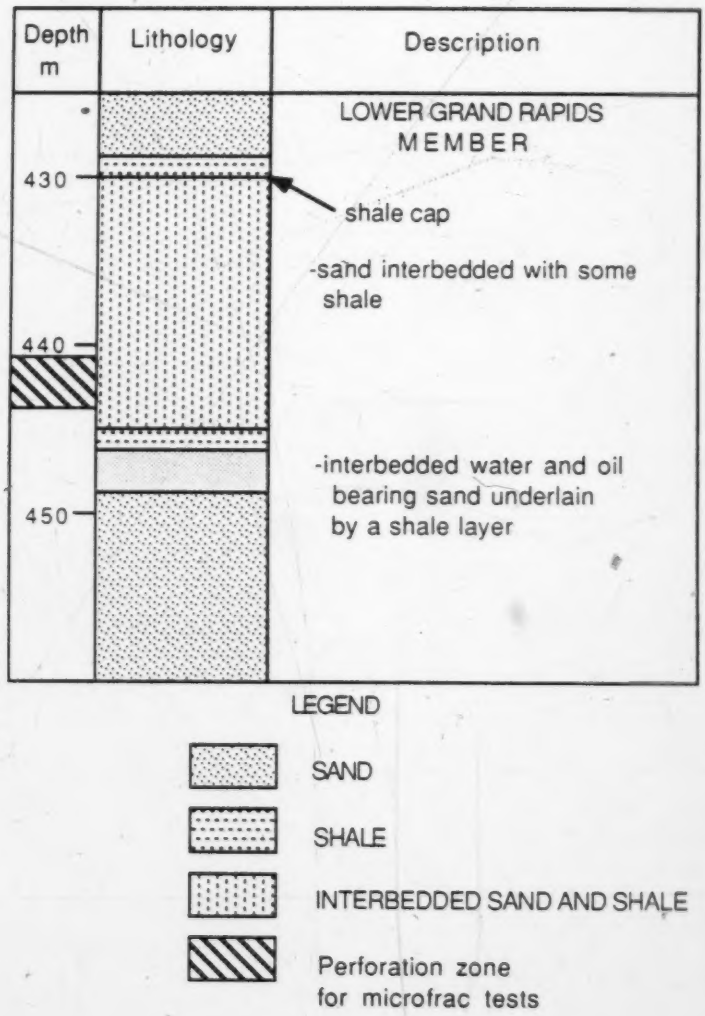

Figure 5.15 Representative lithologic log of the BP OB-B01 and OB-B02 wells.

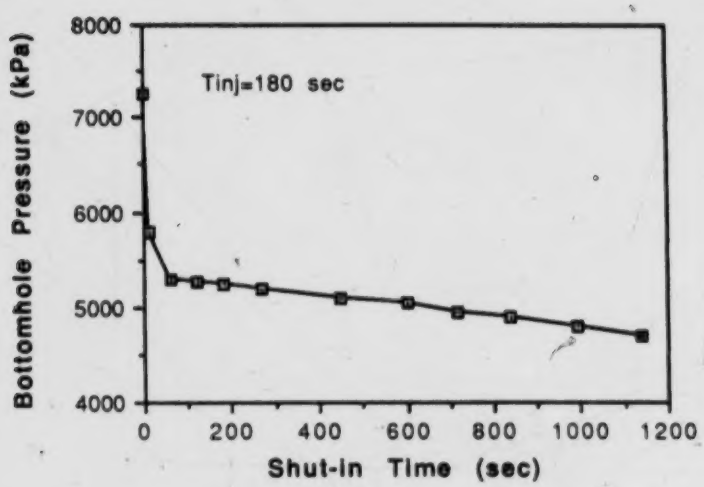

(a) Pressure-shut-in time graph.

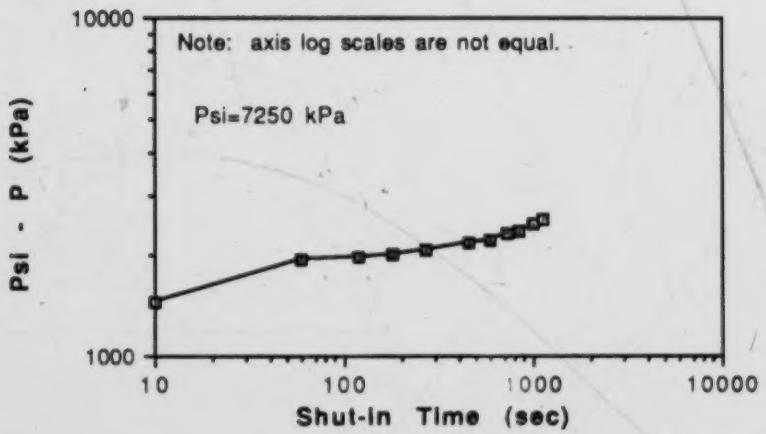

(b) Log-log graph

Figure 5.16 Shut-in pressure interpretation graphs for the BP OB-B01 well microfrac-cycle 1.

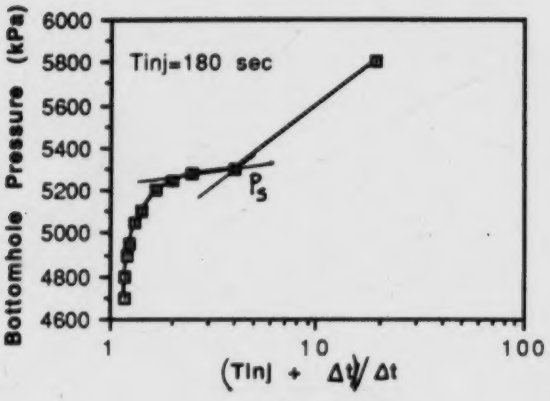

(c) Horner graph

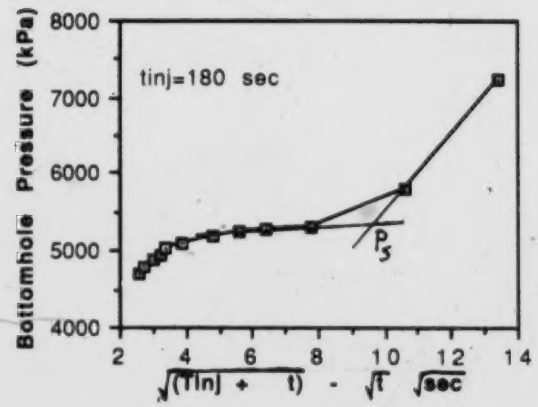

(d) Tandem square root graph

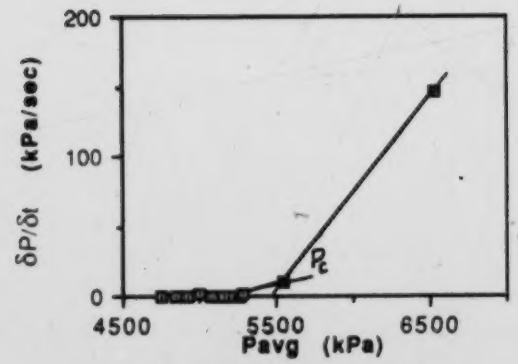

(e) pressure decay rate graph

Figure 5.16 continued

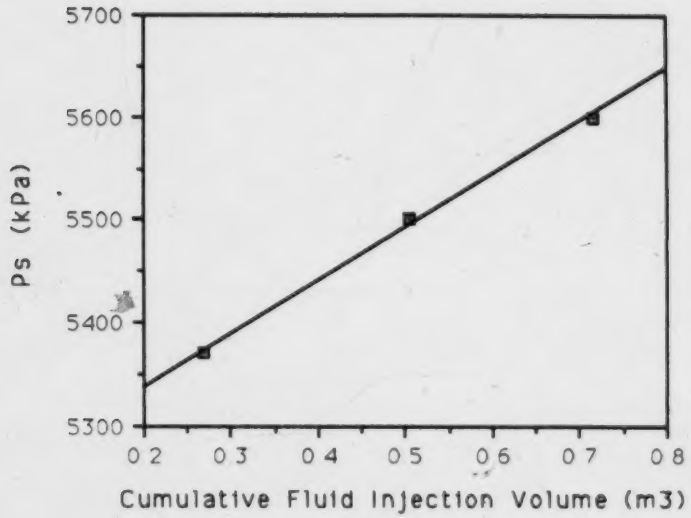

(a) Cycles 1 to 3

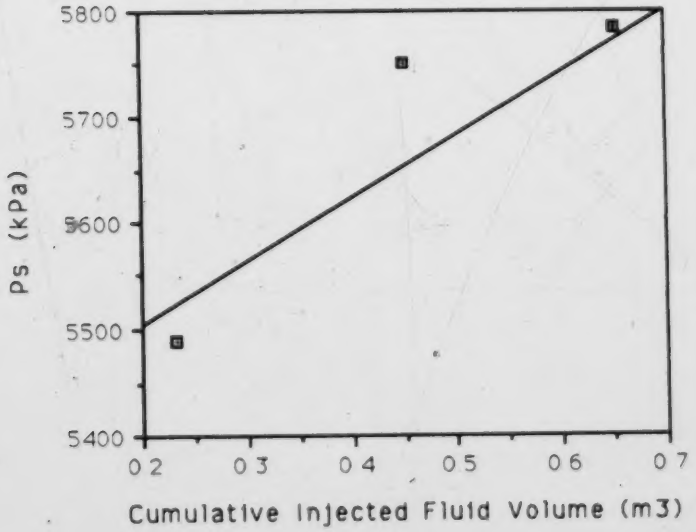

(b) Cycles 4 to 6

Figure 5.17 Variation in the minimum principal stress for the BP OB-B01 well microfrac test.

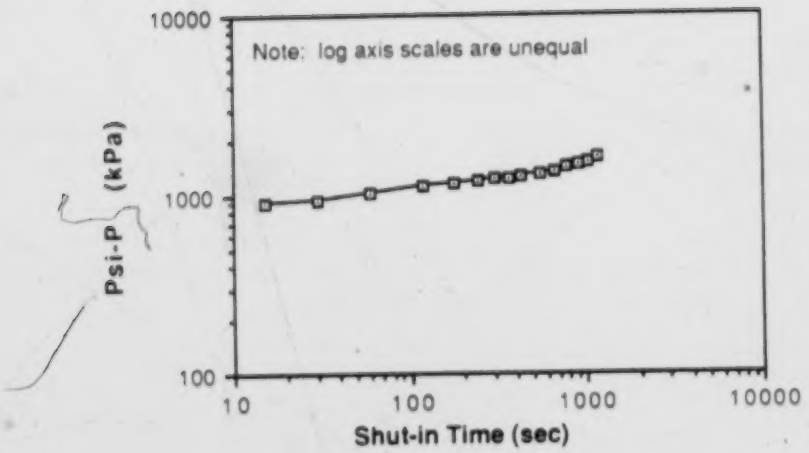

Figure 5.18 Log-log interpretation graph for BP OB-B02 well-cycle 1.

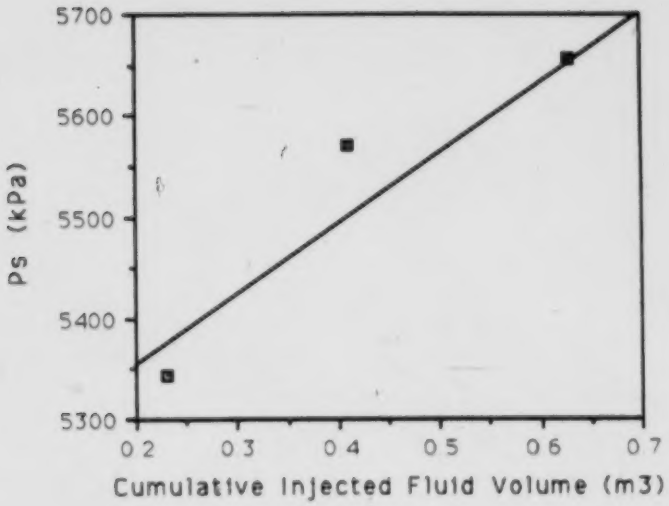

(a) Cycles 1 to 3

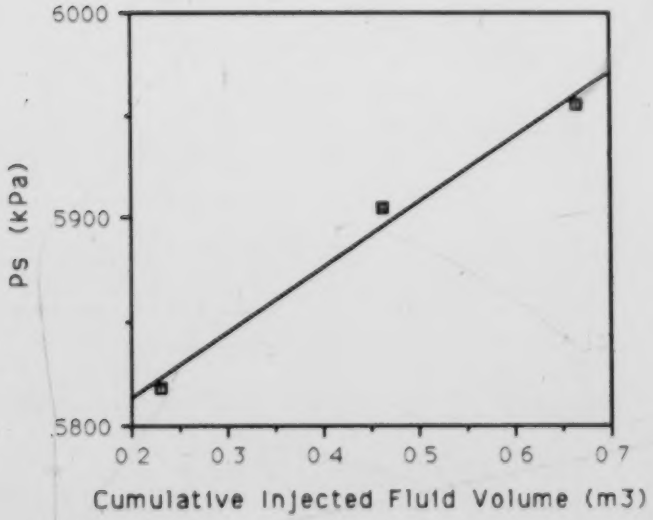

(b) Cycles 4 to 6

Figure 5.19 Variation in the minimum principal stress for the BP OB-B02 well microfrac test.

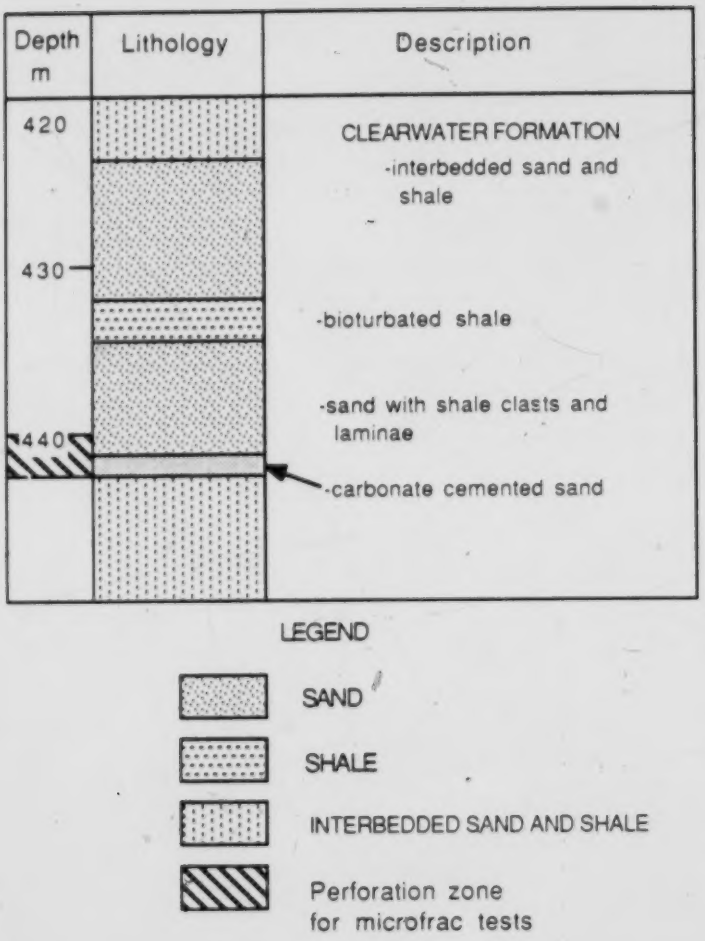

Figure 5.20 Lithologic log of the ABC CH#3 well.

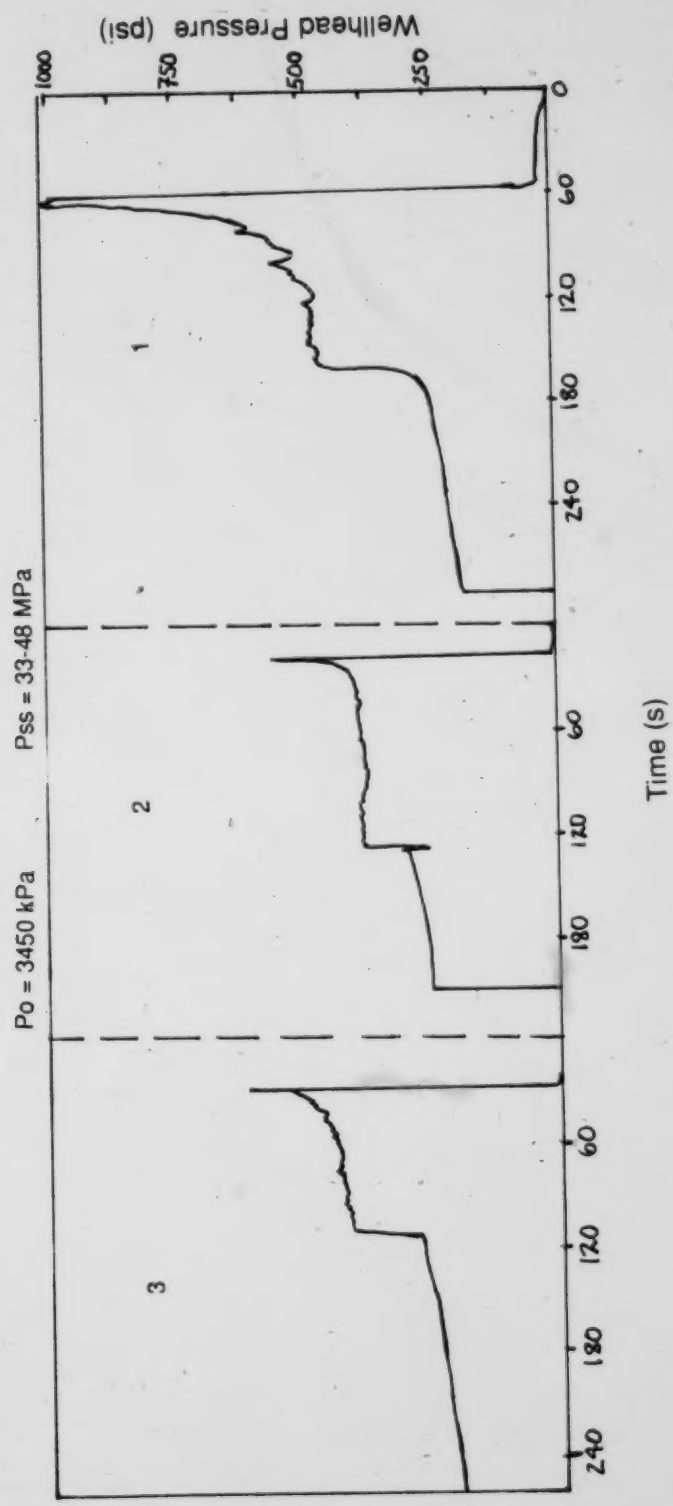

Figure 5.21 Pressure-time graph for the ABC CH#3 well consisting of three injection/shut-in cycles.

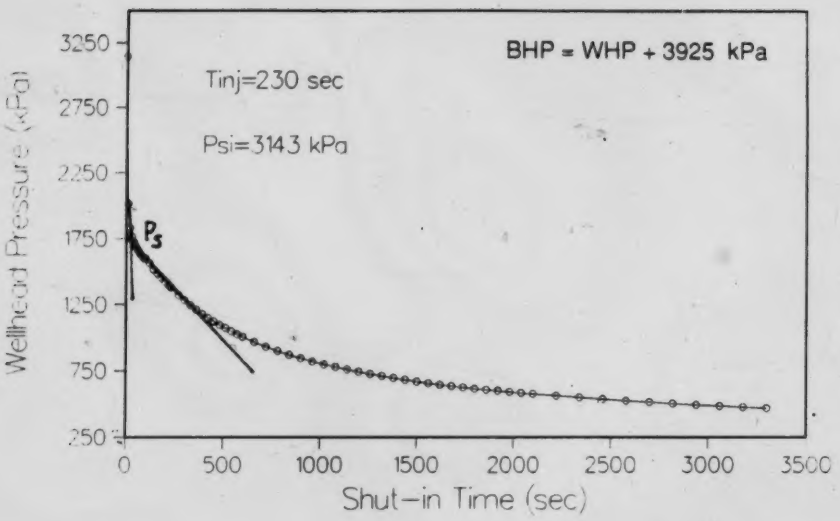

(a) Pressure-shut-in time graph

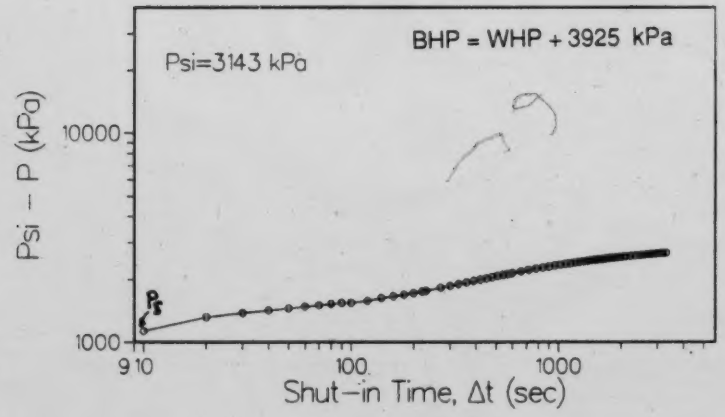

(b) Log-log graph

Figure 5.22 Shut-in pressure interpretation graphs for the ABC CH#3 well microfrac-cycle 1.

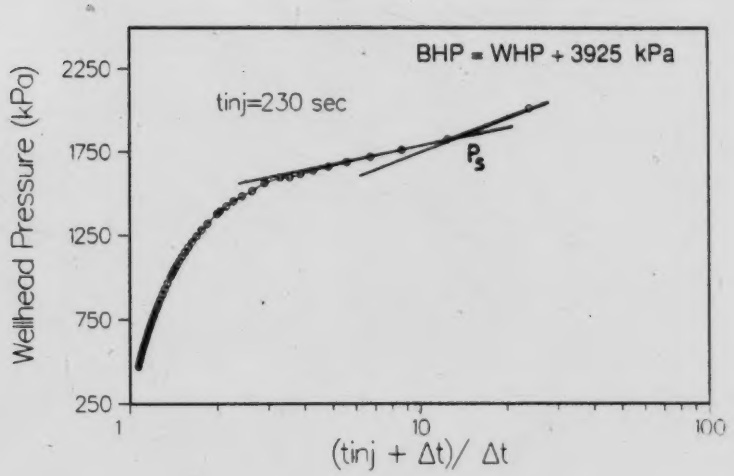

(c) Horner graph

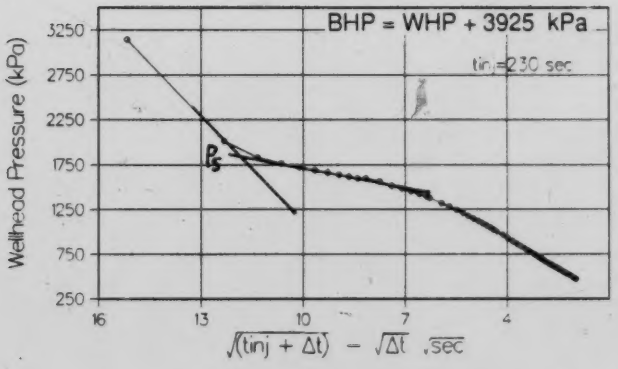

(d) Tandem square root graph

Figure 5.22 continued.

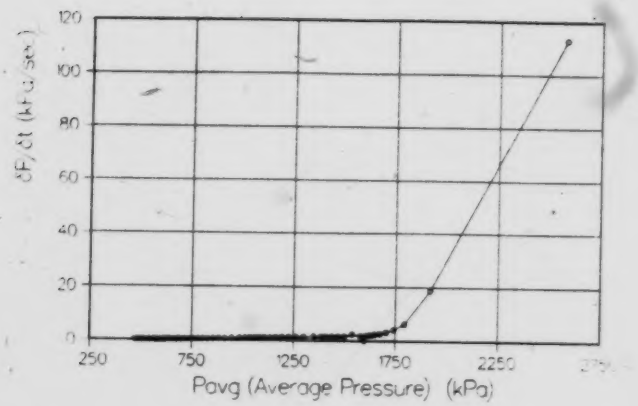

(e) Pressure decay rate graph

Figure 5.22 continued.

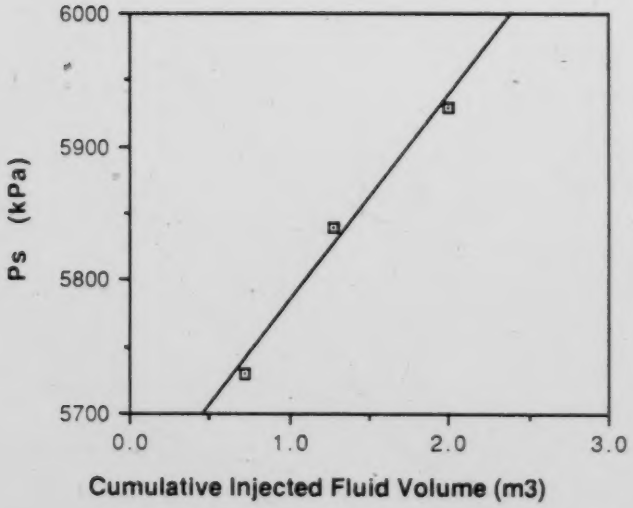

Figure 5.23 Variation in the minimum principal stress for the ABC CH#3 well microfrac test.

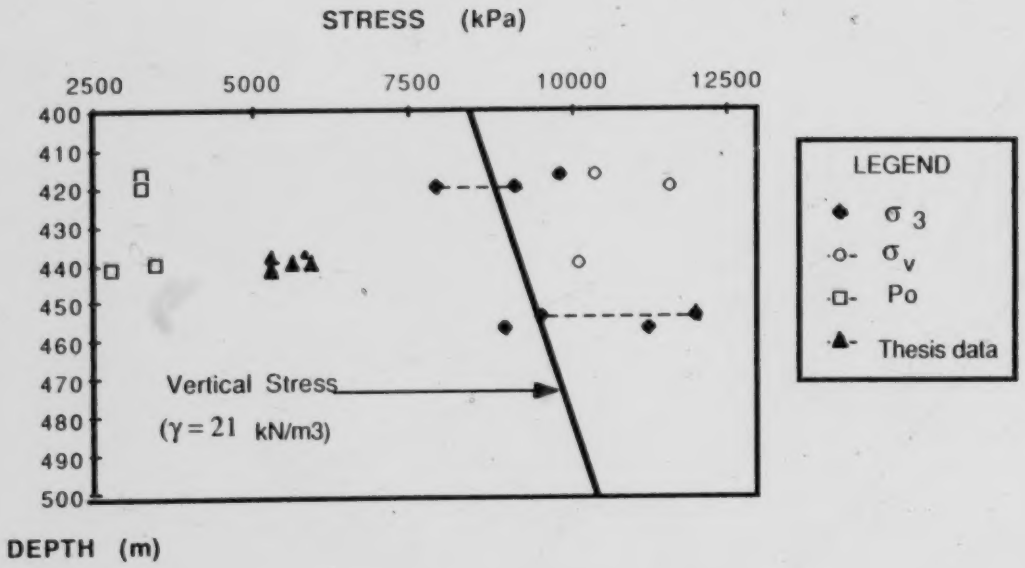

Figure 5.24 Thesis microfrac stress data plotted along with previous in situ stress data for the Cold Lake deposit.

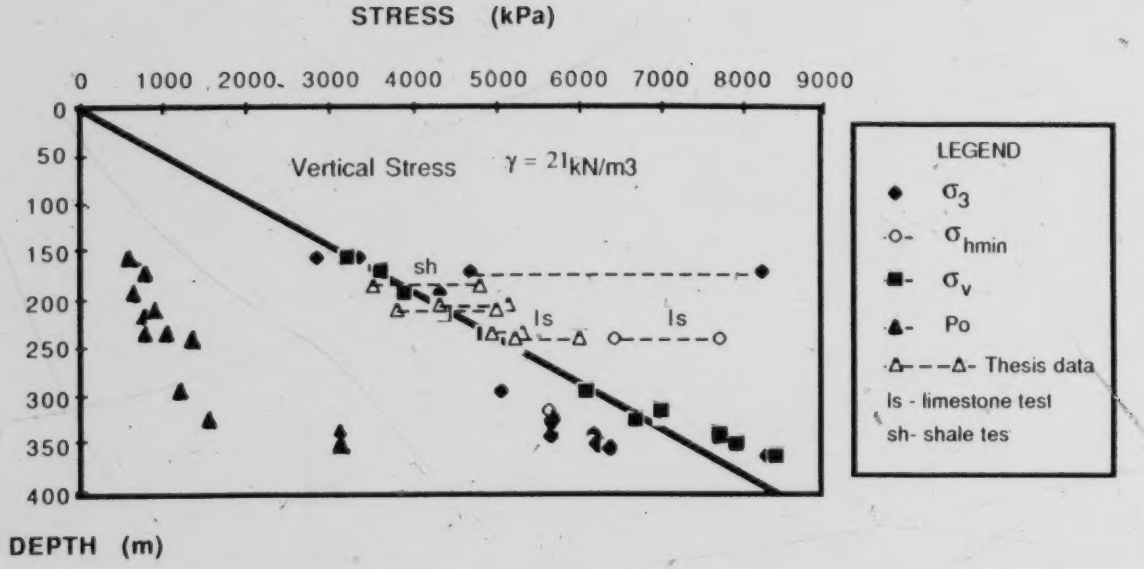

Figure 5.25 Thesis microfrac stress data plotted along with previous in situ stress data for the Athabasca deposit.

6. CONCLUSIONS AND RECOMMENDATIONS

6.1 Conclusions

The primary objective of the thesis was to investigate the validity of hydraulic fracture stress measurement theory for Alberta oil sands deposits. Once the validity of the theory was verified for oil sands, the emphasis was on the analysis of the relationship between the shut-in pressure response and the minimum principal stress. The method developed in this thesis for determining the minimum principal stress from microfrac test data was applied in the analysis of four oil sands deposit microfrac tests. The findings related to the development of the shut-in pressure analysis method and the analysis of the oil sands tests data are summarized below.

(1) A minimum principal stress interpretation method for oil sands tests based on well test methodology was proposed. Review of the various interpretation techniques indicated that the effects of extraneous factors on the shut-in pressure response are still poorly understood. Well test methodology was selected because it has been well developed for analyzing the transient pressure responses of fractured wells affected by fluid leakoff. While this approach does not explicitly consider all of the extraneous factors, such as geologic discontinuities and fracture climbing, its adequate treatment of fluid leakoff puts it ahead of the other techniques.

(2) To check if the microfrac tests did undergo hydraulic fracturing, an analysis of the steady-state injection rate and the steady-state pressure was conducted. The results, along with transmissibility values derived from Horner analyses of the shut-in pressure data, are summarized in Table 5.3.

(3) An analysis of four microfrac tests in oil sand deposits was performed according to the interpretation method developed in chapter 4. The minimum principal stress results for the two Athabasca deposit microfrac

tests are consistent with previous in situ stress data suggesting the development of horizontal fractures. The two Cold Lake deposit microfrac tests gave a minimum horizontal principal stress of approximately 5500 kPa. The data suggests that there is a greater variability in the Cold Lake in situ stress regime.

(4) Comparison of the instantaneous shut-in pressures and the closure pressures for each microfrac test suggest that these two pressures normally coincide. The Amoco H3 oil sands test presented anomalous shut-in pressure responses. The H3 test had an instantaneous shut-in pressure value of 5000 kPa which is close to the vertical stress at 235 m depth. However, the closure stress analysis gave a much lower value of 3500 kPa. This demonstrates the importance of carefully analyzing the shut-in pressure reponse.

The investigation of the primary objective consisted of three components: (i) a review of hydraulic fracture theories and the delineation of their limitations in chapter 2; (ii) a study of the geomechanical behaviour of oil sands relevant to hydraulic fracturing and a review of previous studies of oil sands hydraulic fracturing in chapter 3; and (iii) an in situ stress analysis of four Alberta oil sands microfrac tests in chapter 5. The conclusions regarding the primary objective are summarized below.

(1) The common practice of performing hydraulic fracture tests in cased boreholes prevents a complete analysis of hydraulic fracture intiation theory. Current practice concentrates on determining the minimum principal stress from the shut-in pressure data. The maximum horizontal principal stress is normally not determined from the breakdown pressure. However, the evaluation of the hydraulic fracture initiation theories is summarized below:

- Preliminary evidence indicates that substantial poroelastic effects would exist during hydraulic fracture tests in oil sands. The error involved in assuming the classic equation under such circumstances is potentially large.

- Linear elastic fracture mechanics theory may be useful as a fracture propagation criteria in numerical simulators, but actual oil sands test conditions do not normally provide sufficient information for such an analysis.
- Although Dusseault (1980a,b,c) postulated shear failure as a mechanism accompanying fracture propagation, Callanan's (1983) shear failure initiation theory has limited applications to oil sands.
- The fracture initiation theory of Risnes *et al.* (1982) for unconsolidated plastic rock may be valid for oil sands that has sheared in response to the wellbore stress concentration.

All of these theories ideally should be reviewed on a case by case basis due to the highly variable nature of Alberta oil sands deposits.

(2) The geomechanical properties of oil sands and previous studies of oil sands hydraulic fracturing suggest that hydraulic fracture initiation is a complex process. Non-linear stress-strain behaviour, apparent material anisotropy and heterogeneity, shear and tensile strength properties and poroelastic effects can all affect the application of a particular hydraulic fracture initiation theory. Some of these geomechanical properties have been found to be stress path dependent. The stress path associated with borehole drilling and pressurization in hydraulic fracture tests is substantially different from the stress paths used in conventional laboratory tests. Current geomechanical data, therefore, may be inappropriate for hydraulic fracturing analyses. Initial studies also suggest that oil sands wellbore instability may prohibit the application of hydraulic fracture theory. Previous oil sands hydraulic fracture studies have concentrated on fracture propagation in oil sands since hydraulic fracture initiation is less amenable to analysis and is less relevant to fracture design. At present, only the minimum principal stress can be reliably determined in oil sands microfrac tests.

(3) Three of the four case studies examined in the thesis consisted of microfrac tests performed in cased boreholes. Only the Canterra tests were openhole tests. These tests showed a first cycle breakdown pressure which may be due to excessive wellbore/fracture pressure losses associated with the higher injection rates. Overall, except for the Amoco H3 tests, all the oil sands cased borehole microfrac tests exhibited a substantial first cycle fracture resistance.

Oil sands were also found to have certain effects on the concepts of hydraulic fracture propagation as inferred from oil sands geomechanical properties and previous hydraulic fracture tests. Chapter 3 showed that fluid leakoff and poroelastic properties of oil sands must be considered in fracture propagation. There is also the indirect influence of geomechanical properties, manifested in shear failure and wellbore instability, affecting fracture propagation. Additional studies have shown the influence of geologic discontinuities and in situ stress. However, the fundamental question of whether oil sands actually fractures or "parts" during hydraulic fracturing was not settled. Fortunately, analysis of the minimum principal stress is not affected by this ambiguity. Many of the cited oil sands factors affecting hydraulic fracture propagation are not unique to oil sands. Other researchers have identified leakoff and geologic discontinuities as factors affecting tests in different materials, such as sandstone, limestone and granite. They have proposed various techniques for interpretation of data affected by such factors.

6.2 Practical Implications for Conducting Field Tests

Analysis of the four microfrac case histories revealed the necessity for conducting better controlled small volume hydraulic fracture tests (microfracs) in oil sands. Recommendations for conducting reliable hydraulic fracture stress measurement tests in oil sands include the following:

(1) The ISRM (1987) guidelines for performing small volume hydraulic fracture tests should be followed as closely as possible. Monitoring of the injected fluid rates is essential to conducting well controlled microfrac tests. This monitoring would ensure that: (i) total injected fluid volumes would be less than 2 m^3, thereby ensuring adequate fracture growth, but preventing fracture propagation into other geologic strata (ii) constant injection rates would be maintained, and (iii) the design injection rate could be sustained not only to assure fracture initiation but also to assure that the rate is low enough to prevent excessive pressure losses in the equipment and in the fracture.

(2) Permeability (e.g., falling head tests) tests should be performed both before and after the microfrac tests. The initial tests should be used to calculate the injection rate necessary for fracture initiation. The post-microfrac tests could provide an estimate of the fracture's influence on the reservoir's fluid flow properties.

(3) If openhole conditions are unavailable, the perforation charge, pattern, phasing and arrangement for cased holes should be designed to suit the needs of the hydraulic fracture stress measurement conditions.

(4) An adequate pressure monitoring system situated just above the test zone is necessary for capturing the detail during fracture initiation, propagation and shut-in. A pressure frequency resolution of at least one value per two seconds along with a sufficient shut-in pressure monitoring duration will provide an adequate database for analysis.

(5) A downhole shut-in tool assembly should be used to negate the effects of wellbore storage on the shut-in pressure response.

(6) Observation of the fracture at the wellbore and/or observation of the fracture propagation provides additional information regarding in situ

stress orientation and will aid in the understanding of hydraulic fracture behaviour. Although reservoir engineers often rely on history matching of theoretical and field pressure data to provide a unique fracture solution (Cleary 1988), observation of fracture growth often is essential for a complete analysis. For example, if impression packers, borehole cameras or acoustic televiewers were employed in the microfrac tests, the ambiguity regarding wellbore fracture orientation would most likely be removed. Furthermore, as Holzhausen *et al.* (1980) has shown, tiltmeter measurements may provide crucial information regarding fracture growth away from the borehole.

(7) The interpretation of the pressure-time data should be performed in consideration of the various factors which may affect the induced fracture behaviour.

(8) With the recent advances in automated data acquisition and analysis, the microfrac data should be analyzed in real time. When the data is analyzed in the field as the test progresses, a cycle's results can be used to adjust the test procedure for the following cycles.

6.3 Recommendations for Future Research

During preparation of this thesis, the author concluded that many fundamental aspects of hydraulic fracture behaviour in oil sands are not adequately understood. Analysis of field tests are often inconclusive because of the lack of control over factors affecting hydraulic fracture behaviour in oil sands. For example, the role of fluid leakoff during fluid injection and shut-in in oil sands tests is poorly understood and usually cannot be inferred from field tests. The following recommendations are offered to aid a potential researcher in investigating the fundamental aspects of oil sands hydraulic fracturing.

(1) A well designed laboratory program is necessary to conduct hydraulic fracture experiments under controlled conditions. Experiments would investigate the role of fluid leakoff, poroelastic effects and geologic discontinuities on hydraulic fracturing. Once the basics of hydraulic fracture initiation and propagation have been experimentally verified, the experimental program could be directed to investigate specific aspects of various hydraulic fracture models. However, any experimental program involving oil sands samples is contingent upon the acquisition or fabrication of samples which have in situ oil sands properties.

(2) The experimental program should be conducted in conjunction with numerical modelling efforts which have incorporated the experimental findings.

(3) Carefully designed field tests should eventually follow in order to investigate oil sands fracturing under actual field conditions. The field procedure would be in accordance with ISRM (1987) guidelines modified by the experimental and numerical studies. Pressure monitoring and direct fracture growth monitoring would be required to correlate field results with numerical model predictions.

(4) The evaluation of oil sands geomechanical behaviour relevant to hydraulic fracturing should concentrate on poroelastic properties, fluid leakoff properties, and the stress path dependency of the stress-strain-strength properties.

5) Finally, efforts should be made to liberate proprietory research and field measurements performed by the petroleum industry with respect to oil sands hydraulic fracturing. The scale of present oil sands in situ pilot projects and production projects implies that a substantial amount of potentially valuable data remains unpublished.

REFERENCES

Aamodt, R.L. and Kuriyagawa, M. 1983. Measurement of instantaneous shut-in pressure in crystalline rock. Proceedings of the Workshop on Hydraulic Fracturing Stress Measurements, Monterey, California, pp. 139-142.

Abou-Sayed, A.S., Brechtel, C.E., and Clifton, R.J. 1978. In situ stress determination by hydrofracturing: a fracture mechanics approach. Journal of Geophysical Research, 83: 2851-2862.

Agar, J.G. 1984. Geotechnial behaviour of oil sands at elevated temperatures and pressures. Ph.D. thesis, University of Alberta.

Agar, J.G., Morgenstern, N.R. and Scott, J.D. 1987. Shear strength and stress-strain behaviour of Athabasca oil sand at elevated temperatures and pressures. Canadian Geotechnical Journal, 24(1): 1-10.

Agar, J.G., Morgenstern, N.R. and Scott, J.D. 1989. Fluid transport properties of Athabasca oil sand at elevated temperatures and confining stresses. In preparation.

Aggson, J.R. and Kim, K. 1987. Analysis of hydraulic fracturing pressure histories: a comparison of five methods used to identify shut-in pressure. International Journal of Rock Mechanics and Mining Sciences & Geomechanics Abstracts, 24 (1): 75-80.

Alexander, L.G. 1983. Note on effects of infiltration on the criterion for breakdown pressure in hydraulic fracturing stress measurements. Proceedings of the Workshop on Hydraulic Fracturing Stress Measurements, Monterey, California, pp. 143-148.

AOSTRA. 1987. Twelfth annual report.

Atkinson, B.K. (ed.) 1987. Fracture mechanics of rocks. Academic Press Inc. (London) Ltd., London, U.K.

Au, K.S. 1984. The strength-deformation properties of Alberta oil sands. M.Eng. report, University of Alberta.

Avasthi, J.M. 1981. Hydrofracturing in inhomogeneous, anisotropic and fractured rocks. Ph.D. thesis, Univerisity of Wisconsin-Madison, Madison.

Barnes, D.J. 1980. Micro-fabric and strength studies of oil sands. M.Sc. thesis, University of Alberta.

Baumgärtner, J. and Zoback, M. 1988. Interpretation of hydraulic pressure-time records using interactive analysis methods: application to in situ stress measurements at Moodus, Connecticut. Proceedings of the 2nd International Workshop on Hydraulic Fracturing Stress Measurements, Minneapolis, MN, pp. 619-645.

Bawden, W.F. 1983. Hydraulic fracturing in Alberta tar sand formations, a unique material for in-situ stress stress measurements. Proceedings of

the Workshop on Hydraulic Fracturing Stress Measurements, Monterey, California, pp. 91-103.

Bell, J.S. and Babcock, E.A. 1986. The stress regime of the Western Canadian Basin and implications for hydrocarbon production. Bulletin of Canadian Petroleum Geology, 34(3): 364-378.

Bell. J.S. and Gough, D.I. 1983. The use of borehole breakouts in the study of crustal stress. Proceedings of the Workshop on Hydraulic Fracturing Stress Measurements, Monterey, California, pp. 201-209.

BenNaceur, K., and Roegiers, J.-C. 1988. An automatic system for matching pressure decline during fracturing. Proceedings of the 2nd International Workshop on Hydraulic Fracturing Stress Measurements, Minneapolis, MN, pp. 986-1003.

Bjerrum, L. and Andersen, K.H. 1972. In-situ measurement of lateral pressures in clay. Proceedings of the 5th European Conference, International Society of Soil Mechanics and Foundation Engineering, Madrid, Vol. 1, pp. 11-20.

Bjerrum, L., Nash, J.K.T.L., Kennard, R.M. and Gibson, R.E. 1972. Hydraulic fracturing in field permeability testing. Geotechnique, 22(2): 319-332.

Bredehoeft, J.D., Wolf, R.G., Keys, W.S., and Shuter, E. 1976. Hydraulic fracturing to determine the regional in situ stress field, Piceance Basin, Colorado. Geological Society of Americal Bulletin, 87: 250-258.

Callanan, M.J. 1983. Hydraulic fracture initiation by shear failure in formations at great depths. Proceedings of the Workshop on Hydraulic Fracturing Stress Measurements, Monterey, California, pp. 181-189.

Chan Chim Yuk, C.W. 1986. Geotechnical characteristics of Genesee clay. Ph.D. thesis, University of Alberta.

Charlez, Ph., Herail, R., and Despax, D. 1988. Interpretation of hydraulic fracture parameters by inversion of pressure curves. Proceedings of the 2nd International Workshop on Hydraulic Fracturing Stress Measurements, Minneapolis, MN, pp. 977-985.

Cheatham, J.B. 1984. Wellbore stability. Journal of Petroleum Technology, 36(6): 889-896.

Cheung, L.S. and Haimson, B.C. 1988. Hydraulic fracturing stress measurements in intact and prefractured rock--a laboratory study. Proceedings of the 2nd International Workshop on Hydraulic Fracturing Stress Measurements, Minneapolis, MN, pp. 542-582.

Chhina, H. 1988. Personal communication.

Chhina, H. and Agar, J.G. 1985. Potential use of fracture technology for recovery of bitumen from oil sands. Paper presented at the Third International Conference on Heavy Crude and Tar Sands, UNITAR/UNDP Information Centre, Long Beach, California.

Chhina, H.S., Luhning, R.W., Bilak, R.A., and Best, D.A. 1987. A horizontal fracture test in the Athabasca oil sands. Preprint, 38th Annual Technical Meeting of the Petroleum Society of the CIM, Calgary, Ab, paper no. 87-38-56, pp. 931-966.

Cinco, H. 1982. Evaluation of hydraulic fracturing by transient pressure analysis methods. Paper presented at the International Petroleum Exhibition and Technical Symposium, Beijing, PRC, SPE 10043, pp. 639-665.

Cinco, H. and Samaniego, V.F. 1981 Transient pressure analysis for fractured wells. Journal of Petroleum Technology, **33**: 1749-1766.

Clark, I.B. 1949. A hydraulic process for increasing the productivity of wells. Transactions, AIME, **186**: 1.

Cleary, M.P. 1979. Rate and structure sensitivity in hydraulic fracturing of fluid saturated porous formations. Proceedings of the 20th U.S. Symposium on Rock Mechanics, University of Texas, Austin, pp. 127-142.

Cleary, M.P. 1988. The engineering of hydraulic fractures--state of the art and technology of the future. Journal of Petroleum Technology, **40**(1): 13 -21.

Cornet, F.H. and Valette, B. 1984. In situ stress determination from hydraulic injection test data. Journal of Geophysical Research, **89**(B13): 11527-11537.

Daneshy, A.A. 1973. Experimental investigation of hydraulic fracturing through perforations. Paper presented at the 2nd Annual European Meeting of the SPE of AIME, London, UK, SPE 4333.

de Bree, P. and Walters, J. 1988. Micro/minifrac tests: field test procedures and interpretational techniques. Proceedings of the 2nd International Workshop on Hydraulic Fracturing Stress Measurements, Minneapolis, MN, pp. 718-759.

Detournay, E. and Cheng, A.H.-D. 1988. Poroelastic response of a borehole in a non-hydrostatic stress field. International Journal of Rock Mechanics and Mining Science and Geomechanics Abstracts, **25**(3): 171-182.

Detournay, E., Roegiers, J.-C., and Cheng, A.H.-D. 1987. Some new examples of poroelastic effects in rock mechanics. Proceedings of the 28th U.S. Symposium on Rock Mechanics, Tucson, pp. 575-584.

Detournay, E., Cheng, A.H.-D., Roegiers, J.-C., and McLennan, J.D. 1988. Poroelastic considerations in in situ stress determination by hydraulic fracturing. Proceedings of the 2nd International Workshop on Hydraulic Fracturing Stress Measurements, Minneapolis, MN, pp. 410-424.

Doe, T., Hustrulid, W.A., Leijon, B., Ingevald, K., Strindell, L., 1983. Determination of the state of stress at the Stripa Mine, Sweden. Proceedings of the Workshop on Hydraulic Fracturing Stress Measurements, Monterey, California, pp. 119-129.

Dunlap, I.R. 1963. Factors controlling the orientation and direction of hydraulic fractures. Journal of the Institute of Petroleum, **49**: 282-288.

Dusseault, M.B. 1977a. The geotechnical characteristics of oil sands. Ph.D. thesis, University of Alberta.

Dusseault, M.B. 1977b. Stress state and hydraulic fracturing in the Athabasca oil sands. Journal of Canadian Petroleum Technology, **16**(3): 19-27.

Dusseault, M.B. 1980a. The behaviour of hydraulically induced fractures in oil sands. In Underground Rock Engineering, Proceedings of the 13th Canadian Rock Mechanics Symposium, Canadian Institute of Mining and Metallurgy, Toronto, pp. 36-41.

Dusseault, M.B. 1980b. A conceptual geomechanical model for hydraulic fracture in the Athabasca oil sands. Paper presented at the AOSTRA-University-Industry Symposium, Fort McMurray, Alberta.

Dusseault, M.B. 1980c. The development of permeability in cohesionless bituminous sands. Proceedings of the Tar Sands Permeability Enhancement Seminar, Sandia National Laboratories, Alburqueque, New Mexico, pp. 45-84.

Dusseault, M.B. and Morgenstern, N.R. 1978. Shear strength of Athabasca oil sands. Canadian Geotechnical Journal, **15**: 216-238.

Dusseault, M.B. and Simmons, J.V. 1982. Injection induced stress and fracture orientation changes. Canadian Geotechnical Journal, **19**: 483-493.

Earlougher Jr., R.C. 1977. Advances in well test analysis. Monograph Series No. 5, Society of Petroleum Engineers, Dallas TX.

Edl Jr., J. N. 1973. Mechanical instability of deep walls with particular reference to hydraulic fracturing. M.S. thesis, University of Wisconsin.

Fairhurst, C. 1964. Measurement of in situ rock stresses with particular reference to hydraulic fracturing. Felsmechanik und Ingenieurgeologie, **2**(3,4): 129-147.

Gay, N.C. 1980. The state of stress in the plates. In Dynamics of Plate Interiors. Geodynamics Series. Edited by A. Bally, P.L. Bender, T.R. McGetchin, and R.I. Walcott. American Geophysical Union and the Geological Society of America. Vol. 1, pp. 145-154.

Goodman, R.E. 1980. Introduction to rock mechanics. John Wiley & Sons, New York.

Gough, D.I. and Bell, J.S. 1982. Stress orientations from borehole wall fractures with examples from Colorado, east Texas, and northern Canada. Canadian Journal of Earth Science, **19**: 1358-1370.

Gringarten, A.C., Ramey Jr., H.J.1974. Unsteady-state pressure distributions caused by a well with a single, horizontal fracture, partial penetration, or

restricted entry. Society of Petroleum Engineers Journal, August 1974, pp. 413-426.

Gringarten, A.C., Ramey Jr., H.J., and Raghavan, R. 1974. Unsteady-state pressure distributions created by a well with a single infinite-conductivity vertical fracture. Society of Petroleum Engineers Journal, August 1974, pp. 347-360.

Gronseth, J.M. and Kry, P.R. 1983. Instantaneous shut-in pressure and its relationship to the minimum in situ stress. Proceedings of the Workshop on Hydraulic Fracturing Stress Measurements, Monterey, California, pp. 55-60.

Gronseth, J.M. 1988. Cased hole in situ stress determinations from deviated wellbores in an unconsolidated formation. Proceedings of the 2nd International Workshop on Hydraulic Fracturing Stress Measurements, Minneapolis, MN., pp. 840-855.

Hackbarth, D.A. and Nastasa, N. 1979. Hydrogeology of the Athabasca oil sands area, Alberta. Alberta Research Council, Bulletin 38, 39p.

Haimson, B.C. 1968. Hydraulic fracturing in porous and nonporous rock and its potential for determining in-situ stresses at great depth. Ph.D. thesis, University of Minnesota, Minneapolis, MN.

Haimson, B.C. 1975. Deep in-situ stress measurements by hydrofracturing. Tectonophysics, **29**: 41-47.

Haimson, B.C. 1978. The hydrofracturing stress measuring method and recent field results. International Journal of Rock Mechanics and Mining Sciences and Geomechanics Abstracts, **15**(4): 167-178.

Haimson, B.C. 1981. Confirmation of hydrofracturing results through comparisons with other stress measurements. Proceedings of the 22nd U.S. Symposium on Rock Mechanics, Cambridge, Massachusets, pp. 409-415.

Haimson, B.C. 1982. Deep stress measurements in three Ohio quarries and their comparison to near surface tests. Proceedings of the 23rd U.S. Symposium on Rock Mechanics, Berkeley, California, pp. 190-202.

Haimson, B.C. 1983. A comparative study of deep hydrofracturing and overcoring stress measurements at six locations with particular interest to the Nevada Test Site. Proceedings of the Workshop on Hydraulic Fracturing Stress Measurements, Monterey, California, pp. 107-118.

Haimson, B.C. 1984. The state of stress at the Nevada Test Site: a demonstration of the reliability of hydrofracturing and overcoring techniques. In Field Measurements in Geomechanics, Proceedings of the International Syposium, Zurich, Edited by K. Kovari, pp. 115-126.

Haimson, B.C. and Avasthi, J.M. 1975. Stress measurements in anisotropic rock by hydraulic fracturing. Proceedings of the 15th U.S. Symposium on Rock Mechanics, Custer State Park, SD, pp. 135-156.

Haimson, B.C. and Edl, J.H. 1972. Hydraulic fracturing of deep wells. Paper presented at the 47th Annual Fall Meeting of SPE of AIME, SPE 4061.

Haimson, B.C. and Fairhurst, C. 1967. Initiation and extension of hydraulic fractures in rock. Society of Petroleum Engineers Journal, 7(3): 310-318.

Haimson, B.C. and Fairhurst, C. 1969. Hydraulic fracturing in porous-permeable materials. Journal of Petroleum Technology. 2(7): 811-817.

Haimson, B.C. and Fairhurst, C. 1970. In-situ stress determination at great depth by means of hydraulic fracturing. Proceedings of the 11th U.S. Symposium on Rock Mechanics, University of California, Berkeley, pp. 559-584.

Haimson, B.C. and Voight, B. 1977. Crustal stresses in Iceland. Pure and Applied Geophysics, 115: 153-190.

Hast, N. 1979. Limits of stress measurements in the earth's crust. Rock Mechanics, 11: 143-150.

Hayashi, K., and Sakurai, I. 1988. Interpretation of shut-in curves of hydraulic fracturings for tectonic stress measurements. Proceedings of the 2nd International Workshop on Hydraulic Fracturing Stress Measurements, Minneapolis, MN, pp. 583-618.

Hickman, S.H. and Zoback, M.D. 1983. The interpretation of hydraulic fracturing pressure-time data for in situ stress determination. Proceedings of the Workshop on Hydraulic Fracturing Stress Measurements, Monterey, California, pp. 44-54.

Hickman, S.H., Healy, J.H. and Zoback, M.D. 1985. In situ stress, natural fracture distribution, and borehole elongation in the Auburn Geothermal Well, Auburn, New York. Journal of Geophysical Research, 90(B7): 5497-5512.

Holzhausen, G.R., Wood, M.D., Raisbeck, J.M. and Card, C.C. 1980. Results of deformation monitoring during steam stimulation in a single-well test. Applied Oilsands Geoscience, Edmonton, Alberta.

Horsrud, P., Risnes, R., and Bratli, R.K. 1982. Fracture initiation pressures in permeable poorly consolidated sands. International Journal of Rock Mechanics and Mining Sciences & Geomechanics Abstracts, 19: 255-266.

Hubbert, M.K., and Willis, D.G. 1957. Mechanics of hydraulic fracturing. Transactions of the American Institute of Mining and Metallurgical and Petroleum Engineers, 210:.153-168.

ISRM-Commission on Testing Methods, 1987. Method 2: suggested method for rock stress determination using the hydraulic fracturing technique. International Journal of Rock Mechanics and Mining Sciences & Geomechanics Abstracts, 24(1): 59-62.

Jaworski, G.W. 1979. An experimental study of hydraulic fracturing. Ph.D. thesis, University of California, Berkeley.

Jaworski, G.W. Duncan, J.M. and Seed, H. Bolton. 1981. Laoboratory study of hydraulic fracturing. ASCE Journal of the Geotechnical Engineering Division, **107**(GT6): 713-732.

Kaiser, P.K. 1987. Detection of rock mass rupture modes. Proceedings of the 6th Congress of the International Society of Rock Mechanics, Montreal.

Kaiser, P.K. 1988. Deep borehole rupture mechanics. Final Summary Report for NSERC Strategic Grant No. G1136

Kaiser, P.K. and Maloney, S. 1987. Factors influencing the stability of deep boreholes. Proceedings of the 6th Congress of the International Society of Rock Mechanics, Montreal,

Kehle, R.O. 1964. Determination of tectonic stresses through analysis of hydraulic well fracturing. Journal of Geophysical Research, **69**(2): 259-272.

King, G.E. 1987. Selecting a perforating system. Journal of Petroleum Technology, **39**: 261-262.

Komar, C.A. and Fohne, K.H. 1973. Factors controlling fracture orientation in sandstone. Preprint, 48th Annual Fall Meeting of the Society of Petroleum Engineers of AIME, Las Vegas, Nevada, SPE 4567.

Kosar, K.M. 1989. Geotechnical properties of oil sands and related strata. Ph.D thesis, University of Alberta.

Kosar, K.M., Scott, J.D. and Morgenstern, N.R. 1987. Testing to determine the geotechnical properties of oil sands. Preprint, 38th Annual Technical Meeting of the Petroleum Society of the CIM, Calgary, Alberta, paper no. 87-38-59, pp. 995-1010.

Kular, G.S., Chhina, H.S., Best, D.A., and MacKenzie, W.T. 1988. Multiple hydraulic fracture propagation in oil sands. Preprint, SPE Rocky Mountain Regional Meeting, Casper, WY, SPE 17534, pp. 477-481.

Kuriyagawa, M., Kobayashi, H., Matsunaga, I., Kosugi, M., Yamaguchi, T., Sasaki, S. and Hori, Y. 1985. Determination of in-situ stress to predict direction of hydraulically created fractures for development of hot dry geothermal resources in Japan. Transactions-Geothermal Resources, **9**(2): 111-114.

Lawn, B.R. and Wilshaw, T.R. 1975. Fracture of brittle solids. Cambridge University Press, Cambridge, U.K.

Lefebvre, G., Philibert, A., Bozozuk, M. and Pare, J-J. 1981. Fissuring from hydraulic fracture of clay soil. Proceedings of the 10th International Conference on Soil Mechanics and Foundation Engineering, Stockholm, Sweden, A.A. Balkema, Vol. 2, pp. 513-518.

Lee, J. 1983. Well testing. Society of Petroleum Engineers of AIME, New York.

Lee, M.Y. and Haimson, B.C. 1988. Applications of statistical techniques to field hydraulic fracturing data interpretation. Proceedings of the 2nd International Workshop on Hydraulic Fracturing Stress Measurements, Minneapolis, MN, pp. 502-541.

Li Fang-quan, Li Yan-mei, Wang En-fu, Zhai Qing-shan, Bi Shang-xu, Zhang-Jun, Liu-Peng, Wei Qing-yun, and Zhao Shi-quang. 1983. Experiments of in situ stress measurements using stress relief and hydraulic fracturing techniques. Proceedings of the Workshop on Hydraulic Fracturing Stress Measurements, Monterey, California, pp. 130-134.

Lindner, E.N. and Halpern, J.A. 1978. In situ stress in North America: a compilation. International Journal of Rock Mechanics and Mining Sciences & Geomechanics Abstracts, **15**: 183-204.

Lockner, D., and Byerlee, J.D. 1977. Hydrofracture in Weber sandstone at high confining pressure and differential stress. Journal of Geophysical Research, **82**(14): 2018-2026.

Logan, J.M. 1983. Rock fabric and hydraulic fracturing: the implications for in situ stress measurements and permeability enhancement. Proceedings of the 24th U.S. Symposium on Rock Mechanics, Texas A&M University, College Station, TX, pp. 751-760.

Massarsch, K.R. 1978. New aspects of soil fracturing in clay. ASCE Journal of the Geotechnical Engineering Division, **104**(GT8): 1109-1121.

Massarsch, K.R., Holtz, R.D., Holm, B.G. and Fredriksson, A. 1975. Measurement of horizontal in-situ stresses. Proceedings of the American Society of Civil Engineers Specialty Conference on In-Situ Measurement of Soil Properties, Raleigh, Vol 1., pp. 266-286.

McGarr, A., and Gay, N.C. 1978. State of stress in the earth's crust. Annual Review of Earth and Planetary Science, Volume 6, pp. 405-436.

McKay, J.G. 1988. Personal communication.

McLennan, J.D. 1980. Hydraulic fracturing: A fracture mechanics approach. Ph.D. thesis, University of Toronto.

McLennan, J.D. and Roegiers, J.-C. 1982. How instantaneous are instantaneous shut-in pressures? Paper persented at the 57th Annual Fall Technical Conference and Exhibition of SPE of AIME, New Orleans, SPE 11064.

McLennan, J.D. and Roegiers, J.-C. 1983. Do instantaneous shut-in pressures accurately represent the minimum principal stress? Proceedings of the Workshop on Hydraulic Fracturing Stress Measurements, Monterey, California, pp. 68-78.

Medlin, W.L. and Massé, L. 1979. Laboratory investigation of fracture initiation pressure and orientation. Society of Petroleum Engineers Journal, **19**(2): 129-144.

Medlin, W.L. and Massé, L. 1984. Laboratory experiments in fracture propagation. Society of Petroleum Engineers Journal, 24(3): 256-268.

Mitchell, J.K. 1976. Fundamentals of soil behaviour. John Wiley & Sons, New York.

Morgenstern, N.R. and Vaughan, P.R. 1963. Some observations on allowable grouting pressures. Grouts and Drill Muds, Institution of Civil Engineers, London, pp. 36-42.

Morgenstern, N.R. and Scott, J.D. 1986. NSERC Strategic Grant Application.

Mossop, G.D. 1978. Geological controls on reservoir hetergeneity-Athabasca oil sands. Proc. Seminar on Underground Excavation in Oil Sands. ed. by M.B. Dusseault, Dept. of Civil Engineering, University of Alberta, Edmonton, Paper No. 1.

Nelson, R.A. 1985. Geologic analysis of naturally fractured reservoirs. Gulf Publishing Co., Houston.

Nobari, E.S., Lee, K.L., and Duncan, J.M. 1973. Hydraulic fracturing in zoned earth and rockfill dams. Office of Research Services, University of California, Berkeley, Report No. TE 73-1, Vol 9, No. 8, pp. 17-23.

Nur, A. and Byerlee, J.D. 1971. An exact effective stress law for elastic deformation of rock with fluids. Journal of Geophysical Research, 76(26): 6413-6419.

Pine, R.J., Ledingham, P., and Merrifield, C.M. 1983. In situ stress measurement in the Carnmenellis granite--II. Hydofracture tests at Rosemanowes quarry to depths of 2000 m. International Journal of Rock Mechanics and Mining Sciences & Geomechanics Abstracts, 20(2): 63-72.

Plewes, H.D. 1987. Undrained strength of Athabasca oil sands. M.Sc. thesis, University of Alberta, Edmonton.

Raisbeck, J.M. and Currie, J.B. 1981. A laboratory investigation of hydraulic fracturing in oil sands. In Situ, 5(1): 1-24.

Rice, J.R. and Cleary, M.P. 1976. Some basic stress diffusion solutions for fluid-saturated elastic porous media with compressible constituents. Review of Geophysics and Space Physics, 14(2): 227-241.

Risnes, R., Bratli, R.K., and Horsrud, P.1982. Sand stresses around a wellbore. Society of Petroleum Engineers Journal, 22(6): 883-898.

Roegiers, Jean-Claude. 1974. The development and evaluation of a field method for in situ stress determination using hydraulic fracturing. Ph.D. thesis, University of Minnesota, Minneapolis.

Scheidegger, A.E. 1962. Stresses in the earth's crust as determined from hydraulic fracturing data. Geologie und Bauwesen, 27(2): 45.

Scott, J.D. and Morgenstern, N.R. 1987. Stress-deformation and strength properties of Athabasca oil sands. Progress report on Geotechnical and Thermal Testing of Oil Sands submitted to the Alberta Oil Sands Technology and Research Authority, Edmonton, Alberta.

Settari, A. and Raisbeck, J.M. 1979. Fracture mechanics analysis in in-situ oil sands recovery. Journal of Canadian Petroleum Technology, 18(2): 85-94.

Settari, A. and Raisbeck, J.M. 1981. Analysis and numerical modeling of hydraulic fracturing during cyclic steam stimulation in oil sands. Journal of Petroleum Technology, 33(1): 2201-2212.

Settari, A., Kry, P.R. and Yee, C.T. 1989. Coupling of fluid flow and soil behaviour to model injection into uncemented oil sands. Journal of Canadian Petroleum Technology, 28(1): 81-92.

Shylapobersky, J. 1988. Hydraulic fracture determination of minimum in situ stress from extended pressure falloff and from fracture reopening and flowback tests. Proceedings of the 2nd International Workshop on Hydraulic Fracturing Stress Measurements, Minneapolis, MN, pp. 760-799.

Simonson, E.R., Abou-Sayed, A.S., and Clifton, R.J. 1978. Containment of massive hydraulic fractures. Society of Petroleum Engineers Journal, 18(1): 27-32.

Smith, M.B. 1985. Stimulation design for short, precise hydraulic fractures. Society of Petroleum Engineers Journal, 25: 371-379.

Solberg, P., Lockner, D., and Byerlee, J.D. 1977. Shear and tension hydraulic fractures in low permeability rocks. Pure and Applied Geophysics, 115: 191-198.

Solberg, P., Lockner, D., and Byerlee, J.D. 1980. Hydraulic fracturing in granite under geothermal conditions. International Journal of Rock Mechanics and Mining Sciences & Geomechanics Abstracts, 17: 25-33.

Sookprasong, P.A. 1986. Plot preocedure finds closure pressure. Oil & Gas Journal, September 8, 1986, pp. 110-112.

Sufi, A. H. and Thompson, R.J. 1988. A modified slug test for underpressured reservoirs. Journal of Petroleum Technology, 40(1): 105-110.

Tavenas, F.A., Blanchette, G., Lerouil, S. Roy, M. and LaRochelle, P. 1975. Difficulties in the in-situ determination of K_o in sensitive clay. Proceedings of the American Society of Civil Engineers Specialty Conference on In-Situ Measurement of Soil Properties, Raleigh, Vol 1., pp. 450-476.

Teufel, L.W. 1979. An experimental study of hydraulic fracture propagation in layered rock. Ph.D. thesis, Texas A&M University, College Station, Texas.

Teufel, L.W. 1985. In-situ stress state in the mounds test well as determined by the anelastic strain recovery method. Paper presented at the SPE/DOE Low Permeability Gas Rerservoirs, Denver, CO, SPE/DOE 13896.

Teufel, L.W. and Clark, J.A. 1984. Hydraulic fracture propagation in layered rock: experimental studies of fracture containment. Society of Petroleum Engineers Journal, **24**(1): 19-32.

Teufel, L.W. and Warpinski, N.R. 1983. In-situ stress variations and hydraulic fracture propagation in layered rock--observations from a mineback experiment. Proceedings of the 5th International Congress on Rock Mechanics, Melbourne, Vol. 2, pp. F43-F48.

Teufel, L.W. and Warpinski, N.R. 1987. Influence of geologic discontinuities on hydraulic fracture propagation. Journal of Petroleum Technology, **39**(2): 209-220.

Tunbridge, L. 1988. Interpretation of the shut-in pressure from the rate of pressure decay. Proceedings of the 2nd International Workshop on Hydraulic Fracturing Stress Measurements, Minneapolis, MN, pp. 686-717.

Vaziri, H. 1987. A methodology for predicting sand failure around wellbores. Preprint, 38th Annual Technical Meeting of the Petroleum Society of the CIM, Calgary, Paper No. 97-38-60, pp. 1011-1034.

Von Schonfeldt, Hilmar A. 1970. An experimental study of open-hole hydraulic fracturing as a stress measurement method with particular emphasis on field tests. Ph.D. thesis, University of Minnesota, Minneapolis.

Warpinski, N.R. 1983. Investigation of the accuracy and reliability of in situ stress measurements using hydraulic fracturing in perforated cased boreholes. Proceedings of the 24th U.S. Symposium on Rock Mechanics,Texas A&M University, College Station, TX, pp. 773-786.

Warpinski, N.R. 1988. Determining the minimum in situ stress from hydraulic fracturing through perforations. Proceedings of the 2nd International Workshop on Hydraulic Fracturing Stress Measurements, Minneapolis, MN, pp. 800-839.

Warpinski, N.R., Branagan, P. and Wilmer, R. 1985. In-situ stress measurements at U.S. DOE's Multiwell Experiment Site, Mesaverde Group, Rifle, Colorado. Journal of Petroleum Technology, **37**(3): 527-536.

Warpinski, N.R., Schmidt, R.A. and Northrop, D.A. 1982. In-situ stresses: the predominant influence on hydraulic fracture containment. Journal of Petroleum Technology, **34**(3): 653-664.

Warren, W.E. 1981. Packer induced stresses during hydraulic well fracturing. ASME Journal of Energy Resources Technology, **103**(12): 336-343.

Warren, W.E. 1983. Determination of in-situ stresses from hydraulically fractured spherical cavities. ASME Journal of Energy Resources Technology, **105**(6): 125-127.

Whitehead, W.S., Gatens, J.M., and Holditch, S.A. 1988. Determination of in-situ stress profiles through hydraulic fracturing measurements in two distinct geologic areas. Proceedings of the 2nd International Workshop

on Hydraulic Fracturing Stress Measurements, Minneapolis, MN, pp. 856-915.

Widjaja, H., Duncan, J.M., and Seed, H.B. 1984. Scale and time effects in hydraulic fracturing. Report prepared for the U.S. Army Corps of Engineers, Geotechnical Laboratory, Waterways Experiment Station, Vicksburg, 189 p.

Wooten, C., and Elbel, J. 1988. State of the art determination of fracture closure pressure. Proceedings of the 2nd International Workshop on Hydraulic Fracturing Stress Measurements, Minneapolis, MN, pp. 916-952.

Zoback, M.D. and Haimson, B.C. 1982. Status of the hydraulic fracturing method for in situ stress measurements. Proceedings fo the 23rd U.S. Symposium on Rock Mechanics, Berkeley, pp. 143-157.

Zoback, M.D. and Pollard, D.D. 1978. Hydraulic fracture propagation and the interpretation of pressure-time records for in situ stress determinations. Proceedings of the 19th U.S. Symposium on Rock Mechanics, Vol. 1., pp. 14-21.

Zoback, M.D., Rummel, F., Jung, R., and Raleigh, C.B. 1977. Laboratory hydraulic fracturing experiments in intact and pre-fractured rock. International Journal of Rock Mechanics and Mining Sciences & Geomechanics Abstracts, **14**: 49-58.

Zoback, M.D., Moos, D., Mastin, L., and Anderson, R.N. 1985. Well bore breakouts and in situ stress. Journal of Geophysical Research, **90**(B7): 5523-5530.